University of Nevada, Reno

Trapping the Elusive Aza-Oxyallylic Cation Intermediate: Aza-[4+3] Cycloaddition Reactions and their Application Toward Target Directed Synthesis

A dissertation submitted in partial fulfillment of the
requirements for the degree of Doctor of Philosophy in Chemistry

By

Korry Lee Barnes

Dr. Christopher S. Jeffrey/Dissertation Advisor

December, 2014

THE GRADUATE SCHOOL

We recommend that the dissertation
prepared under our supervision by

KORRY LEE BARNES

Entitled

Trapping the Elusive Aza-Oxyallylic Cation: Aza-[4+3] Cycloaddition Reactions and their Application Toward Target Directed Synthesis

be accepted in partial fulfillment of the
requirements for the degree of

DOCTOR OF PHILOSOPHY

Christopher S. Jeffrey, Ph. D., Advisor

Benjamin T. King, Ph. D., Committee Member

Sean S. Casey, Ph. D., Committee Member

Regina M. Tempel, Ph. D., Committee Member

James L. Kenyon, Ph. D., Graduate School Representative

David W. Zeh, Ph. D., Dean, Graduate School

December, 2014

Abstract

The aza-oxyallylic cation is a reactive intermediate that undergoes a [4+3] cycloaddition reaction with dienes to form seven-membered nitrogen heterocycles. Although the existence of this intermediate had been proposed for over 50 years, only recently has experimental evidence been established to support its existence. The intermediate was generated by base-mediated dehydrohalogenation of α-haloamide precursors synthesized from the corresponding acid halide in dichloromethane, respectively. From the analogous aza-oxyallylic cation intermediates generated *in situ*, a series of bicyclic lactam scaffolds were easily prepared from a [4+3]-cycloaddition reaction of the corresponding α-haloamide and either furan or cyclopentadiene as the diene moiety. With the exception of one case, all monoaryl and monoalkyl haloamides provided selectively the *endo* diastereoisomer (≥19:1). Computational and experimental evidence suggest that an *N*-alkoxy substituent provides necessary stabilization to the aza-oxyallylic cation intermediate.

Balanol is a fungal metabolite first isolated from *Verticillium balanoides* and has been shown to be a potent protein kinase C (PKC) inhibitor. Starting from the α-chlorocycloadduct synthesized in Chapter 2, a concise synthesis of the hexahydroazepine-containing fragment was undertaken that was both scalable and stereoselective. Polyhydroxylated azepanes are a relatively new class of compounds with broad therapeutic potential in a variety of biological and pharmaceutical applications. A general synthesis of (±)-(4*R*, 5*R*, 6*R*)-4,5,6-trihydroxy-3,3-dimethylazepane is achieved in only five short synthetic steps starting from the corresponding cycloadduct, allowing for rapid access to the seven-membered iminosugar class of compounds. The reaction sequence is efficient, diastereoselective, scalable, and has the capability of incorporating a wide variety of functional groups at the ring three-postion.

Polyhydroxylated piperidines are a functionally rich class of biologically active compounds that also have broad therapeutic potential. Previously described aza-[4+3]

cycloadditions of putative aza-oxyallylic cations provide heterocyclic scaffolds that enabled a concise synthesis of polyhydroxylated piperidines. Chemoselective amide reduction and subsequent hemiaminal ether ring opening of four α-chlorocycloadducts by aluminum hydride provided in one pot four novel 3-chloroazepines. Aziridinium ion-mediated ring contraction and chloride displacement was triggered by silver acetate, followed by acetate hydrolysis under basic conditions to give the corresponding tetrahydropyridine diols. Alkene dihydroxylation catalyzed by osmium tetroxide installed the final hydroxyl groups, which yielded four novel polyhydroxylated *N*-alkoxypiperidine iminosugar analogs in good overall yield and high diastereoselectivity.

Expanding on the originally reported methodology of dehyrohalogenation of α-haloamides as a means to generate aza-oxyallylic cation intermediates, efforts were undertaken to explore alternative methods to generate the afformentioned intermediates that could incorporate heteroatoms at the α-position. 2-methoxy-*N*-(phenylmethoxy)acetamide and 2-phthalyl-*N*-(phenylmethoxy)acetamide were synthesized to serve as model substrates and screened according to solvent, base, and oxidant in order to determine conditions that would allow for aza-oxyallylic cation formation.

All compounds were fully characterized by NMR, IR, and high-resolution mass spectrometry. Additionally, six compounds that were of exceptionally high crystallinity were characterized by single crystal X-ray diffraction.

Dedication

For Ashley Lynn. Thank you for embarking on this journey with me and for your never ending love and support along the way.

Acknowledgements

First and foremost, I wish to thank my advisor, Dr. Chris Jeffrey. He has been a constant source of encouragement and guidance throughout my graduate career and has not only provided academic advice, but also advice towards life decisions. I have gone through a lot of personal and academic growth over the last 5 years, and Dr. Jeffrey has been there every step of the way providing nothing but unwavering support. He has taught me so much about organic chemistry in a way that has been both challenging and fun at the same time. It would be impossible to thank him enough and let him know how much he is appreciated.

I would also like to thank the members of my doctoral committee Dr. Benjamin King, Dr. Sean Casey, Dr. James Kenyon, and Dr. Regina Tempel for reading all of my manuscripts and donating their valuable time to giving me feedback on all of my written and oral exams. To Dr. Stephen Spain for his continued assistance with any instrumentation needs I may have had. To Dr. Vincent Catalano, Dr. Lyndsay Munro, and Kelly Chen for all of your help with X-Ray crystallography. You were all an integral part of the success of the aza-sugars project and it could not have been completed without your assistance and crystallographic expertise. To all of the Jeffrey group members, especially Tracy, Devendar, and Arjun. We all started this adventure with Dr. Jeffrey together at the same time, and it seems like just yesterday we all met each other as first-year graduate students. Much has changed over the years, however one thing remains the same, and that's our close friendship and the bonds that we have formed from working with each other. I will never forget the memories we made together from traveling, to the jokes in lab, to lifting each other up when we were down, to celebrating each other's milestones.

To all of my family members back home, especially mom, dad, Kenny, Klayton, Kaleb, Beth, and Skye. Although you weren't here physically through my graduate career you were always sending me your love and support and I could not have done it without you. Thank you

for supporting me and listening even though most of the time what I was talking about sounded like a foreign language. To my aunt Netty, cancer took you away from our family too soon, and ever since your passing you have been a constant motivation in driving me to succeed. It is your legacy that continues to feed my passion for working toward discovering new treatments for this terrible disease that impacts so many lives. To my in-laws Mr. Jerry and Mrs. Kerry Thompson, Mr. Ken Thompson, and Mr. Billy and Mrs. Ginger Larsen. I want to first and foremost thank you for entrusting me to take care of your beloved daughter, and also for providing nothing but love and support throughout our marriage and my academic career. You all truly mean the world to me and I don't know that any of this would have been possible without you.

Finally, I wish to thank my wife Ashley. Although you are listed last, you are without a doubt the most important. Your love and support throughout this entire process has been unrivaled and even though it has been anything but easy, you have chosen to stand by my side through thick and thin. We have endured very trying circumstances over the last few years, but when I look back on everything, in a strange way it makes me smile and I feel accomplished for pushing forward together and never giving up. When I think about all you've done from working full-time at the hospital while finishing your degree, to birthing Liam and being a phenomenal mother to him, it truly makes me proud to be your husband. These have been trying times but I feel confident that we are a better family because of them. I don't know that there are actual words for the depth of gratitude I have toward your never-ending love and support.

Table of Contents

List of Schemes

List of Figures

List of Tables

Chapter 1: Introduction

1.1 Natural Products as a Template to Organic Synthesis

Natural products, also known as secondary metabolites, are organic compounds produced by plants that are not directly part of normal growth, development, or reproduction of the organism.[1] Unlike primary metabolites, the absence of secondary metabolites does not result in immediate death, but rather may in the long term impair the organism's survivability, fecundity, aesthetics, or could in contrast not result in any significant change at all. Plants utilize secondary metabolites for their defense characteristics against herbivorous predators and as interspecies defense strategies, whereas humans have found these compounds to have wide applications in medicinal drugs and food flavorings.[2,3] Throughout history, organic chemists have continued to draw inspiration from natural products as motivation for total synthesis, or the development of new reaction methodology. In 1828 Friedrich Wöhler discovered that urea could be synthesized from the simple inorganic starting materials silver cyanate and ammonium chloride (Figure 1.1.1).[4] This significant finding represented a major milestone in chemistry because it was

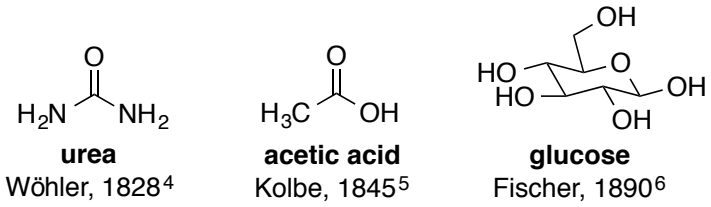

Figure 1.1.1. Selected examples of nineteenth century landmarks in total synthesis.

demonstrated that a substance previously thought to be only a biological product could be synthesized in the lab. The synthesis of acetic acid from elemental carbon by Kolbe in 1845 marked the second major feat in the field of total synthesis, and additionally was the first time the word "synthesis" was used to describe the process of assembling a compound from other substances.[5] Perhaps the most striking and spectacular early total synthesis was that of glucose by

Fischer, not only for its structural complexity, which for the first time included stereogenic centers, but also for the exceptional degree of stereochemical control that accompanied his method.[6] These compounds, although simple and primitive in form, piqued the curiosity of early synthetic chemists and represent the foundations from which the fields of total synthesis and organic reaction methodology were built.

Natural products of significant biological and pharmaceutical importance have been and continue to be a driving force for the development of new organic reaction methodologies to either aid in their total synthesis, or provide a general means to construct an important but challenging aspect of their architecture. For example, the spirocyclopentaneoxindole scaffold is a common structural motif found in a wide variety of biologically active natural products (**1**, **2**, **3**, Scheme 1.1.1), and motivated Kanger and co-workers to develop an organocatalytic cascade reaction of simple isatin derivatives **4** and nitroketones **5** to access the core skeleton **6**.[7] Inspired by the indolizine core being a common structural unit found in many bioactive natural alkaloids (**7-11**, Scheme 1.1.2), Barbas and co-workers utilized a pyrrole enolate intermediate **12** formed *in situ* as an electron donor for the general synthesis of 5,6-dihydroindolizine frameworks **14**.[8] As new natural products continue to emerge with pharmaceutical relevance, organic chemists will be challenged with the task of devising methods to aid in the synthesis of these complex compounds.

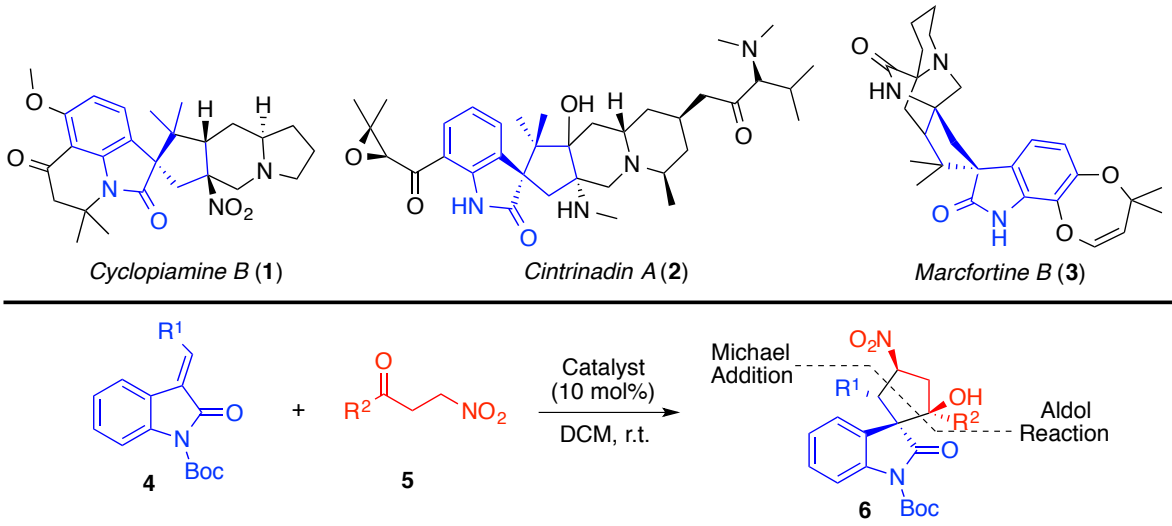

Scheme 1.1.1. Spirocyclopentaneoxindole natural products and organocatalytic cascade reaction.[7]

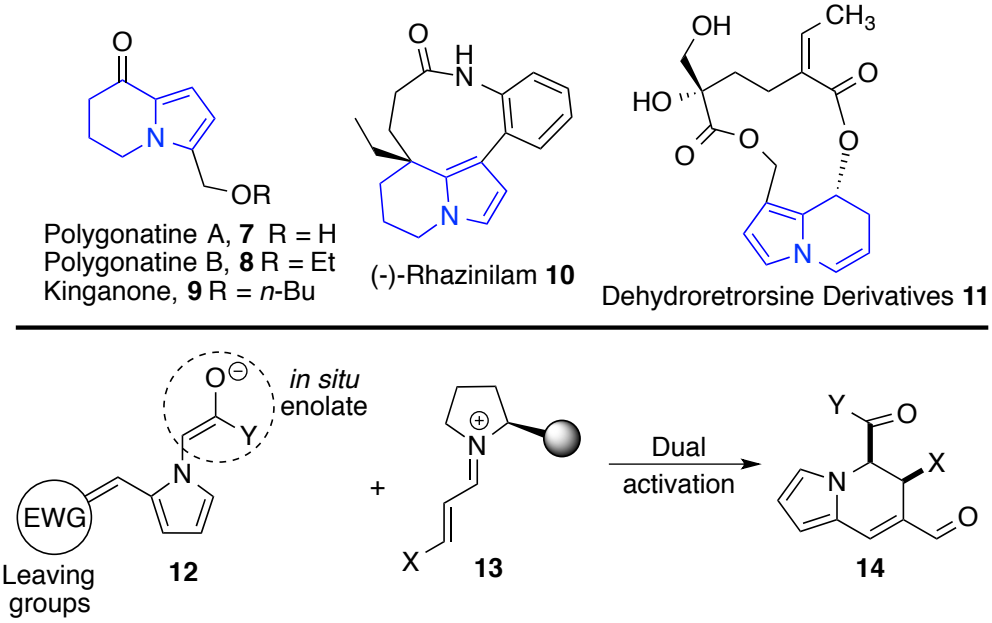

Scheme 1.1.2. Representative hydroindolizine-containing natural and biologically active products. Dual iminium-enolate activated catalytic strategy.[8]

1.2 Heterocycle Synthesis Using Dipolar Aza-Electrophilic Intermediates: Toward New Dipoles for Cycloaddition Reactions

Nitrogen containing heterocycles are a common moiety found in many pharmaceuticals, materials, and natural products. In the last 40 years, the dipolar cycloaddition reaction has been

established as an invaluable method in the synthesis of heterocyclic natural products.[9] Despite extensive research in this area, reactions of dipolar intermediates that feature an electrophilic nitrogen atom at one terminus of the dipole have not been comprehensively explored. Indeed, methods for forming C-N bonds that avoid the use of azides and hydrazine, as well as green souces of electrophilic nitrogen species remain a priority in pharmaceutical manufacturing.[10] Lactams are nitrogen-containing heterocycles that are an important functional group in organic chemistry, and have been widely used in the synthesis of complex molecules, with applications being found in medicinal chemistry and materials research. This structural unit can be found in many natural products and biologically active compounds such as the bengamides **15**, vitronecin antagonist receptors **16**, and tuberostemonone **17** (Figure 1.2.1). With the flexible and direct synthesis of lactams still posing a challenge, it was recognized that a modular and concise synthesis that afforded highly substituted and stereodefined nitrogen heterocycles was needed. We envisioned that the types of compounds in Figure 1.2.1 could be accessed by a hetero [4+3] cycloaddition of an aza-oxyallylic cation intermediate **18** with a diene **19** to give a seven-membered lactam **20**.

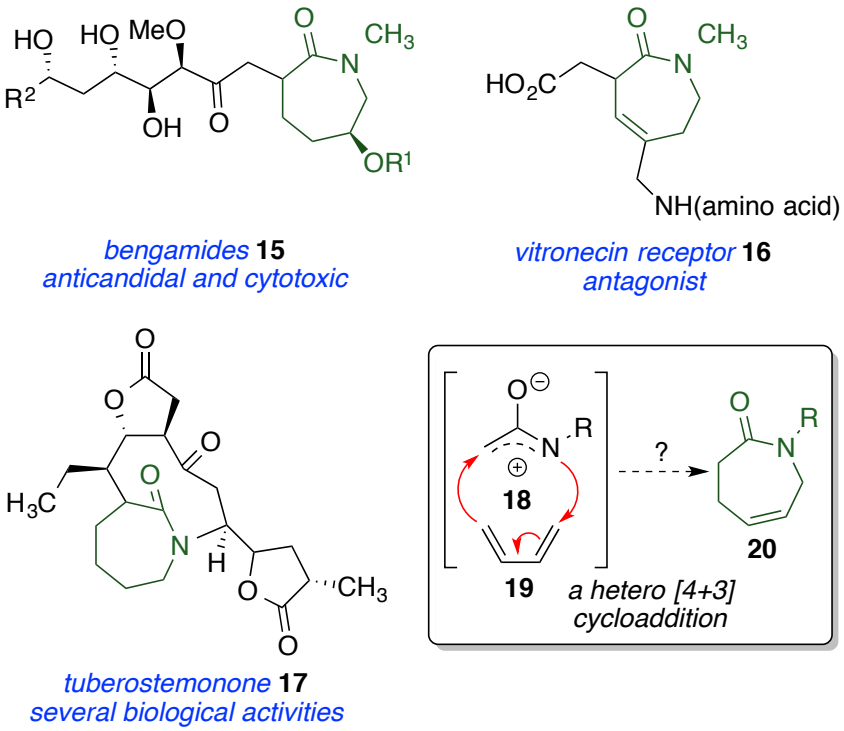

Figure 1.2.1. Representative lactam-containing natural products and proposed access via aza-[4+3] cycloaddition.

If lactam skeletons could be accessed from this intermediate, it would provide insight into novel reactivity as well as entry into several classes of biologically active target compounds. The use of oxyallylic cationic intermediates in [4+3] cycloaddition reactions with dienes has become a powerful method for the construction of seven-membered carbocycles.[11] Our group considered that an analogous aza-oxyallylic cation intermediate could be employed for the synthesis of seven-membered azacycles. The aza-oxyallyic cation intermediate has previously been discussed in the context of α-lactams **21**, namely their synthesis, reactions, and rearrangements (Scheme 1.2.1). Sheehan and Lengyl suggested that these intermediates could possibly be relevant to the regioselectivity trends of the nucleophilic ring opening of α-lactams.[12] Conversely, Stang and Anderson proposed an aza-oxyallylic cation intermediate to be involved in the conversion of an alkylidine oxazirine **22** to an α-lactam.[13] However despite both theoretical and stereochemical studies on the nucleophilic ring opening of alkyl-substituted α-lactams, attempts to trap the

proposed intermediate have failed to provide any experimental and thus compelling evidence for its involvement in these types of processes.[14,15] Base mediated dehydrohalogenation of α-haloketones has been a commonly employed method of generating oxyallylic cation intermediates,[11] therefore we considered that a similar dehydrohalogenation reaction of an α-haloamide **23** could provide an aza-oxyallylic cation intermediate **18** *in situ*. Research efforts towards the exploration of aza-oxyallylic cations as intermediates for heterocycle synthesis are outlined in more detail in Chapter 2.

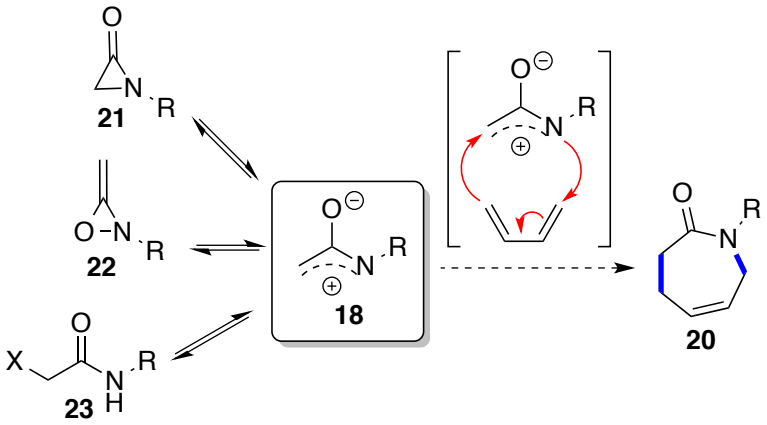

Scheme 1.2.1. Previously proposed methods to access aza-oxyallylic cation intermediate **18**, proposal to trap intermediate with a diene to generate seven-membered heterocycles **20**.

1.3 Balanol and Iminosugars: Target Directed Studies Utilizing Aza-[4+3] Cycloaddition Scaffolds

Recently, there has been a growing recognition of the importance of protein kinase inhibitors and their important role in an variety of cellular events.[16] Although the number of known protein kinases continues to expand, the significance associated with protein kinase C (PKC) has remained incomparable.[17] Phosphorylation of proteins by PKC is known to lead to a number of cell responses including cell proliferation and gene expression.[18] Activated PKC has been associated with a broad range of clinical conditions such as cancer, asthma, HIV,

cardiovascular disorders, inflammation, diabetes, and CNS disfunction.[18] With regard to cancer, the observation that tumor-promoting phorbol esters cause PKC activation has led to the conclusion that PKC inhibitors could prove beneficial in cancer therapy applications. Balanol **24** (Scheme 1.3.1) is a fungal metabolite produced by *Verticillium balanoides* and represents an significant new discovery in the ongoing search for effective PKC inhibitors.[19] Balanol has been observed to inhibit the majority of PKC isozymes in nanomolar concentrations, and its unique novel structure has provided a guiding template in the advancement of new potent and selective PKC inhibitors.[16] The assets of devising a concise and flexible synthesis of balanol and derivatives of balanol include providing understanding into single transduction pathways involving PKC, and also allowing for the discovery of new drug candidates with substantial therapeutic value.[18] The structural features of balanol led us to consider the strategic bond disconnections shown in Scheme 1.3.1. The hexahydroazepine ring could be simplified by removal of the 4-hydroxybenzoic acid residue through the amide bond, and further dissection of the ester linkage would provide the necessary seven-membered heterocyclic core **25**. We envisioned the hexahydroazepine ring **25** to be a reduced form of cycloadduct **27**, with the amine functionality arising from nucleophilic displacement of a leaving group on **26** by nitrogen. Finally, **27** could be formed from the reaction of a simple functionalized α-haloamide **28** and furan **29**. Progress in utilizing simple aza-[4+3] scaffolds toward the synthesis of balanol are described in Chapter 3.

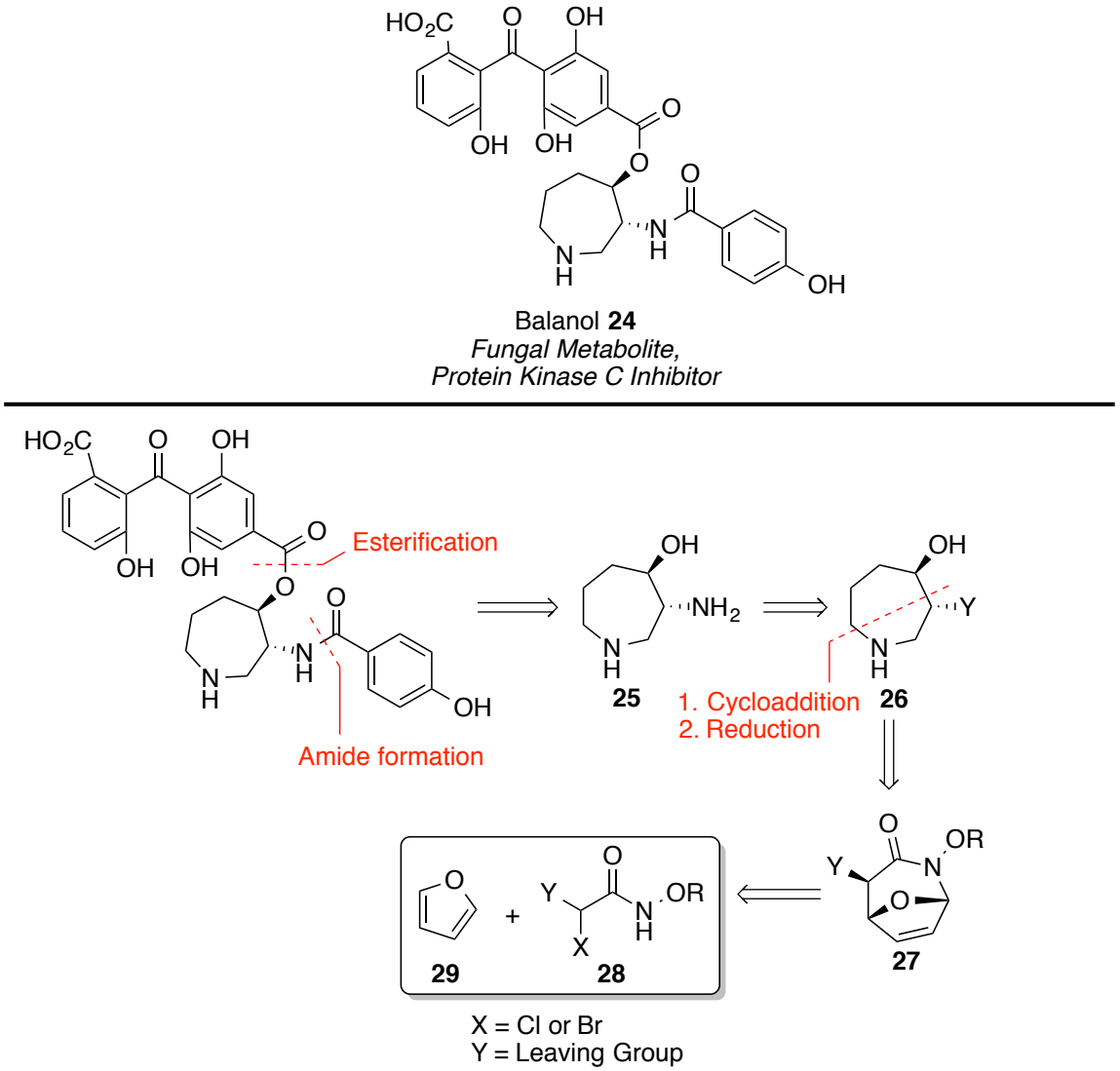

Scheme 1.3.1. Balanol **24** and retrosynthetic analysis to lead back to simple starting materials.

Polyhydroxylated azepanes and piperidines, also referred to as iminosugars, are a class of small organic compounds where the endocyclic oxygen atom has been replaced with a nitrogen atom. Iminosugars have received considerable attention from researchers due to their glycosidase inhibitory properties, which make them good candidates for therapeutic applications in the treatment of HIV, cancer, and diabetes.[20, 21] They occupy a region of space similar to traditional carbohydrates but on the same hand they remain different from other small heterocyclic compounds.[22] On the basis of space, iminosugars provide an opportunity for new drug leads to

complement compound libraries for pharmaceutical companies. As small polar molecules, they resemble carbohydrates enough to allow efficient cellular uptake, but remain chemically distinct enough from traditional sugars to avoid degredation by carbohydrate-modifying enzymes.[23] This "dual personality" allows for iminosugars to serve as a special class of compounds in the ongoing search for new drug targets.[24] Many types of iminosugars exist, both natural and synthetic, and can range from five to seven-membered ring sizes as well as bicyclic systems. Our curiosity was piqued towards the possibility of using aza-[4+3] cycloaddition skeletons to provide a concise and general synthesis of iminosugars (Scheme 1.3.2). We envisioned that polyhydroxylated azepanes **32** (seven-membered iminosugars) and polyhydroxylated piperidines **33** (six-membered iminosugars) could be accessed by simple synthetic manipulations of a richly functionalized cycloadduct **31**. Chapters 3 and 4 provide a detailed description of our synthetic efforts to access the iminosugars class of compounds.

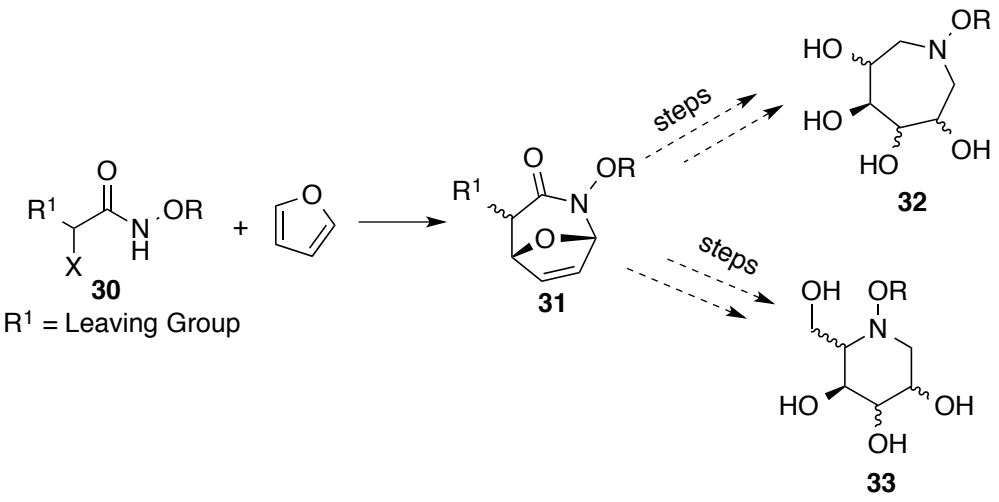

Scheme 1.3.2. Polyhydroxylated azepanes and piperidines through a general aza-[4+3] cycloadduct.

1.4 Alternative Methods for Generating Aza-Oxyallylic Cation Intermediates

Our initial report of the first experimental evidence supporting the existence of aza-oxyallylic cations was centered around base mediated dehydrohalogenation of α-haloamides as a

means of generating the desired intermediates.[28,29] As part of our lab's ongoing interest in electrophilic nitrogen species, we were eager to explore the viability of utilizing other starting materials and alternative methods to generate aza-oxyallylic cations. Chapter 5 details progress toward the alternative generation of aza-oxyallylic cation intermediates beyond our current methodology.

The intriguing properties of aza-oxyallylic cations and the highly functionalized and stereodefined scaffolds they could potentially afford led us to further exploration of these intermediates and their application toward the synthesis of seven-membered heterocycles. This dissertation is divided into four major sections, with additional chapters including an introduction, conclusion, and appendix. Chapter 2 describes our studies on aza-oxyallylic cations and their application for the synthesis of 7-membered heterocycles, and includes computational and experimental results toward developing this new methodology. Chapter 3 highlights our target directed studies on utilizing the aforementioned scaffolds for the synthesis of balanol and polyhydroxylated azepanes. Chapter 4 involves utilizing an unexpected ring contraction to access polyhydroxylated *N*-alkoxypiperidines in good overall yield and high diastereoselectivity. Chapter 5 outlines our work on the exploration of using α-heteroatom substituted amides and alternative methods to generate aza-oxyallylic cations other than dehydrohalogenation of α-haloamides. Finally, Chapter 6 concludes with a general summary and future directions based on the results of this dissertation.

1.5 References

1. Gottfried, F.S. *Science* **1959**, *129*, 1466.
2. Stamp, N. *The Quarterly Review of Biology* **2003**, *79*, 23.
3. Raven, P.H. *Biology of Plants* 6th edn., W.H. Freeman, 1999 ISBN 1 5725 9041 6.
4. Wöhler, F. *Ann. Phys. Chem.* **1828**, *12*, 253.
5. Kolbe, H. *Ann. Chem. Pharm.* **1845**, *54*, 145.
6. Fischer, E. *Ber. Dtsch. Chem. Ges.* **1890**, *23*, 799.
7. Noole, A.; Ilmarinen, K.; Järving, I.; Lopp, M.; Kanger, T. *J. Org. Chem.* **2013**, *78*, 8117.
8. Jiang, X.; Tan, B.; Barbas, C.F. *Angew. Chem. Int. Ed.* **2013**, *52*, 9261.
9. (a) Antiline, J.E.; Hsung, R.P.; Huang, J.; Song, Z.; Li, G. *Org. Lett.* **2007**, *9*, 1275. (b) Huang, J.; Hsung, R.P. *J. Am. Chem. Soc.* **2005**, *127*, 50. (c) Harmata, M.; Ghosh, S.K.; Hong, X.; Wacharasindhu, S.; Kirchhoefer, P. *J. Am. Chem. Soc.* **2003**, *125*, 2058. (d) Walters, M.A.; Arcand, H.R. *J. Org. Chem.* **1996**, *61*, 1478.
10. Constable, D.J.C.; Dunn, P.J.; Hayler, J.D.; Humphrey, G.R.; Leazer, J.L.; Linderman, R.J.; Lorenz, K.; Manley, J.; Pearlman, B.A.; Wells, A.; Zaks, A.; Zhang, T.Y. *Green Chemistry* **2007**, *9*, 411.
11. (a) Lohse, A.G.; Hsung, R.P. *Chem.-Eur. J.* **2011,** *17,* 3812. (b) Harmata, M. *Chem. Commun.* **2010,** 8904. (c) Harmata, M. *Chem. Commun.* **2010,** 8886. (d) Huan, J.; Hsung, R.P. *Chemtracts* **2005,** *18,* 207. (e) Harmata, M. *Adv. Synth. Catal.* **2006,** 2297. (f) Harmata, M. *Acc. Chem. Res.* **2001,** *34,* 595. (g) Cha, J.K.; Oh, J. *Curr. Org. Chem.* **1998,** *2,* 217. (h) Harmata, M. In *Advances in Cycloaddition;* Lautens, M., Ed.; JAI: Greenwich, 1997; Vol. 4, pp 41-86. (i) West, F.G. In *Advances in Cycloaddition;* Lautens, M., Ed.; JAI: Greenwich, CT, 1997; Vol. 4 pp 1-40. (j) Harmata, M. *Tetrahedron* **1997,** *53,* 6235. (k) Padwa, A.; Schoffstall, A. In *Advances in Cycloaddition;* Curran D.P., Ed.; JAI Press: Greeenwich, CT, 1990; Vol. 2, pp1-89. (l)

Harmata, M. *Recent Res. Dev. Org. Chem.* **1997,** *1,* 523. (m) Rigby, J.H.; Pigge, F.C. *Org. React.* **1997,** *51,* 351. (n) Mann, J. *Tetrahedron* **1986,** *42,* 4611. (o) Hoffmann, H.M.R. *Angew. Chem., Int. Ed. Engl.* **1984,** *23,* 1. (p) Hoffmann, H.M.R. *Angew. Chem., Int. Ed. Engl.* **1973,** *12,* 819.

12. Lengyel, I.; Sheehan, J.C. *Angew. Chem. Int. Ed.* **1968**, *7*, 25.
13. Stang, P.J.; Anderson, G.H. *Gazz. Chim. Itl.* **1995**, *125*, 329.
14. Tantillo, D.J.; Houk, K.N.; Hoffman, R.V.; Tao, J. *J. Org. Chem.* **1999**, *64*, 3830.
15. Hoffman, R.V. In *The Amide Linkage: Selected Structural Aspects in Chemistry, Biochemistry, and Material Science;* Greenberg, A.; Breneman, C.M., Liebman, J.F., Eds.; John Wiley & Sons Inc.: New York, 2000; p 137.
16. Nicolaou, K.C.; Koide, K.; Bunnage, M.E. *Chem. Eur. J.* **1995**, *1*, 455.
17. (a) Newton., A.C. *Annu. Rev. Eiophys. Eiomol. Srrucr.* **1993**, *22*, 1. (b) Farago, A.; Nishizuka, Y. *FEBS Lett*. **1990,** *268*, 350. (c) Stabel, S.; Parker, P.J. *Pharmac. Ther.* **1991**, *51*, 71. d) Nishizuka, Y. *Nature* **1988**, *334*, 661. (e) Nishizuka, Y. *Science* **1986**, *233*, 305. (f) Nishizuka, Y. *Nature* **1984**, *308*, 693. (g) Nishizuka, Y. *Science* **1992**, *258*, 607.
18. Bradshaw, D.; Hill, C.H.; Nixon, J.S.; Wilkinson, S.E. *Agents Actions* **1993**, *38*, 135.
19. (a) Kulanthaivel, P.; Hallock, Y.F.; Boros, C.; Hamilton, S.M.; Janzen, W.P.; Ballas, L.M.; Loomis, C.R.; Jiang, J.B.; Katz, B.; Steiner, J.R.; Clardy, J. *J. Am. Chem. Soc.* **1993**, *115*, 6452. (b) Ohshima, Y.; Yanagisawa, M.; Katoh, A.; Fujii, T.; Sano, T.; Matsukuma, S.; Furumai, T.; Fujiu, M.; Watanabe, K.; Yokose, K.; Arisawa, M.; Okuda, T. *J. Antibiot.* **1994**, *47*, 639.
20. Davis, B.G. *Tetrahedron: Asymmetry* **2009**, *20*, 652.
21. Winchester, B.G. *Tetrahedron: Asymmetry* **2009**, *20*, 645.

22. Horne, G.; Wilson, F.X.; Tinsley, J.; Williams, D.H.; Storer, R. *Drug Discovery Today* **2011**, *16*, 107.

23. Mellor, H.R. *Biochem. J.* **2004**, *381*, 861.

24. D'Alonzo, D. *Curr. Med. Chem.* **2009**, *16*, 473.

25. Baliah, V.; Jeyraman, R.; Chandrasekaran, L. *Chem. Rev.* **1983**, *83*, 379.

26. (a) Laschat, S.; Dickner, T. *Synthesis* **2000**, *13*, 1781. (b) Bates, R.W.; Sa-Ei, K. *Tetrahedron* **2002**, *58*, 5957.

27. Buffat, M.G.P. *Tetrahedron* **2004**, *60*, 1701.

28. Jeffrey, C.S.; Barnes, K.L.; Eickhoff, J.E.; Carson, C.R. *J. Am. Chem. Soc.* **2011**, *133*, 7688.

29. Barnes, K.L.; Koster, A.K.; Jeffrey, C.S. *Tetrahedron Lett.* **2014**, *55*, 4690.

Chapter 2: Generation and Reactivity of Aza-Oxyallylic Cations: Aza-[4+3] Cycloaddition Reactions for Heterocycle Synthesis

2.1 Introduction

The aza-oxyallylic cation is a reactive intermediate that has eluded chemists for decades, with its existence only being hypothesized but never proven with experimental evidence. The Jeffrey lab's interest in the generation of electrophilic nitrogen species piqued our curiosity towards exploring this intermediate and its potential use for the rapid synthesis of 7-membered aza-cycles. The proposal to intercept the aza-oxyallylic cation **45** was largely inspired by the comprehensive body of work related to oxyallylic cation intermediates (**46**, Scheme 2.1.1) and their reactivity in [4+3]-cycloaddition reactions with dienes to form 7-

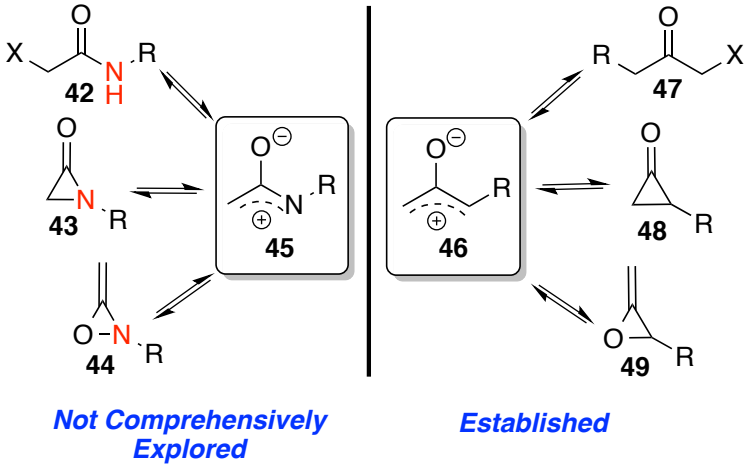

Scheme 2.1.1. Established methods to access oxyallylic cation intermediate and the analogous underexplored aza-oxyallylic cation equilibrium.

membered rings.[1] More specifically, we envisioned a base-mediated dehydrohalogenation event of an α-halo amide **42** as a way to generate the desired intermediate, much in the same way that the dehydrohalogenation process of α-halo ketones **47** to give oxy-allyl cations **46**.[1] With the larger goal of developing new C-N bond forming reactions with broad applications in target directed syntheses, we envisioned that cycloadditions of aza-oxyallylic cations could be employed as a powerful method to prepare nitrogen-containing seven-membered heterocycles.

Trapping or even establishing the existence of the aza-oxyallylic cation has been a long road and was not a novel idea when we began experimenting with the intermediate. The aza-oxyallylic cation **45** was first proposed by Sheehan in the 1960s during his foray into the chemistry of α-lactams such as **43** (Scheme 2.1.1).[2] The first α-lactam to be isolated and characterized was synthesized in 1962 by Baumgarten.[3] Prior to this, α-lactams were believed to be intermediates in a variety of reactions, but it was still unknown if the 3-membered ring would encumber too much ring strain to permit isolation. Building on the work of Baumgarten, Sheehan and Lengyel observed that the stability of the α-lactams was enhanced by the presence of a *tert*-butyl group or other bulky substituent on the nitrogen atom.[2] Despite this general trend however, attempted syntheses of α-lactams with bulky phenyl substituents on the nitrogen atom were surprisingly unsuccessful. Sheehan hypothesized that charge delocalization through the phenyl rings made possible a highly reactive acyclic intermediate **45** (an aza-oxyallylic cation) that was more stable than the corresponding α-lactam **43** he was trying to synthesize, but was not isolable.[2] Sheehan also suggested the involvement of this dipolar intermediate in the thermal decomposition of some α-lactams and their nucleophilic ring opening. Following the analogy of the oxyallylic cation in the Favorskii rearrangement previously described by House and Gilmore,[4] Sheehan did not rule out the possibility of an analogous dipolar aza-oxyallylic cation intermediate in the nucleophilic substitution reaction of isolable α-lactams. Moreover, the proposed intermediate could explain the dichotomous C-2 versus C-3 nucleophilic ring opening of this highly reactive aza-cycle (Scheme 2.1.2).

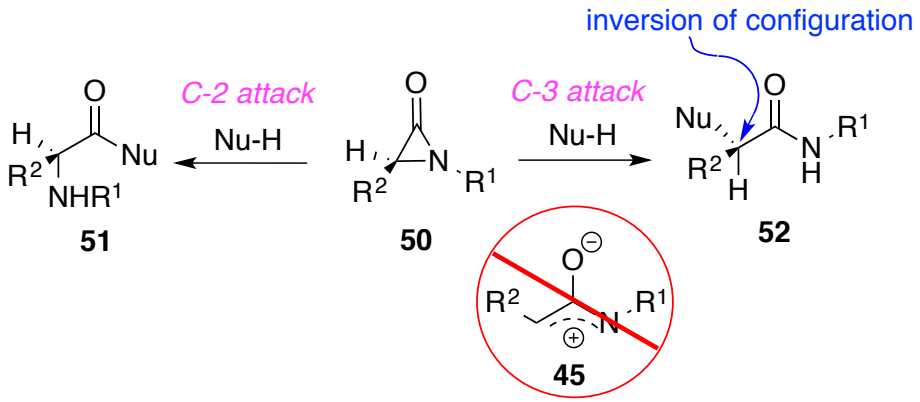

Scheme 2.1.2. The stereospecific nucleophilic ring opening of enantiopure α-lactams to give products **51** and **52**.

The proposal of Sheehan and Lengyel along with the ambivalent reactivity of α-lactam electrophiles **50** stimulated numerous theoretical and mechanistic studies of their nucleophilic ring opening.[5] While it remained difficult to predict whether nucleophilic attack would be favored at the C-2 or C-3 position of the lactam **50**, an elegant set of experiments by Hoffman and co-workers using enantiopure α-lactams **50** established that attack at the C-2 position consistently produced an amino acid derivative **51** with retention in stereochemistry, while attack at the C-3 position produced an amide **52** with inversion of stereochemistry (Scheme 2.1.2).[5] The stereospecificity of the reaction at C-3 was inconsistent with the formation of a planar aza-oxyallylic cation intermediate, which instead would have resulted in product racemization. Several other research groups also suggested the role of the aza-oxyallylic cation as an intermediate or transition state in transformations involving α-lactams α-haloamides, and related species. In 1955, Stang and Anderson proposed an aza-oxyallylic cation intermediate in their studies of the interactions of alkylidene carbenes with nitroso compounds.[6] In 2004, Toscano and co-workers performed a computational study that illustrated an aza-oxyallylic cationic transition state in their isomerization studies of the conversion of an alkylidene oxazirine **44** to the α-lactam (Scheme 2.1.1).[7] Despite all of these hypotheses however, the intermediacy of an aza-oxyallylic cation was yet to be experimentally supported.

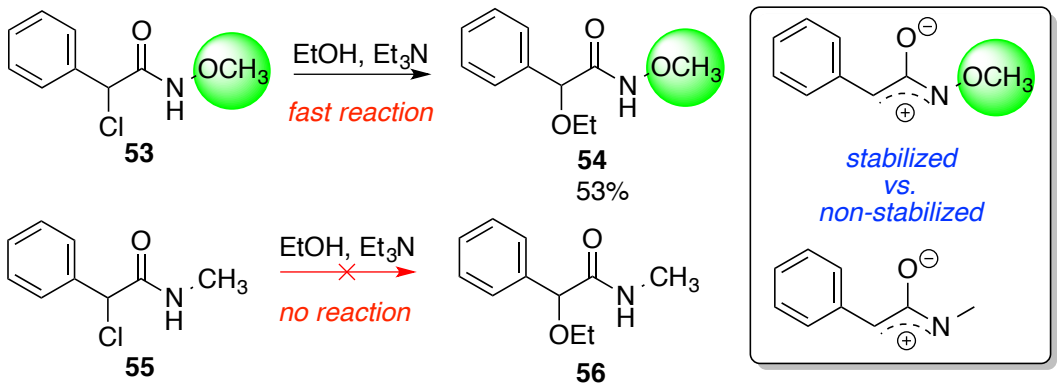

Scheme 2.1.3. The solvolysis experiment of Kikugawa and co-workers that highlights the importance of a donor group in the possible strategy for stabilizing aza-oxyallylic cations.

The most promising evidence of the viability of an aza-oxyallylic cation intermediate came from the Kikugawa group in 1993.[8] A series of solvolysis experiments on α-haloamides **53** and **55** demonstrated the importance of an alkoxy donor group on the nitrogen atom (Scheme 2.1.3). They observed that the 2-chloro-*N*-alkoxyphenylacetamide **53** underwent rapid solvolysis when treated with a base in ethanol to provide the amide **54**; however, no reaction was observed when the *N*-methylamide **55** was subjected to the same conditions. This result implied that the alkoxy-substituent in **53** could stabilize a pathway through a highly electrophilic aza-oxyallylic cation, thereby accelerating the rate of solvolysis of the *N*-methoxyphenylacetamide **53**. Coupled with the previously described reports of an increase in the stability of oxyallylic cations and *N*-acyl nitrenium ions[9] with the addition of an alkoxy donor group, the Kikugawa experiment led us to believe that an electron-donating substituent could potentially stabilize an aza-oxyallylic cation intermediate and give it enough of a lifetime to react with a diene in a [4+3]-cycloaddition reaction (Scheme 2.1.4).

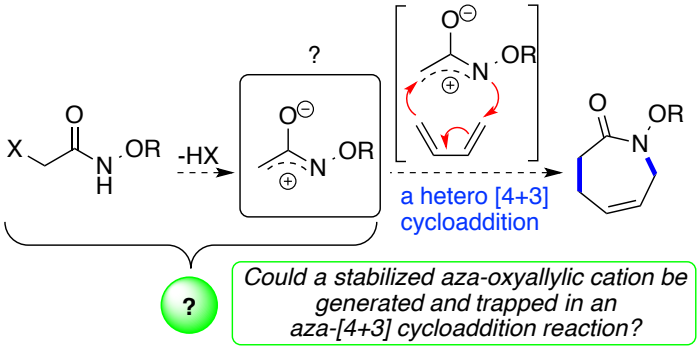

Scheme 2.1.4. Proposed aza-[4+3] cycloaddition reaction of a stabilized aza-oxyallylic cation with a diene.

One of the primary methods of generating oxyallylic cations for [4+3]-cycloadditions is through the dehydrohalogenation of α-haloketones.[1] The first example of such a reaction was reported by Fort in 1962.[9] In this experiment, Fort reacted α-chlorodibenzylketone with furan in the presence of a base to yield a 7-membered carbocycle with a bridging oxygen atom. Hoffman continued work in this area, pioneering much of the chemistry surrounding the synthesis of 7-membered rings through the reaction of allyl cations with dienes.[10] In 1965, Woodward and Hoffman published a Letter proposing that a concerted cycloaddition reaction of a diene and an allyl cation was thermally allowed by orbital symmetry.[11] To support his theory, Hoffman published the first example of such a reaction in 1968.[12] Following Hoffman's work, numerous examples of [4+3]-cycloaddition reactions through oxyallylic cations have been reported.[1] Strategic incorporation of electron-donating groups such as nitrogen,[13] oxygen,[14] or sulfur,[15] on the dienophile have been shown to facilitate [4+3]-cycloaddition reactions of oxyallylic cations through the extra stability afforded to the intermediate. It was this very simple but thus far overlooked observation that led us to the capture of the aza-oxyallylic cation. The difference between the aza-oxyallylic cation and the oxyallylic cation is, of course, the replacement of a carbon atom with a more electronegative nitrogen atom.

2.2 Preliminary Computational Studies of Stabilized Aza-Oxyallylic Cations

Initial studies of stabilized aza-oxyallylic cations began by computationally modeling our hypothesis.[16] Two α-lactams, one *N*-substituted with an ethyl group **57**, and one *N*-substituted with a methoxy group **58** (Figure 2.2.1) were chosen as model systems. The relaxed potential energy plot for the heterolytic cleavage of the C(2)-N bond of each α-lactam to an aza-oxyallylic cation **59** in methanol was predicted using a B3LYP/6-31G* level of theory with a conductor polarized continuum model (CPCM)[17] to simulate solvent effects.[18,19]

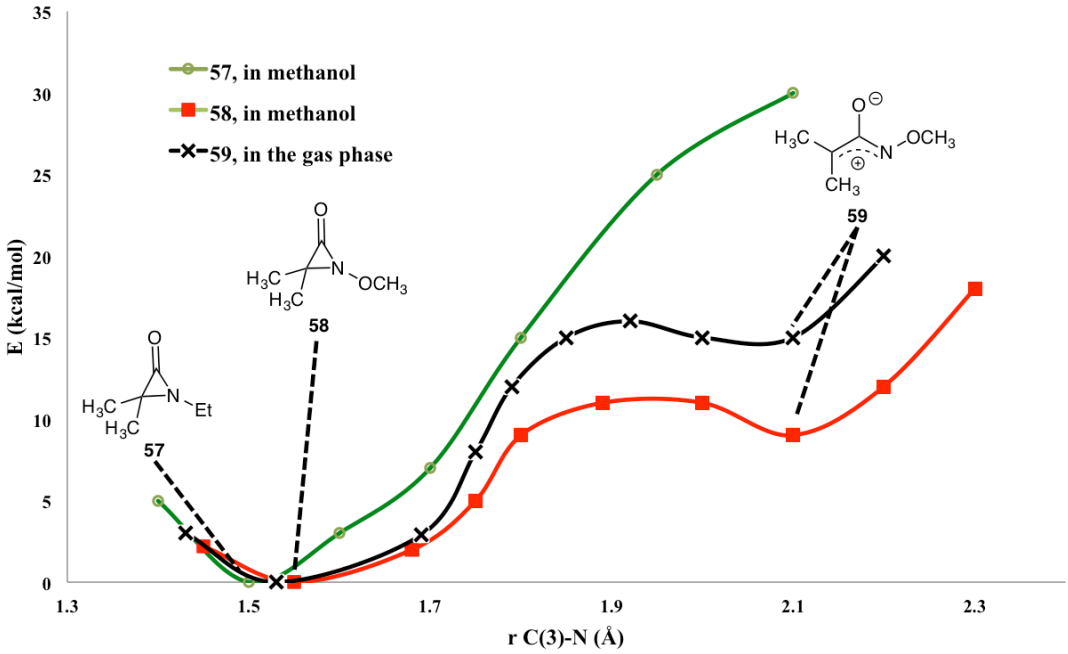

Figure 2.2.1. Relaxed potential energy scans along the C(3)-N(1) coordinate of α-lactams **57** and **58**. Green line = **57** in methanol, red line = **58** in methanol, black line = **59** in the gas phase.

As expected, the ethyl-substituted α-lactam **57** did not arrive at a second energy minimum corresponding to the aza-oxyallylic cation intermediate. However, the α-lactam with a strongly electron-donating methoxy substitutent **58** showed that the aza-oxyallylic cation **59** was in a second energy minimum, consistent with our hypothesis and with Kikugawa's solvolysis experiments. Comparison of isomerization in the gas phase and in methanol for the methoxy α-lactam demonstrated qualitative differences in the well depth for the intermediate

59. According to these calculations, the aza-oxyallylic cation intermediate was more stable in a polar solvent than in the gas phase, which was consistent with the proposed zwitterionic structure of an aza-oxyallylic cation intermediate.

2.3 Preliminary Experimental Studies of the Reaction of Stabilized Aza-Oxyallylic Cations with Furan

Experimentally, our investigation began with synthesizing 2-bromo-*N*-benzylbutyramide **60** from the corresponding acid bromide and benzylamine (Scheme 2.3.1). As expected for the reaction of an α-haloamide lacking a donor group, treatment of this substrate with a base in the presence of furan as the diene and trifluoroethanol (TFE) as the solvent only resulted in recovery of the starting material. To test our hypothesis of a donor group being crucial for stabilizing the desired intermediate, a 2-bromohydroxamate **62** was synthesized from again the corresponding acid bromide but this time *O*-benzylhydroxylamine. Treatment of **62** to the Föhlisch conditions[20] provided the desired cycloadduct **63** and trifluoroether **64**, providing the first example of a reaction of an aza-oxyallylic cation with a diene.

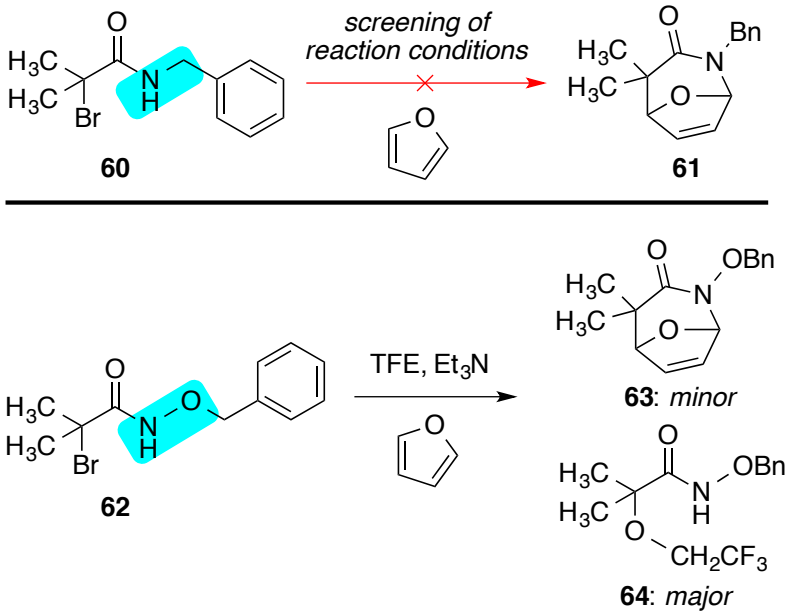

Scheme 2.3.1. First example of an aza-[4+3] reaction and a control experiment that demonstrates the importance of an alkoxy donor group.

2.4 The Aza-[4+3] Cycloaddition Reaction as a New Method for the Synthesis of Caprolactams

Initial optimization studies were aimed at minimizing the solvolysis product **64** and thereby increase the yield of the cycloadduct. Switching to the bulkier hexafluoroisopropanol solvent was found to circumvent solvolysis and provide the desired product in 78% yield.[21] Carbonate bases were found to provide the desired cycloadduct in comparable yields to the reaction using triethylamine (entries 4-6, Table 2.4.1). The reaction could also be effected in ether by using triethylamine with lithium perchlorate as a Lewis acid additive,[22] but under these reaction conditions a methacrylamide was isolated as the major product from elimination of the cationic intermediate or a transient α-lactam.

Table 2.4.1. Solvent and Base Effects on the Yield of the Aza-[4+3] Reaction of 62 with Furan

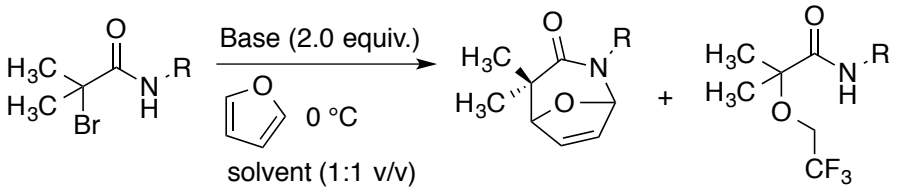

60: R = Bn
62: R = OBn

61: R = Bn
63: R = OBn

64: R = OBn

Entry	R	Solvent	Base	Yield[a] %
1	**Bn**	**TFE**	**Et_3N**	**no reaction**
2	OBn	TFE	Et_3N	38%[b]
3	OBn	HFIP	Et_3N	78%
4	OBn	HFIP	Cs_2CO_3	58%
5	OBn	HFIP	K_2CO_3	67%
6	OBn	HFIP	Na_2CO_3	74%
7	OBn	TFE	imidazole	decomp.
8	OBn	TFE	pyridine	no reaction
9	OBn	Et_2O	Et_3N, $LiClO_4$	See text

[a]Isolated yield of **63**. [b]Provided a 56% yield of **64**.

The aza-[4+3] cycloaddition reaction was found to be general, providing the desired cycloadducts in good to excellent yields with a variety of alkyl and halo substrates substituted at the α-carbon (Table 2.4.2). Monoalkyl stubstituted bromo amides (entries b-f) provided the highest yields of the cycloadduct, and all monoaryl and monoalkyl haloamides selectively demonstrated a preference for the *endo*-diastereoisomer ($\geq$ 19:1).[23] In the case of entry f, it was observed that the ratio of diastereoisomers at about 40% conversion was $\geq$ 19:1 *endo:exo*, but upon complete consumption of the starting material equilibrated to a ratio of 2:1 *endo:exo*. Monoalkyl bromoamides were found to react slower than aryl and dialkyl substituted haloamides, and α-chloroamides reacted slower than α-bromoamides (*cf.* b and e). α -Chloromethoxyacetamide proved difficult to handle and decomposed under the cycloaddition conditions, and the unsubstituted bromoacetamide (X = Br, $R^1 = R^2 = H$, entry a) was unreactive and resulted in recovery of the starting material. Dialkyl and aryl substrates provided the desired cycloadduct in moderate yields when run in HFIP (entries h, i, and l). Cyclopentadiene was also found to be a viable diene for the [4+3] cycloaddition, affording the cycloadducts in comparable yields to those of furan, albeit with less selectivity for the *endo* diastereoisomer (entries j-l). As mentioned previously for the case of the α,α-dichloroamide substrate, the ratio of diastereoisomers at early conversion ($\geq$ 19:1, *endo:exo* at *ca.* 40%) was greater than at complete conversion (2:1, *endo:exo*). In order to gain more insight on this observation, the purified *endo* cycloadduct was resubjected to the reaction conditions. After 24 hours, it was found that the *endo* cycloadduct had equilibrated to a 1:1 mixture of diastereoisomers, suggesting that there is a kinetic preference for the *endo*-product. The exact nature of this selectivity is a project still under investigation.

Table 2.4.2. Evaluation of the Substrate Scope of the Aza-[4+3] Reaction

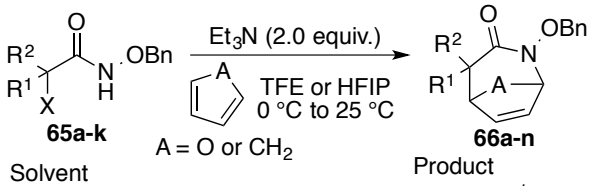

Entry	Solvent Reaction Time	Substrate	Product dr (endo:exo)[b]	Yield[c]
a b c d	TFE 16 h	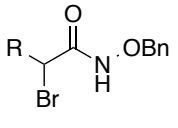	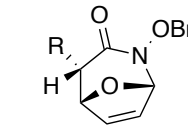 dr ≥ 19:1 (endo:exo)	R = H (0%) R = Me (67%) R = Et (86%) R = *t*Bu (54%)
e	TFE 48 h	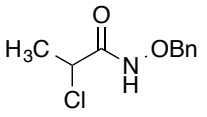	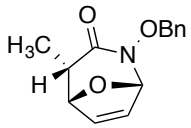 dr ≥ 19:1 (endo:exo)	78%
f	TFE 72 h	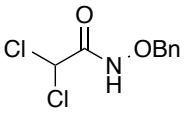	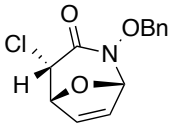 dr = 2:1 (endo:exo)	73%
g	TFE 1h	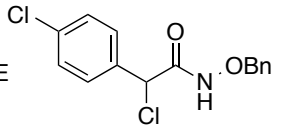	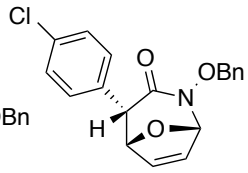 dr ≥ 19:1 (endo:exo)	52%
h	HFIP 30 min	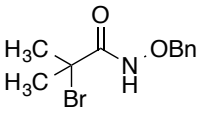	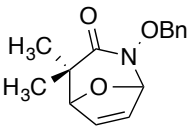	78%
i	HFIP 30 min	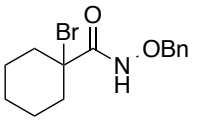	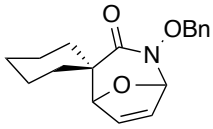	65%
j	TFE 16 h	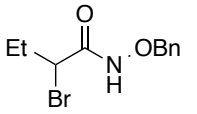	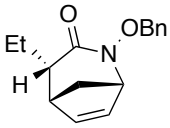 dr = 3:1 (endo:exo)	85%
k	TFE 16 h	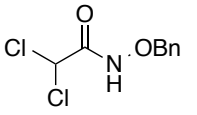	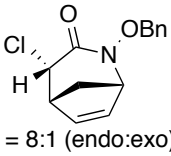 dr = 8:1 (endo:exo)	64%
l	HFIP 30 min	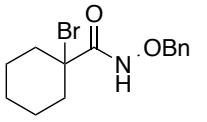	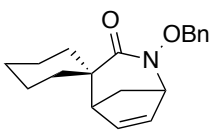	81%

[a]Conditions: solvent was furan or cyclopentadiene (1:1 v/v, 0.25 M) at 0 to 25 °C with Et_3N (2.0 equiv.). Diastereoisomeric ratio (dr) was determined from crude ^1H NMR analysis. [b] ≥ 19:1 dr indicates that the minor diastereoisomer was not detected. [c]Isolated yield of both diastereoisomers.

The experimental and computaional data support a mechanism whereby dehydrohalogenation of an α-haloamide **67** under basic conditions generates an aza-oxyallylic cation intermediate **68** that reacts as a dienophile in an aza-[4+3] cycloaddition (Scheme 2.4.1). An alkoxy electron donating group (OBn) is essential for allowing the cycloaddition to take place, and was computationally found to stabilize the proposed intermediate. Aryl substituents accellerate the overall rate of conversion. In conjunction with the all-carbon [4+3] cycloaddition with cyclic dienes, the aza-[4+3] cycloaddition demonstrates a preference for the formation of the *endo* diastereoisomer. The observation that the diastereoisomeric ratio of cycloadducts (entry f, Table 2.4.1) was high at early conversion and that the purified *endo*-adduct isomerized to a 1:1 ratio of diastereoisomers (**69**-*endo* to **69**-*exo*, R = Cl, Scheme 2.4.1) under the reaction conditions suggests that there is a kinetic preference for the *endo*-cycloadduct.

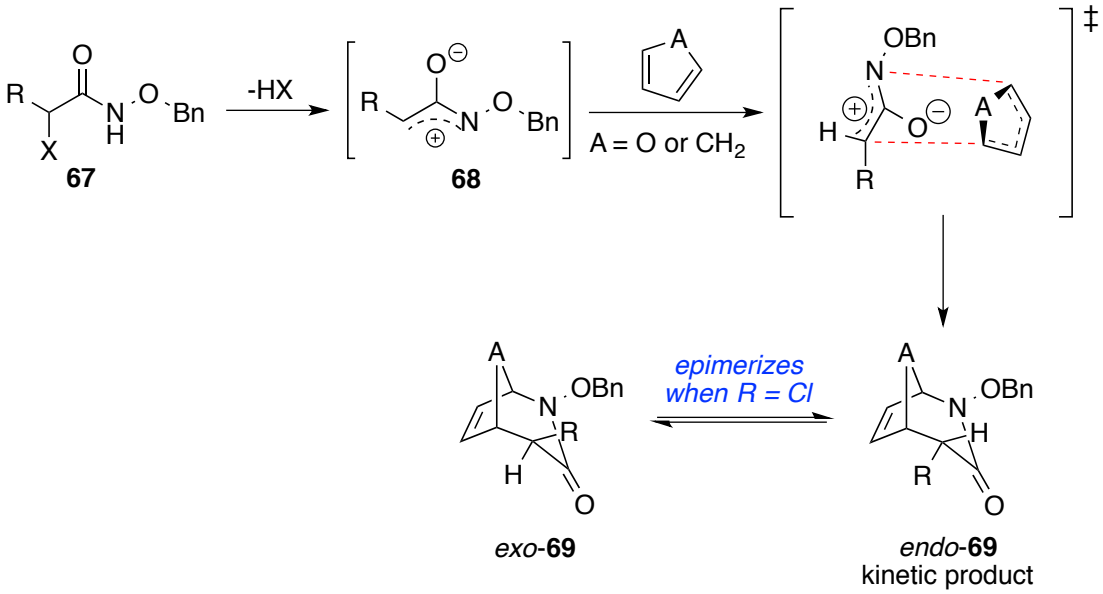

Scheme 2.4.1. Proposed mechanism for the aza-[4+3] cycloaddition reaction with furan (A = O) and cyclopentadiene (A = CH_2).

2.5 Experimental

All reactions were carried out under an atmosphere of nitrogen in oven-dried glassware with magnetic stirring, unless otherwise specified. Dichloromethane was purified by passage through a bed of activated alumina. Cyclopentadiene was distilled from dicyclopentadiene immediately prior to use. All other reagents and solvents were purchased from Sigma-Aldrich Chemical Company and used without any further purification. TLC information was recorded on Silicycle glass 60 F254 plates and developed by staining with $KMnO_4$ or ceric ammonium molybdate. Purification of reaction products was carried out by flash chromatography using Silicycle Siliaflash® P60 (230-400 mesh). ^{1}H-NMR spectra were measured on Varian 400 (400 MHz), Varian MR400 (400 MHz), or Varian 500 (500 MHz) spectrometers and are reported in ppm (s = singlet, d = doublet, t = triplet, q = quartet, m = multiplet, br = broad; integration; coupling constant(s) in Hz), using TMS as an internal standard (TMS at 0.00 ppm) in $CDCl_3$ or the solvent peak (1.94 ppm) in CD_3CN. ^{13}C-NMR spectra were recorded on V400 or V500 spectrometer and reported in ppm using solvent as an internal standard ($CDCl_3$ at 77.16 ppm) or (CD_3CN at 118.26 ppm). Infrared (IR) spectra were recorded on a Nicolet 6700 FT-IR with a diamond ATR and data are reported as cm^{-1} (br = broad, st = strong). High-resolution mass spectra were obtained using an Agilent 6230 TOF LC/MS with an (atmospheric pressure photo- ionization (APPI) or electrospray (ESI) source with purine and HP-0921 as an internal calibrants. Haloamides HRMS were obtained with an inlet temperature of 200 °C.

General Procedure A: For the synthesis of alpha-haloamides

To a suspension of the *O*-benzylhydroxylamine hydrochloride in dichloromethane (0.25 M) and triethylamine was added the alpha-haloacid halide dropwise at 0 °C. The reaction mixture was stirred at that same temperature until TLC analysis (3:1 hexanes:ethyl acetate) revealed complete consumption of the starting material. The mixture was then warmed to room temperature and quenched with water. The aqueous phase was extracted 3x with dichloromethane and the combined organic extracts were washed with water, brine, and

dried over anhydrous sodium sulfate. The solvent was removed under reduced pressure and the crude residue was purified by column chromatography (3:1 hexanes:ethyl acetate) to afford the pure haloamides in 45 – 90% yield as white crystalline solids.

General Procedure B: For the cycloaddition reaction of furan or cyclopentadiene in trifluoroethanol or hexafluoroisopropanol.

To a solution of the haloamide (1 equiv.) in CF_3CH_2OH and furan [1:1 (v/v) 0.25 M] or $(CF_3)_2CHOH$ was added triethylamine (2 equiv.) dropwise at 0 °C. The solution was then allowed to warm to room temperature and the reaction progress monitored by TLC (3:1 or 2:1 hexanes:ethyl acetate) until complete consumption of the haloamide. The volatiles were removed under reduced pressure and the crude residue purified by flash column chromatography (4:1 to 3:1 hexanes:ethyl acetate) to afford the pure cycloadducts as oils (54 – 85% yield).

2-bromo-2-methyl-*N*-(phenylmethyl)propanamide (60):

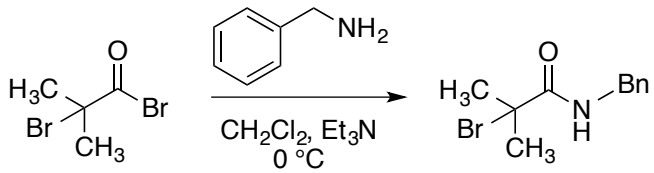

Prepared in 91% yield (0.42 mmol, 10.7 g) from the reaction of 2-bromo-2-methylpropanoyl bromide (0.46 mmol, 10.6 g) with benzylamine (0.46 mmol, 5.1 mL) via general procedure A. R_f = 0.84 (3:1 hexanes:ethyl acetate); M.P. = 73.4 – 75.5 °C; ^{1}H NMR (400 MHz, $CDCl_3$): δ 7.41 – 7.23 (m, 5H), 7.03 (br s, 1H), 4.46 (d, J = 5.8 Hz, 2H), and 1.99 (s, 6H); ^{13}C NMR (125 MHz, $CDCl_3$): δ 172.0, 137.8, 128.8, 127.6, 62.8, 44.4, and 32.6; IR (neat) 3291 (br), 3065, 3014, 3008, 2938, 2919, 1642 (st), and 1533 cm^{-1}; HR-ESIMS requires for $C_{11}H_{15}BrNO$ $(M+H)^+$ 256.0332, found 256.0329.

2-bromo-2-methyl-*N*-(phenylmethoxy)propanamide (62, 65h):

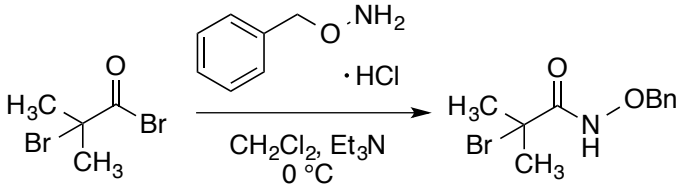

Prepared in 87% yield (11.3 mmol, 3.53 g) from the reaction of 2-bromo-2-methylpropanoyl bromide (13 mmol, 3.0 g) with *O*-benzylhydroxylamine hydrochloride (13 mmol, 2.13 g) via general procedure A. R_f = 0.58 (3:1 hexanes:ethyl acetate); M.P. = 88.6 – 91.1 °C; ^{1}H NMR (500 MHz, $CDCl_3$): δ 9.05 (br s, 1H), 7.45 – 7.34 (m, 5H), 4.94 (s, 2H), and 1.93 (s, 6H); ^{13}C NMR (126 MHz, $CDCl_3$): δ 169.7, 134.9, 129.6, 129.1, 128.8, 78.4, 59.5, and 32.6; IR (neat) 3195 (br), 3034, 2954, 2890, 1652 (st), 1505, 1469, 1454, 1112, 1032, and 1004 cm^{-1}; HR-ESIMS requires for $C_{11}H_{18}BrNO_2$ $(M+NH_4)^+$ 289.0546, found 289.0543.

(±)-2-bromo-*N*-(phenylmethoxy)propanamide (65b):

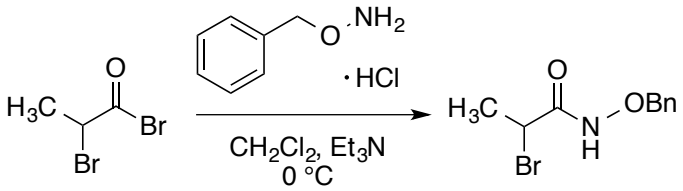

Prepared in 53% yield (631 mg, 2.44 mmol) from the reaction of 2-bromo-2-methylpropanoyl bromide (1.0 g, 4.6 mmol) with *O*-benzylhydroxylamine hydrochloride (742 mg, 4.6 mmol) via general procedure A. R_f= 0.28 (3:1 hexanes:ethyl acetate); M.P. = 75.3-77.4 °C; ^{1}H-NMR (500 MHz, $CDCl_3$): δ 9.61 (br s, 1H), 7.44 – 7.26 (m, 5H), 4.90 (s, 2H), 4.31 (q, *J* = 7.7 Hz, 1H), and 1.77 (d, *J* = 6.4 Hz, 3H); ^{13}C-NMR (126 MHz, $CDCl_3$): δ 167.5, 134.8, 129.45, 128.9, 128.7, 78.3, 40.5, and 22.2; IR (neat) 3110 (br), 2924, 2852, 1675 (st), 1508, 1495, 1453, 1364, 1188, 1038, and 1023 cm^{-1}; HR-ESIMS requires for $C_{10}H_{12}BrNO_2$ $(M+H)^+$ 259.1225, found 259.1222.

(±)-2-bromo-*N*-(phenylmethoxy)butanamide (65c):

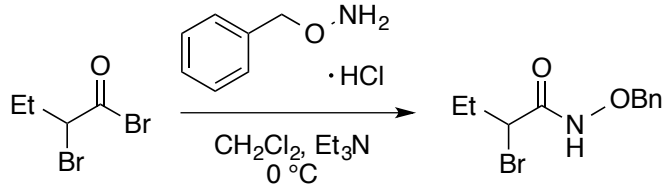

Prepared in 72% yield (4.71 g, 17.3 mmol) from the reaction of 2-bromobutyryl bromide (5.0 g, 24 mmol) with *O*-benzylhydroxylamine, hydrochloride via general procedure A. R_f = 0.49 (3:1 hexanes:ethyl acetate); M.P. = 99.3 - 101.6 °C; ^{1}H-NMR (500 MHz, $CDCl_3$): δ 8.92 (br s, 1H), 7.52 – 7.31 (m, 5H), 4.93 (s, 2H), 4.12 (app q, *J* = 7.2 Hz 1H), 2.02 - 1.94 (m, 2H), and 1.00 (t, *J* = 7.0 Hz, 3H); ^{13}C-NMR (126 MHz, $CDCl_3$): δ 166.6, 134.8, 129.5, 129.0, 128.7, 78.4, 48.8, 28.8, and 11.8; IR (neat) 3112, 2963, 2933, 2874, 1695, 1668 (s), 1528, 1496, 1454, 1364, 1177, 1089, 1023 cm^{-1}; HR-ESIMS requires for $C_{11}H_{15}BrNO_2$ $(M+H)^+$ 256.0332, found 256.0329.

(±)-2-bromo-2,2-dimethyl-*N*-(phenylmethoxy)butanamide (65d):

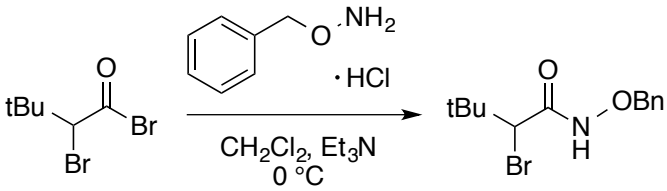

Prepared in 61% yield (11.8 mmol, 3.5 g) from the reaction of 2-bromo-2,2-dimethylpropanoyl chloride (19.3 mmol, 4.98 g) with *O*-benzylhydroxylamine (19.3 mmol, 3.12 g), hydrochloride via general procedure A. R_f = 0.33 (3:1 hexanes:ethyl acetate); ^{1}H-NMR (500 MHz, $CDCl_3$): δ 8.73 (br s, 1H), 7.55 – 7.29 (m, 4H), 4.92 (s, 2H), 3.95 (s, 1H), 1.11 (s, 9H); ^{13}C-NMR (126 MHz, $CDCl_3$): δ 166.1, 135.0, 129.6, 129.0, 128.8, 78.3, 59.4, 35.2, and 27.4; IR (neat): 3179 (br), 3037, 2985, 2960, 2944, 2885, 1657 (st), 1511, 1479, 1371, 1241, 1159, 1052 cm^{-1}; HR-ESIMS requires for $C_{13}H_{19}BrNO_2$ $(M+H)^+$ 300.0594, found 300.0595.

(±)-2-chloro-*N*-(phenylmethoxy)propanamide (65e):

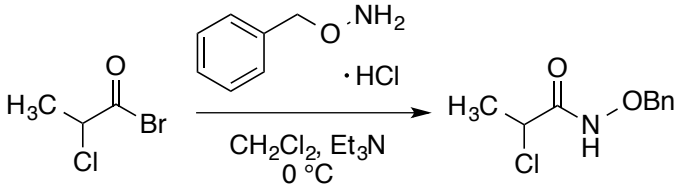

Prepared in 48% yield (3.9 mmol, 0.97 g) from the reaction of 2-chloropropanoyl chloride (8.2 mmol, 1.03 g) with *O*-benzylhydroxylamine, hydrochloride (8.2 mmol, 1.03 g) via general procedure A. R_f = 0.43 (3:1 hexanes:ethyl acetate); M.P. = 70.1-72.8 °C; ^{1}H-NMR (500 MHz, $CDCl_3$): δ 9.09 (br s, 1H), 7.44 – 7.35 (m, 5H), 4.93 (s, 4H), 4.33 (q, *J* = 7.1 Hz, 1H), and 1.69 (d, *J* = 6.8 Hz, 3H); ^{13}C-NMR (126 MHz, $CDCl_3$): δ 167.1, 134.8, 129.5, 129.1, 128.8, 78.5, 53.2, and 22.3.; IR (neat): 3112 (br), 2931, 1678 (st), 1494, 1454, 1364, 1222, 1204, 1074 cm^{-1}; HR-ESIMS requires for $C_{10}H_{12}ClNO_2$ $(M+Na)^+$ 236.0449, found 236.0445.

2,2-dichloro-*N*-(phenylmethoxy)acetamide (65f):

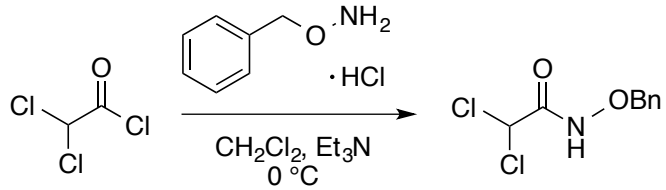

Prepared in 82% yield (11.1 mmol, 2.6 g) from the reaction of 2,2-dichloroacetyl chloride (13.6 mmol, 2.0 g) with *O*-benzylhydroxylamine, hydrochloride (13.6 mmol, 2.15 g) via general procedure A. R_f = 0.52 (3:1 hexanes:ethyl acetate); ^{1}H NMR (400 MHz, CD_3CN) δ 9.89 (br s, 1H), 7.63 – 7.17 (m, 4H), 6.02 (s, 1H), and 4.89 (s, 2H); ^{13}C NMR (101 MHz, CD_3CN) δ 162.2, 136.1, 130.4, 129.7, 129.4, 78.8, and 65.6; IR (film) 3135 (br), 2996, 2880, 2860, 1700, 1677 (st), 1531, 1468, 1454, 1367, 1341, 1214, 1200, 1046, 1027 cm^{-1}; HR-APPIMS requires for $C_9H_9Cl_2NO_2$ $(M^*)^+$ 233.0005, observed 232.9976.

(±)-2-chloro-2-(4-chlorophenyl)-*N*-(phenylmethoxy)acetamide (65g):

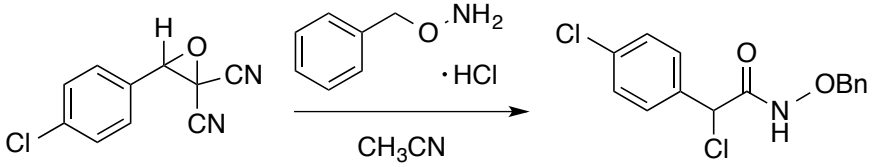

A suspension of the epoxynitrile (1.2 mmol, 315 mg ~ 80 % pure) and *O*-benzylhydroxylamine hydrochloride (1.5 mmol, 240 mg) in acetonitrile (0.1 M, 15 mL) was heated to reflux overnight. The suspension was cooled and the mixture was concentrated to 5 mL. The residue was partitioned between water and ethyl acetate and the aqueous phase was extracted with ethyl acetate (3 x 15 mL). The combined organic layers were washed with brine (15 mL), dried over Na_2SO_4, filtered, and evaporated under reduced pressure. The residue was recrystallized from hexanes and ethyl acetate to provide the product as a colorless solid (0.69 mmol, 215 mg, 58% yield). R_f = 0.20 (3:1 hexanes:ethyl acetate); ^{1}H NMR (400 MHz, CD_3CN) δ 9.76 (s, 1H), 7.51 – 7.29 (m, 9H), 5.27 (s, 1H), and 4.84 (s, 2H). ^{13}C NMR (101 MHz, CD_3CN) δ 165.2, 136.6, 136.3, 135.5, 130.6, 130.4, 129.8, 129.6, 129.4, 78.6, and 57.9; IR (neat): 3115.8 (br), 2942, 2842, 2662, and 1492 (st) cm^{-1}; HR-ESIMS requires for $C_{15}H_{13}Cl_2NO_2$ $(M+Na)^+$ 332.0216, found 332.0216.

(±)-2-bromo-*N*-(phenylmethoxy)carboxamide (65i, 65l):

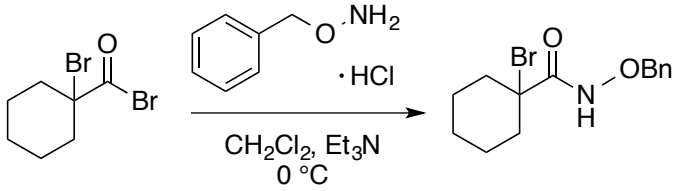

Prepared in 72% yield (14.5 mmol, 4.5 g) from the reaction of 2-bromocyclohexanoyl bromide (20.1 mmol, 4.53 g) with *O*-benzylhydroxylamine, hydrochloride (20.1 mmol, 3.21 g) via general procedure A. R_f = 0.47 (3:1 hexanes:ethyl acetate); M.P. = 84.6-86.1 °C; ^{1}H NMR (400 MHz, $CDCl_3$) δ 8.98 (br s, 1H), 7.51 – 7.31 (m, 5H), 4.94 (s, 2H), 2.13 (ddd, *J* =

14.6, 10.9, 4.0 Hz, 2H), 2.00 (dt, *J* = 14.0, 4.1 Hz, 2H), 1.80 – 1.57 (m, 5H), 1.42 – 1.23 (m, 1H); ^{13}C NMR (101 MHz, $CDCl_3$) δ 169.6, 135.0, 129.6, 129.0, 128.7, 78.2, 38.1, 24.7, and 22.6. IR (neat): 3235 (br), 3034, 2936, 2862, 1680, 1651 (st), 1470, 1459, 1270, 1249, 1210, 1122, 1025, 1000 cm^{-1}; HR-APPIMS requires for $C_{14}H_{16}BrNO_2$ $(M+H)^+$ 312.0594, found 312.0206.

(±)-(4*S*, 5*R*, 1*S*)-4-methyl-8-oxo-2-(phenylmethoxy)-2-azabicyclo[3.2.1]oct-6-en-3-one (66b):

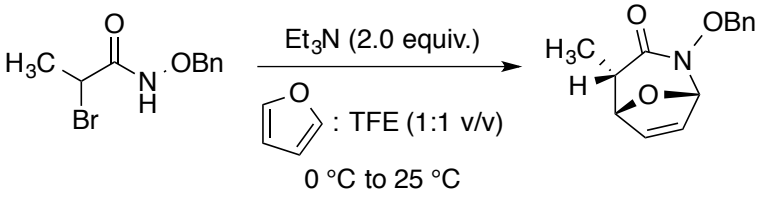

Prepared in 67% yield (0.26 mmol, 63.3 mg) from the reaction of 2-bromo-*N*-(phenylmethoxy)propanamide (0.39 mmol, 100.7 mg) with furan via general procedure B. R_f = 0.3 (3:1 hexanes:ethyl acetate); ^{1}H-NMR (500 MHz, $CDCl_3$): δ 7.47 – 7.32 (m, 5H), 6.57 (dd, *J* = 6.2, 1.0 Hz, 1H), 6.41 (dd, *J* = 6.0, 1.7 Hz, 1H), 5.25 (d, *J* = 1.5 Hz, 1H), 5.00 (d, *J* = 11.0 Hz, 1H), 4.87 (d, *J* = 11.0 Hz, 1H), 4.85 (dd, *J* = 5.0, 1.9 Hz, 1H), 3.17 (qd, *J* = 7.4, 5.0 Hz, 1H), and 1.09 (d, *J* = 7.4 Hz, 3H); ^{13}C-NMR (126 MHz, $CDCl_3$): δ 172.7, 136.1, 135.8, 133.8, 129.7, 128.9, 128.7, 91.6, 82.9, 78.1, 45.1, and 10.6; IR (film) 3089, 2970, 2970, 2934, 2876, 1697, 1497, 1455, 1377, 1209, and 1053 cm^{-1}; HR-ESIMS requires for $C_{14}H_{16}NO_3$ $(M+H)^+$ 246.1125, found 246.1118.

(±)-(4*S*, 5*R*, 1*S*)-4-ethyl-8-oxo-2-(phenylmethoxy)-2-azabicyclo[3.2.1]oct-6-en-3-one (66c):

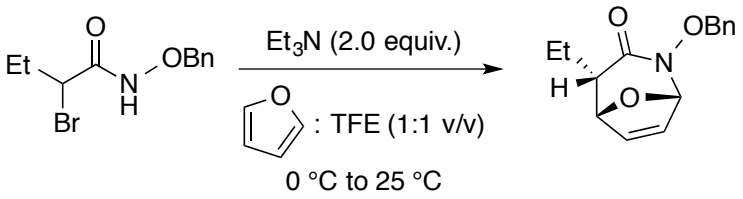

Prepared in 86% yield (0.157 mmol, 40.6 mg) from the reaction of 2-bromo-*N*-(phenylmethoxy)butanamide (0.183 mmol, 50.0 mg) with furan via general procedure B. R_f = 0.3 (3:1 hexanes:ethyl acetate); R_f 0.50 (3:1, hexanes: ethyl acetate); ^{1}H-NMR (500 MHz, $CDCl_3$): δ 7.45 – 7.42 (m, 2H), 7.41 – 7.32 (m, 3H), 6.51 (dd, *J* = 6.0, 1 Hz, 1H), 6.38 (dd, *J* = 6.0, 1.8 Hz, 1H), 5.25 (d, *J* = 1.2 Hz, 1H), 4.99 (d, *J* = 11.0 Hz, 1H), 4.95 (dd, *J* = 5.1, 1.8 Hz, 1H), 4.87 (d, *J* = 11.0 Hz, 1H), 2.99 (dt, *J* = 10.1, 5.1 Hz, 1H), 2.01 (dqd, *J* = 15.4, 7.5 5.3, 7.5, 15.4 Hz, 1H), 1.24 – 1.14 (m, 1H), and 1.03 (t, *J* = 7.5 Hz, 3H). ^{13}C-NMR (126 MHz, $CDCl_3$): δ 172.1, 135.8, 133.6, 129.7, 128.8, 128.6, 91.4, 91.4, 81.3, 78.0, 51.8, 19.5, and 12.3; IR (film) 3250 (br), 3032, 2966, 2929, 2877, 1696 (st), 1497, 1455, 1371, 1209, 1104, 1055, and 1033 cm^{-1}; HR-ESIMS requires for $C_{15}H_{17}NO_3$ $(M+Na)^+$ 282.1101, found 282.1083.

(±)-(4*S*, 5*R*, 1*S*) 4-(2,2-dimethylethyl)-8-oxo-2-(phenylmethoxy)-2- azabicyclo[3.2.1]oct-6-en-3-one (66d):

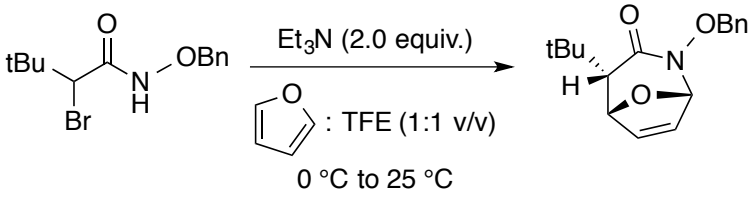

Prepared in 54% yield (52.7 mg, 0.18 mmol) from the reaction of 2-bromo-2,2-dimethyl-*N*- (phenylmethoxy)propanamide (103.5 mg, 0.34 mmol) with furan via general procedure B. R_f = 0.49 (3:1 hexanes:ethyl acetate); ^{1}H-NMR (500 MHz, $CDCl_3$): δ 7.43 (m, 2H), 7.41 – 7.33 (m, 3H), 6.42 (dd, *J* = 6.0, 1.8 Hz, 2H), 6.35 (dd, *J* = 6.0, 1.5 Hz, 1H), 5.20

(d, J = 1.3 Hz, 1H), 5.00 (dd, J = 4.8, 1.8 Hz, 1H), 4.98 (d, J = 11.0 Hz, 1H), 4.88 (d, J = 11.0 Hz, 1H), 3.04 (d, J = 4.8 Hz, 1H), and 1.10 (s, 9H); ^{13}C-NMR (126 MHz, $CDCl_3$): δ 141.6, 136.0, 134.5, 134.0, 129.8, 128.8, 128.6, 91.6, 81.5, 78.0, 60.5, 32.3, and 29.8; IR (film): 3210, 3090, 3064, 3032, 2958, 2871, 1672 (st), 1497, 1480, 1455, 1365(s), 1231, 1211, 1162, 1054, and 1038 cm^{-1}; HR-ESIMS requires for $C_{17}H_{21}NO_3$ $(M+Na)^+$ 312.1455, found 312.1446.

(±)-(4*S*, 5*R*, 1*S*)-4-chloro-8-oxo-2-(phenylmethoxy)-2-azabicyclo[3.2.1]oct-6-en-3-one (*endo*-66f) and (±)-(4*R*, 5*R*, 1*S*)-4-chloro-8-oxo-2-(phenylmethoxy)-2-azabicyclo[3.2.1]oct-6-en-3-one (*exo*-66f):

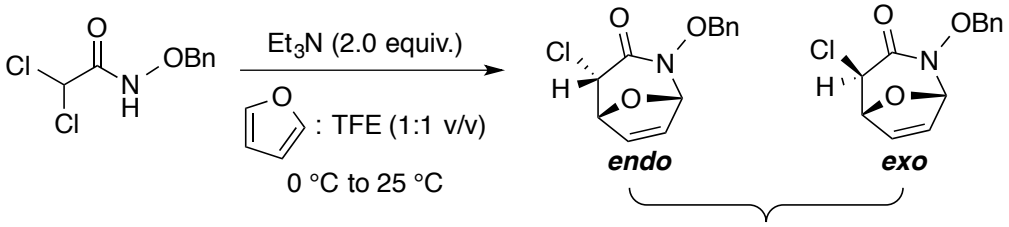

Prepared in 73% yield (0.31 mmol, 72 mg) from the reaction of 2,2-dichloro-*N*-(phenylmethoxy)acetamide (0.43 mmol, 100.2 mg) with furan via general procedure B. R_f = 0.50 (3:1 hexanes:ethyl acetate) ^{1}H NMR (400MHz, $CDCl_3$) δ 7.51 – 7.30 (m, 3H), 6.54 (dd, J = 6.0, 1.1 Hz, 1H), 6.51 (dd, J = 6.0, 1.7 Hz, 1H), 5.27 (d, J = 1.1 Hz, 1H), 5.09 (dd, J = 5.1, 1.6 Hz, 1H), 5.00 (d, J = 11.0 Hz, 1H), 4.89 (d, J = 11.0 Hz, 1H), and 4.76 (d, J = 5.2 Hz, 1H); ^{13}C NMR (101 MHz, $CDCl_3$) δ 165.9, 136.8, 135.3, 133.1, 129.8, 129.2, 128.2, 92.1, 82.1, 78.3, and 56.9; IR (film): 3032, 2950, 2922, 2852, 1712 (st), 1455, 1369, 1213, 1189, 1059, and 1023 cm^{-1}. HR-ESIMS requires for $C_{13}H_{12}ClNO_3$ $(M+Na)^+$ 288.0398, found 288.0391. ***exo*-diastereoisomer:** R_f = 0.3 (3:1 hexanes:ethyl acetate); ^{1}H NMR (400MHz, $CDCl_3$): δ 7.48 – 7.35 (m, 2H), 6.68 (d, J = 5.9 Hz, 1H), 6.34 (dd, J = 6.0, 1.1 Hz, 1H), 5.28 (s, 1H), 5.02 (d, J = 10.9 Hz, 1H), 4.98 (s, 1H), 4.92 (d, J = 10.9 Hz, 1H), and 4.09 (s, 1H); ^{13}C NMR (101 MHz, $CDCl_3$) δ 165.5, 138.2, 135.0, 131.4, 129.9, 129.2, 128.8, 91.3, 84.2,

78.4, and 56.1; IR (neat): 3067, 3034, 2946, 2885, 1694, and 1046 cm^{-1}; HR-ESIMS requires for $C_{13}H_{12}ClNO_3$ $(M+Na)^+$ 288.0398, found 288.0399.

(±)-(4*S*, 5*R*, 1*S*)-4-(4-chlorophenyl)-8-oxo-2-(phenylmethoxy)-2-azabicyclo[3.2.1]oct-6-en-3-one (66g):

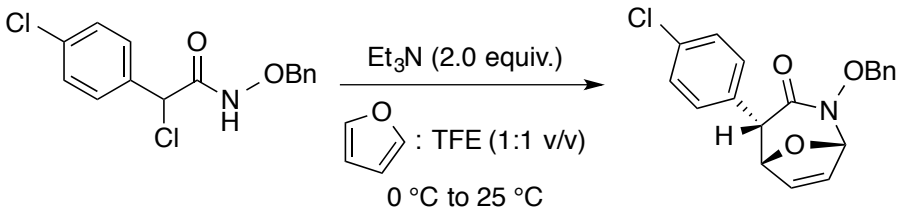

Prepared in 53% yield (0.16 mmol, 54.4 mg) from the reaction of 2-choro-2-(4-chlorophenyl)-*N*-(phenylmethoxy)acetamide (0.31 mmol, 95.5 mg) with furan via general procedure B. R_f = 0.48 (3:1 hexanes:ethyl acetate); ^{1}H-NMR (500 MHz, $CDCl_3$): δ 7.50 – 7.44 (m, 2H), 7.44 – 7.34 (m, 3H), 7.28 (ABd, *J* = 8.5 Hz, 2H), 7.05 (ABd, *J* = 8.5 Hz, 2H), 6.55 (dd, *J* = 6.0, 1.1 Hz, 1H), 6.19 (dd, *J* = 6.0, 1.7 Hz, 1H), 5.36 (d, *J* = 1.3 Hz, 1H), 5.05 (d, *J* = 11.0 Hz, 1H), 4.96 (d, *J* = 11.0 Hz, 1H), 4.94 (dd, *J* = 5.3, 1.8 Hz, 1H), and 4.38 (d, *J* = 5.3 Hz, 1H); ^{13}C-NMR (126 MHz, $CDCl_3$): δ 169.7, 136.0, 136.0, 135.6, 133.8, 133.8, 132.0, 131.1, 129.83, 129.1, 128.8, 128.7, 91.8, 91.8, 83.1, 83.1, 78.3, and 56.5; IR (film): 3089, 3064, 3031, 2924, 1688 (st), 1492, 1454, 1368, 1275, 1260, 1211, 1091, 1059, and 1017 cm^{-1}; HR-ESIMS requires for $C_{19}H_{17}ClNO_3$ $(M+H)^+$ 342.0891, found 342.0886.

(±)-(1*R*, 5*S*)-4,4-dimethyl-8-oxo-2-(phenylmethoxy)-2-azabicyclo[3.2.1]oct-6-en-3-one (63, 66h):

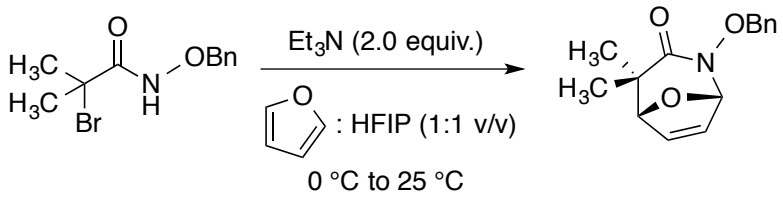

Prepared in 78% yield (0.32 mmol, 85.2 mg) from the reaction of 2-bromo-2-methyl *N*- (phenylmethoxy)propanamide (0.42 mmol, 115.0 mg) with furan via general procedure B. R_f = 0.40 (3:1 hexanes:ethyl acetate); ^{1}H-NMR (500 MHz, $CDCl_3$): δ 7.46 – 7.28 (m, 5H), 6.56 (dd, *J* = 5.9, 1 Hz, 1H), 6.43 (dd, *J* = 5.9, 1.9 Hz, 1H), 5.21 (d, *J* = 1.1 Hz, 1H), 4.97 (d, *J* = 10.9 Hz, 1H), 4.87 (d, *J* = 10.9 Hz, 1H), 4.46 (d, *J* = 1.8 Hz, 1H), 1.49 (s, 3H), and 1.05 (s, 3H); ^{13}C-NMR (126 MHz, $CDCl_3$): δ 175.7, 135.7, 135.5, 134.6, 129.8, 128.9, 128.6, 91.5, 87.4, 78.0, 49.3, 27.1, and 19.9; IR (film): 3055 (br), 1692 (st), 1470, 1385, 1362, 1265, 1217, 1174, 1055, 1008 cm^{-1}; HR-ESIMS requires for $C_{15}H_{17}NO_3$ $(M+Na)^+$ 282.1101, found 282.1098.

(±)-(1'*R*, 5'*S*)-spiro[cyclohexane-1,2'-[8]oxo-4'-(phenylmethoxy)-4'-azabicyclo[3.2.1]oct[6]en]-3'-one (66i):

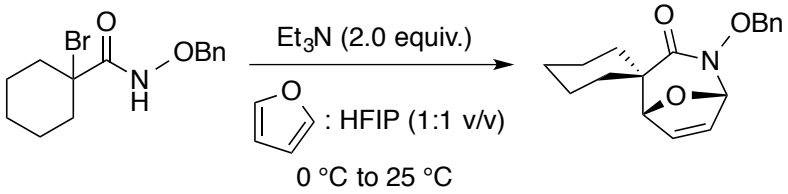

Prepared in 65% yield (0.22 mmol, 65.9 mg) from the reaction of 2-bromo-*N*-(phenylmethoxy)cyclohexane carboxamide (0.34 mmol, 107.2 mg) with furan via general procedure B. R_f = 0.62 (3:1 hexanes:ethyl acetate); ^{1}H-NMR (500 MHz, $CDCl_3$): δ 7.48 – 7.29 (m, 5H), 6.54 (d, *J* = 5.8 Hz, 1H), 6.43 (dd, *J* = 6.0, 1.7 Hz, 1H), 5.18 (d, *J* = 1.1Hz, 1H), 4.96 (d, *J* = 10.9 Hz, 1H), 4.93 (d, *J* = 1.4 Hz, 1H), 4.86 (d, *J* = 10.9 Hz, 1H), 2.06 (d, *J* = 12.7 Hz, 2H), 1.89 (td, *J* = 13.5, 6.8 Hz, 3H), 1.75 (s, 2H), 1.62 (dd, *J* = 13.3, 7.5 Hz, 5H),

and 1.47 – 1.19 (m, 6H); ^{13}C-NMR (101 MHz, $CDCl_3$): δ 175.7, 135.8, 135.5, 134.5, 129.8, 128.8, 128.6, 91.2, 82.9, 77.9, 53.3, 33.7, 28.9, 25.5, 21.7, and 21.5; IR (film): 3063, 3031, 2927, 2858, 1690, 1496, 1454, 1367, 1210, 1187, 1076, and 1064 cm^{-1}. HR-ESIMS requires for $C_{18}H_{21}NO_3$ $(M+Na)^+$, 322.1414, found 322.1424.

(±)-(4*S*, 5*R*, 1*S*)-4-ethyl-2-(phenylmethoxy)-2-azabicyclo[3.2.1]oct-6-en-3-one (*endo*-66j) and (±)-(4R, 5R, 1S) 4-ethyl- -2-(phenylmethoxy)-2-azabicyclo[3.2.1]oct-6-en-3- one (*exo*-66j):

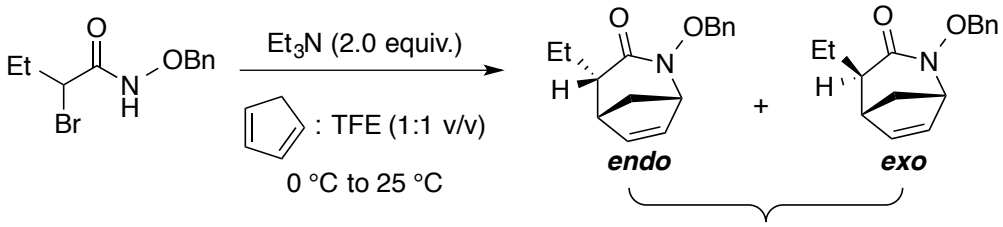

Prepared in 85% yield (0.32 mmol, 82.3 mg) from the reaction of 2-bromo-*N*-(phenylmethoxy)butanamide (0.37 mmol, 100.4 mg) with cyclopentadiene via general procedure B (characterized as a mixture 2.5:1 exo:endo). ***Endo* diastereoisomer**: R_f = 0.54 (3:1 hexanes:ethyl acetate); ^{1}H-NMR (500 MHz, $CDCl_3$): δ 7.53 – 7.28 (m, 5H), 6.30 (dd, *J* = 5.5, 2.0 Hz, 1H), 6.12 (dd, *J* = 5.4, 2.7 Hz, 1H), 4.95 (d, *J* =10.8 Hz, 1H), 4.88 (d, *J* = 10.8 Hz, 1H), 3.90 (d, *J* = 6.1 Hz, 1H), 2.93 (app q, *J* = 4.2 Hz, 1H), 2.59 (dt, *J* = 10.4, 4.1 Hz, 1H), 2.09 (dt, *J* = 12.1, 7.8 Hz, 1H), 1.99 (dd, J = 11.0, 5.3 Hz, 1H), 1.85 (d, *J* = 10.8 Hz, 1H), 1.37 – 1.16 (m, 2H), and 1.01 (t, *J* = 7.5 Hz, 3H); ^{13}C-NMR (101 MHz, $CDCl_3$): δ 171.6, 137.2, 137.0, 136.0, 129.8, 129.7, 128.7, 128.5, 77.19, 64.5, 51.5, 42.4, 40.8, 21.6, and 12.3; IR (film): 3063, 3031, 2961, 2874, 1668 (st), 1455, and 1368 cm^{-1}; HR-ESIMS requires for $C_{16}H_{19}NO_2$ $(M+Na)^+$ 280.1308, found 280.1296. ***Exo* diastereoisomer:** R_f = 0.41 (3:1 hexanes:ethyl acetate); ^{1}H NMR (500 MHz, $CDCl_3$): δ 7.5 – 7.3 (m, 5H), 6.30 (dd, *J* = 5.5, 2.5 Hz, 1H), 6.17 (dd, *J* = 5.5, 2.9 Hz, 1H), 4.93 (d, *J* = 10.7 Hz, 1H), 4.86 (d, *J* = 10.7 Hz, 1H), 3.86 (br s, 1H), 2.73 (app t, *J* = 4.2 Hz, 1H), 2.20 (dd, *J* = 10.1, 5.3 Hz, 1H), 2.12-2.16 (m, 1H), 2.05-1.98 (m 1H), 1.92 (d, *J* = 11.3 Hz, 1H), 1.74 (ddd, *J* = 10, 5, 5 Hz, 1H), 1.62-

1.59 (m, 1H), 1.31-1.18 (m, 1H), and 1.05 (t, J = 7.1 Hz, 3H); ^{13}C NMR (101 MHz, $CDCl_3$) δ 174.5, 138.3, 136.4, 136.0, 129.9, 128.8, 128.5, 77.0, 64.4, 51.5, 42.2, 38.8, 34.3, 30.5, 25.7, 21.6, and 21.3. IR (film): 3063, 3031, 2961, 2874, 1679, 1496, 1455, 1370 cm^{-1}; HR-ESIMS requires for $C_{16}H_{19}NO_2$ $(M+Na)^+$ 280.1308, found 280.1303.

(±)-(4*S*, 5*R*, 1*S*)-4-chloro-2-(phenylmethoxy)-2-azabicyclo[3.2.1]oct-6-en-3-one (*endo*-66k) and

(±)-(4*R*, 5*R*, 1*S*)-4-chloro-2-(phenylmethoxy)-2-azabicyclo[3.2.1]oct-6-en-3-one (*exo*-66k):

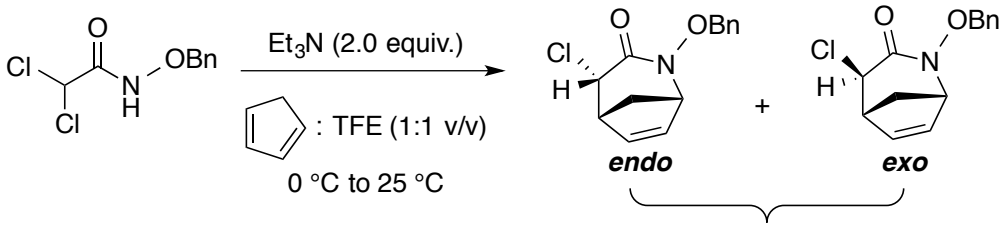

Prepared in 64 % yield (0.28 mmol, 73.8 mg) from the reaction of 2-bromo-*N*-(phenylmethoxy)butanamide (0.43 mmol, 100.8 mg) with cyclopentadiene via general procedure B. R_f = 0.53 (3:1 hexanes:ethyl acetate); ^{1}H-NMR (500 MHz, $CDCl_3$): δ 7.46 – 7.34 (m, 3H), 6.32 (dd, J = 5.7, 2.2 Hz, 1H), 6.31 – 6.28 (m, 1H), 4.98 (d, J = 10.9 Hz, 1H), 4.92 (d, J = 10.9 Hz, 1H), 4.71 (d, J = 4.4 Hz, 1H), 2.06 (dt, J = 11.6, 4.8 Hz, 1H), and 1.90 (d, J = 11.5 Hz, 1H); ^{13}C-NMR (126 MHz, $CDCl_3$): δ 164.7, 138.0, 136.5, 135.5, 129.9, 129.0, 128.6, 77.4, 65.0, 61.0, 46.8, and 41.7; IR (film): 3066, 3033, 2926, 2853, 1679, 1455, and 1372 cm^{-1}; HR-ESIMS requires for $C_{14}H_{15}ClNO_2$ $(M+H)^+$ 264.0786, found 264.0779.

(±)-(1'*R*, 5'*S*)-spiro[cyclohexane-1,2' -4'-(phenylmethoxy)-4'- azabicyclo[3.2.1]oct[6]en]-3'-one (66l):

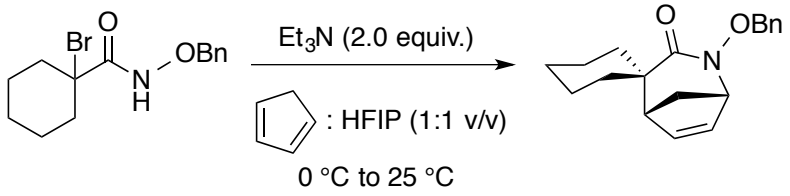

Prepared in 81 % yield (0.26 mmol, 72.9 mg) from the reaction of 2-bromo-*N*-(phenylmethoxy)butanamide (0.32 mmol, 100.4 mg) with cyclopentadiene via general procedure B. R_f = 0.6 (3:1 hexanes:ethyl acetate); ^{1}H-NMR (400 MHz, $CDCl_3$): 7.42 (d, *J* = 7.5 Hz, 2H), 7.40 – 7.29 (m, 3H), 6.25 (dd, *J* = 5.6, 2.0 Hz, 1H), 6.16 (dd, *J* = 5.6, 2.9 Hz 1H), 4.92 (d, *J* = 10.4 Hz, 2H), 4.88 (d, *J* = 10.3 Hz, 2H), 3.84 (dd, *J* = 4.2, 3.5 Hz, 1H), 2.98 (dd, *J* = 4.1, 3.1 Hz, 1H), 1.98 (d, *J* = 11.2 Hz, 1H), 1.94 (dt, J = 16.6, 12.6 Hz, 1H) 1.88-1.84 (m, 1H), 1.83 (dt, J = 10.6, 4.5 Hz, 1H), 1.75 (dq, *J* = 13.4, 3.6 Hz, 1H), 1.70- 1.60 (m, 3H), 1.55-1.42 (m, 2H), and 1.42-1.31 (m, 2H); ^{13}C NMR (101 MHz, $CDCl_3$) δ 174.5, 138.6, 136.4, 136.0, 130.0, 128.7, 128.5, 77.0, 64.4, 51.5, 42.3, 38.8, 34.3, 30.5, 25.7, 21.6, and 21.3; IR (film): 3062, 3030, 2925, 2858, 1662 (st), 1454, and 1371 cm^{-1}; HR-ESIMS requires for $C_{19}H_{24}NO_2$ $(M+Na)^+$ 321.1699, found 321.1651.

2-methyl-2-(2,2,2-trifluoroethoxy)-*N*-(phenylmethoxy)-propanamide (64):

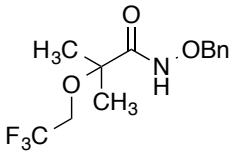

Produced as a byproduct in 56% yield from the reaction of 2-bromo-2-methyl-*N*-(phenylmethoxy) propanamide with TEA in furan and trifluoroethanol. R_f = 0.26 (3:1 hexanes:ethyl acetate); ^{1}H NMR (500 MHz, $CDCl_3$) δ 8.88 (s, 1H), 7.56 – 7.31 (m, 5H), 4.94 (s, 2H), 3.68 (q, *J* = 8.3 Hz, 2H), 1.43 (s, 6H); ^{13}C NMR (125 MHz, $CDCl_3$) δ 170.8, 134.9, 129.4, 129.0, 128.7, 123.7 (q, *J* = 278 Hz), 80.4, 78.3, 61.6 (q, *J* = 35 Hz), and 23.6; IR

(neat): 3218 (br), 3036; 2942, 2886, 1663 (st), 1430, 1455, 1485, 1386, 1369, 1307, 1285, 1217, 1181, 1145, 1029, and 1010 cm^{-1}; HR-ESIMS requires for $C_{13}H_{17}F_3NO_3$ $(M+H)^+$ 292.1155, found 292.1160.

2-methyl-*N*-(phenylmethoxy)-2-propenamide: Elimination product from the reaction attempted cycloaddition of **62** with $LiClO_4/Et_3N$ in diethyl ether.

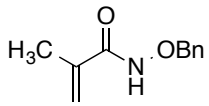

Produced in 61% yield from the reaction of 2-bromo-2-methyl-*N*- (phenylmethoxy) propanamide with $LiClO_4/Et_3N$ in furan and diethyl ether. R_f = 0.4 (3:1 hexanes:ethyl acetate); ^1H NMR (400 MHz, $CDCl_3$) δ 8.19 (br s, 1H), 7.49 – 7.29 (m, 5H), 5.55 (pent, *J* = 1 Hz, 1H), 5.32 (dq, *J* = 1.6, 1.0 Hz, 1H), 4.96 (s, 2H), and 1.92 (dd, *J* = 1.6, 1.2 Hz, 3H); ^{13}C NMR (101 MHz, $CDCl_3$) δ 167.2, 138.0, 135.4, 129.5, 129.0, 128.8, 120.4, 78.3, and 18.6; IR (film): 3199 (br), 3064, 3032, 2954, 2878, 1658, 1620, 1496, 1453, 1372, 1322, 1209, and 1039 cm^{-1}; HR-ESIMS requires for $C_{11}H_{13}NO_2$ $(M+Na)^+$ 215.0871, found 215.0869.

2.6 References

1. (a) Harmata, M. *Chem. Commun.* **2010**, 8886. (b) Harmata, M. *Chem. Commun.* **2010**, 8904. (c) Harmata, M. *Adv. Synth. Catal.* **2006**, 2297. (d) Harmata, M. *Acc. Chem. Res.* **2001**, *34*, 595. (e) Harmata, M. In *Advances in Cycloaddition;* Lautens, M., Ed.; JAI: Grenwich, 1997; Vol. 4, pp 41-86. (f) Harmata, M. *Tetrahedron* **1997**, *53*, 6235. (g) Harmata, M. *Recent Res. Dev. Org. Chem.* **1997**, *1*, 523. (h) Lohse, A.G.; Hsung, R.P. *Chem. Eur. J.* **2011**, *17*, 3812. (i) Huan, J.; Hsung, R.P. *Chemtracts* **2005**, *18*, 207. (j) Cha, J.K.; Oh, J. *Curr. Org. Chem.* **1998**, *2*, 217, (k) Rigby, J.H.; Pigge, F.C. *Org. React.* **1997**, *51*, 351. (l) Mann, J. *Tetrahedron* **1986**, *42*, 4611.
2. For reviews on the reactivity and synthesis of α-lactams, see: (a) Lengyel, I.; Sheehan, J.C. *Angew. Chem., Int. Ed. Engl.* **1968**, *7*, 25. (b) L'Abbe, G. *Angew. Chem., Int. Ed. Engl.* **1980**, *19*, 276.
3. Baumgarten, H.E. *J. Am. Chem. Soc.* **1962**, *84*, 4975.
4. House, H.O.; Gilmore, W.F. *J. Am. Chem. Soc.* **1961**, *83*, 3980.
5. For a comprehensive review of the mechanistic studies of the nucleophilic ring opening of α-lactams see: Hoffman, R.V. In *The Amide Linkage: Selected Structural Aspects in Chemistry Biochemistry and Material Science*; Greenberg, A.; Breneman, C.M., Liebman, J.F., Eds.; John Wiley & Sons: New York, 2000; p 137.
6. Stang, P.J.; Anderson, G.H. *Gazz. Chim. Ital.* **1995**, *125*, 329.
7. Cohen, A.D.; Showalter, B.M.; Toscano, J.P. *Org. Lett.* **2004**, *6*, 401.
8. Kikugawa, Y.; Shimada, M.; Kato, M.; Sakamoto, T. *Chem. Pharm. Bull.* **1993**, *41*, 2192.
9. Fort, A.W. *J. Am. Chem. Soc.* **1962**, *84*, 4979.
10. (a) Hoffman, H.M.R. *Angew. Chem., Int. Ed. Engl.* **1984**, *23*, 1. (b) Hoffman, H.M.R. *Angew. Chem., Int. Ed. Engl.* **1973**, *12*, 819.
11. Hoffman, R.; Woodward, R.B. *J. Am. Chem. Soc.* **1965**, *87*, 2046.

12. (a) Wardrop, D.J.; Bowen, E.G. In *Nitrenes and Nitrenium Ions*; Falvey, D.E. Gudmundsdottir, A.D. Eds.; Wiley-VCH: Weinheim, 2013; pp 347-449. (b) Kikugawa, Y. *Heterocycles* **2009**, *78*, 571 and references therein.

13. For examples of (4+3) cycloaddition reactions of nitrogen-stabilized oxyallylicic cations see: (a) Antoline, J.E.; Hsung, R.P. *Synlett* **2008,** 739. (b) Antoline, J.E.; Hsung, R.P.; Huang, J.; Song, Z.; Li, G. Org. Lett. **2007,** *9,* 1275. (c) MaGee, D.I.; Godineau, E.; Thornton, P.D.; Walters, M. A.; Sponholtz, D. J. *Eur. J. Org. Chem.* **2006,** 3667. (d) Huang, J.; Hsung, R.P. *J. Am. Chem. Soc.* **2005,** *127,* 50. (e) Rameshkumar, C.; Hsung, R.P. *Angew. Chem., Int. Ed.* **2004,** *43,* 615. (f) Xiong, H.; Huang, J.; Ghosh, S.K.; Hsung, R.P. *J. Am. Chem. Soc.* **2003,** *125,* 12694. (g) Harmata, M.; Ghosh, S.K.; Hong, X.; Wacharasindhu, S.; Kirchhoefer, P. *J. Am. Chem. Soc.* **2003,** *125,* 2058. (h) Xiong, H.; Hsung, R.P.; Berry, C.R.; Rameshkumar, C. *J. Am. Chem. Soc.* **2001,** *123,* 7174. (i) Walters, M.A.; Arcand, H.R. *J. Org. Chem.* **1996,** *61,* 1478.

14. For recent examples of cycloaddition reactions of oxygen-stabilized oxyallylicic cations see: (a) Harmata, M.; Huang, C. *Tetrahedron Lett.* **2009,** *50,* 5701. (b) Armstrong, A.; Dominguez-Fernandez, B.; Tsuchiya, T. *Tetrahedron* **2006,** *62,* 6614. (c) Aungst, R.A., Jr.; Funk, R.L. *Org. Lett.* **2001,** *3,* 3553. (d) Stark, C.B.W.; Pierau, S.; Wartchow, R.; Hoffmann, H.M.R. *Chem.-Eur. J.* **2000,** *6,* 684. (e) Misske, A.M.; Hoffmann, H.M.R. *Chem. Eur. J.* **2000,** *6,* 3313. (f) Lee, J.C.; Cha, J.K. *Tetrahedron* **2000,** *56,* 10175. (g) Harmata, M.; Sharma, U. *Org. Lett.* **2000,** *2,* 2703. (h) Harmata, M.; Rashatasakhon, P. *Synlett* **2000,** 1419 and references cited within.

15. For examples of cycloaddition reactions of sulfur-stabilized oxyallylicic cations see: (a) Harmata, M.; Kahraman, M.; Adenu, G.; Barnes, C.L. *Heterocycles* **2004,** *62,* 583. (b) Masuya, K.; Domon, K.; Tanino, K.; Kuwajima, I. *J. Am. Chem. Soc.* **1998,** *120,* 1724. (c) Harmata, M.; Carter, K.W. *ARKIVOC* **2002,** 62. (d) Harmata, M.; Jones, D.E. *Tetrahedron Lett.* **1996,** *37,* 783. (e) Harmata, M.; Fletcher, V.R.;

Claassen, R.J., II. *J. Am. Chem. Soc.* **1991,** *113,* 9861. (f) Ogura, K.; Ishida, M.; Fujita, M. *Bull. Chem. Soc. Jpn.* **1989,** *62,* 3987.

16. (a) Jeffrey, C.S.; Barnes, K.L.; Eickhoff, J.E.; Carson, C.R. *J. Am. Chem. Soc.* **2011,** *133,* 7688. (b) Barnes, K.L.; Koster, A.K.; Jeffrey, C.S. *Tett. Lett.* **2014**, *55*, 4690.
17. (a) Barone, V.; Cossi, M. *J. Phys. Chem. A* **1998**, *102*, 1995– 2001. (b) Barone, V.; Cossi, M.; Tomasi, J. *J. Comput. Chem*. **1998**, *19*, 404–417.
18. Frisch, M. J. *Gaussian 03*, revision C.02; Gaussian, Inc.: Wall- ingford, CT, 2004.
19. Density functional theory (DFT) methods are demonstrated to accurately model various aspects of the [4+3] cycloaddition of oxyallylic cations: (a) Krenske, E. H.; Houk, K. N.; Lohse, A. G.; Antoline, J. E.; Hsung, R. P. *Chem. Sci*. **2010**, *1*, 387–392. (b) Krenske, E. H.; Houk, K. N; Harmata, M. *Org. Lett*. **2010**, *12*, 444–447. (c) Domingo, L. R.; Arno, M.; Saez, J. A. *J. Org. Chem*. **2009**, *74*, 5934–5940. (d) Arno, M.; Picher, M. T.; Domingo, L. R.; Andres, J. *Chem.—Eur. J.* **2004**, *10*, 4742–4749. (e) Saez, J. A.; Arno, M.; Domingo, L. R. *Org. Lett*. **2003**, *5*, 4117–4120. (f) Cramer, C. J.; Barrows, S. E. *J. Phys. Org. Chem*. **2000**, *13*, 176–186. (g) Cramer, C. J.; Barrows, S. E. *J. Org. Chem*. **1998**, *63*, 5523–5532.
20. Föhlisch, B.; Gehrlach, E.; Herter, R. *Angew. Chem., Int. Ed. Engl.* **1982,** *21*, 137.
21. Hexafluoroisopropanol improves the yield of reactions proceeding through reactive oxyallylic cationic intermediates; see: (a) Harmata, M.; Huang, C.; Rooshenas, P.; Schreiner, P.R. *Angew. Chem., Int. Ed. Engl.* **2008,** *47*, 8696. (b) Myers, A.G.; Barbay, J.K. *Org. Lett.* **2001**, *3*, 425.
22. Herter, R.; Föhlisch, B. *Synthesis* **1982**, 976.
23. The relative configuration of entry 3, Table 2 was assigned by coupling constant analysis [$J \sim 5$ Hz C(5) – C(4) for the *endo* vs. $J < 3$ Hz C(4) – C(5) for the *exo*] and NOE correlations.

Chapter 3: Target Directed Studies Of Aza-[4+3] Cycloaddition Scaffolds

3.1 Introduction

The family of protein kinase C (PKC) enzymes catalyzes the transfer of the γ-phosphate from adenosine triphosphate (ATP) to serine or threonine residues on their respective substrate proteins.[1-7] Phosphorylation that is mediated by PKC had been found to be pivitol in a number of cellular processes, including but not limited to gene expression and cell proliferation. Unregulated PKC activation has been discovered to play a part in a variety of clinical disease states, with the most prominent being carcinogenesis.[8] Thus, extensive efforts have been made over the last several years to identify selective and potent inhibitors of PKC. Balanol **70** is a secondary metabolite of the fungus *Verticillium balanoides*, and was first isolated and characterized in 1993 by Kulanthaivel and co-workers.[9] Balanol was found to be a powerful inhibitor of PKC at low nanomolar concentrations, and its total synthesis has been reported by several research groups.[10-13] Given the seven-membered nitrogen ring at the core of its structure, we were curious to explore the possibility of utilizing our cycloaddition methodology (described in Chapter 2) toward a new approach to synthesizing balanol in an overall shorter and more concise route (Scheme 3.1.1). The first portion of this chapter outlines our progress in applying an aza-[4+3] cycloaddition substrate to the synthesis of balanol.

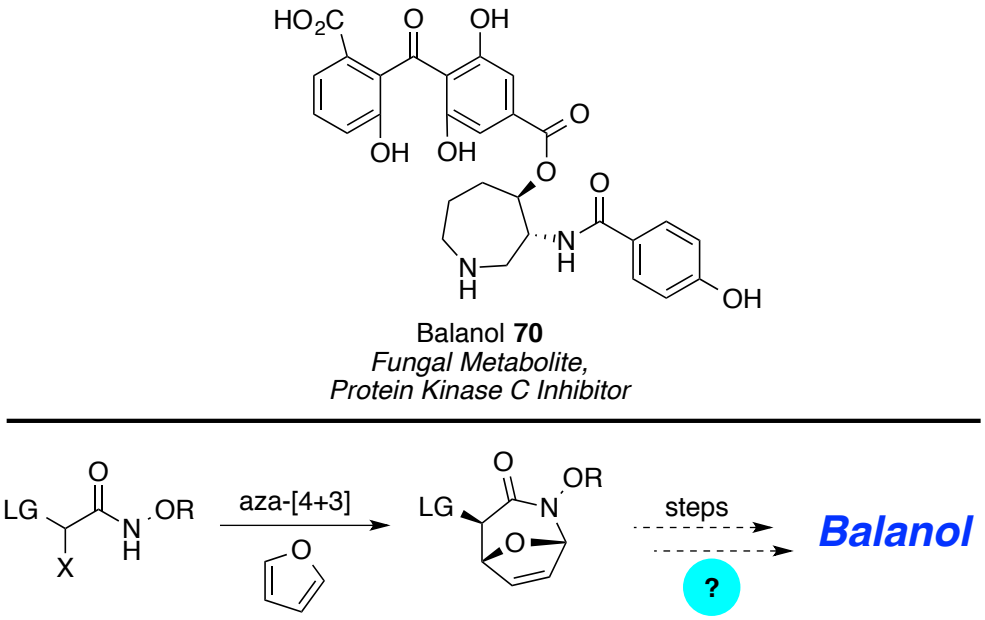

Scheme 3.1.1. Proposal to synthesize balanol **70** starting from a simple pre-functionalized α-haloamide.

Iminosugars are analogues of monosaccharides where the endocyclic oxygen is replaced with a nitrogen atom, a substitution that prevents the metabolism of these compounds.[14] Polyhydroxylated piperidines, or six-membered ring-size iminosugars, have received the most attention to detail, owing to their ability to mimic their analogous pyranoses in interactions with carbohydrate-processing enzymes. Deoxynojirimycin **71** (DNJ) (Figure 3.1.1), an analogue of glucose, is the archetypal iminosugar and occurs naturally in mulberry plants, *Streptomyces,* and *Bacillus.*[15] Miglitol **72** is an FDA approved anti-diabetic drug that functions by inhibiting the

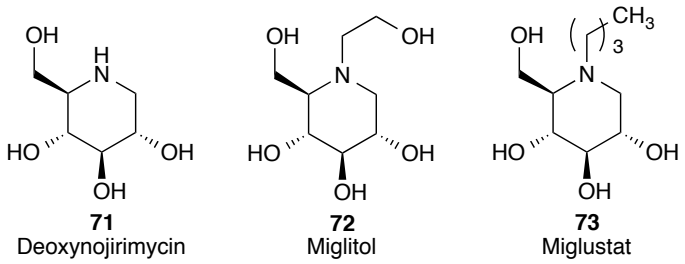

Figure 3.1.1. Representative examples of biologically and pharmaceutically relevant iminosugars.

body's ability to breakdown carbohydrates into glucose, and has more recently been shown to reduce plasma lipids as well as inhibit free radical generation.[16] Miglustat **73** (marketed under the trade name Zavesca) is an inhibitor of glucosylceramide synthase, and is used to treat adults with mild to moderate Type I Gaucher disease.[17] Due to their similarity, iminosugars share many chemical features with mono- and disaccharides. With respect to spatial aspects, they occupy an area of chemical space similar to that of carbohydrates, but different from that of other small heterocyclic molecules typically explored in screening libraries.[18] The attraction of iminosugars however extends beyond being simply different. As small polar molecules they possess the ability for efficient uptake by the body,[19] while at the same time they remaining adequately distinct from carbohydrates to avoid processing by carbohydrate-modifying enzymes, thus giving them chemical and biological stability. This "dual nature" of properties sets apart iminosugars as a special class in the on-going search for new drug molecules. Continuing developments in the depths of understanding of glycobiology are constantly identifying new targets to which iminosugars can appropriately be applied in the search for drug candidates.[18] Since the commercialization of the first iminosugar-based drug (Glyset^{TM}) in 1996, the rate at which new discoveries in the field of sugar mimetics with nitrogen replacement of the endocyclic oxygen has been steadily on the rise.[20] Several structures either have been, or are currently involved in clinical trials for the treatment of cancers,[21] diabetes,[22] viral infections,[23] and rare genetic diseases.[24,25]

Our goal in the contribution to this rapidly growing field of research was to demonstrate the utility of our new reaction methodology (described in Chapter 2) to provide a general means to access iminosugar scaffolds. More specifically, we wanted to establish a versatile synthetic strategy that allowed for the option to access a variety of derivatives from our general aza-[4+3] cycloaddition scheme. Herein, the latter part of this chapter describes synthetic efforts devoted to

the construction of seven-membered iminosugar analogues from commercially available starting materials and a common intermediate in high yields and diastereoselectivity.

3.2 Towards a Concise and Stereoselective Synthesis of Balanol

Synthetic studies toward the total synthesis of balanol began with α-chlorocycloadduct **74** (from Chapter 2) (Scheme 3.2.1), thinking that the halogen functionality could provide a necessary handle for functional group manipulation at the 3-position of the azepane ring. Reduction of **74** using lithium aluminum hydride and aluminum trichloride proceeded cleanly to give azepine **75** in good yield. The next step of our synthesis would involve displacement of chloride by a nitrogen-centered nucleophile. Reaction of **75** with sodium azide in dimethyl sulfoxide (DMSO) at 90 °C was found to effectively install a nitrogen functionality. A one-pot reductive acylation sequence was carried out, using first palladium-catalyzed hydrogenation followed by acylation of the resulting free amine with *p*-methoxybenzoyl chloride. However upon purification, instead of the expected seven-membered azepane, piperidine **78** was recovered as the sole product, presumably to have arisen from ring contraction during the azide displacement step. Although we observed an unwanted ring size, we were able to demonstrate proof of concept toward realizing the core structure of balanol by esterifying the alcohol of **78** with benzoic anhydride, catalyzed by 4-dimethylaminopyridine (DMAP) to give **79** in good yield.

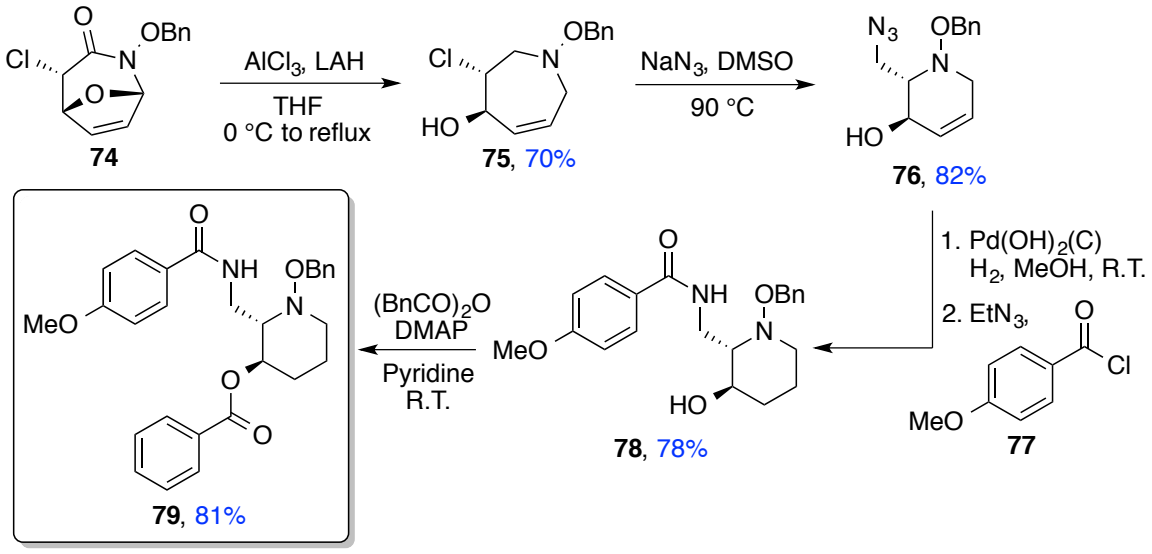

Scheme 3.2.1. Synthetic efforts directed toward balanol starting from cycloadduct **74**.

Given the exceptional electron rich character on the nitrogen atom due to the electron-donating benzyloxy group, we proposed a plausible mechanism for the observed ring contraction in which intramolecular nucleophilic attack by nitrogen would give aziridinium ion **80** (Scheme 3.2.2). Subsequent nucleophilic attack by azide to relieve the three-membered ring strain would ultimately give rise to piperidine **79**. Attempts to directly displace chloride from the starting cycloadduct **74** including microwave and the previously described conditions all resulted in decomposition of the substrate. In light of ring contraction being an inevitable result of our current methodology, current work on this project is being focused on the development of new cycloaddition conditions that avoid the use of halogens. We are investigating conditions whereby an aza-oxyallylic cation intermediate **82** is generated by direct oxidation of α-nitrogen substituted amides **81**, giving a cycloadduct such as **83**. Reduction would provide pre-functionalized azepine **84** with no need for nucleophilic substitution and circumventing the ring contraction problem.

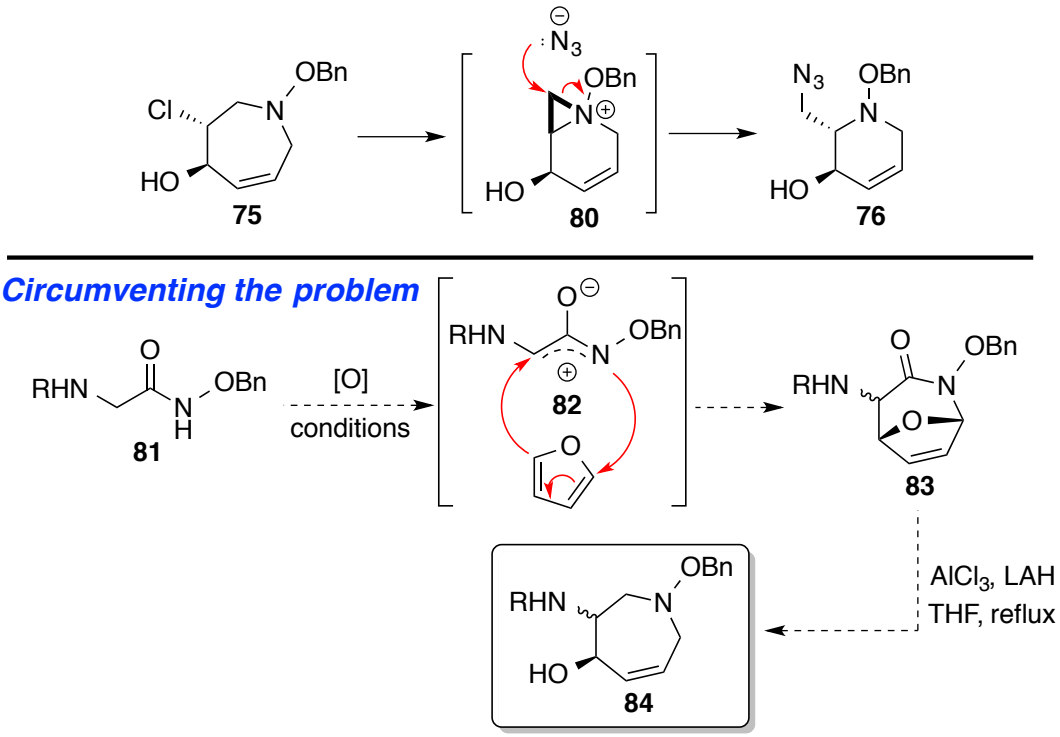

Scheme 3.2.2. Proposed ring contraction mechanism and current work to circumvent problem.

3.3 Synthesis of 7-Membered Iminosugar Analogues: A General Strategy for the Rapid Construction of Polyhydroxylated Azepane Derivatives

Compared to naturally occurring five- and six-membered iminosugar homologues, polyhydroxylated azepanes or azepane iminosugars have garnered less attention and thus been less investigated. The first azepane iminosugars were first synthesized in 1967 by Paulsen,[26] with more interest in this field being acquired thirty years later when Wong studied their bioactivities and found comparable outcomes with their five- and six-membered relatives.[27-32] Over the past several years, new azepane iminosugar family members have surfaced including seven-membered DNJ homologues,[28] and 1-*N*-iminosugars,[29] both of which showed promising inhibitory properties. Additionally, acetylamino group substituted azepanes have been shown to be potent inhibitors of *N*-acetyl-*β*-hexosaminidases.[30] Azepanes in bicyclic form, known as polyhydroxylated perhydroazaazulenes, have been synthesized although no significant biological

activity has been reported yet.[31] Several other higher homologues of calystegine have also shown promising inhibitory properties.[32] Despite all of the promising biological leads and increased interest in these types of compounds, currently no general synthetic strategies exist that allow for convenient structural modifications. We considered the possibility of utilizing aza-[4+3] cycloaddition reactions and the privileged scaffolds they afford, as well as the rich functionality produced from a single synthetic step, as potential building blocks for azepane iminosugars. Given the versatility of our method and the ability to readily tune the substituent groups at the 3-position (Scheme 3.3.1), we sought to consider if seven-membered iminosugars could be accessed diastereoselectively and in only a few short synthetic steps.

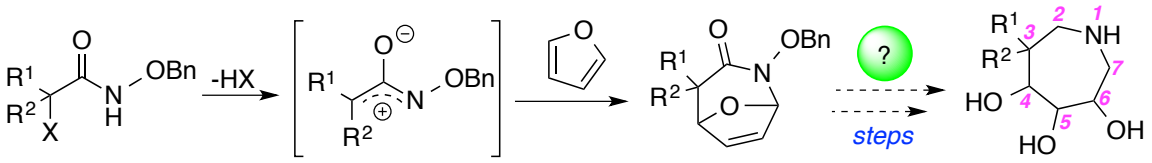

Scheme 3.3.1. Using aza-[4+3] cycloaddition scaffolds to access seven-membered iminosugar derivatives.

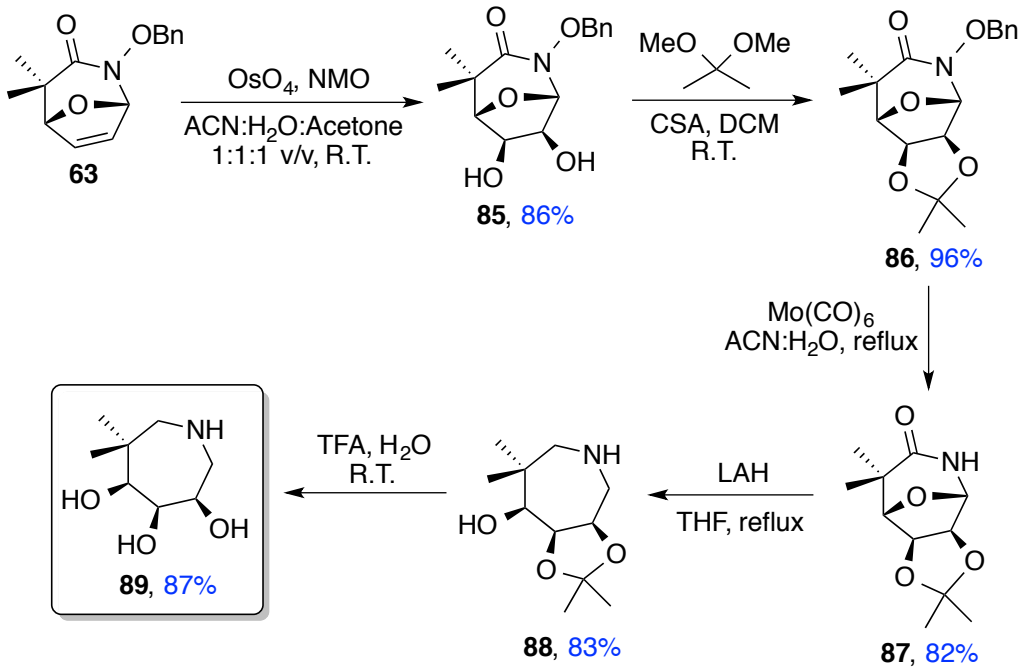

Scheme 3.3.2. Synthesis of polyhydroxylated azepane **89** starting from cycloadduct **63**.

To explore the viability of our proposal, dimethyl cycloadduct **63** (Scheme 3.3.2) was chosen as a model substrate. Alkene dihydroxylation of **63** catalyzed by osmium tetroxide proceeded in high yield, giving *syn*-diol **85** as a single diastereoisomer. Protection of the diol as its acetal using 2,2-dimethoxypropane and catalyzed by camphor sulfonic acid gave cleanly **86** in excellent yield.[33] Selective reductive N-O bond cleavage was accomplished by the action of $Mo(CO)_6$ in refluxing acetonitrile and water to provide amide **87** in high yield.[34] For the next step, it was found that refluxing of **87** in excess lithium aluminum hydride (LAH) not only provided reduction of the carbonyl, but also ring opening of the hemiaminal ether had occurred to give the desired azepane **88** in excellent yield and install the first hydroxyl group. The structure and relative stereochemistry of **88** was unambiguously assigned by single crystal X-ray diffraction (Figure 3.3.1). Finally, stirring of **88** in trifluoroacetic acid and water was found to cleanly deprotect the diols to give the desired polyhydroxylated azepane **89** in good overall yield starting from cycloadduct **63**.

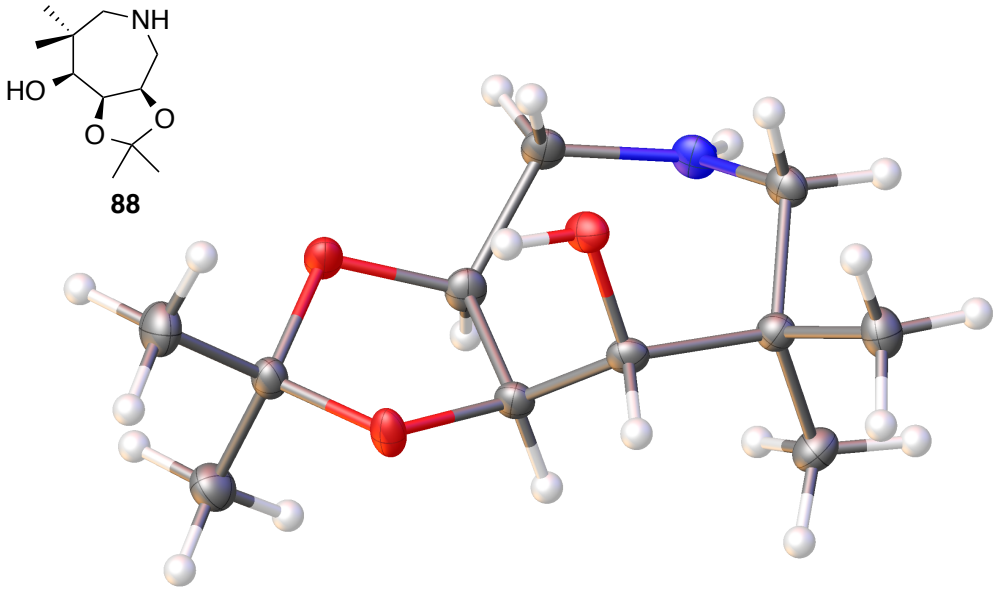

Figure 3.3.1. Thermal ellipsoid plot of azepane **88** at 50% probability. Hydrogen atoms are represented as spheres of arbitrary radius. Grey = carbon, red = oxygen, blue = nitrogen.

Alternatively, it was found that we could eliminate the protection/deprotection steps and synthesize **89** more directly and efficiently simply by reordering the reaction sequence. Reductive cleavage of the N-O bond of **63** by $Mo(CO)_6$ provided amide **90** with no sacrifice in yield (Scheme 3.3.3). Next, LAH mediated amide reduction and subsequent hemiaminal ether ring opening gave azepine **91**. Catalytic dihydroxylation again by osmium tetroxide yielded **89** in excellent overall yield, completing the synthesis and providing access to the seven-membered iminosugar family of compounds in only five synthetic steps and excellent overall yield from commercially available starting materials. Although simple in form, the reaction sequence described provides access to seven-membered iminosugar scaffolds in only 5 short synthetic steps and relatively easy reactions. Additionally, the methodology provides for a large degree of variability at the *C*-terminus of a simple α-haloamide starting material. This type of methodology could easily be employed to assist in the construction of libraries of compounds to test for biological activity as well as structure activity relationship (SAR) studies.

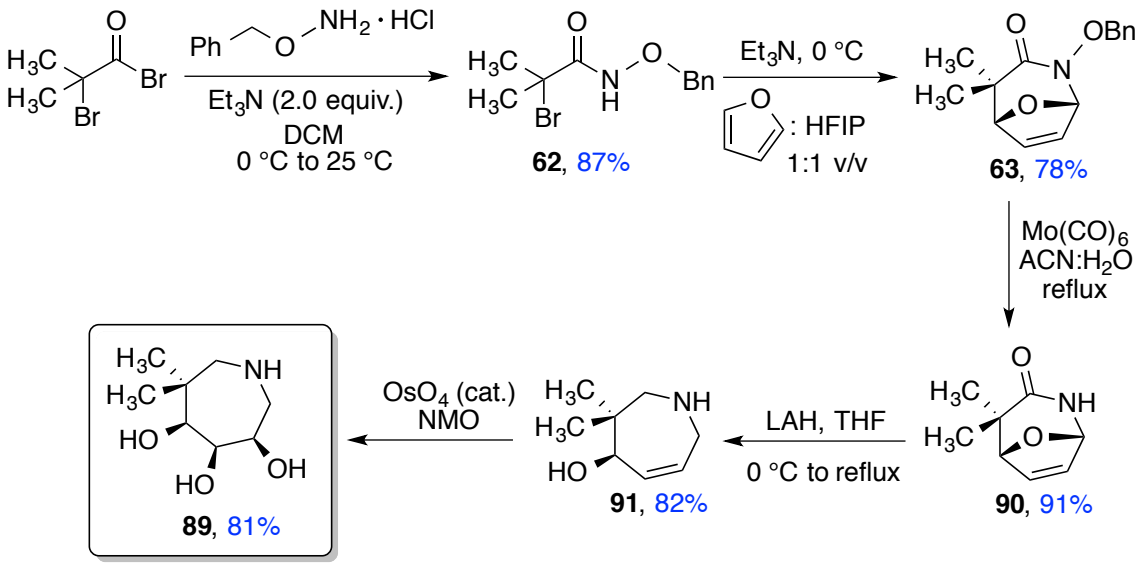

Scheme 3.3.3. Alternative synthesis of polyhydroxylated azepane **89** starting from a simple acid halide.

Attention was turned towards the α-chloro-cycloadduct, thinking that the halogen functionality could provide the necessary handle for installing a fourth hydroxyl group on the ring. Initial studies began by subjecting either *endo* or *exo* α-chloro-cycloadduct **66** to N-O bond cleaving conditions, however this reaction proved ineffective and resulted in decomposition of the starting material (Scheme 3.3.4). Other reductive conditions including Zn/AcOH, SmI_2, and a titanocene (III) chloride procedure reported by Miller and co-workers[35] were all found to be incompatible with the substrate and could not affect the desired N-O bond cleavage. Under palladium catalyzed hydrogenation conditions, C-O bond reduction resulted in recovery of undesired hydroxamic acid **92** as the sole product.

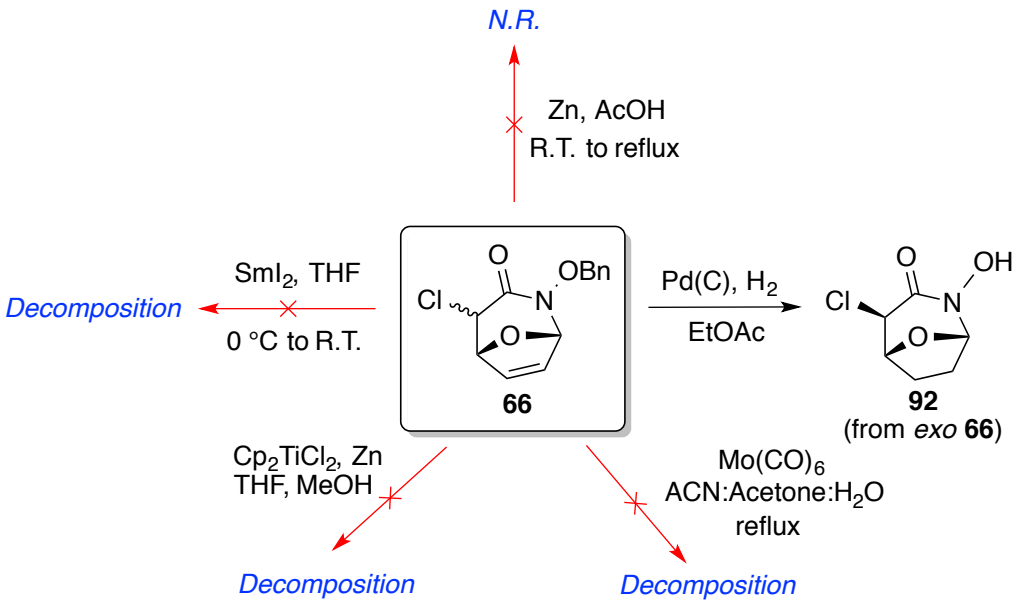

Scheme 3.3.4. Screening of N-O reduction conditions of **66**.

Since all of the above reagents involve one-electron reducing mechanisms and are usually not tolerant of halogens, efforts were focused on first displacing the chloride with oxygen-centred nucleophiles to install the desired functionality before moving on to N-O bond reduction. To our dismay however, all attempts to displace chloride with various oxygen-centered nucleophiles

proved to be unproductive and resulted in either decomposition or recovery of the starting material (Scheme 3.3.5). In an effort to circumvent these issues, we thought that re-ordering of the reaction scheme could provide a solution to the observed difficulties. At this point, studies were conducted on α-alkyl-substituted substrates as model systems in parallel with the α-chloro cycloadduct material for purposes of reaction exploration/optimization. Dihydroxylation of cycloadducts *endo* **66f** and **66c** by osmium tetroxide was found to proceed in good yield providing *syn*-diols **93** and **95** (Scheme 3.3.6). Subsequent protection of the alcohols using 2,2-dimethoxypropane and catalyzed by camphor sulfonic acid as previously described gave acetals **94** and **96** in excellent yield, setting the stage for reduction of the amide and ring opening of the hemiaminal ether.[33] Treatment of **96** to LAH following the previously mentioned conditions however was found to be unproductive, which instead of the desired product, resulted in recovery of carbinol amine **97**, albeit as a single diastereoisomer. The structure of **97** was confirmed as well as the relative stereochemical configuration unambiguously assigned by single crystal X-ray analysis (Figure 3.3.2).

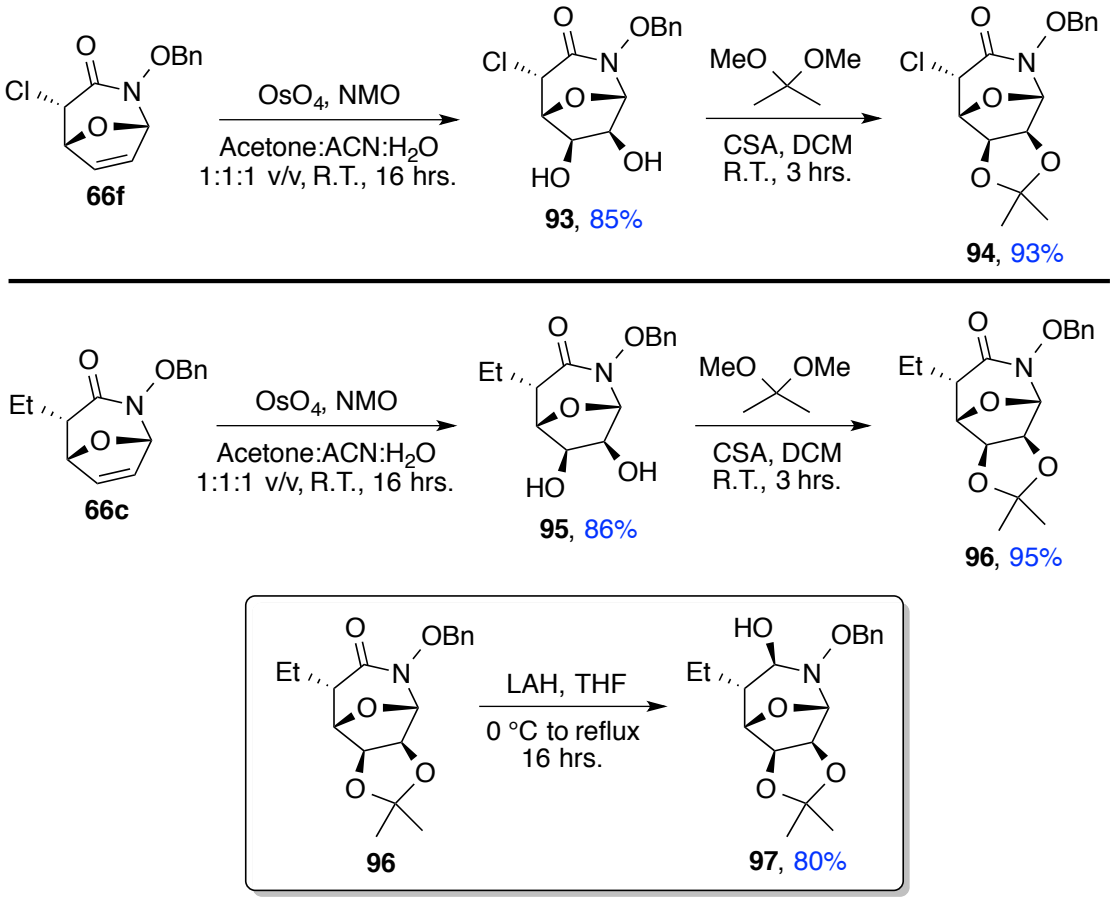

Scheme 3.3.6. Synthesis of acetal-protected diols **94** and **96** starting from cycloadducts *endo* **66f** and **66c**. LAH reduction of **96** to give carbinol amine **97**.

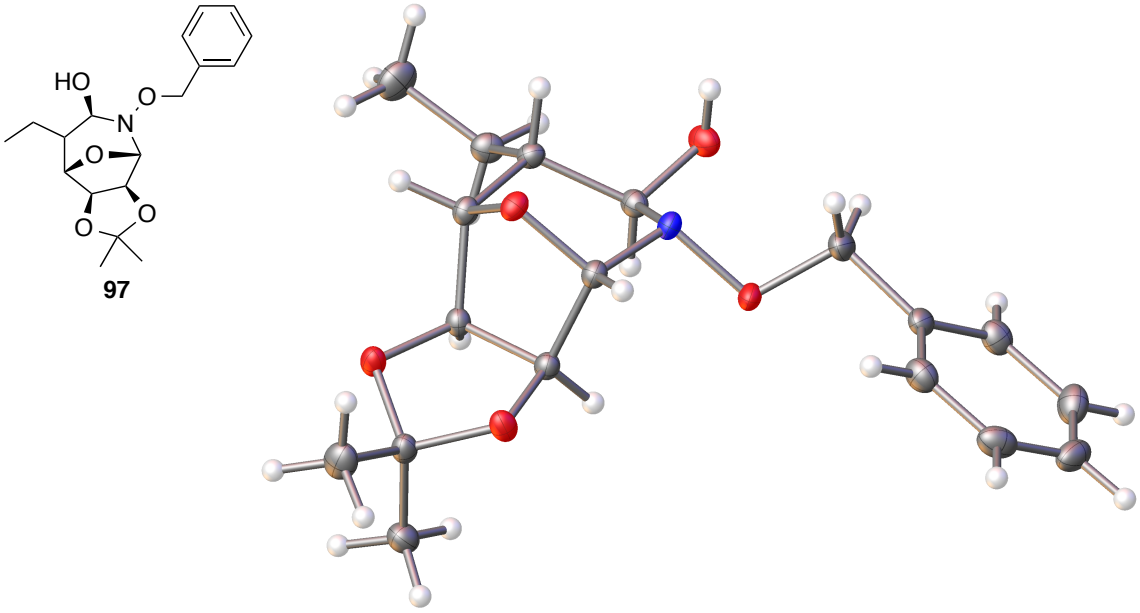

Figure 3.3.2. Thermal ellipsoid plot of carbinol amine **97** at 50% probability. Hydrogen atoms are represented as spheres of arbitrary radius. Grey = carbon, red = oxygen, blue = nitrogen.

Aluminum hydride, or alane (generated *in situ* from lithium aluminum hydride and aluminum trichloride), has been shown to be an excellent overall reducing agent that reduces a wide variety of functional groups while leaving unaltered halogens, alkenes, and nitro groups.[36] Although evidence supporting single electron pathway mechanisms has been reported,[37] reductions by alane take place primarily by a two-electron mechanism.[38,39] In this light, we proposed that alane would be a suitable reducing reagent that could chemoselectively reduce the amide while at the same time leaving the chloride unaffected. Indeed, upon subjection of acetal-protected diol **94** to a solution of LAH and aluminum trichloride in THF, it was found that the amide was reduced to the desired amine as well as the aminal ether ring opened to give an alcohol, however the acetal had also been reduced to give isopropyl ether **98** as the final product (Scheme 3.3.6). After consulting the literature we discovered that reduction of acetals by alane to give the half protected diol is a known transformation.[40] Other reducing agents such as borane, lithium triethylborohydride (super hydride), diisobutylaluminum hydride (DIBAL), and sodium

borohydride all failed to give the desired reactivity as well and resulted in recovery of the starting material.

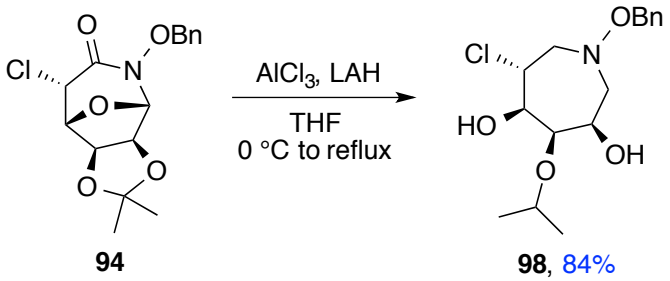

Scheme 3.3.7. Alane reduction of **94** to give isopropyl ether **98**.

Once again we thought that perhaps re-ordering of the reaction scheme could possibly circumvent the observed unwanted reactivity. Since alane has been shown to be tolerant of both halogens and double bonds, it was hypothesized that reduction of α-chloro cycloadduct *endo* **66f** as the first step in our synthesis could be a viable option. Exposure of *endo* **66f** to a slight excess of aluminum hydride under refluxing conditions was found to effectively provide azepine **75** (previously synthesized in Section 3.2) in good yield and as a single diastereoisomer (Scheme 3.3.8). Attempts to displace chloride with oxygen-centered nucleophiles under previously described conditions (Scheme 3.3.5) resulted in either decomposition or recovery of the starting material, with the exception of one case. We found that 3-chloroazepine **75** underwent facile ring contraction when reacted with silver acetate in DMF at 90 °C, giving tetrahydropyridine **100** in modest yield, albeit as a single diastereoisomer. Again, given the exceptional electron-rich character of the nitrogen atom, a plausible mechanism would involve the ring contraction going through an aziridinium ion intermediate such as **99** and ultimately collapsing to the six-membered ring similar to our observed ring contraction observation in Section 3.2. We saw this serendipitous result as an opportunity to extend our aza-[4+3] cycloaddition scaffolds to the synthesis of piperidine iminosugars. As previously stated, we were unable to reductively cleave the N-O bond of α-chloro cycloadduct **66f** in the presence of the halogen and thus de-tune the

electron donating character on the nitrogen atom. Therefore, ring contraction turned out to be an inevitable result and we were unable to install a fourth oxygen functionality with our current methodology and retain the seven-membered ring, regardless of reaction conditions or re-ordering of the synthetic scheme.

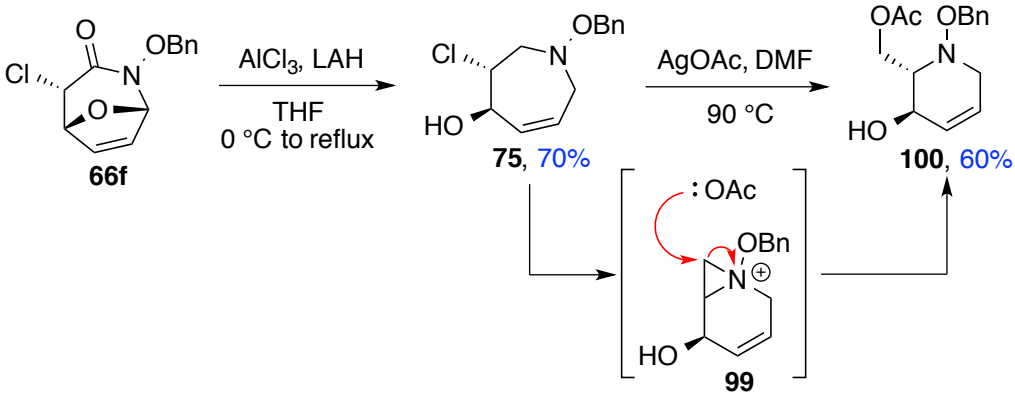

Scheme 3.3.8. Alane reduction of cycloadduct *endo* **66f** to give azepine **75** and subsequent silver acetate-mediated ring contraction to give tetrahydropyridine **100**.

3.4 Experimental

All reactions were carried out under an atmosphere of nitrogen in oven-dried glassware with magnetic stirring, unless otherwise specified. All reagents and solvents were purchased from Sigma-Aldrich Chemical Company and used without any further purification. TLC information was recorded on Silicycle glass 60 F_{254} plates and developed by staining with $KMnO_4$ or ceric ammonium molybdate. Purification of reaction products was carried out by flash chromatography using Silicycle Siliaflash® P60 (230-400 mesh). ^{1}H-NMR spectra were measured on Varian 400 (400 MHz) or Varian 500 (500 MHz) spectrometers and are reported in ppm (s = singlet, d = doublet, t = triplet, q = quartet, m = multiplet, br = broad; integration; coupling constant(s) in Hz using TMS as an internal standard (TMS at 0.00 ppm) in $CDCl_3$, CD_3CN, or CD_3OD. ^{13}C-NMR spectra were recorded on V400 or V500 spectrometers and reported in ppm using solvent as an

internal standard ($CDCl_3$ at 77.36 ppm), (CD_3CN at 118.26 ppm) or (CD_3OD at 49.86 ppm). Infrared (IR) spectra were recorded on a Nicolet 6700 FT-IR with a diamond ATR and data are reported as cm^{-1} (br = broad, st = strong). High-resolution mass spectra were obtained using an Agilent 6230 TOF LC/MS with an atmospheric pressure photo-ionization (APPI) or electrospray (ESI) source with purine and HP-0921 as internal calibrants.

(±)-(4*S*, 5*R*, 1*S*)-4-chloro-8-oxo-2-(phenylmethoxy)-2-azabicyclo[3.2.1]oct-6-en-3-one (66f *endo*, 74)

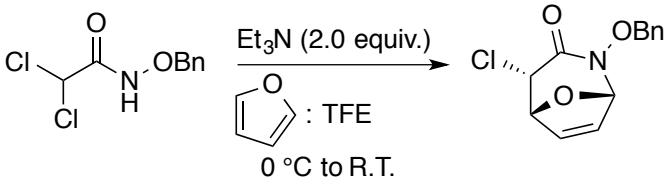

To a solution of 2,2-dichloro-*N*-(phenylmethoxy)acetamide (100.2 mg, 0.43 mmol) in CF_3CH_2OH (TFE) and furan [1:1 (v/v) 0.25 M] at 0 °C was added triethylamine (2 equiv.) dropwise. The solution was allowed to warm to room temperature and the reaction mixture was stirred for 72 hours. After removal of the volatiles under reduced pressure, the crude mixture was purified by flash column chromatography (3:1 hexanes:ethyl acetate) to afford 72 mg of **74** *endo* (0.31 mmol, 79% yield) (2:1 *endo:exo*) as a yellow oil. R_f = 0.50 (3:1 hexanes:ethyl acetate); ^1H NMR (400 MHz, $CDCl_3$) δ 7.51 – 7.30 (m, 3H), 6.54 (dd, *J* = 6.0, 1.1 Hz, 1H), 6.51 (dd, *J* = 6.0, 1.7 Hz, 1H), 5.27 (d, *J* = 1.1 Hz, 1H), 5.09, (dd, *J* = 5.1, 1.6 Hz, 1H), 5.00 (d, *J* = 11.0 Hz, 1H), 4.89 (d, *J* = 11.0 Hz, 1H), 5.09 (dd, *J* = 5.1, 1.6 Hz, 1H), 5.00 (d, *J* = 11.0 Hz, 1H), 4.89 (d, *J* = 11.0 Hz, 1H), and 4.76 (d, *J* = 5.2 Hz, 1H); ^{13}C NMR (101 MHz, $CDCl_3$) δ 165.9, 136.8, 135.3, 133.1, 129.8, 129.2, 128.2, 92.1, 82.1, 78.3, and 56.9; IR (film) 3032, 2950, 2922, 2852, 1712 (s), 1455, 1369, 1213, 1189, 1059, 1023 cm^{-1}. HR-ESIMS requires for $C_{13}H_{12}ClNNaO_3$ $(M+Na)^+$ 288.0398, found 288.0391.

(±)-(3*S*, 4*R*)-*N*-phenylmethoxy-3-chloro-4-hydroxy-2,3,4,7-tetrahydro-1*H*-azepine (75)

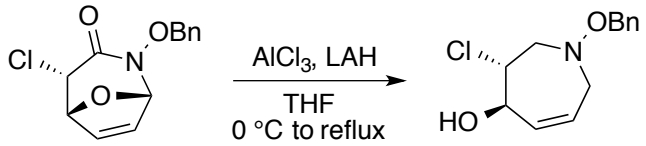

To an oven dried 100 mL Schlenk flask equipped with a magnetic stir bar was added dry THF (19 mL) under an atmosphere of nitrogen. The flask was placed in an ice bath and aluminum chloride (7.57 mmol, 1.01 g) was added in portions over a period of 5 minutes. Upon complete dissolution of the aluminum chloride, a solution of lithium aluminum hydride in dry THF (11.4 mmol, 5.7 mL) was added dropwise at that same temperature over a period of 15 minutes and the resulting solution was stirred at 0 °C for 20 minutes. The cycloadduct **74** (3.79 mmol, 1.01 g) was then added in THF (25 mL) dropwise over a period of 20 minutes and the reaction mixture was refluxed under nitrogen for 1.5 hours. The reaction flask was cooled to 0 °C and quenched with water followed by 10% NaOH. The aluminum salts were filtered off and the filtrate was dried over Na_2SO_4 and concentrated under reduced pressure. The crude residue was purified by column chromatography (10% - 33% Hex:EtOAc) to afford 0.67 g of **75** as a white crystalline solid (2.64 mmol, 70% yield). R_f = 0.54 (2:1 hexanes:ethyl acetate); M.P. 59.5 – 62.0 °C; ^{1}H NMR (500 MHz, $CDCl_3$): δ 7.35 – 7.30 (m, 5H), 5.81 (dt, *J* = 11.9, 3.1 Hz, 1H), 5.67 (dt, *J* = 12.0, 6.0 Hz, 1H), 4.69 (s, 2H), 4.36 (d, *J* = 8.2 Hz, 1H), 4.18 (td, *J* = 8.3, 4.7 Hz, 1H), 3.77 (dd, *J* = 14.1, 4.7 Hz, 1H), 3.62 (dd, *J* = 15.9, 6.2 Hz, 1H), 3.44 – 3.39 (m, 1H), 3.22 (dd, *J* = 14.0, 8.0 Hz, 1H), and 2.86 – 2.83 (m, 1H); ^{13}C NMR (101 MHz, $CDCl_3$): δ 137.20, 132.20, 128.71, 128.38, 128.03, 126.27, 74.64, 73.34, 64.26, 61.87, and 57.41; IR (neat) 3556, 3105 (br), 3006, 2987, 2965, 1464, 1376, 1055 (s), and 1037 cm^{-1}; HR-ESIMS requires for $C_{13}H_{17}ClNO_2$ $(M+H)^+$ 254.0948, found 254.0950.

(±)- (2*S*, 3*R*)-*N*-phenylmethoxy-2-azidomethyl-3-hydroxy-1,2,3,6-tetrahydropyridine (76)

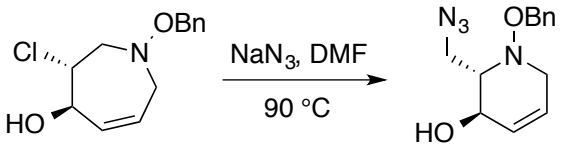

To a solution of **75** (4.94 mmol, 1.46 g) in DMSO (36 mL) was added sodium azide (28.8 mmol, 1.88 g) all at once and the resulting solution was stirred at 90 °C until TLC analysis indicated complete consumption of the starting material (3 days). The reaction was quenched with water and the aqueous layer was extracted with ethyl acetate (3 x 25 mL). The combined organic extracts were washed with water, brine, and then dried over anhydrous sodium sulfate. After concentration under reduced pressure the crude residue was purified by column chromatography to afford 1.05 g of azide **76** (4.03 mmol, 82% yield) as a pale yellow oil. R_f = 0.4 (2:1 hexanes:ethyl acetate); ^{1}H NMR (400 MHz, CD_3OD): δ 7.35 – 7.25 (m, 5H), 5.69 (t, *J* = 6.2 Hz, 1H), 5.62 (ddd, *J* = 9.9, 4.0, 1.9 Hz, 1H), 4.80 (s, 1H), 4.74 (d, *J* = 1.7 Hz, 2H), 4.21 (d, *J* = 9.6 Hz, 1H), 3.73 (d, *J* = 13.2 Hz, 1H), 3.65 – 3.57 (m, 2H), 3.31 (d, *J* = 15.3 Hz, 1H), and 2.72 (br s, 1H); ^{13}C NMR (101 MHz, CD_3OD): δ 137.16, 128.82, 128.56, 128.01, 127.67, 123.94, 74.72, 67.76, 65.05, 53.49, and 48.63; IR (neat) 3361 (br), 3087, 3063, 3031, 2919, 2872, 2822, 2094 (st), 1493, 1451, 1363, 1280, 1260, 1207, 1080, 1018, 909, 868, 844, and 741 cm^{-1}; HR-ESIMS requires for $C_{13}H_{16}N_4O_2$ $(M+H)^+$ 261.1346, found 261.1344.

(±)- (2*S*, 3*R*)-*N*-phenylmethoxy-2-((4-methoxybenzene)amido)-3-hydroxypiperidine (78)

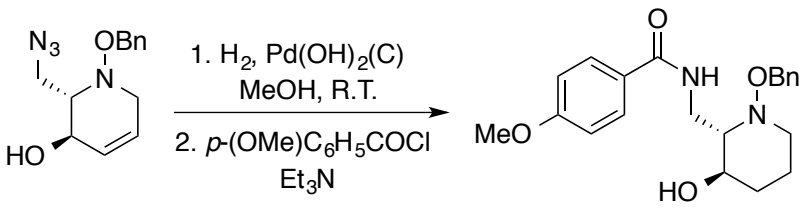

To a solution of **76** (2.0 mmol, 520 mg) in methanol (10 mL) was added palladium hydroxide on activated carbon (10 mol%, 5 mg) and the resulting black suspension was placed under an atmosphere of hydrogen (atmospheric pressure) and stirred at room temperature until TLC analysis indicated complete consumption of the starting material and appearance of a polar spot (4 hours). The reaction mixture was filtered over celite and the pad washed with methanol (3 x 10 mL) and then concentrated under reduced pressure. The resulting residue was then taken up in dichloromethane (20 mL) and triethylamine (2.4 mmol, 0.3 mL) and cooled to 0 °C. 4-methoxybenzoyl chloride was added dropwise and the reaction mixture was allowed to reach room temperature. When TLC analysis indicated complete consumption of the polar spot the solvent was removed under reduced pressure and the crude residue was purified by column chromatography (3:1 to 2:1 hexanes:ethyl acetate) to give 580 mg of **78** (1.6 mmol, 78% yield) as a yellow oil. R_f = 0.2 (1:1 hexanes:ethyl acetate); ^{1}H NMR (400 MHz, $CDCl_3$): δ 7.54 – 7.27 (m, 6H), 6.88 – 6.76 (m, 2H), 5.46 (s, 1H), 5.01 – 4.96 (m, 1H), 4.69 (dd, *J* = 12.1, 4.2 Hz, 1H), 4.57 (dd, *J* = 12.1, 4.1 Hz, 1H), 4.09 – 4.03 (m, 1H), 3.94 (ddt, *J* = 11.9, 7.5, 4.1 Hz, 1H), 3.79 (s, 3H), 3.48 – 3.40 (m, 2H), 3.13 (br s, 1H), 2.44 – 2.26 (m, 2H), 1.98 (d, *J* = 4.8 Hz, 1H), 1.91 – 1.84 (m, 1H), 1.70 (d, *J* = 9.2 Hz, 1H), 1.42 – 1.24 (m, 2H), and 1.20 (td, *J* = 7.1, 3.0 Hz, 1H); ^{13}C NMR (101 MHz, $CDCl_3$): δ 162.29, 138.22, 129.51, 129.04, 128.71, 128.31, 125.76, 122.62, 113.44, 73.19, 66.80, 60.31, 55.37, 37.01, 31.10, 20.98, and 14.17; IR (neat) 3420, (br), 3343 (br), 3028, 2939, 2860, 2833, 1631, 1605, 1534, 1496, 1457, 1443, 1298, 1251, 1177, 1098, 1030, 912, 844, and 768 cm^{-1}; HR-ESIMS requires for $C_{21}H_{27}N_2O_4$ $(M+H)^+$ 371.1965, found 371.1964.

(±)-(2*S*, 3*R*)-*N*-phenylmethoxy-2-((4-methoxybenzene)amido)-3-hydroxybenzoic acid piperidine (79)

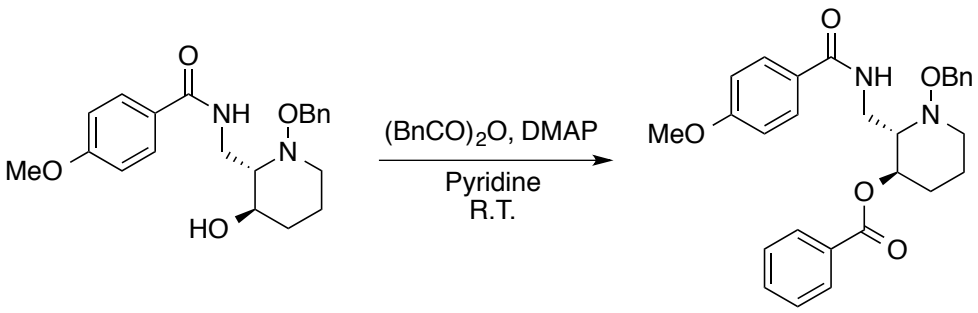

To a solution of **78** (0.7 mmol, 250 mg) in pyridine was added benzoic anhydride (1.4 mmol, 318 mg) and DMAP (20 mol%, 30 mg) and the resulting solution was stirred at room temperature overnight. Upon completion, the reaction was quenched with saturated sodium bicarbonate solution and extracted with ether (3 x 15 mL). The combined organic extracts were washed with water, brine, dried over anhydrous sodium sulfate, and concentrated under reduced pressure to give 273 mg of **79** (0.6 mmol, 82% yield) as a pale yellow oil that was used without further purification. R_f = 0.4 (2:1 hexanes:ethyl acetate); ^{1}H NMR (400 MHz, $CDCl_3$): δ 8.62 – 8.59 (m, 1H), 8.06 – 8.01 (m, 3H), 7.55 – 7.51 (m, 3H), 7.44 – 7.39 (m, 3H), 7.30 – 7.25 (m, 5H), 6.83 (d, *J* = 8.8 Hz, 2H), 4.72 (d, *J* = 7.5 Hz, 2H), 3.82 (s, 3H), 3.50 (d, *J* = 11.7 Hz, 1H), 2.63 (s, 1H), 2.23 (d, 11.3 Hz, 1H), 1.79 – 1.70 (m, 2H), and 1.50 – 1.40 (m, 1H); ^{13}C NMR (101 MHz, $CDCl_3$): δ 166.58, 161.86, 149.78, 135.92, 133.05, 132.85, 129.72, 129.53, 128.68, 128.55, 128.38, 128.31, 123.69, 113.48, 106.48, 55.33, 39.14, 38.13, and 29.65; IR (neat) 3063, 3031, 3007, 2945, 2860, 2836, 1717 (st), 1658, 1605, 1531, 1493, 1452, 1313, 1295, 1251, 1177, 1107, 1065, 1027, 989, 936, 912, 841, and 762 cm^{-1}; HR-ESIMS requires for $C_{28}H_{30}N_2O_5$ $(M+H)^+$ 475.2227, found 475.2224.

(±)-(6*R*, 7*R*, 5*R*, 1*S*)-4,4-dimethyl-6,7-dihydroxy-8-oxo-2-(phenylmethoxy)-2-azabicyclo[3.2.1]oct-3-one (85)

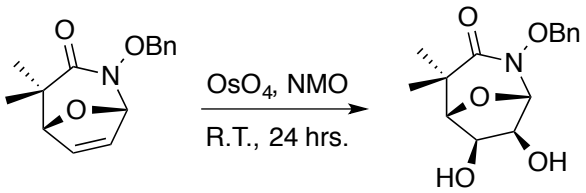

To a solution of **63** (3.86 mmol, 1.00g) in acetonitrile, water, and acetone (23 mL total, 1:1:1 v/v) at room temperature was added NMO (7.72 mmol, 0.8 mL, 50 wt% in H_2O) followed by an OsO_4 solution (5.02 mL of 1 wt% in H_2O). The reaction mixture was stirred overnight at that same temperature followed by filtering of the solution over a pad of celite. The pad was washed with ethyl acetate (3 x 15 mL) and the solvent removed under reduced pressure. The crude product was recrystallized from DCM:hexanes to give the pure diol 975 mg of **85** as light green crystals (3.32 mmol, 86% yield). R_f = 0.2 (1:1 hexanes:ethyl acetate); M.P. = 116.4 – 117.9 °C; ^{1}H NMR (500 MHz, $CDCl_3$): δ 7.45 – 7.34 (m, 5H), 4.96 (d, *J* = 10.6 Hz, 1H), 4.84 (d, *J* = 10.7 Hz, 1H), 4.82 (d, *J* = 1.0 Hz, 1H), 4.36 (dd, *J* = 5.2, 1.0 Hz, 1H), 4.22 (q, *J* = 6.2 Hz, 2H), 3.48 (s, 2H), 2.72 (dt, *J* = 9.4, 5.4 Hz, 1H), 1.27 (s, 3H), and 1.19 (s, 3H); ^{13}C NMR (126 MHz, $CDCl_3$): δ 169.19, 134.60, 129.67, 129.11, 128.66, 93.94, 85.53, 77.58, 74.02, 69.75, 47.49, 18.70, and 12.26; IR (neat) 3272 (br), 3031, 2992, 2969, 2928, 2869, 1690, 1658 (st), 1454, 1401, 1384, 1357, 1333, 1242, 1216, 1107, 1095, 1051, 1036 (st), 1009, 989, 933, 824, 765, 741, and 700 cm^{-1}; HR-ESIMS requires for $C_{15}H_{19}NO_5$ $(M+Na)^+$ 316.1155, found 316.1160.

(±)-(6*R*, 7*R*, 5*R*, 1*S*)-4,4-dimethyl-6,7-dimethyldioxolan-8-oxo-2-(phenylmethoxy)-2-azabicyclo[3.2.1]oct-3-one (86)

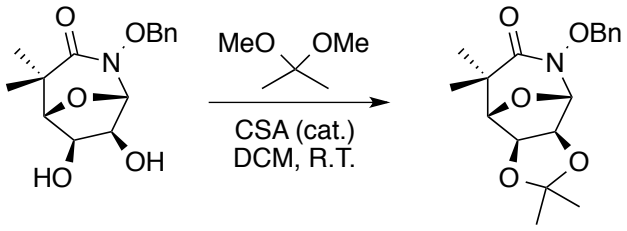

To a solution of **85** (8.3 mmol, 2.4 g) in dichloromethane (35.0 mL) and 2,2-dimethoxypropane (12.5 mmol, 1.5 mL) was added camphor-10-sulfonic acid (2 mol%, 39 mg) and the resulting solution was stirred at room temperature for 3 hours. The reaction mixture was quenched with saturated sodium bicarbonate and the aqueous layer was extracted with dichloromethane (3 x 25 mL). The combined organic layers were washed with brine, dried over anhydrous sodium sulfate, and concentrated under reduced pressure. The crude residue was purified by column chromatography (3:1 hexanes:ethyl acetate) to afford 1.86 g of **86** as a white crystalline solid (5.6 mmol, 96% yield). R_f = 0.5 (3:1 hexanes:ethyl acetate); M.P. = 101.3 °C; ^{1}H NMR (500 MHz, $CDCl_3$): δ 7.43 – 7.35 (m, 5H), 4.97 (d, *J* = 10.7 Hz, 1H), 4.87 (d, *J* = 10.7 Hz, 1H), 4.79 (s, 1H), 4.74 (d, *J* = 5.6 Hz, 1H), 4.69 (d, *J* = 5.6 Hz, 1H), 3.98 (s, 1H), 1.44 (s, 3H), 1.41 (s, 3H), 1.27 (s, 3H), and 1.19 (s, 3H); ^{13}C NMR (121 MHz, $CDCl_3$): δ 172.67, 134.81, 129.82, 129.09, 128.64, 112.82, 92.22, 89.23, 82.41, 79.05, 43.87, 27.37, 25.96, 24.86, and 19.54; IR (neat) 3034, 2984, 2931, 2869, 1672 (st), 1490, 1472, 1457, 1395, 1378, 1254, 1230, 1207, 1163, 1065 (st), 1045, 1009, 962, 892, 818, and 744 cm^{-1}; HR-ESIMS requires for $C_{18}H_{23}NO_5$ $(M+Na)^+$ 356.1468, found 356.1467.

(±)-(6*R*, 7*R*, 5*R*, 1*S*)-4,4-dimethyl-6,7-dimethyldioxolan-8-oxo-2-azabicyclo[3.2.1]oct-3-one (87)

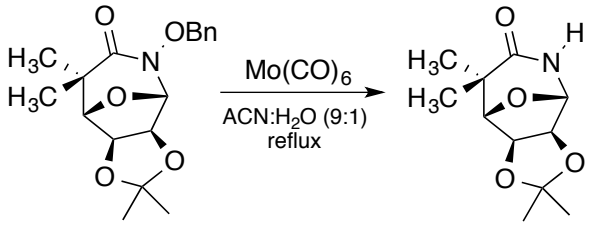

To a stirred solution of **86** (3.6 mmol, 1.2 g) degassed under nitrogen in ACN:H_2O (35.0 mL, 9:1 v/v) was added $Mo(CO)_6$ (4.32 mmol, 1.14 g) all at once and the resulting solution was degassed again. The reaction mixture was refluxed vigorously overnight followed by filtering through a pad of celite. The pad was washed with 3 x 20 mL portions of ethyl acetate and the filtrate was concentrated under reduced pressure. The crude residue was purified by column chromatography (1:1 hexanes:ethyl acetate) to afford 668 mg of the pure amide **87** as a white solid (2.94 mmol, 82% yield). R_f = 0.1 (1:1 hexanes:ethyl acetate); M.P. = 194.8 °C; ^{1}H NMR (500 MHz, $CDCl_3$): δ 6.87 (br s, 1H), 5.04 (d, *J* = 3.3 Hz, 1H), 4.87 (d, *J* = 5.6 Hz, 1H), 4.65 (d, *J* = 5.6 Hz, 1H), 4.04 (s, 1H), 1.48 (s, 3H), 1.40 (s, 3H), 1.32 (s, 3H), and 1.19 (s, 3H); ^{13}C NMR (121 MHz, $CDCl_3$) δ 174.70, 112.87, 88.67, 85.83, 85.51, 79.12, 42.27, 27.51, 26.10, 25.04, and 19.86; IR (neat) 3181 (br), 2989, 2975, 2945, 2877, 1672 (st), 1634, 1484, 1469, 1451, 1366, 1263, 1224, 1207, 1189, 1166, 1092, 1059 (st), 1042, 1015, 971, 933, 871, 836, 818, and 785 cm^{-1}; HR-ESIMS requires for $C_{11}H_{17}NO_4$ $(M+Na)^+$ 250.1055, found 250.1054.

(±)-(6*R*, 7*R*, 5*R*, 1*S*)-4,4-dimethyl-6,7-dimethyldioxolan-2,3,4,7-tetrahydro-1*H*-azepine (88)

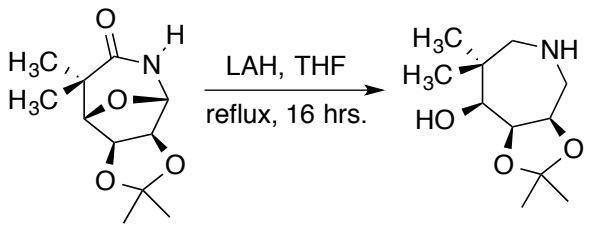

To a stirred solution of **87** (0.44 mmol, 100 mg) in dry THF (5 mL) at 0 °C was added a solution of LAH (1.76 mmol, 0.88 mL) in dry THF dropwise. Upon addition the ice bath was removed and the reaction mixture was refluxed overnight. Upon completion the reaction mixture was quenched with water and sodium hydroxide at 0 °C followed by filtration of the inorganic salts. The filtrate was dried over anhydrous magnesium sulfate, filtered, and concentrated under reduced pressure. The crude residue was purified by column chromatography (EtOAc:MeOH:Et_3N 2% MeOH, 1% Et_3N) to afford 78.4 mg of the pure azepane **88** as an opaque solid (0.36 mmol, 83% yield). X-ray quality crystals were grown by slow evaporation of a dichloromethane/hexanes solution of **88**. R_f = 0.3 (EtOAc:MeOH:Et_3N 2% MeOH, 1% Et_3N); M.P. = 126.9 °C; ^{1}H NMR (500 MHz, $CDCl_3$): δ 4.36 (dd, *J* = 7.8, 2.9 Hz, 1H), 4.30 (ddd, *J* = 10.5, 7.8, 5.5 Hz, 1H), 3.64 (d, *J* = 2.7 Hz, 1H), 3.10 (d, *J* = 10.0 Hz, 1H), 3.01 (dd, *J* = 12.8, 10.5 Hz, 1H), 2.34 (d, *J* = 13.0 Hz, 1H), 1.49 (s, 3H), 1.36 (s, 3H), 1.01 (s, 3H), and 0.98 (s, 3H); ^{13}C NMR (121 MHz, $CDCl_3$): δ 107.96, 78.07, 77.52, 56.11, 49.85, 37.47, 27.43, 26.61, 23.66, and 22.23; IR (neat) 3087 (br), 2984, 2954, 2916, 2866, 2845, 1466, 1451, 1378, 1354, 1266, 1213, 1168, 1145, 1104, 1060 (st), 1033, 1009, 978, 877, 827, and 809 cm^{-1}; HR-ESIMS requires for $C_{11}H_{21}NO_3$ $(M+H)^+$ 216.1594, found 216.1593.

(±)-(4*R*, 5*R*, 6*R*)-4,5,6-trihydroxy-3,3-dimethylazepane (89)

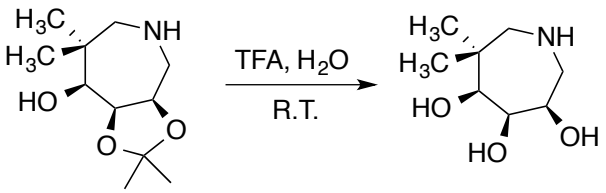

To a solution of trifluoroacetic acid (10 mL) and water (5 mL) was added **88** (0.23 mmol, 50 mg) and the resulting solution was stirred at room temperature for 3 hours. After removal of the volatiles under reduced pressure, the crude residue was ran through a short plug of silica gel (EtOAc:MeOH:Et_3N 20% MeOH, 1% Et_3N, eluent) and concentrated to give 35 mg of **89** as a colourless oil (0.2 mmol, 87% yield). R_f = 0.3 (EtOAc:MeOH:Et_3N 20% MeOH, 1% Et_3N); ^1H NMR (400 MHz, CD_3OD): δ 4.15 – 4.07 (m, 1H), 4.00 (t, *J* = 2.2 Hz, 1H), 3.51 (d, *J* = 2.0 Hz, 1H), 3.28 (dtd, *J* = 3.4, 2.0, 1.2 Hz, 1H), 3.25 (d, *J* = 4.6 Hz, 1H), 3.16 (d, *J* = 0.7 Hz, 1H), 2.87 (d, *J* = 13.8 Hz, 1H), 1.12 (s, 3H), and 1.07 (s, 3H); ^{13}C NMR (101 MHz, CD_3OD): δ 78.92, 74.95, 68.86, 53.33, 46.39, 36.50, 25.12, and 23.20; IR (neat) 3352 (br), 3090, 2975, 2913, 2880, 1666, 1472, 1425, 1198, 1177, 1089, 1062, 1012, 936, 836, 800, and 718 cm^{-1}; HR-ESIMS requires for $C_8H_{17}NO_3$ $(M+H)^+$ 176.1281, found 176.1282.

(±)-(1R, 5S)-4,4-dimethyl-8-oxo-2-azabicyclo[3.2.1]oct-6-en-3-one (90)

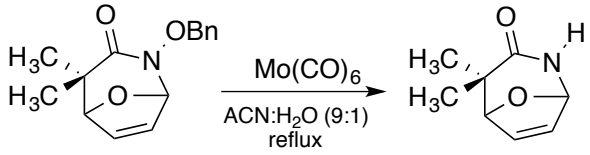

To a stirred solution of **63** (3.02 mmol, 783.5 mg) degassed under nitrogen in ACN:H_2O (20.1 mL, 9:1 v/v) was added $Mo(CO)_6$ (3.62 mmol, 957 mg) all at once and the resulting solution was degassed again. The reaction mixture was refluxed vigorously overnight followed by filtering through a pad of celite. The pad was washed with 3 x 15 mL portions of ethyl acetate and

the filtrate was concentrated under reduced pressure. The crude residue was purified by column chromatography (1:1 hexanes:ethyl acetate) to afford 420 mg of the pure amide **90** as a white solid (2.74 mmol, 91% yield). R_f = 0.1 (1:1 hexanes:ethyl acetate); M.P. = 130.5 – 133.5 °C; ^{1}H NMR (500 MHz, $CDCl_3$): δ 7.65 (s, 1H), 6.55 (dd, *J* = 6.0, 1.4 Hz, 1H), 6.40 (dd, *J* = 5.9, 1.9 Hz, 1H), 5.44 (dd, *J* = 3.0, 1.4 Hz, 1H), 4.50 (d, *J* = 1.9 Hz, 1H), 1.46 (s, 3H), and 1.04 (s, 3H); ^{13}C NMR (101 MHz, $CDCl_3$): δ 176.17, 136.80, 132.08, 86.26, 84.65, 47.21, 27.29, and 19.79; IR (neat) 3163 (br), 3053, 2998, 2961, 2933, 2903, 2872, 1647 (st), 1473, 1460, 1393, 1356, 1326, 1262, 1246, 1179, 1048, 944, 892, 852, and 742 cm^{-1}; HR-ESIMS requires for $C_8H_{11}NO_2$ $(M+Na)^+$ 176.0682, found 176.0682.

(±)-4-hydroxy-3,3-dimethyl-2,4,7-trihydro-1*H*-azepine (91)

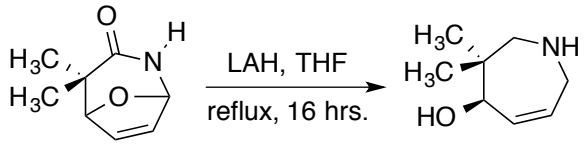

To a solution of **90** (0.71 mmol, 100 mg) in dry THF (3 mL) at 0 °C was added a solution of LAH (2.84 mmol, 1.42 mL) in dry THF dropwise. The ice bath was removed and the reaction mixture was refluxed overnight under a nitrogen atmosphere. Upon completion, the reaction was quenched with water and 10% NaOH. The inorganic salts were filtered and the filtrate was dried over anhydrous sodium sulfate followed by concentration under reduced pressure. The crude residue was purified by flash chromatography (EtOAc:MeOH:Et_3N 10% MeOH, 1% Et_3N) to afford 82 mg of azepine **91** as a light brown oil (0.6 mmol, 82% yield). (R_f = 0.3 (ethyl acetate, 10 % methanol, 1% triethylamine); ^{1}H NMR (400 MHz, $CDCl_3$): δ 5.99 – 5.92 (m, 1H), 5.65 (dtd, *J* = 11.5, 3.9, 0.8 Hz, 1H), 3.74 (d, *J* = 6.3 Hz, 1H), 3.59 – 3.52 (m, 1H), 3.42 (s, 2H), 3.36 – 3.28 (m, 1H), 2.91 (dd, *J* = 13.6, 1.0 Hz, 1H), 2.58 (d, *J* = 13.6 Hz, 1H), 1.09 (s, 3H), and 0.84 (s, 3H); ^{13}C NMR (101 MHz, $CDCl_3$): δ 133.54, 129.73, 76.32, 60.18, 50.70, 39.74, 26.23, and

25.16; IR (neat) 3308 (br), 3022, 2948, 2901, 2866, 1646, 1622, 1454, 1407, 1384, 1360, 1307, 1278, 1216, 1121, 1042 (st), 1021, 956, and 871 cm^{-1}; HR-ESIMS requires for $C_8H_{15}NO$ $(M+H)^+$ 142.1226, found 142.1224.

(±)-(4*R*, 5*R*, 6*R*)-4,5,6-trihydroxy-3,3-dimethylazepane (89)

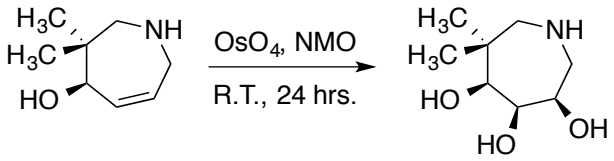

Osmium tetroxide (0.5 mL of a 1 wt% solution in water) and NMO (0.71 mmol, 0.1 mL) were added to a stirred solution of **91** (0.35 mmol, 50 mg) in acetonitrile, water, and acetone (2.1 mL, 1:1:1 v/v) and the resulting reaction mixture was stirred under nitrogen overnight. The reaction mixture was filtered over celite and the pad washed with methanol (3 x 10 mL) followed by concentration under reduced pressure. The residue was passed through a plug of silica gel (EtOAc:MeOH:Et_3N 20% MeOH, 1% Et_3N, eluent) followed by concentration to give 49.5 mg of **89** as a colourless oil (0.28 mmol, 81% yield). R_f = 0.3 (EtOAc:MeOH:Et_3N 20% MeOH, 1% Et_3N); ^1H NMR (400 MHz, CD_3OD): δ 4.15 – 4.07 (m, 1H), 4.00 (t, *J* = 2.2 Hz, 1H), 3.51 (d, *J* = 2.0 Hz, 1H), 3.28 (dtd, *J* = 3.4, 2.0, 1.2 Hz, 1H), 3.25 (d, *J* = 4.6 Hz, 1H), 3.16 (d, *J* = 0.7 Hz, 1H), 2.87 (d, *J* = 13.8 Hz, 1H), 1.12 (s, 3H), and 1.07 (s, 3H); ^{13}C NMR (101 MHz, CD_3OD): δ 78.92, 74.95, 68.86, 53.33, 46.39, 36.50, 25.12, and 23.20; IR (neat) 3352 (br), 3090, 2975, 2913, 2880, 1666, 1472, 1425, 1198, 1177, 1089, 1062, 1012, 936, 836, 800, and 718 cm^{-1}; HR-ESIMS requires for $C_8H_{17}NO_3$ $(M+H)^+$ 176.1281, found 176.1282.

(±)-(4R, 5R, 1S)-4-chloro-8-oxo-2-(hydroxy)-2-azabicyclo[3.2.1]oct-3-one (92)

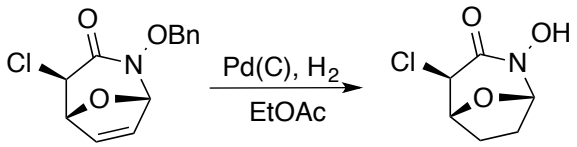

To a solution of **66f** (4.22 mmol, 1.12 g) in ethyl acetate (21.1 mL) was added palladium on activated carbon (10% by mass, 0.11 g) and the resulting suspension was evacuated under vacuum and hydrogenated at atmospheric pressure for 30 minutes. The reaction mixture was filtered over a pad of celite and the pad washed with 3 x 10 mL portions of ethyl acetate to give 675 mg of hydroxamic acid **92** (3.8 mmol, 90% yield) as an orange solid that was used without any further purification. R_f = 0.1 (1:1 hexanes:ethyl acetate); M.P. = Decom. ^{1}H NMR (500 MHz, $CDCl_3$): δ 9.74 (br s, 1H), 6.10 (s, 1H), 5.41 (d, *J* = 4.1 Hz, 1H), 4.77 (d, *J* = 2.7 Hz, 2H), 2.55 (ddd, *J* = 12.4, 9.4, 2.7 Hz, 1H), 2.33 – 2.24 (m, 1H), 2.15 (dddd, *J* = 13.2, 11.1, 6.2, 2.7 Hz, 1H), and 2.05 (tdd, *J* = 11.7, 6.7, 4.0 Hz, 1H); ^{13}C NMR (126 MHz, $CDCl_3$): δ 162.66, 91.25, 78.77, 64.11, 56.28, 32.13, and 22.19; IR (neat) 3072 (br), 3031, 2998, 2951, 2842, 1646 (st), 1501, 1460, 1437, 1354, 1289, 1245, 1204, 1142, 1068, 1042, 947, 921, 838, 782, 724, and 656 cm^{-1}; HR-ESIMS requires for $C_6H_8ClNO_3$ $(M+Na)^+$ 200.0085, found 200.0087.

(±)-(4*S*, 6*R*, 7*R*, 5*R*, 1*S*) 4-chloro-6,7-dihydroxy-8-oxo-2-(phenylmethoxy)-2-azabicyclo[3.2.1]oct-3-one (93)

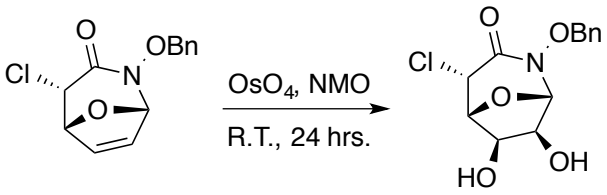

To a solution of **66f** *endo* (1.0 mmol, 275.3 mg) in acetonitrile, water, and acetone (6 mL total, 1:1:1 v/v) at room temperature was added NMO (2.0 mmol, 0.24 mL, 50 wt% in H_2O)

followed by an OsO_4 solution (1.3 mL of 1 wt% in H_2O). The reaction mixture was stirred overnight at that same temperature followed by filtering of the solution over a pad of celite. The pad was washed with ethyl acetate (3 x 10 mL) and the solvent removed under reduced pressure. The crude product was recrystallized from dichloromethane:hexanes to give 255 mg of the pure diol **93** as a colourless oil (0.85 mmol, 85% yield). R_f = 0.3 (1:1 hexanes:ethyl acetate); ^{1}H NMR (500 MHz, $CDCl_3$): δ 7.38 (tdd, *J* = 7.0, 3.3, 1.4 Hz, 5H), 4.98 (dd, *J* = 10.6, 1.2 Hz, 1H), 4.90 – 4.85 (m, 1H), 4.59 (dd, *J* = 5.4, 1.3 Hz, 1H), 4.55 (t, *J* = 6.1 Hz, 1H), 4.47 (dd, *J* = 5.4, 1.2 Hz, 1H), 4.24 (td, *J* = 6.0, 1.4 Hz, 1H), 4.10 (qd, *J* = 7.2, 1.5 Hz, 1H), and 3.72 (ddd, *J* = 15.5, 10.1, 5.7 Hz, 1H); ^{13}C NMR (121 MHz, $CDCl_3$): δ 161.88, 133.65, 129.97, 129.50, 128.80, 93.72, 87.90, 73.17, 71.20, and 55.10; IR (neat) 3408 (br), 3378, 3057, 3001, 2981, 2954, 2922, 1702 (st), 1440, 1369, 1339, 1295, 1233, 1210, 1101, 1001, 945, 906, 838, 753, 715, and 659 cm^{-1}; HR-ESIMS requires for $C_{13}H_{14}ClNO_5$ $(M+Na)^+$ 322.0453, found 322.0452.

(±)-(4*S*, 6*R*, 7*R*, 5*R*, 1*S*) 4-chloro-6,7-dimethyldioxolan-8-oxo-2-(phenylmethoxy)-2-azabicyclo[3.2.1]oct-3-one (94)

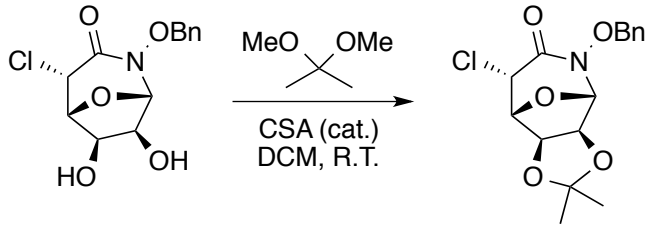

To a solution of **93** (2.12 mmol, 740 mg) in dichloromethane (10.0 mL) and 2,2-dimethoxypropane (4.24 mmol, 0.4 mL) was added camphor-10-sulfonic acid (2 mol%, 10 mg) and the resulting solution was stirred at room temperature for 3 hours. The reaction mixture was quenched with saturated sodium bicarbonate and the aqueous layer was extracted with dichloromethane (3 x 10 mL). The combined organic layers were washed with brine, dried over anhydrous sodium sulfate, and concentrated under reduced pressure. The crude residue was

purified by column chromatography (3:1 hexanes:ethyl acetate) to afford 670 mg of **94** as a white crystalline solid (0.82 mmol, 95% yield). R_f = 0.5 (3:1 hexanes:ethyl acetate); M.P. = 112.3 – 114.1 °C; ^{1}H NMR (500 MHz, $CDCl_3$): δ 7.45 – 7..37 (m, 5H), 5.03 (d, *J* = 10.8 Hz, 1H), 4.96 (d, *J* = 5.7 Hz, 1H), 4.92 (d, *J* = 10.8 Hz, 1H), 4.90 (t, *J* = 0.5 Hz, 1H), 4.70 (d, *J* = 5.7 Hz, 1H), 4.65 (d, *J* = 5.6 Hz, 1H), 4.58 (dd, *J* = 5.6, 0.6 Hz, 1H), 1.45 (d, *J* = 0.9 Hz, 3H), 1.29 (d, *J* = 0.9 Hz, 3H); ^{13}C NMR (101 MHz, $CDCl_3$): δ 163.15, 134.45, 130.37, 129.39, 128.08, 113.31, 93.38, 83.21, 81.75, 79.34, 53.83, 52.60, 26.25, and 25.44; IR (neat) 3031, 2987, 2945, 2895, 1699 (st), 1496, 1463, 1454, 1381, 1333, 1278, 1242, 1204, 1157, 1092 (st), 1071, 1048, 1012, 986, 965, 945, 909, 862, 853, 812, and 700 cm^{-1}; HR-ESIMS requires for $C_{16}H_{18}ClNO_5$ $(M+H)^+$ 340.0946, found 340.0949.

(±)-(4*S*, 6*R*, 7*R*, 5*R*, 1*S*) 4-ethyl-6,7-dihydroxy-8-oxo-2-(phenylmethoxy)-2-azabicyclo[3.2.1]oct-3-one (95)

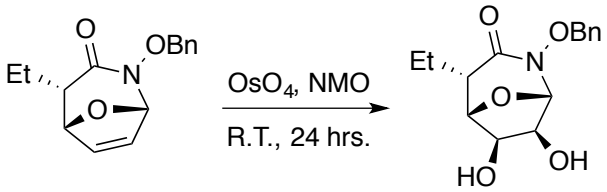

To a solution of **66c** (3.86 mmol, 1.00g) in acetonitrile, water, and acetone (23 mL total, 1:1:1 v/v) at room temperature was added NMO (7.72 mmol, 0.8 mL, 50 wt% in H_2O) followed by an OsO_4 solution (5.02 mL of 1 wt% in H_2O). The reaction mixture was stirred overnight at that same temperature followed by filtering of the solution over a pad of celite. The pad was washed with ethyl acetate (3 x 15 mL) and the solvent removed under reduced pressure. The crude product was recrystallized from DCM:hexanes to give 975 mg of the pure diol **95** as light green crystals (3.32 mmol, 86% yield). R_f = 0.2 (1:1 hexanes:ethyl acetate); M.P. = 116.4 – 117.9 °C; ^{1}H NMR (500 MHz, $CDCl_3$): δ 7.45 – 7.34 (m, 5H), 4.96 (d, *J* = 10.6 Hz, 1H), 4.84 (d, *J* =

10.7 Hz, 1H), 4.82 (d, *J* = 1.0 Hz, 1H), 4.36 (dd, *J* = 5.2, 1.0 Hz, 1H), 4.22 (q, *J* = 6.2 Hz, 2H), 3.48 (s, 2H), 2.72 (dt, *J* = 9.4, 5.4 Hz, 1H), 2.06 (dqd, *J* = 15.3, 7.7, 5.4 Hz, 1H), 1.37 – 1.25 (m, 1H), and 1.04 (t, 3H); ^{13}C NMR (126 MHz, $CDCl_3$): δ 169.19, 134.60, 129.67, 129.11, 128.66, 93.94, 85.53, 77.58, 74.02, 69.75, 47.49, 18.70, and 12.26; IR (neat) 3272 (br), 3031, 2992, 2969, 2928, 2869, 1690, 1658 (st), 1454, 1401, 1384, 1357, 1333, 1242, 1216, 1107, 1095, 1051, 1036 (st), 1009, 989, 933, 824, 765, 741, and 700 cm^{-1}; HR-ESIMS requires for $C_{15}H_{19}NO_5$ $(M+Na)^+$ 316.1155, found 316.1160.

(±)-(4*S*, 6*R*, 7*R*, 5*R*, 1*S*) 4-ethyl-6,7-dimethyldioxolan-8-oxo-2-(phenylmethoxy)-2-azabicyclo[3.2.1]oct-3-one (96)

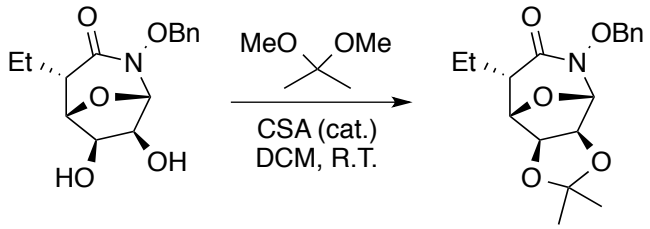

To a solution of **95** (0.871 mmol, 255.4 mg) in dichloromethane (2.0 mL) and 2,2-dimethoxypropane (1.31 mmol, 0.16 mL) was added camphor-10-sulfonic acid (2 mol%, 4 mg) and the resulting solution was stirred at room temperature for 3 hours. The reaction mixture was quenched with saturated sodium bicarbonate and the aqueous layer was extracted with dichloromethane (3 x 5 mL). The combined organic layers were washed with brine, dried over anhydrous sodium sulfate, and concentrated under reduced pressure. The crude residue was purified by column chromatography (3:1 hexanes:ethyl acetate) to afford 275 mg of **96** as a white crystalline solid (0.82 mmol, 95% yield). R_f = 0.5 (3:1 hexanes:ethyl acetate); M.P. = 111.3 – 114.1 °C; ^{1}H NMR (500 MHz, $CDCl_3$): δ 7.49 – 7.33 (m, 5H), 5.00 (dd, *J* = 10.6, 0.6 Hz, 1H), 4.87 (d, *J* = 5.6 Hz, 1H), 4.85 (s, 1H), 4.71 (d, *J* = 5.7 Hz, 1H), 4.63 (d, *J* = 5.7 Hz, 1H), 4.45 (d, *J* = 5.4 Hz, 1H), 2.76 (dt, *J* = 9.4, 5.5 Hz, 1H), 2.17 – 2.05 (m, 1H), 1.45 (s, 3H), 1.34 (dtd, *J* =

15.1, 7.1, 2.1 Hz, 1H), 1.27 (s, 3H), and 1.07 (t, J = 7.5 Hz, 3H); ^{13}C NMR (101 MHz, $CDCl_3$): δ 169.43, 134.91, 129.60, 128.97, 128.62, 112.76, 92.05, 82.96, 78.56, 47.02, 25.87, 24.72, 18.70, and 12.30; IR (neat) 2995, 2981, 2966, 2936, 2872, 1687 (st), 1460, 1448, 1378, 1348, 1333, 1269, 1233, 1207, 1157, 1080 (st), 1051, 1018, 986, 974, 900, 862, 812, 750, and 691 cm^{-1}; HR-ESIMS requires for $C_{18}H_{23}NO_5$ $(M+H)^+$ 334.1649, found 334.1659.

(±)-(4*S*, 3*R*, 6*R*, 7*R*, 5*R*, 1*S*) 4-ethyl-3-hydroxy-6,7-dimethyldioxolan-8-oxo-2-(phenylmethoxy)-2-azabicyclo[3.2.1]octane (97)

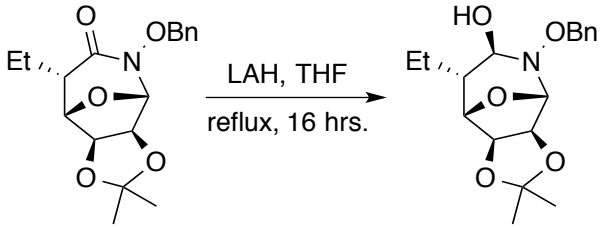

To a solution of LAH (3.0 mmol, 114 mg) in dry THF under a nitrogen atmosphere at 0 °C was added **96** dropwise over a period of 10 minutes. The reaction mixture was then refluxed overnight followed by cooling to 0 °C. The reaction was quenched with water and 10% sodium hydroxide, filtered, and dried over anhydrous Na_2SO_4. The solvent was removed under reduced pressure and the crude residue was recrystallized from hexanes to give **97** as a white solid (1.2 mmol, 402 mg, 80% yield). X-ray quality crystals were grown by slow evaporation of a dichloromethane/hexanes solution of **93**. R_f = 0.4 (2:1 hexanes:ethyl acetate); M.P. = 64.6 – 66.4 °C; ^{1}H NMR (400 MHz, $CDCl_3$): δ 7.40 – 7.30 (m, 5H), 4.86 (s, 1H), 4.81 (s, 2H), 4.51 (d, J = 5.7 Hz, 1H), 4.25 (d, J = 3.7 Hz, 1H), 3.73 (dd, J = 9.4, 7.6 Hz, 1H), 1.80 – 1.70 (m, 2H), 1.48 (s, 3H), 1.32 (s, 3H), and 0.99 (t, J = 7.4 Hz, 3H); ^{13}C NMR (101 MHz, $CDCl_3$): δ 136.85, 129.02, 128.54, 128.34, 111.78, 82.19, 81.57, 78.42, 75.56, 42.22, 25.95, 24.65, 20.46, 19.76, 11.93, and 11.25; IR (neat) 3154 (br), 3031, 2936, 2925, 1702, 1678, 1499, 1481, 1451, 1378, 1257, 1080,

980, 815, 765, and 729 cm^{-1}; HR-ESIMS requires for $C_{18}H_{25}NO_5$ $(M+H)^+$ 336.1805, found 336.2492.

(±)-(3*S*, 4*R*, 5*R*, 6*R*)-*N*-phenylmethoxy-3-chloro-4-hydroxy-5-isopropyloxy-6-hydroxy-azepane (98)

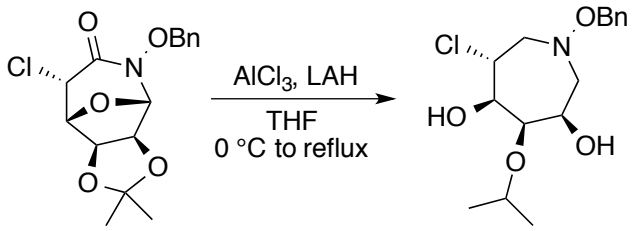

To an oven dried 100 mL Schlenk flask equipped with a magnetic stir bar was added dry THF (25 mL) under an atmosphere of nitrogen. The flask was placed in an ice bath and aluminum chloride (5.3 mmol, 704 mg) was added in portions over a period of 10 minutes. Upon complete dissolution of the aluminum chloride, a solution of lithium aluminum hydride in dry THF (7.9 mmol, 4.0 mL) was added dropwise at that same temperature over a period of 15 minutes and the resulting solution was stirred at 0 °C for 20 minutes. The acetal-protected diol **90** (2.6 mmol, 895 mg) was then added in THF (10 mL) dropwise over a period of 20 minutes and the reaction mixture was refluxed under nitrogen for 1.5 hours. The reaction flask was cooled to 0 °C and quenched with water followed by 10% NaOH. The aluminum salts were filtered off and the filtrate was dried over Na_2SO_4 and concentrated under reduced pressure. The crude residue was purified by column chromatography (3:1 – 2:1 Hex:EtOAc) to afford **94** as a white crystalline solid (2.2 mmol, 730 mg, 84% yield). R_f = 0.2 (2:1 hexanes:ethyl acetate); M.P. 70.4 – 75.8 °C; ^{1}H NMR (500 MHz, $CDCl_3$): δ 7.39 – 7.29 (m, 5H), 4.69 (d, *J* = 2.8 Hz, 2H), 4.15 (ddd, *J* = 7.2, 5.3, 4.2 Hz, 1H), 4.08 – 4.05 (m, 1H), 3.89 (td, *J* = 6.8, 2.1 Hz, 1H), 3.64 (ddd, *J* = 8.0, 5.9, 2.2 Hz, 1H), 3.61 (d, *J* = 5.5 Hz, 1H), 3.60 – 3.57 (m, 1H), 3.39 (dd, *J* = 15.1, 5.9 Hz, 1H), 3.19 (dd, *J* = 11.3, 5.8 Hz, 1H), 3.05 (dd, *J* = 12.3, 7.6 Hz, 1H), 2.97 (d, *J* = 6.8 Hz, 1H), and 1.13 (dd, *J* =

9.8, 6.1 Hz, 1H); ^{13}C NMR (126 MHz, $CDCl_3$): δ 137.22, 128.99, 128.35, 128.04, 77.54, 75.10, 74.61, 73.13, 71.07, 63.09, 61.58, 59.63, 22.69, and 22.27; IR (neat) 3305 (br), 3087, 3060, 2972, 2925, 2889, 2845, 1496, 1454, 1366, 1322, 1269, 1222, 1157, 1121, 1080, 1018 (st), 968, 921, 862, 735, and 694 cm^{-1}; HR-ESIMS requires for $C_{16}H_{24}ClNO_4$ $(M+Na)^+$ 352.1286, found 352.1256.

(±)-(2*S*, 3*R*)-*N*-phenylmethoxy-2-acetoxymethyl-3-hydroxy-1,2,3,6-tetrahydropyridine (100)

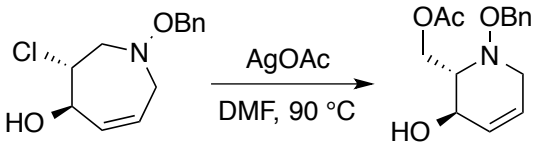

To a stirred solution of **75** (1.0 mmol, 250 mg,) in DMF (12 mL) was added AgOAc (2.0 mmol, 334 mg,) all at once and the resulting suspension was heated in a sealed flask at 90 °C for 72 hours. The crude reaction mixture was filtered through a pad of celite and the pad was washed with ethyl acetate (2 x 15 mL) followed by methanol (15 mL). The filtrate was concentrated under reduced pressure at 65 °C to remove DMF and the crude residue was purified by column chromatography (33% to 50% hexanes:ethyl acetate) to afford 224 mg of **100** as a pale yellow oil (0.81 mmol, 60% yield). R_f = 0.33 (1:1 hexanes:ethyl acetate); ^{1}H NMR (500 MHz, CD_3OD): δ 7.34 – 7.24 (m, 5H), 5.74 – 5.66 (m, 2H), 4.83 (s, 1H), 4.70 (d, *J* = 10.7 Hz, 1H), 4.65 (d, *J* = 10.6 Hz, 1H), 4.48 (d, *J* = 12.7 Hz, 1H), 4.40 (dd, *J* = 11.5, 5.0 Hz, 1H), 4.24 (dd, *J* = 8.3, 3.6 Hz, 1H), 3.66 (d, *J* = 15.8 Hz, 1H), 3.39 – 3.32 (m, 1H), 2.81 (s, 1H), and 2.05 (s, 3H); ^{13}C NMR (101 MHz, CD_3OD): δ 171.54, 137.13, 128.78, 128.60, 127.90, 127.60, 123.97, 74.88, 66.99, 64.61, 60.89, 53.67, and 19.49; IR (neat) 3405 (br), 3034, 2917, 2860, 1736, 1451, 1363, 1236, 1024, and 698 cm^{-1}; HR-ESIMS requires for $C_{15}H_{19}NO_4$ $(M+H)^+$ 278.1387, found 278.1384.

3.5 References

1. Newton, A.C. *Annu. Rev. Biophys. Biomol. Struct.* **1993**, *22*, 1.
2. Farago, A.; Nishizuka, Y. *FEBS Lett.* **1990**, *268*, 350.
3. Stabel, S.; Parker, P.J. *Pharmacol. Ther.* **1991**, *51*, 71.
4. Nishizuka, Y. *Nature* **1984**, *308*, 693.
5. Nishizuka, Y. *Science* **1986**, *233*, 305.
6. Nishizuka, Y. *Nature* **1988**, *334*, 661.
7. Nishizuka, Y. *Science* **1992**, *258*, 607.
8. Bradshaw, D.; Hill, C.H.; Nixon, J.S.; Wilkinson, S.E. *Agents Actions* **1993**, *38*, 135.
9. Kulanthaivel, P.; Hallock, Y.F.; Boros, C.; Hamilton, S.M.; Janzen, W.P.; Lawrence, M.B.; Loomis, C.R.; Jiang, J.B. *J. Am. Chem. Soc.* **1993**, *115*, 6452.
10. Ohshima, S.; Okuda, T. *J. Antibiot. (Tokyo)* **1994**, *47*, 639.
11. Nicolaou, K.C.; Bunnage, M.E.; Koide, K. **1994**, *116*, 8402.
12. Lampe, J.W.; Hughes, P.F.; Biggers, C.K.; Smith, S.H.; Hu, H. *J. Org. Chem.* **1994**, *59*, 5147.
13. Nicolaou, K.C.; Koide, K.; Bunnage, M.E. *Chem. Eur. J.* **1995**, *1*, 454.
14. Mellor, H.R.; Neville, D.C.A.; Harvey, D.J.; Platt, F.M.; Dwek, R.A.; Butters, T.D. *Biochem. J.* **2004**, *381*, 861.
15. Davis, B.G. *Tetrahedron: Asymmetry* **2009**, *20*, 652.
16. Shrivastava, A.; Chaturvedi, U.; Singh, C.V.; Saxena, J.K.; Bhatia, G. *Lipids* **2013**, *48*, 597.
17. (a) van Giersbergen, P.L.; J. Dingemanse, J. *J. Clinical Pharm.* **2007**, *47*, 1277. (b) Cox, T. *J. Inherit Metabol. Diseases,* **2003**, *26,* 513. (c) Kolodny, E.H.; Neudorfer, O.; Gianutsos, J.; Zaroff, C.; Barnett, N.; Zeng, B.J.; Raghavan, S.; Torres, P.; and Pastores, G.M. *J. Neurochemistry* **2004**, *90,* 54.

18. Horne, G.; Wilson, F.X.; Tinsley, J.; Williams, D.H.; Storer, R. *Drug Discovery Today* **2011**, *16*, 107.

19. Mellor, H.R. *Biochem. J.* **2004**, *381*, 861.

20. *Iminosugars: From Synthesis to Therapeutic Applications*; Compain, P., Martin, O.R. Eds.; Wiley-VCH: Weinheim, 2007.

21. Nishimura, Y. In *Iminosugars, from Synthesis to Therapeutic Applications;* Compain, P., Martin, O.R., Eds.; Wiley-VCH: Weinheim, 2007; pp 269-294.

22. Somsak, L.; Nagy, V.; Hadazy, Z.; Docsa, T.; Gergely, P. *Curr. Pharm. Des.* **2003**, *9*, 1177.

23. (a) Greimel, P.; Spreitz, J.; Stutz, A.E.; Wrodnigg, T.M. *Curr. Top. Med. Chem.* **2003**, *3*, 513. (b) Robina, L.; Moreno-Vargas, A.J.; Carmona, A.T.; Vogel, P. *Curr. Drug. Met.* **2004**, *5*, 329. (c) Norton, P.A.; Baohua, G.; Block, T.M. in *Iminosugars, from Synthesis to Therapeutic Applications;* Compain, P., Martin, O.R., Eds.; Wiley-VCH: Weinheim, 2007; pp 209-224.

24. (a) Butters, T.D.; Dwek, R.A.; Platt, F.M. *Chem. Rev.* **2000**, *100*, 4683. (b) Butters, T.D.; Dwek, R.A.; Platt, F.M. *Glycobiology* **2005**, *10*, 43R.

25. Norez, C.; Noel, S.; Wilke, M.; Bijvelds, M.; Jorna, H.; Melin, P.; DeJonge, H.; Becq, F. *FEBS Lett.* **2006**, *580*, 2081.

26. Paulsen, H.; Todt, K.; *Chem. Ber.* **1967**, *100*, 512.

27. a) Andreana, P.R.; Sanders, T.; Janczuk, A.; Warrick, J.I.; Wang, P.G. *Tetrahedron Lett*. **2002**, *43*, 6525. (b) Joseph, C.C.; Regeling, H.; Zwanenburg, B.; Chittenden, G.J.F. *Tetrahedron* **2002**, *58*, 6907. (c) Fuentes, J.; Gasch, C.; Olano, D.; Pradera, M.Á.; Repetto, G.; Sayago, F.J. *Tetrahedron: Asymmetry* **2002**, *13*, 1743. (d) Tilekar, J.N.; Patil, N.T.; Jadhav, H.S.; Dhavale, D.D. *Tetrahedron* **2003**, *59*, 1873. (e) Dhavale, D.D.; Chaudhari, V.D.; Tilekar, J.N. *Tetrahedron Lett*. **2003**, *44*, 7321. (f) Painter, G.F.;

Eldridge, P.J.; Falshaw, A. *Bioorg. Med. Chem.* **2004**, *12*, 225. (g) Moutel, S.; Shipman, M.; Martin, O.R.; Ikeda, K.; Asano, N. *Tetrahedron: Asymmetry* **2005**, *16*, 487 and references cited therein.

28. (a) Li, H.Q.; Bleŕiot, Y.; Chantereau, C.; Mallet, J.M.; Sollogoub, M.; Zhang,Y.M.; Rodríguez-García,E.; Vogel,P.; Jimeńez- Barbero, J.; Sinay¨, P. *Org. Biomol. Chem.* **2004**, *2*, 1492. (b) Dhavale, D.D.; Markad, S.D.; Karanjule, N.S.; PrakashaReddy, J. *J. Org. Chem.* **2004**, *69*, 4760. (c) Li, H.Q.; Schütz, C.; Favre, S.; Zhang, Y.M.; Vogel, P.; Sinay¨, P.; Bleŕiot,Y. *Org. Biomol. Chem.* **2006**, *4*, 1653.

29. (a) Mehta, G.; Lakshminath, S. *Tetrahedron Lett.* **2002**, *43*, 331. (b) Li, H.Q.; Zhang, Y.M.; Vogel, P.; Sinay¨, P.; Bleŕiot, Y. *Chem. Commun.* **2007**, *183*. (c) Jabgunde, A.M.; Kalamkar, N.B.; Chavan, S.T.; Sabharwal, S.G.; Dhavale, D.D. *Bioorg. Med. Chem.* **2011**, *19*, 5912. (d) Deschamp, J.; Mondon, M.; Nakagawa, S.; Kato, A.; Alonzi, D.S.; Butters, T.D.; Zhang, Y.M.; Sollogoub, M.; Bleŕiot, Y. *Bioorg. Med. Chem.* **2012**, *20*, 641.

30. (a) Li, H.Q.; Marcelo, F.; Bello, C.; Vogel, P.; Butters, T.D.; Rauter, A.P.; Zhang, Y.M.; Sollogoub, M.; Bleŕiot, Y. *Bioorg.Med. Chem.* **2009**, *17*, 5598. (b) Marcelo, F.; He, Y.; Yuzwa, S.A.; Nieto, L.; Jimeńez-Barbero, J.; Sollogoub, M.; Vocadlo, D.J.; Davies, G.D.; Bleŕiot, Y. *J. Am. Chem. Soc.* **2009**, *131*, 5390.

31. (a) Bande, O.P.; Jadhav, V.H.; Puranik, V.G.; Dhavale, D.D. *Tetrahedron: Asymmetry* **2007**, *18*, 1176. (b) Bande, O.P.; Jadhav, V.H.; Puranik, V.G.; Dhavale, D.D. *Synlett* **2009**, 1959. (c) Lindsay, K.B.; Pyne, S.G. *Tetrahedron* **2004**, *60*, 4173. (d) Markad, S.D.; Karanjule, N.S.; Sharma, T.; Sabharwal, S.G.; Puranik, V.G.; Dhavale, D.D. *Org. Biomol. Chem.* **2006**, *4*, 2549. (e) Torres-Sańchez, M.I.; Borrachero, P.; Cabrera-Escribano, F.; Gomez-Guilleń, M.; Angulo- Álvarez, M.; Dianez, M.J.; Estrada, M.D.; Lopez-Castro, A.; Perez- Garrido, S. *Tetrahedron: Asymmetry* **2005**, *16*, 3897.

32. Chagnault, V.; Compain, P.; Lewinski, K.; Ikeda, K.; Asano, N.; Martin, O.R. *J. Org. Chem*. **2009**, *74*, 3179.

33. Ahmed, M.M.; Berry, B.P.; Hunter, T.J.; Tomcik, D.J.; O'Doherty, G.A. *Org. Lett.* **2005**, *7*, 745.

34. Zhao, G.L.; Lin, S.; Korotvička, A.; Deiana, L.; Kullberg, M.; Córdova, A. *Adv. Synth. Catal.* **2010**, *352*, 2291.

35. Cesario, C.; Lawrence, P.T.; Miller, M. *J. Org. Chem.* **2009**, *74*, 448.

36. (a) Seyden-Penne, J. *Reductions by the Alumino- and Borohydrides in Organic Synthesis*; Wiley-VCH: New York, 1997, 2nd edition. (b) Brown, H.C.; Krishnamurthy, S. *Tetrahedron* **1979**, *35*, 567.

37. (a) Ashby, E.C.; Goel, A.B. *Tetrahedron Lett.* **1981**, *22*, 4783. (b) Ashby, E.C.; DePriest, R.N.; Pham, T.N. *Tetrahedron Lett.* **1983**, *24*, 2825. (c) Ashby, E.C.; DePriest, R.N.; Goel, A.B.; Wenderoth, B.; Pham, T.N. *J. Org. Chem.* **1984**, *49*, 3545. (d) Ashby, E.C.; Pham, T.N. *J. Org. Chem.* **1986**, *51*, 3548. (e) Ashby, E.C.; Pham, T.N. *Tetrahedron Lett.* **1987**, *28*, 3197.

38. Laszlo, P.; Teston, M. *J. Am. Chem. Soc.* **1990**, *112*, 8751.

39. (a) Park, S.-U.; Chung, S.-K.; Newcomb, M. *J. Org. Chem.* **1987**, *52*, 3275. (b) Yamataka, H.; Hanafusa, T. *J. Org. Chem.* **1988**, *53*, 773.

40. (a) Danishefsky, S.; Regan, J. *Tetrahedron Lett.* **1981**, *22*, 3919. (b) Takano, S.; Akiyama, M.; Sato, S.; Ogasawara, K. *Chem. Lett.* **1983**, 1593. (c) Richter, W.J. *J. Org. Chem.* **1981**, *46*, 5119.

Chapter 4: New Building Blocks for Iminosugars: A Concise Synthesis of Polyhydroxylated *N*-Alkoxypiperidines through an Aza-[4+3] Cycloaddition

4.1 Introduction

Recently, iminosugars functionalized through a hydroxylamine N-O bond have been an attractive synthetic target due to the fact that the barrier to inversion at the nitrogen atom of trialkylhydroxylamines is higher than simple amines.[1] However, at approximately 15 kcal/mol this barrier is not sufficient to prevent rapid inversion at room temperature.[1] Ideally with this low barrier to inversion, it is anticipated that any iminosugar derivative possessing a hydroxylamine motif could sample the full extent of conformational space available at room temperature and adapt in order to effectively bind to enzymes specific for either axial or equatorially linked substrates.[2] Therefore, we saw this void as a motive for developing a general and concise synthesis of *N*-alkoxy iminosugar analogs that had the potential for incorporating a wide variety of alkyl chains and functional groups at the N-O terminus.

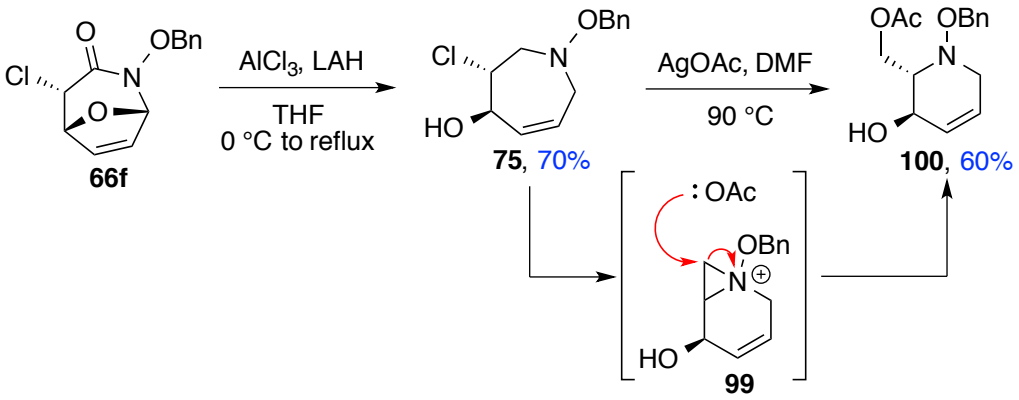

Scheme 4.1.1. Facile ring contraction observed from Chapter 3.

We recently found that α-chloroazepane **75** (Scheme 4.1.1) underwent facile ring contraction when treated with a nucleophile to give tetrahydropyridine **100**. Given the exceptional

electron rich character of the nitrogen atom, a plausible mechanism would involve the ring contraction going through an aziridinium ion intermediate such as **99** and ultimately collapsing to the six-membered ring. It was this discovery that led us to believe that simple functional group manipulations could provide access to the iminosugar class of compounds in a way that was not only stereoselective and concise, but that also was scalable. Moreover, we envisioned that the stereochemical flexibility our methodology afforded would enable a diversity-oriented approach for the synthesis of a library of compounds for biological screening as well as structure activity relationship (SAR) studies. With the goal of developing new C-N bond forming reactions with broad applications in target directed syntheses, we envisioned an α-chlorocycloadduct formed from the cycloaddition of an aza-oxyallylic cation as a general means to easily and stereoselectively construct the cyclic core of polyhydroxylated *N*-alkoxypiperidines (Scheme 4.1.2). Additionally, we thought that the rich functionality our method afforded could provide the necessary handles needed for functional group manipulations in order to elaborate these cores to the desired targets. We also envisioned that our synthesis could provide easy access to stereoisomers that are traditionally difficult to synthesize with current methodology. This chapter focuses on our report of a general strategy for the preparation of polyhydroxylated *N*-alkoxypiperidines that is concise, scalable, diastereoselective, and highly versatile to allow for the construction of a library of derivatives for both biological activity and SAR studies.

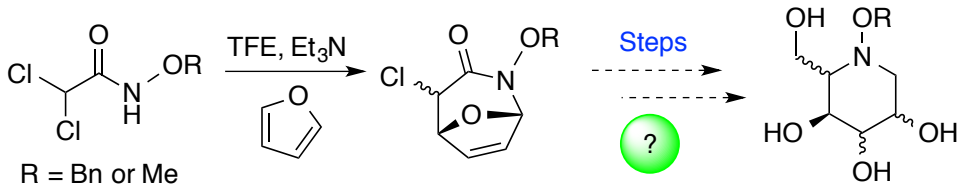

Scheme 4.1.2. Proposal to synthesize polyhydroxylated *N*-alkoxypiperidines from general aza-[4+3] cycloaddition scaffolds.

4.2 A Concise and Diastereoselective Synthesis of Polyhydroxylated *N*-Alkoxypiperidines through an Aza-[4+3] Cycloaddition

Initial studies commenced with synthesizing dichloroamides **101** (Synthesized in Chapter 2) and **104** from dichloroacetyl chloride and either *O*-benzylhydroxylamine or methoxy amine hydrochloride (Scheme 4.2.1). Cycloaddition of the amide substrates provided α-chlorocycloadducts **102** and **103** (previously reported in Chapter 2), as well as **105** and **106** in good overall yield with a diastereoisomeric ratio of 2:1 *endo*:*exo*.[3,4] It is worth mentioning that

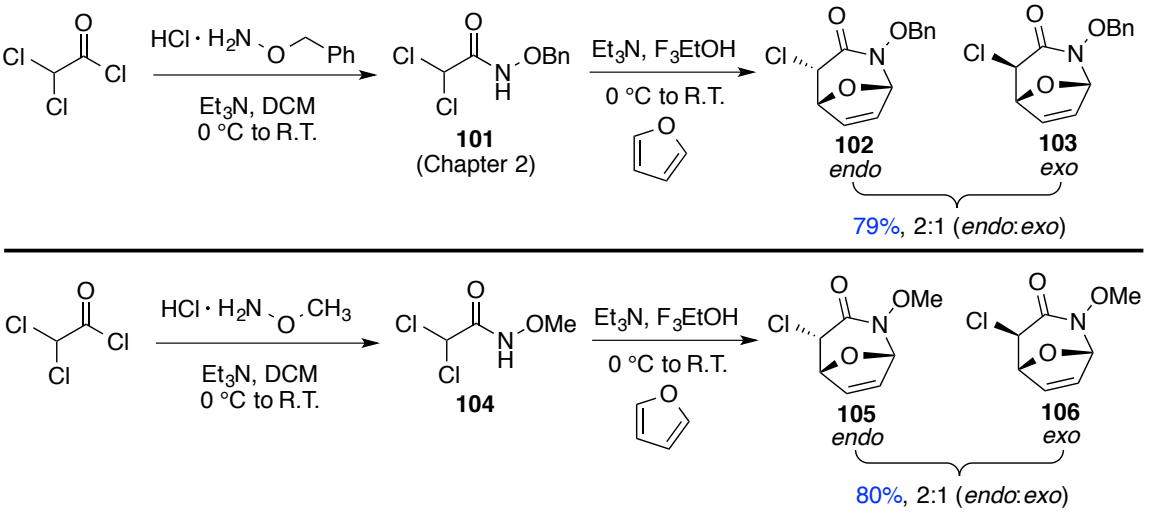

Scheme 4.2.1. Synthesis of cycloadducts **102**, **103**, **105**, and **106** from a simple acid halide starting material.

although the diastereoselectivity of these reactions was rather poor, our goal was to develop a methodology that could access a variety of stereoisomers, thus both diastereoisomers were considered useful and elaborated to the desired targets. Slow addition of the corresponding cycloadducts to a solution of aluminum hydride at 0 °C followed by refluxing for 90 minutes gave cleanly 3-chloroazepine products **107-108** and **111-112** in good yield and as single diastereoisomers (Scheme 4.2.2). The exceptionally high crystalline quality of azepine **108** allowed for its analysis by single crystal X-ray diffraction, thus confirming its structure as well as

the relative *trans* stereochemical configuration of the 3-chloride and 4-hydroxyl group (Figure 4.2.1). Silver acetate mediated ring contraction provided tetrahydropyridine products **109-110** and **113-114** in fair yield and as single diastereoisomers.

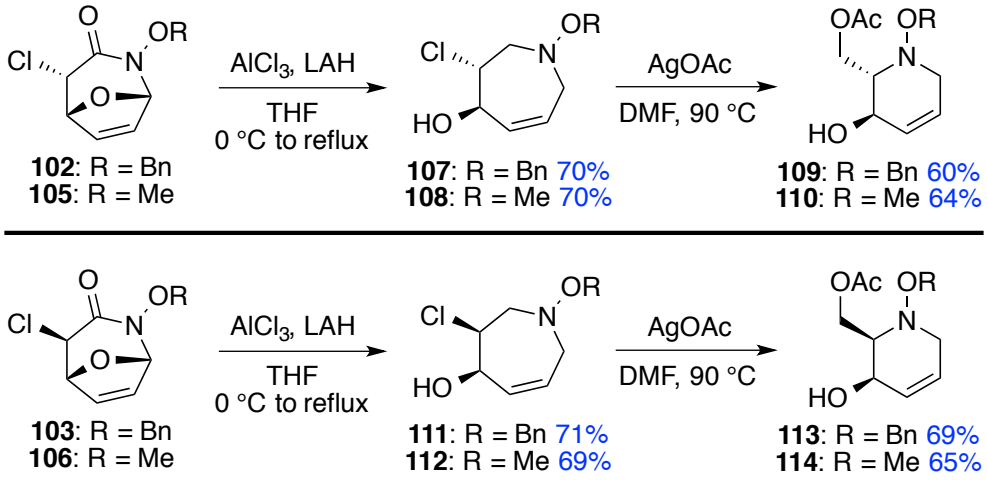

Scheme 4.2.2. Synthesis of 3-chloroazepines **107-108** and **111-112**; subsequent ring contraction to give tetrahydropyridines **109-110** and **113-114**.

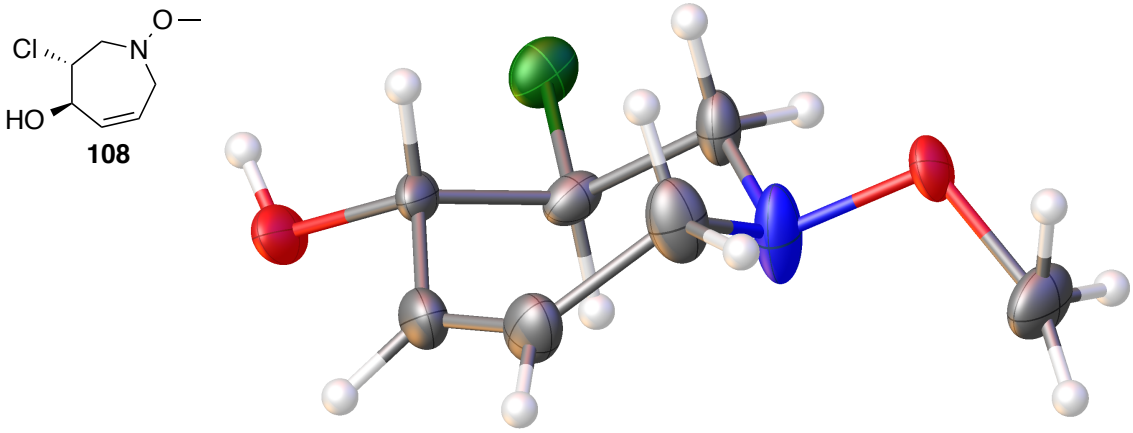

Figure 4.2.1. Thermal ellipsoid plot of azepine **108** at 50% probability. Hydrogen atoms are represented as spheres of arbitrary radius. Gray = carbon, red = oxygen, blue = nitrogen, green = chlorine.

To the best of our knowledge, this reaction represents the first example of an intramolecular azepine ring contraction whereby the substrate is pre-functionalized at the 2-

position with a leaving group. A similar azepine ring contraction example was reported in the literature by Davies and co-workers, albeit their substrate was not pre-functionalized with an appended leaving group.[5] In this respect, we have developed a new methodology for the rapid and stereoselective construction of tetrahydropyridine cores in only a few short synthetic steps from commercially available starting materials. Additionally, the resulting skeletons are richly functionalized and could be envisioned as versatile building blocks for the construction of other iminosugar derivatives or piperidine natural products of interest. Acetate hydrolysis using potassium carbonate in methanol[6] produced diols **115-116** and **119-120** (Scheme 4.2.3) in high yields, with **119** being of particular interest due to its high crystallinity and potential for X-ray analysis. Indeed, slow evaporation of benzene from **119** afforded crystals of suitable quality for X-ray diffraction studies (Figure 4.2.2).

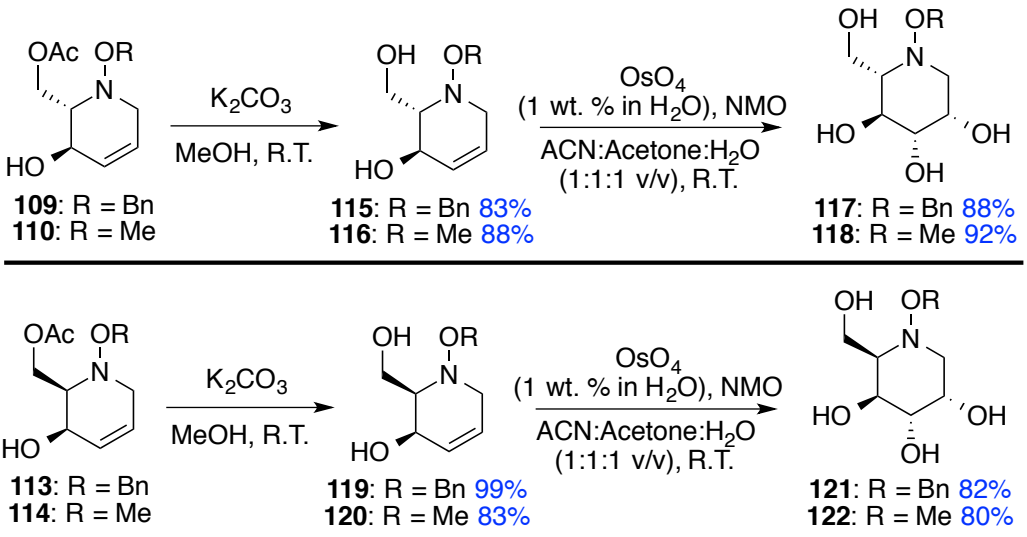

Scheme 4.2.3. Acetate hydrolysis products **115-116** and **119-120**; Osmium tetroxide-mediated olefin oxidation to install final hydroxyl groups to give iminosugar derivatives **117-118** and **121-122**.

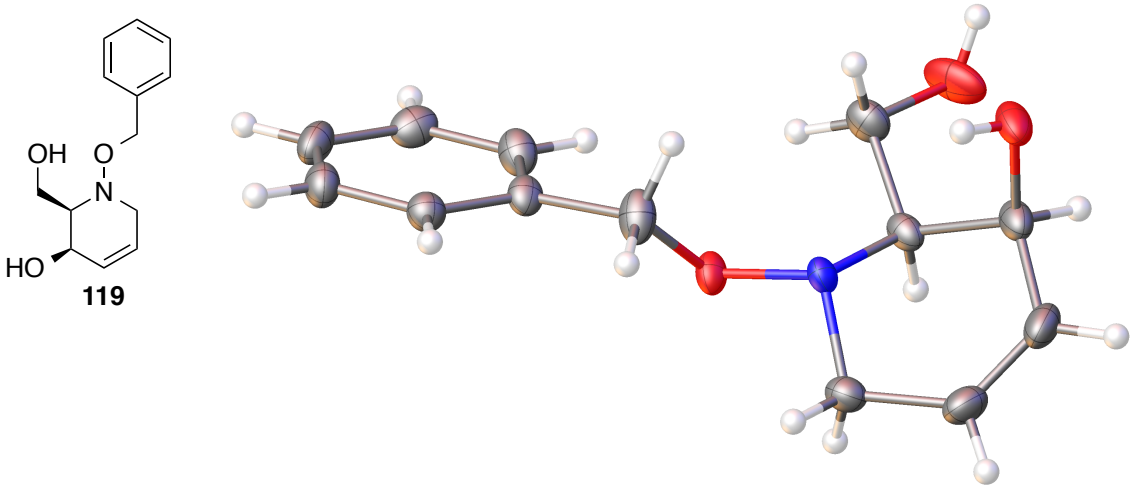

Figure 4.2.2. Thermal ellipsoid plot of tetrahydropyridine **119** at 50% probability. Hydrogen atoms are represented as spheres of arbitrary radius. Gray = carbon, red = oxygen, blue = nitrogen.

We found the observed stereochemistry of diol **119** intriguing, and led us to consider the following mechanistic hypothesis. The resulting stereochemistry suggests a double inversion-type mechanism, whereby a Lewis acid catalyzed abstraction of chloride by silver would lead to backside nucleophilic attack by ring nitrogen to form the aziridinium ion intermediate **123** (Scheme 4.2.4). Subsequent nucleophilic attack by acetate onto the aziridinium ion **123** would

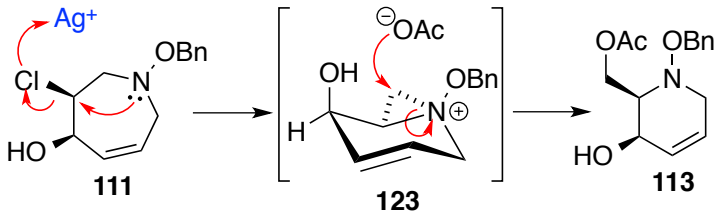

Scheme 4.2.4. Mechanistic proposal of aziridinium ion-mediated ring contraction of **111** to **113**.

provide tetrahydropyridine **113**. With the desired diols in hand, the last step to complete the syntheses would involve utilization of the alkene to install the remaining alcohol groups. Dihydroxylation of the alkene using catalytic osmium tetroxide was found to be a simple and high-yielding method for installing the remaining hydroxyl groups. Exposure of the substrates **115-116** and **119-120** to a solution of osmium tetroxide in water and NMO as the co-oxidant

provided the final polyhydroxylated products **117-118** and **121-122** in good yields and as single diastereoisomers (Scheme 4.2.3). Upon analysis of **121** by single crystal X-ray diffraction, the oxidation was determined to occur selectively from the opposite face of the allylic carbinol group resulting in a *trans*-configuration relative to the C-3 alcohol group in all cases (Figure 4.2.3). These scaffolds represent 4 novel iminosugar derivatives with unique stereochemical configurations that are scarcely found in the literature.[7]

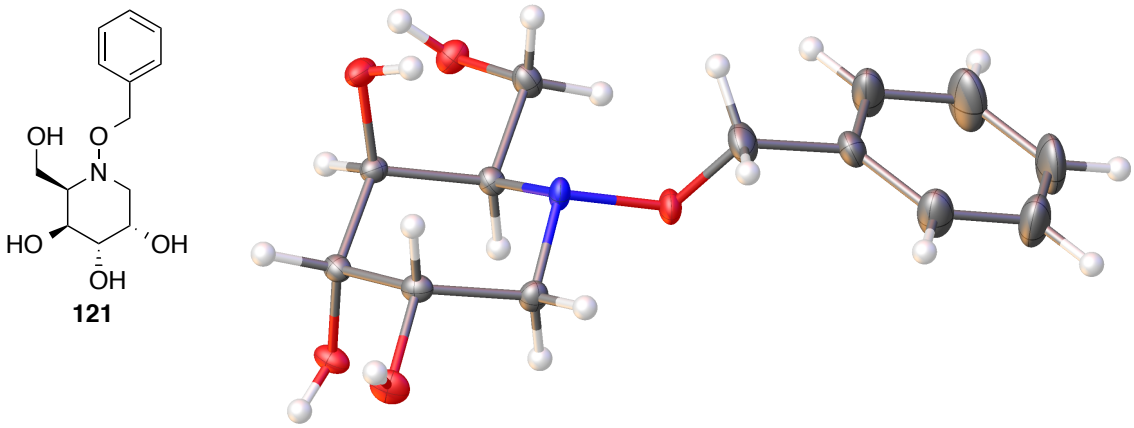

Figure 4.2.3. Thermal ellipsoid plot of polyhydroxylated piperidine **121**. Hydrogen atoms are represented as spheres of arbitrary radius. Gray = carbon, red = oxygen, blue = nitrogen.

4.3 Experimental

All reactions were carried out under an atmosphere of nitrogen in oven-dried glassware with magnetic stirring, unless otherwise specified. All reagents and solvents were purchased from Sigma-Aldrich Chemical Company and used without any further purification. TLC information was recorded on Silicycle glass 60 F_{254} plates and developed by staining with $KMnO_4$ or ceric ammonium molybdate. Purification of reaction products was carried out by flash chromatography using Silicycle Siliaflash® P60 (230-400 mesh). ^{1}H-NMR spectra were measured on Varian 400 (400 MHz) or Varian 500 (500 MHz) spectrometers and are reported in ppm (s = singlet, d = doublet, t = triplet, q = quartet, m = multiplet, br = broad; integration; coupling constant(s) in Hz using TMS as an internal standard (TMS at 0.00 ppm) in $CDCl_3$, CD_3CN, or CD_3OD. ^{13}C-NMR spectra were recorded on V400 or V500 spectrometers and reported in ppm using solvent as an internal standard ($CDCl_3$ at 77.36 ppm), (CD_3CN at 118.26 ppm) or (CD_3OD at 49.86 ppm). Infrared (IR) spectra were recorded on a Nicolet 6700 FT-IR with a diamond ATR and data are reported as cm^{-1} (br = broad, st = strong). High-resolution mass spectra were obtained using an Agilent 6230 TOF LC/MS with an atmospheric pressure photo-ionization (APPI) or electrospray (ESI) source with purine and HP-0921 as internal calibrants. Single crystal X-ray diffraction was performed at 100 K on a Bruker SMART Apex II CCD instrument using graphite-monochromated Mo K_α radiation. The crystals were covered in Paratone oil and mounted on glass fibers. Lorentz and polarization effects were corrected using SAINT[SI] and absorption corrections were applied using SADABS.[S2] The structures were solved using direct methods using OLEX2.[S3]

References

[S1] *SAINT: Program for data reduction, Version 7.68A; Bruker AXS: Madison, WI,* **2009**.

[S2] G. M. Sheldrick. *Acta Crystallogr., Sect. A.: Found. Crystallogr.* **2008**, *64*, 112.

[S3] O. V. Dolomanov, L. J. Bourhis, R. J. Gildea, J. A. K. Howard, and H. Puschmann, *J. Appl. Cryst.* **2009**, *42*, 339.

(±)-2,2-dichloro-*N*-(methoxy)acetamide (104):

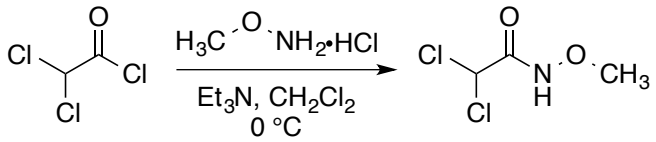

To a suspension of methoxyamine hydrochloride (27.1 mmol, 2.26 g) and triethylamine (54.2 mmol, 5.48) in CH_2Cl_2 (0.25 M) at 0 °C was added dropwise 2,2-dichloroacetyl chloride (27.1 mmol, 4.0 g,) dropwise. The reaction mixture was then warmed to room temperature and stirred until TLC analysis (3:1 hexanes:ethyl acetate) indicated complete consumption of the starting material (1 hour). The solvent was then removed under reduced pressure and the crude product was purified via flash column chromatography (2:1 hexanes:ethyl acetate) to provide 3.5 g of the pure haloamide **104** as a white crystalline solid (3.5 g, 22.2 mmol, 82% yield). R_f = 0.3 (2:1 hexanes: ethyl acetate); M.P. = 40.5 – 42.8 °C; ^{1}H NMR (500 MHz, $CDCl_3$) δ 11.38 (br s, 1H), 6.28 (s, 1H), and 3.90 (s, 3H); ^{13}C NMR (101 MHz, $CDCl_3$) δ 162.51, 64.17, and 63.95; IR (neat) 3172 (br), 2998, 2940, 1674 (st), 1500, 1439, 1335, 1210, 1057, and 974 cm^{-1}; HR-ESIMS requires for $C_3H_5ClNO_2$ $(M+H)^+$ 158.9798, found 158.9784.

(±)-(4*S*, 5*R*, 1*S*)-4-chloro-8-oxo-2-(methoxy)-2-azabicyclo[3.2.1]oct-6-en-3-one (*endo*) and (±)-(4*R*, 5*R*, 1*S*)-4-chloro-8-oxo-2-(methoxy)-2-azabicyclo[3.2.1]oct-6-en-3-one (*exo*) (105, 106):

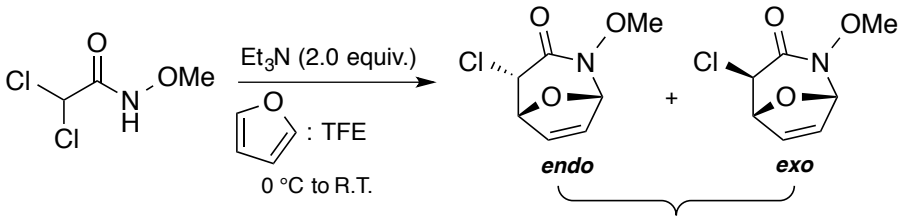

To a solution of 2,2-dichloro-*N*-(phenylmethoxy)acetamide (22.2 mmol, 3.5 g) in CF_3CH_2OH and furan [1:1 (v/v) 0.25 M] at 0 °C was added triethylamine (2 equiv.) dropwise.

The solution was allowed to warm to room temperature and the reaction mixture was stirred for 24 hours. After removal of the volatiles under reduced pressure, the crude mixture was purified by flash column chromatography (3:1 hexanes:ethyl acetate) to afford 3.4 g (17.9 mmol, 80 % yield) of the pure cycloadduct *endo* isomer as a yellow solid and the *exo* isomer as a yellow oil (2:1 *endo:exo*). ***Endo*-diastereoisomer:** R_f = 0.4 (2:1 hexanes:ethyl acetate); M.P. = 87.8 °C; ^{1}H NMR (500 MHz, $CDCl_3$): δ 6.81 (dd, *J* = 6.0, 1.3 Hz, 1H), 6.60 (dd, *J* = 6.0, 1.8 Hz, 1H), 5.63 (d, *J* = 1.4 Hz, 1H), 5.18 (dd, *J* = 5.1, 1.9 Hz, 1H), 4.80 (d, *J* = 5.1 Hz, 1H), 3.82 (s, 3H); ^{13}C NMR (101 MHz, $CDCl_3$): δ 165.53, 136.79, 133.22, 90.80, 82.05, 63.56, and 56.67; IR (neat) 3101, 3015, 3091, 2990, 2942, 1679 (st), 1442, 1394, 1325, 1242, 1062, 1030, 926, and 834 cm^{-1}; HR-ESIMS requires for $C_7H_8ClNO_3$ $(M+Na)^+$ 212.0085, found 212.0083. ***Exo*-diastereoisomer:** R_f = 0.3 (2:1 hexanes:ethyl acetate); ^{1}H NMR (500 MHz, $CDCl_3$): δ 6.87 (dd, *J* = 6.1, 1.4 Hz, 1H), 6.50 (dd, *J* = 5.9, 2.0 Hz, 1H), 5.70 (d, *J* = 1.5 Hz, 1H), 5.08 (d, *J* = 2.1 Hz, 1H), 4.16 (d, *J* = 1.0 Hz, 1H), and 3.84 (s, 3H); ^{13}C NMR (101 MHz, $CDCl_3$): δ 165.16, 137.88, 131.70, 89.90, 84.06, 63.41, and 55.69; IR (neat) 3094, 2987, 2939, 2901, 1692 (st), 1439, 1363, 1274, 1236, 1157, 1046 (st), 986, 903, and 834 cm^{-1}; HR-ESIMS requires for $C_7H_8ClNO_3$ $(M+Na)^+$ 212.0085, found 212.0087.

(±)-(3*S*, 4*R*)-*N*-phenylmethoxy-3-chloro-4-hydroxy-2,3,4,7-tetrahydro-1*H*-azepine (107)

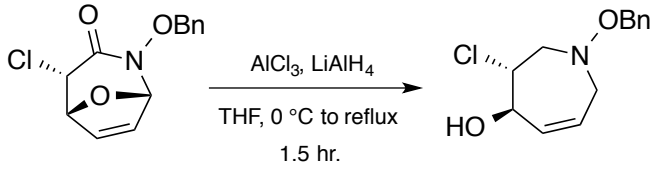

To an oven dried 100 mL Schlenk flask equipped with a magnetic stir bar was added dry THF (19 mL) under an atmosphere of nitrogen. The flask was placed in an ice bath and aluminum chloride (7.57 mmol, 1.01 g) was added in portions over a period of 5 minutes. Upon complete dissolution of the aluminum chloride, a solution of lithium aluminum hydride in dry THF (11.4

mmol, 5.7 mL) was added dropwise at that same temperature over a period of 15 minutes and the resulting solution was stirred at 0 °C for 20 minutes. The cycloadduct **102** (3.79 mmol, 1.01 g) was then added in THF (25 mL) dropwise over a period of 20 minutes and the reaction mixture was refluxed under nitrogen for 1.5 hours. The reaction flask was cooled to 0 °C and quenched with water followed by 10% NaOH. The aluminum salts were filtered off and the filtrate was dried over Na_2SO_4 and concentrated under reduced pressure. The crude residue was purified by column chromatography (10% - 33% Hex:EtOAc) to afford 0.67 g of **107** as a white crystalline solid (2.64 mmol, 70% yield). R_f = 0.54 (2:1 hexanes:ethyl acetate); M.P. 59.5 – 62.0 °C; ^{1}H NMR (500 MHz, $CDCl_3$): δ 7.35 – 7.30 (m, 5H), 5.81 (dt, *J* = 11.9, 3.1 Hz, 1H), 5.67 (dt, *J* = 12.0, 6.0 Hz, 1H), 4.69 (s, 2H), 4.36 (d, *J* = 8.2 Hz, 1H), 4.18 (td, *J* = 8.3, 4.7 Hz, 1H), 3.77 (dd, *J* = 14.1, 4.7 Hz, 1H), 3.62 (dd, *J* = 15.9, 6.2 Hz, 1H), 3.44 – 3.39 (m, 1H), 3.22 (dd, *J* = 14.0, 8.0 Hz, 1H), and 2.86 – 2.83 (m, 1H); ^{13}C NMR (101 MHz, $CDCl_3$): δ 137.20, 132.20, 128.71, 128.38, 128.03, 126.27, 74.64, 73.34, 64.26, 61.87, and 57.41; IR (neat) 3556, 3105 (br), 3006, 2987, 2965, 1464, 1376, 1055 (s), and 1037 cm^{-1}; HR-ESIMS requires for $C_{13}H_{17}ClNO_2$ $(M+H)^+$ 254.0948, found 254.0950.

(±)-(3*S*, 4*R*)-*N*-methoxy-3-chloro-4-hydroxy-2,3,4,7-tetrahydro-1*H*-azepine (108)

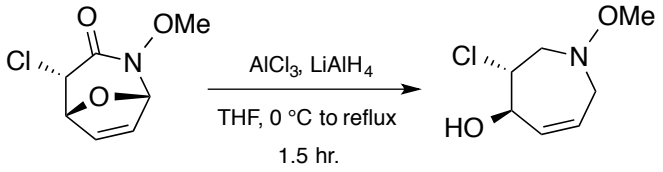

To an oven dried 100 mL Schlenk flask equipped with a magnetic stir bar was added dry THF (19 mL) under an atmosphere of nitrogen. The flask was placed in an ice bath and aluminum chloride (12.1 mmol, 1.61 g) was added in portions over a period of 5 minutes. Upon complete dissolution of the aluminum chloride, a solution of lithium aluminum hydride in dry THF (18.1 mmol, 9.1 mL) was added dropwise at that same temperature over a period of 15 minutes and the

resulting solution was stirred at 0 °C for 20 minutes. The cycloadduct **105** (6.03 mmol, 1.14 g) was then added in THF (40 mL) dropwise over a period of 20 minutes and the reaction mixture was refluxed under nitrogen for 1.5 hours. The reaction flask was cooled to 0 °C and quenched with water followed by 10% NaOH. The aluminum salts were filtered off and the filtrate was dried over Na_2SO_4 and concentrated under reduced pressure. The crude residue was purified by column chromatography (25% - 33% Hex:EtOAc) to afford 0.75 g of **108** as a white crystalline solid (4.22 mmol, 70% yield). X-ray quality crystals were grown by slow evaporation of a dichloromethane/hexanes solution of **108**. R_f = 0.55 (1:1 hexanes:ethyl acetate); M.P. = 63.9 – 65.4 °C; ^{1}H NMR (500 MHz, $CDCl_3$): δ 5.84 (dt, *J* = 11.9, 2.9 Hz, 1H), 5.75 – 5.70 (m, 1H), 4.39 (d, *J* = 7.2 Hz, 1H), 4.19 (td, *J* = 8.6, 4.5 Hz, 1H), 3.82 (ddd, *J* = 13.9, 4.5, 1.5 Hz, 1H), 3.68 (ddd, *J* = 15.9, 6.5, 1.2 Hz, 1H), 3.53 (s, 3H), 3.42 (d, *J* = 16.2 Hz, 1H), 3.19 (dd, *J* = 13.8, 8.4 Hz, 1H), and 2.86 (br s, 1H); ^{13}C NMR (101 MHz, $CDCl_3$): δ 132.97, 125.91, 73.42, 63.72, 62.07, 59.68, and 56.50; IR (neat) 3326 (br), 3031, 2949, 2810, 1458, 1385, 1350, 1283, 1198, 1062, 1024 (st), 897, and 774 cm^{-1}; HR-ESIMS requires for $C_7H_{12}ClNO_2$ $(M+H)^+$ 178.0629, found 178.0627.

(±)-(2*S*, 3*R*)-*N*-phenylmethoxy-2-acetoxymethyl-3-hydroxy-1,2,3,6-tetrahydropyridine (109)

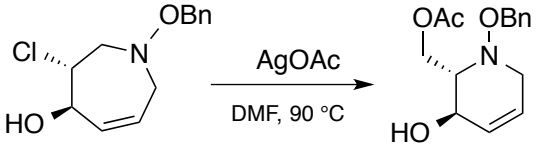

To a stirred solution of **107** (1.0 mmol, 250 mg,) in DMF (12 mL) was added AgOAc (2.0 mmol, 334 mg,) all at once and the resulting suspension was heated in a sealed flask at 90 °C for 72 hours. The crude reaction mixture was filtered through a pad of celite and the pad was washed with ethyl acetate (2 x 15 mL) followed by methanol (15 mL). The filtrate was concentrated under reduced pressure at 65 °C to remove DMF and the crude residue was purified

by column chromatography (33% to 50% hexanes:ethyl acetate) to afford 224 mg of **109** as a pale yellow oil (0.81 mmol, 60% yield). R_f = 0.33 (1:1 hexanes:ethyl acetate); ^{1}H NMR (500 MHz, CD_3OD): δ 7.34 – 7.24 (m, 5H), 5.74 – 5.66 (m, 2H), 4.83 (s, 1H), 4.70 (d, *J* = 10.7 Hz, 1H), 4.65 (d, *J* = 10.6 Hz, 1H), 4.48 (d, *J* = 12.7 Hz, 1H), 4.40 (dd, *J* = 11.5, 5.0 Hz, 1H), 4.24 (dd, *J* = 8.3, 3.6 Hz, 1H), 3.66 (d, *J* = 15.8 Hz, 1H), 3.39 – 3.32 (m, 1H), 2.81 (s, 1H), and 2.05 (s, 3H); ^{13}C NMR (101 MHz, CD_3OD): δ 171.54, 137.13, 128.78, 128.60, 127.90, 127.60, 123.97, 74.88, 66.99, 64.61, 60.89, 53.67, and 19.49; IR (neat) 3405 (br), 3034, 2917, 2860, 1736, 1451, 1363, 1236, 1024, and 698 cm^{-1}; HR-ESIMS requires for $C_{15}H_{19}NO_4$ $(M+H)^+$ 278.1387, found 278.1384.

(±)-(2*S*, 3*R*)-*N*-methoxy-2-acetoxymethyl-3-hydroxy-1,2,3,6-tetrahydropyridine (110)

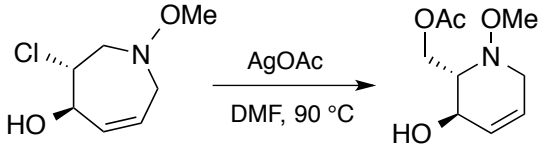

To a stirred solution of **108** (1.1 mmol, 200 mg,) in DMF (15 mL) was added AgOAc (2.2 mmol, 367 mg,) all at once and the resulting suspension was heated in a sealed flask at 90 °C for 72 hours. The crude reaction mixture was filtered through a pad of celite and the pad was washed with ethyl acetate (2 x 15 mL) followed by methanol (15 mL). The filtrate was concentrated under reduced pressure at 65 °C to remove DMF and the crude residue was purified by column chromatography (33% to 50% hexanes:ethyl acetate) to afford 143 mg of **110** as a pale yellow oil (0.71 mmol, 64% yield). R_f = 0.23 (1:1 hexanes:ethyl acetate); ^{1}H NMR (500 MHz, $CDCl_3$): δ 5.81 – 5.77 (m, 1H), 5.73 (dddd, *J* = 10.1, 3.8, 2.3, 1.3 Hz, 1H), 4.55 (dd, *J* = 11.7, 4.3 Hz, 1H), 4.35 (dd, *J* = 11.7, 4.2 Hz, 1H), 4.23 (d, *J* = 7.6 Hz, 1H), 3.70 – 3.64 (m, 1H), 3.57 (s, 3H), 3.43 – 3.38 (m, 1H), 2.97 – 2.93 (m, 1H), 2.56 (d, *J* = 11.3 Hz, 1H), and 2.12 (s, 3H); ^{13}C NMR (101 MHz, CD_3OD): δ 170.92, 126.54, 124.31, 75.52, 68.85, 60.70, 59.39, 58.22, and

19.65; IR (neat) 3444 (br), 2937, 2891, 2845, 2811, 1729 (st), 1454, 1439, 1372, 1228 (st), 1029, 965, and 901 cm^{-1}; HR-ESIMS requires for $C_9H_{15}NO_4$ $(M+Na)^+$ 224.0893, found 224.0890.

(±)-(3*R*, 4*R*)-*N*-phenylmethoxy-3-chloro-4-hydroxy-2,3,4,7-tetrahydro-1*H*-azepine (111)

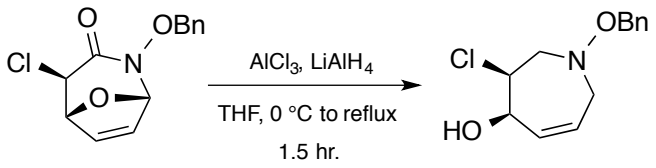

To an oven dried 250 mL Schlenk flask equipped with a magnetic stir bar was added dry THF (55 mL) under an atmosphere of nitrogen. The flask was placed in an ice bath and aluminum chloride (21.8 mmol, 2.91 g) was added in portions over a period of 5 minutes. Upon complete dissolution of the aluminum chloride, a solution of lithium aluminum hydride in dry THF (32.7 mmol, 16.4 mL) was added dropwise at that same temperature over a period of 15 minutes and the resulting solution was stirred at 0 °C for 20 minutes. The cycloadduct **103** (10.9 mmol, 2.89 g) was then added in THF (72 mL) dropwise over a period of 20 minutes and the reaction mixture was refluxed under nitrogen for 1.5 hours. The reaction flask was cooled to 0 °C and quenched with water followed by 10% NaOH. The aluminum salts were filtered off and the filtrate was dried over Na_2SO_4 and concentrated under reduced pressure. The crude residue was purified by column chromatography (10% - 33% Hex:EtOAc) to afford 1.96 g of **111** as a colorless oil (1.96 g, 7.72 mmol, 71% yield). R_f = 0.36 (3:1 hexanes:ethyl acetate); ^{1}H NMR (500 MHz, $CDCl_3$): δ 7.35 – 7.31 (m, 5H), 5.86 (dd, *J* = 11.7, 6.2 Hz, 1H), 5.72 (dt, *J* = 11.6, 4.7 Hz, 1H), 4.69 (s, 2H), 4.45 (td, *J* = 8.0, 1.3 Hz, 1H), 4.32 (ddd, *J* = 8.0, 6.0, 2.2 Hz, 1H), 3.70 (dd, *J* = 16.5, 5.0 Hz, 1H), 3.59 (dd, *J* = 13.8, 7.8 Hz, 1H), 3.55 – 3.49 (m, 2H), 2.91 (d, *J* = 8.9 Hz, 1H); ^{13}C NMR (101 MHz, $CDCl_3$): δ 137.01, 131.06, 129.20, 128.77, 128.46, 128.17, 74.74, 71.45, 62.00, 60.19, and 57.05; IR (neat) 3498 (br), 3150, 2976, 2865, 2852, 1489, 1424, 1176, and 1054 cm^{-1}; HR-ESIMS requires for $C_{13}H_{17}ClNO_2$ $(M+H)^+$ 254.0948, found 254.0940.

(±)-(3*R*, 4*R*)-*N*-methoxy-3-chloro-4-hydroxy-2,3,4,7-tetrahydro-1*H*-azepine (112)

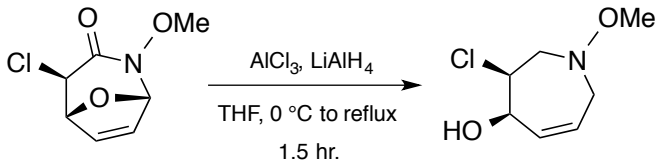

To an oven dried 100 mL Schlenk flask equipped with a magnetic stir bar was added dry THF (19 mL) under an atmosphere of nitrogen. The flask was placed in an ice bath and aluminum chloride (7.48 mmol, 0.997 g) was added in portions over a period of 5 minutes. Upon complete dissolution of the aluminum chloride, a solution of lithium aluminum hydride in dry THF (11.2 mmol, 5.6 mL) was added dropwise at that same temperature over a period of 15 minutes and the resulting solution was stirred at 0 °C for 20 minutes. The cycloadduct **106** (3.74 mmol, 1.01 g) was then added in THF (25 mL) dropwise over a period of 20 minutes and the reaction mixture was refluxed under nitrogen for 1.5 hours. The reaction flask was cooled to 0 °C and quenched with water followed by 10% NaOH. The aluminum salts were filtered off and the filtrate was dried over Na_2SO_4 and concentrated under reduced pressure. The crude residue was purified by column chromatography (10% - 33% Hex:EtOAc) to afford 0.46 g of **112** as a colorless oil (2.59 mmol, 69% yield). R_f = (2:1 hexanes:ethyl acetate); ^{1}H NMR (500 MHz, $CDCl_3$): δ 5.94 – 5.89 (m, 1H), 5.78 (dt, *J* = 11.4, 4.8 Hz, 1H), 4.49, (ddd, *J* = 8.7, 6.6, 2.4 Hz, 1H), 4.41 – 4.35 (m, 1H), 3.75 (dd, *J* = 16.3, 5.0 Hz, 1H), 3.66 – 3.60 (m, 1H), 3.58 – 3.55 (m, 1H), and 3.55 (s, 3H); ^{13}C NMR (101 MHz, $CDCl_3$): δ 131.40, 129.12, 71.47, 61.17, 60.21, 59.75, and 55.96; IR (neat) 3405 (br), 2971, 2939, 2860, 2825, 1458, 1435, 1369, 1312, 1052 (st), 1033, 1017, 926, and 745 cm^{-1}; HR-ESIMS requires for $C_7H_{12}ClNO_2$ $(M+Na)^+$ 200.0449, found 200.0447.

(±)-(2*R*, 3*R*)-*N*-phenylmethoxy-2-acetoxymethyl-3-hydroxy-1,2,3,6-tetrahydropyridine (113)

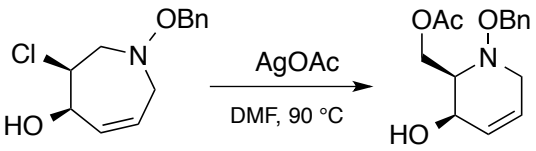

To a stirred solution of **111** (0.9 mmol, 229 mg,) in DMF (11 mL) was added AgOAc (1.81 mmol, 302 mg,) all at once and the resulting suspension was heated in a sealed flask at 90 °C for 72 hours. The crude reaction mixture was filtered through a pad of celite and the pad was washed with ethyl acetate (2 x 10 mL) followed by methanol (10 mL). The filtrate was concentrated under reduced pressure at 65 °C to remove DMF and the crude residue was purified by column chromatography (20% to 33% hexanes:ethyl acetate) to afford 174 mg of **113** as a pale yellow oil (0.63 mmol, 69% yield). R_f = 0.36 (2:1 hexanes:ethyl acetate); ^{1}H NMR (500 MHz, CD_3OD): δ 7.37 – 7.25 (m, 5H), 5.88 – 5.81 (m, 1H), 5.74 (dd, *J* = 10.0, 4.9 Hz, 1H), 4.81 (d, *J* = 1.8 Hz, 1H), 4.73 – 4.69 (m, 1H), 4.65 (dd, *J* = 11.0, 1.6 Hz, 1H), 4.56 (dd, *J* = 10.8, 5.5 Hz, 1H), 4.32 (ddd, *J* = 11.2, 7.3, 1.7 Hz, 1H), 4.12 (d, *J* = 4.1 Hz, 1H), 3.74 (dd, *J* = 16.6, 4.5 Hz, 1H), 3.28 – 3.22 (m, 1H), 3.04 (s, 1H), and 2.00 (d, *J* = 1.7 Hz, 3H); ^{13}C NMR (101 MHz, CD_3OD): δ 171.42, 137.22, 128.67, 127.95, 127.66, 126.71, 125.74, 75.32, 64.99, 62.20, 58.72, 54.23, and 19.56; IR (neat) 3467 (br), 3028, 2922, 2860, 2816, 1728 (st), 1454, 1366, 1236, 1086, 1039, and 735 cm^{-1}; HR-ESIMS requires for $C_{15}H_{19}NO_4$ $(M+H)^+$ 278.1387, found 278.1388.

(±)-(2*R*, 3*R*)-*N*-methoxy-2-acetoxymethyl-3-hydroxy-1,2,3,6-tetrahydropyridine (114)

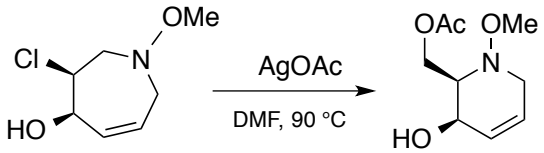

To a stirred solution of **112** (1.4 mmol, 252 mg,) in DMF (13 mL) was added AgOAc (2.8 mmol, 467 mg,) all at once and the resulting suspension was heated in a sealed flask at 90 °C

for 72 hours. The crude reaction mixture was filtered through a pad of celite and the pad was washed with ethyl acetate (2 x 15 mL) followed by methanol (15 mL). The filtrate was concentrated under reduced pressure at 65 °C to remove DMF and the crude residue was purified by column chromatography (33% to 50% hexanes:ethyl acetate) to afford 186 mg of **114** as a pale yellow oil (0.92 mmol, 186 mg, 65% yield). R_f = 0.23 (1:1 hexanes:ethyl acetate); ^{1}H NMR (400 MHz, CD_3OD): δ 5.89 – 5.83 (m, 1H), 5.79 (ddd, *J* = 10.0, 4.5, 1.9 Hz, 1H), 4.55 (dd, *J* = 10.9, 5.7 Hz, 1H), 4.34 (dd, *J* = 10.9, 7.5 Hz, 1H), 4.11 (d, *J* = 7.2 Hz, 1H), 3.82 (dd, *J* = 16.6, 4.6 Hz, 1H), 3.52 (s, 3H), 3.26 – 3.20 (m, 1H), 3.02 (t, *J* = 5.8 Hz, 1H), and 2.07 (s, 3H); ^{13}C NMR (101 MHz, CD_3OD): δ 171.37, 126.71, 125.56, 64.55, 61.95, 59.72, 58.65, 53.46, and 19.49; IR (neat) 3443, 3003, 2967, 2939, 2920, 2860, 2844, 1727 (st), 1454, 1369, 1236, 1052 (st), 1012, and 748 cm^{-1}; HR-ESIMS requires for $C_9H_{15}NO_4$ $(M+Na)^+$ 224.0893, found 224.0893.

(±)-(2*S*, 3*R*)-*N*-phenylmethoxy-2-hydroxymethyl-3-hydroxy-1,2,3,6-tetrahydropyridine (115)

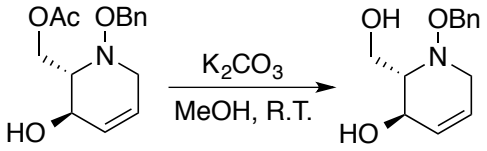

To a solution of **109** (2.24 mmol, 620 mg) in methanol (45 mL) was added potassium carbonate (46.6 mmol, 6.44 g) all at once and the resulting suspension was stirred for 16 hours at room temperature. After concentration under reduced pressure, the crude residue was taken up in 45 mL of water and extracted with $CHCl_3$:*i*-PrOH (3:1 v:v, 3 x 25 mL). The combined organic extracts were washed with brine, dried over Na_2SO_4, and concentrated to afford the crude diol. The crude product was then ran through a short plug of silica gel (eluent 1:1 hexanes:ethyl acetate) to give 440 mg of the pure diol **115** as a colorless oil (1.87 mmol, 83% yield). R_f = 0.14 (1:1 hexanes:ethyl acetate); ^{1}H NMR (400 MHz, CD_3OD): δ 7.39 – 7.21 (m, 5H), 5.72 – 5.61 (m,

2H), 4.76 (s, 2H), 4.24 (d, *J* = 8.2 Hz, 1H), 3.94 (dd, *J* = 10.94, 2.55 Hz, 1H), 3.85 (dd, *J* = 11.1, 5.2 Hz, 1H), 3.66 – 3.59 (m, 1H), 3.37 – 3.30 (m, 1H), and 2.65 (s, 1H); ^{13}C NMR (101 MHz, CD_3OD): δ 137.35, 128.79, 128.51, 127.87, 127.53, 123.95, 74.83, 69.62, 65.12, 58.89, and 53.49; IR (neat) 3364, 3063, 3028, 2930, 2879, 2825, 1496, 1451, 1366, 1264, 1242, 1030, 1002, 913, and 736 cm^{-1}; HR-ESIMS requires for $C_{13}H_{17}NO_3$ $(M+Na)^+$ 258.1101, found 258.1097.

(±)-(2*S*, 3*R*)-*N*-methoxy-2-hydroxymethyl-3-hydroxy-1,2,3,6-tetrahydropyridine (116)

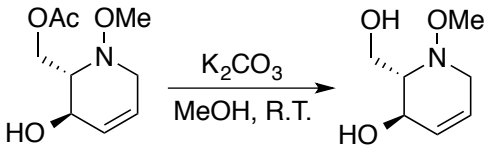

To a solution of **110** (1.36 mmol, 273 mg) in methanol (27 mL) was added potassium carbonate (28.3 mmol, 3.9 g) all at once and the resulting suspension was stirred for 16 hours at room temperature. After concentration under reduced pressure, the crude residue was taken up in 10 mL of water and extracted with $CHCl_3$:*i*-PrOH (3:1 v:v, 3 x 15 mL). The combined organic extracts were washed with brine, dried over Na_2SO_4, and concentrated to afford 190 mg of diol **116** as a white solid that was used without further purification (1.19 mmol, 88% yield). R_f = 0.4 (5% DCM:MeOH); M.P. = 121.2 – 123.4 °C; ^{1}H NMR (400 MHz, CD_3OD): δ 5.85 – 5.79 (m, 1H), 5.74 (dd, *J* = 9.7, 4.2 Hz, 1H), 4.15 (s, 1H), 3.96 (ddd, *J* = 10.9, 5.6, 1.0 Hz, 1H), 3.88 (ddd, *J* = 10.9, 6.7, 1.0 Hz, 1H), 3.77 (ddd, *J* = 16.5, 4.5, 1.2 Hz, 1H), 3.51 (s, 3H), 3.18 (d, *J* = 16.6 Hz, 1H), and 2.78 (s, 1H); ^{13}C NMR (101 MHz, CD_3OD): δ 127.01, 125.51, 67.74, 65.12, 59.82, 59.63, and 53.75; IR (neat) 3352 (br), 3245 (br), 2921, 2851, 2808, 1457, 1384, 1265, 1243, 1225, 1121, 1026, 947, 895, 870, and 846 cm^{-1}; HR-ESIMS requires for $C_7H_{13}NO_3$ $(M+Na)^+$ 182.0788, found 182.0785.

(±)-(2*S*, 3*R*, 4*S*, 5*S*)-*N*-phenylmethoxy-2-hydroxymethyl-3,4,5-trihydroxypiperidine (117)

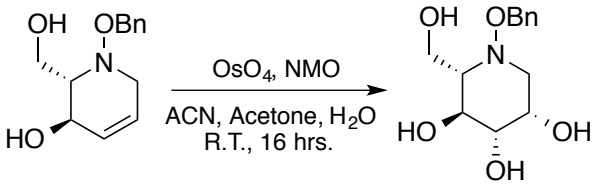

To a solution of **115** (1.83 mmol, 430 mg) in acetonitrile, acetone, and deionized water (11 mL, 1:1:1 v/v) was added NMO (3.66 mmol, 0.4 mL) followed by 2.4 mL of a 1 wt. % solution of osmium tetroxide in deionized water and the resulting solution was stirred overnight at room temperature. The reaction mixture was then filtered through a pad of celite and the pad washed with methanol (3 x 15 mL). After concentration under reduced pressure, the crude residue was purified by column chromatography (5% - 10% DCM:MeOH) to afford 431 mg of the pure piperidine **117** as an off white solid (1.6 mmol, 88% yield). R_f = 0.3 (10% DCM:MeOH); M.P. = 98.6 – 100.8 °C; ^{1}H NMR (400 MHz, CD_3OD): δ 7.38 – 7.22 (m, 5H), 4.73 (d, *J* = 1.0 Hz, 1H), 4.00 (ddd, *J* = 11.2, 2.8, 1.0 Hz, 1H), 3.91 – 3.88 (m, 1H), 3.79 (td, *J* = 9.7, 1.0 Hz, 1H), 3.54 (ddd, *J* = 11.4, 3.5, 1.0 Hz, 1H), 3.35 (ddd, *J* = 9.6, 3.6, 1.0 Hz, 1H), 3.29 (dq, *J* = 3.0, 1.5 Hz, 1H), 2.67 (dd, *J* = 11.6, 1.8 Hz, 1H), and 2.34 (d, *J* = 9.7 Hz, 1H); ^{13}C NMR (101 MHz, CD_3OD): δ 136.94, 128.54, 127.93, 127.61, 74.77, 74.61, 70.91, 68.18, 67.40, 58.50, and 58.25; IR (neat) 3225 (br), 3031, 2978, 2951, 2919, 2842, 1460, 1451, 1437, 1366, 1319, 1210, 1101, 1062, 1042, 974, 909, and 856 cm^{-1}; HR-ESIMS requires for $C_{13}H_{19}NO_5$ $(M+Na)^+$ 292.1155, found 292.1155.

(±)-(2*S*, 3*R*, 4*S*, 5*S*)-*N*-methoxy-2-hydroxymethyl-3,4,5-trihydroxypiperidine (118)

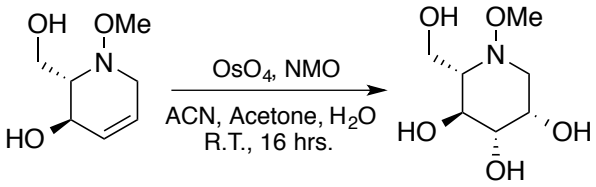

To a solution of **116** (0.69 mmol, 109 mg) in acetonitrile, acetone, and deionized water (4.05 mL, 1:1:1 v/v) was added NMO (1.37 mmol, 0.2 mL) followed by 0.9 mL of a 1 wt. % solution of osmium tetroxide in deionized water and the resulting solution was stirred overnight at room temperature. The reaction mixture was then filtered through a pad of celite and the pad washed with methanol (3 x 10 mL). After concentration under reduced pressure, the crude residue was purified by column chromatography (5% - 20% DCM:MeOH) to afford 122 mg of the pure piperidine **118** as a colorless gum (0.6 mmol, 92%). R_f = 0.5 (20% DCM:MeOH); ^{1}H NMR (400 MHz, CD_3OD): δ 3.99 (ddd, *J* = 7.0, 3.7, 1.8 Hz, 1H), 3.73 (td, *J* = 7.6, 3.2 Hz, 1H), 3.66 (ddd, *J* = 5.9, 1.8, 0.5 Hz, 1H), 3.47 (s, 3H), 3.33 (s, 1H), 3.23 – 3.16 (m, 1H), 3.11 (dd, *J* = 3.2, 0.9 Hz, 1H), 3.09 – 3.07 (m, 1H), and 3.06 – 3.03 (m, 1H); ^{13}C NMR (101 MHz, CD_3OD): δ 76.42, 75.11, 70.78, 67.43, 59.86, 58.99, and 58.00; IR (film) 3346 (br), 2952, 2921, 2903, 2851, 2072, 1463, 1375, 1225, 1118, 1087, 1057, 1042, 971, 898, and 818 cm^{-1}; HR-ESIMS requires for $C_7H_{15}NO_5$ $(M+Na)^+$ 216.0842, found 216.0840.

(±)-(2*R*, 3*R*)-*N*-phenylmethoxy-2-hydroxymethyl-3-hydroxy-1,2,3,6-tetrahydropyridine (119)

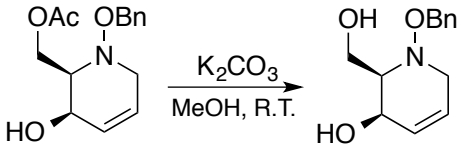

To a solution of **114** (0.958 mmol, 266 mg) in methanol (19 mL) was added potassium carbonate (20.0 mmol, 2.75 g) all at once and the resulting suspension was stirred for 16 hours at

room temperature. After concentration under reduced pressure, the crude residue was taken up in 25 mL of water and extracted with $CHCl_3$:*i*-PrOH (3:1 v:v, 3 x 15 mL). The combined organic extracts were washed with brine, dried over Na_2SO_4, and concentrated to afford 224 mg of diol **119** as an off-white solid that was used without further purification (0.95 mmol, 99% yield). X-ray quality crystals were grown by slow evaporation of a benzene solution of **119**. R_f = 0.15 (1:1 hexanes:ethyl acetate); M.P. = 89.5 – 91.8 °C; ^{1}H NMR (500 MHz, CD_3OD): δ 7.41 – 7.25 (m, 5H), 5.87 – 5.81 (m, 1H), 5.73 (ddd, *J* = 9.9, 4.8, 1.9 Hz, 1H), 4.84 (s, 2H), 4.71 (q, *J* = 10.9 Hz, 2H), 4.20 (br s, 1H), 4.01 (dd, *J* = 10.9, 5.3 Hz, 1H), 3.92 (dd, *J* = 10.9, 7.0 Hz, 1H), 3.73 (dd, *J* = 16.8, 4.6 Hz, 1H), 3.24 (d, *J* = 16.8 Hz, 1H), and 2.85 (br s, 1H); ^{13}C NMR (101 MHz, CD_3OD): δ 137.31, 128.63, 127.95, 127.64, 127.00, 125.71, 75.32, 67.82, 65.48, 59.83, and 54.55; IR (neat) 3322 (br), 3034, 2872, 2813, 1454, 1401, 1369, 1124, 1089, 1045, 998, and 953 cm^{-1}; HR-ESIMS requires for $C_{13}H_{17}NO_3$ $(M+H)^+$ 236.1281, found 236.1283.

(±)-(2*R*, 3*R*)-*N*-methoxy-2-hydroxymethyl-3-hydroxy-1,2,3,6-tetrahydropyridine (120)

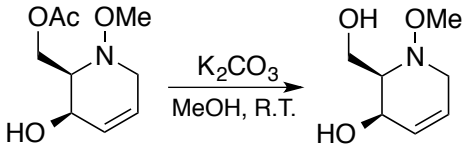

To a solution of **114** (0.82 mmol, 165 mg) in methanol (16 mL) was added potassium carbonate (17.1 mmol, 2.36 g) all at once and the resulting suspension was stirred for 16 hours at room temperature. After concentration under reduced pressure, the crude residue was taken up in 10 mL of water and extracted with $CHCl_3$:*i*-PrOH (3:1 v:v, 3 x 15 mL). The combined organic extracts were washed with brine, dried over Na_2SO_4, and concentrated to afford 117 mg of diol **120** as an off-white solid that was used without further purification (0.73 mmol, 89% yield). R_f = 0.3 (5% DCM:MeOH); M.P. = 67.4 – 70.1 °C; ^{1}H NMR (400 MHz, CD_3OD): δ 5.85 – 5.79 (m, 1H), 5.74 (dd, *J* = 9.7, 4.2 Hz, 1H), 4.15 (s, 1H), 3.96 (ddd, *J* = 10.9, 5.6, 1.0 Hz, 1H), 3.88 (ddd,

J = 10.9, 6.7, 1.0 Hz, 1H), 3.77 (ddd, *J* = 16.5, 4.5, 1.2 Hz, 1H), 3.51 (s, 3H), 3.18 (d, *J* = 16.6 Hz, 1H), and 2.78 (s, 1H); ^{13}C NMR (101 MHz, CD_3OD): δ 127.01, 125.51, 67.74, 65.12, 59.82, 59.63, and 53.75; IR (neat) 3303, 2980, 2930, 2885, 2816, 1470, 1451, 1388, 1337, 1299, 1223, 1125, 1078, 1049, 1008, 986, 935, and 751 cm^{-1}; HR-ESIMS requires for $C_7H_{13}NO_3$ $(M+Na)^+$ 182.0788, found 182.0788.

(±)-(2*R*, 3*R*, 4*S*, 5*S*)-*N*-phenylmethoxy-2-hydroxymethyl-3,4,5-trihydroxypiperidine (121)

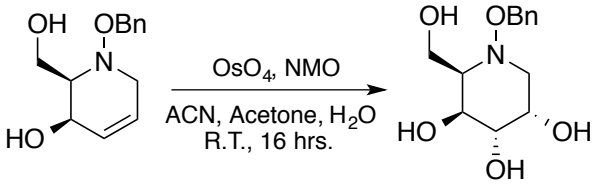

To a solution of **119** (0.992 mmol, 233.3 mg) in acetonitrile, acetone, and deionized water (6 mL, 1:1:1 v/v) was added NMO (1.98 mmol, 0.21 mL) followed by 1.3 mL of a 1 wt. % solution of osmium tetroxide in deionized water and the resulting solution was stirred overnight at room temperature. The reaction mixture was then filtered through a pad of celite and the pad washed with methanol (3 x 10 mL). After concentration under reduced pressure, the crude residue was purified by column chromatography (5% - 10% DCM:MeOH) to afford 220 mg of the pure piperidine **121** as a white solid (0.82 mmol, 82% yield). X-ray quality crystals were grown by vapor diffusion of pentane into an ethanol solution of **121**. R_f = 0.2 (10% DCM:MeOH); M.P. = 130.7 – 133.5 °C; ^{1}H NMR (400 MHz, CD_3OD): δ 7.40 – 7.21 (m, 5H), 4.83 (s, 2H), 4.70 (d, *J* = 10.7 Hz, 1H), 4.63 (d, *J* = 10.6 Hz, 1H), 3.97 (d, *J* = 8.9 Hz, 1H), 3.95 – 3.92 (m, 1H), 3.89 (d, *J* = 10.8 Hz, 1H), 3.76 (s, 1H), 3.23 (ddd, *J* = 9.6, 4.6, 1.0 Hz, 1H), 2.84 (s, 1H), and 2.76 (d, *J* = 10.4 Hz, 1H); ^{13}C NMR (101 MHz, CD_3OD): δ 137.17, 128.56, 127.94, 127.60, 74.87, 70.61, 70.15, 65.51, 64.32, 59.72, and 55.90; IR (neat) 3225 (br), 3031, 2978, 2951, 2919, 2842, 1460,

1451, 1437, 1366, 1319, 1210, 1101, 1062, 1042, 974, 909, and 856 cm^{-1}; HR-ESIMS requires for $C_{13}H_{19}NO_5$ $(M+H)^+$ 270.1336, found 270.1337.

(±)-(2*R*, 3*R*, 4*S*, 5*S*)-*N*-methoxy-2-hydroxymethyl-3,4,5-trihydroxypiperidine (122)

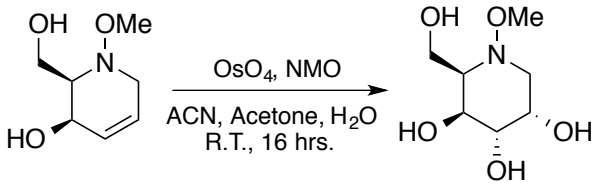

To a solution of **120** (0.63 mmol, 100 mg) in acetonitrile, acetone, and deionized water (3.75 mL, 1:1:1 v/v) was added NMO (1.26 mmol, 0.13 mL) followed by 0.8 mL of a 1 wt. % solution of osmium tetroxide in deionized water and the resulting solution was stirred overnight at room temperature. The reaction mixture was then filtered through a pad of celite and the pad washed with methanol (3 x 10 mL). After concentration under reduced pressure, the crude residue was purified by column chromatography (5% - 20% DCM:MeOH) to afford 97.3 mg of the pure piperidine **122** as an off white gum (0.5 mmol, 80%). R_f = 0.4 (20% DCM:MeOH); ^{1}H NMR (500 MHz, CD_3OD): δ 4.03 – 3.93 (m, 2H), 3.89 (dt, *J* = 12.1, 6.0 Hz, 2H), 3.80 – 3.72 (m, 1H), 3.48 (s, 3H), 3.23 (dd, *J* = 9.7, 4.6 Hz, 1H), 2.77 (s, 1H), and 2.69 (s, 1H); ^{13}C NMR (500 MHz, CD_3OD): δ 70.42, 70.18, 65.37, 64.36, 59.68, 59.15, and 55.04; IR (neat) 3297, (br), 2961, 2940, 2918, 2891, 2845, 1454, 1369, 1228, 1103, 1072, 1051, 1039, 1014, 974, and 950 cm^{-1}; HR-ESIMS requires for $C_7H_{15}NO_5$ $(M+Na)^+$ 216.0842, found 216.0840.

4.4 References

1. (a) Riddell, F.G.; Turner, E.S.; Boyd, A. *Tetrahedron* **1979**, *35*, 259. (b) Hassan, A.; Wazeer, M.I.M.; Perzanowski, H.P.; Ali, S.A. *J. Chem. Soc. Perkin Trans.* **1997**, *2*, 411. (c) Raban, M.; Kost, D. *Tetrahedron* **1984**, *40*, 3345.
2. Malik, G.; Ferry, A.; Guinchard, X.; Cresteil, T.; Crich, D. *Chem. Eur. J.* **2013**, *19*, 2168.
3. Jeffrey, C.S.; Barnes, K.L.; Eickhoff, J.E.; Carson, C.R. *J. Am. Chem. Soc.* **2011**, *133*, 7688.
4. Barnes, K.L.; Koster, A.K.; Jeffrey, C.S. *Tetrahedron Lett.* **2014**, *55*, 4690.
5. For a similar azepine ring contraction see: Bagal, S.K.; Davies, S.G.; Lee, J.A.; Roberts, P.M.; Russell, A.J.; Scott, P.M.; Thomson, J.E. *Org. Lett.* **2010**, *12*, 136.
6. Baga, S.K.; Davies, S.G.; Lee, J.A.; Roberts, P.M.; Scott, P.M.; Thomson, J.E. *J. Org. Chem.* **2010**, *75*, 8133.
7. For examples see: (a) Baxter, E.W.; Reitz, A.B. *Bioorg. Med. Chem. Lett.,* **1992**, *2*, 1419. (b) Baxter, E.W.; Reitz, A.B. *J. Org. Chem.,* **1994**, *59*, 3175. (c) Johnson, C.R.; Golebiowski, A.; Schoffers, E.; Sundram, H.; Braun, M.P. *Synlett,* **1994**, *4*, 313.

Chapter 5: Alternative Methods of Generating Aza-Oxyallylic Cations

5.1 Introduction

As discussed in Chapter 2, one of the limitations encountered in our methodology was the inability to incorporate heteroatoms at the α-carbon of the α-haloamide starting materials. This disadvantage turned out to be quite significant, as the only way to incorporate oxygen or nitrogen into a cycloadduct was by nucleophilic displacement of a chloride atom and always resulted in ring contraction to a six-membered tetrahydropyridine core. Recently, our group has reported the oxidative 1,4-diamination of dienes using simple urea derivatives **124** to construct diaza-seven-membered heterocycles **126** (Scheme 5.1.1).[1] This reaction hinges on formation of a diaza-oxyallylic cation intermediate **125** *in situ* through a series of deprotonation and oxidation events of a dibenzyloxyurea derivative respectively. Given that hypervalent iodide reagents have been shown to be effective oxidants for the generation of *N*-acylnitrenium ions from *O*-alkyl hydroxamates,[2,3] it was our vision to explore the possibility of generating an aza-oxyallylic cation by deprotonation followed by oxidation of an *O*-alkyl hydroxamate functionalized at the α-position with either oxygen or nitrogen.

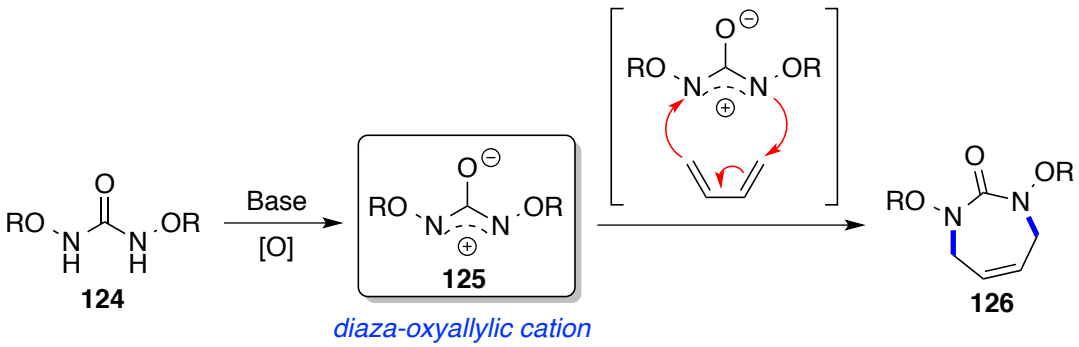

Scheme 5.1.1. Oxidative 1,4-diamination of dienes through a diaza-oxyallylic cation intermediate.

5.2 Toward an Oxidative Generation of Aza-Oxyallylic Cations

In order to explore the feasibility of our hypothesis, two substrates were synthesized, 2-methoxy-*N*-(phenylmethoxy)acetamide **128** and 2-(*N*-phthalyl)-*N*-(phenylmethoxy)acetamide **130** from the corresponding commercially available acid chlorides **127** and **129** respectively (Scheme 5.2.1). Given that (diacetoxyiodo)benzene (DIB) was found to be the optimal oxidant for the 1,4-

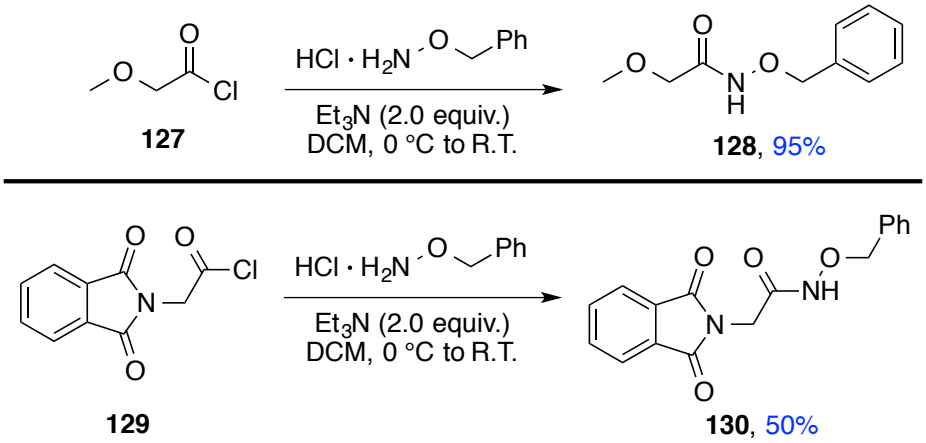

Scheme 5.2.1. Synthesis of α-heteroatom-substituted amide starting materials.

diamination cases, we initially set out to screen bases using 2,2,3,3-tetrafluoro-1-propanol as the solvent.[4] First studied was α-methoxy hydroxamate **128** and was dissolved in the solvent and diene followed by addition of the oxidant and base at 0 °C. Various bases were evaluated in their ability to affect the desired reactivity including triethylamine, 2,6-lutidine, cesium carbonate, sodium carbonate, diisopropylamine, potassium *t*-butoxide, and $CHF_2CF_2CH_2ONa$, with the results being tabulated in Table 5.2.1 below. Amine bases such as triethylamine, diisopropylamine, and 2,6-lutidine gave undesired reactivity and resulted in either no reaction or solvolysis of the intermediate (entries 1-3). Sodium carbonate and cesium carbonate were both found to be ineffective, providing almost a quantitative recovery of the starting material (entries 4 and 5). We were optimistic about the sodium salt of 2,2,3,3-tetrafluor-1-propanol being able to give at least a small amount of the desired cycloadduct given the success of the oxidative 1,4-diamination reaction, however to our dismay this base too proved to fail and gave solvolysis of

the intermediate (entry 5). Interestingly, potassium *t*-butoxide appeared to have given the desired product in a trace amount as observed by crude ^{1}H NMR (entry 6), however attempts to optimize the reaction to provide enough of the pure cycloadduct for characterization including slow addition of the substrate to the reaction mixture, changing the order of addition of reagents, and lowering of the temperature were all unproductive. Using potassium *t*-butoxide as the base and switching to the more bulkier hexafluoroisopropanol solvent was thought to be helpful, however no reaction was observed including no solvolysis and gave recovery of the starting material (entry 7).

Table 5.2.1. Solvent and Base Effects in the Oxidative Generation of Alpha-Methoxy Substituted Aza-Oxyallylic Cations

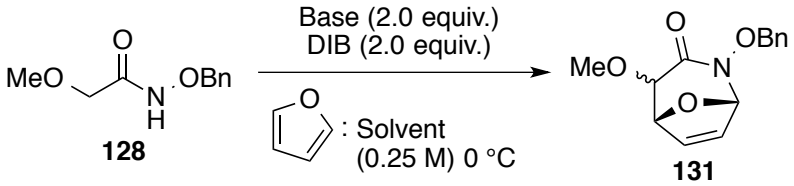

Entry	Solvent	Base	% Yield
1	$CHF_2CF_2CH_2OH$	Et_3N	solvolysis
2	$CHF_2CF_2CH_2OH$	$(i\text{-pr})_2NH$	solvolysis
3	$CHF_2CF_2CH_2OH$	2,6-lutidine	N.R.
4	$CHF_2CF_2CH_2OH$	Na_2CO_3	N.R.
5	$CHF_2CF_2CH_2OH$	Cs_2CO_3	N.R.
6	$CHF_2CF_2CH_2OH$	$CHF_2CF_2CH_2ONa$	solvolysis
7	$CHF_2CF_2CH_2OH$	*t*-BuOK	trace[a]
8	HFIP	*t*-BuOK	N.R.

[a]Trace amount of **131** detected by crude ^{1}H NMR analysis.

Next studied was α-*N*-phthalyl hydroxamate **130** in a similar fashion, with hexafluoroisopropanol being chosen as the solvent in an effort to minimize competitive solvolysis products. Once again, triethylamine, diisopropylamine, and 2,6-lutidine gave no reaction and resulted in recovery of the starting material (entries 1-3, Table 5.2.2). Sodium carbonate and cesium carbonate were observed to be incompatible bases, giving decomposition of the reactant (entries 4 and 5). The sodium salt of 2,2,3,3-tetrafluor-1-propanol and potassium *t*-butoxide both appeared to have provided the desired cycloadduct **132**, albeit once again in trace amounts as detected by crude ^{1}H NMR analysis (entries 6 and 7). Optimization attempts to provide enough product for unambiguous characterization including temperature changes, order of reagent addition changes, and different solvents were all unfruitful. Initially, it appears that more promising results could be obtained with the α-*N*-phthalyl substrate. One hypothesis could be that the acidity of the α-protons is higher due to the electron withdrawing phthalimide group. However, an equally viable argument could be made that the resulting aza-oxyallylic cation intermediate is now being destabilized and not allowing for formation of the desired cycloadduct. Nonetheless, it appears that this project could have viable merit and continued work on this methodology could be worthwhile, especially in the context of target directed synthesis.

Table 5.2.2. Solvent and Base Effects in the Oxidative Generation of Alpha-*N*-Phthalyl Substituted Aza-Oxyallylic Cations

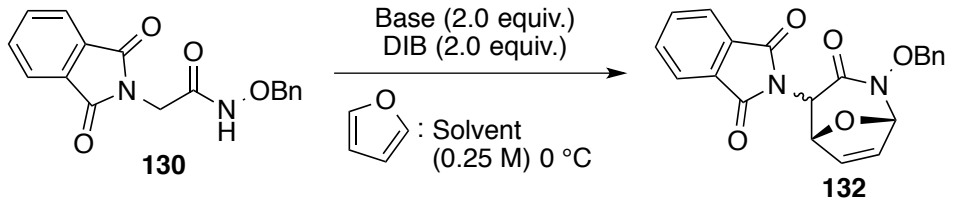

130 **132**

Entry	Solvent	Base	% Yield
1	HFIP	Et_3N	N.R.
2	HFIP	$(i\text{-pr})_2NH$	N.R.
3	HFIP	2,6-lutidine	N.R.
4	HFIP	Na_2CO_3	decomposition
5	HFIP	Cs_2CO_3	decomposition
6	HFIP	$CHF_2CF_2CH_2ONa$	trace[a]
7	HFIP	*t*-BuOK	trace[a]
8	$CHF_2CF_2CH_2OH$	$CHF_2CF_2CH_2ONa$	solvolysis
9	$CHF_2CF_2CH_2OH$	*t*-BuOK	solvolysis

[a]Trace amount of **132** detected by crude ^1H NMR analysis.

5.3 Experimental:

All reactions were carried out under an atmosphere of nitrogen in oven-dried glassware with magnetic stirring, unless otherwise specified. All reagents and solvents were purchased from Sigma-Aldrich Chemical Company and used without any further purification. TLC information was recorded on Silicycle glass 60 F_{254} plates and developed by staining with $KMnO_4$ or ceric ammonium molybdate. Purification of reaction products was carried out by flash chromatography using Silicycle Siliaflash® P60 (230-400 mesh). ^{1}H-NMR spectra were measured on Varian 400 (400 MHz) or Varian 500 (500 MHz) spectrometers and are reported in ppm (s = singlet, d = doublet, t = triplet, q = quartet, m = multiplet, br = broad; integration; coupling constant(s) in Hz using TMS as an internal standard (TMS at 0.00 ppm) in $CDCl_3$, CD_3CN, or CD_3OD. ^{13}C-NMR spectra were recorded on V400 or V500 spectrometers and reported in ppm using solvent as an internal standard ($CDCl_3$ at 77.36 ppm), (CD_3CN at 118.26 ppm) or (CD_3OD at 49.86 ppm). Infrared (IR) spectra were recorded on a Nicolet 6700 FT-IR with a diamond ATR and data are reported as cm^{-1} (br = broad, st = strong). High-resolution mass spectra were obtained using an Agilent 6230 TOF LC/MS with an atmospheric pressure photo-ionization (APPI) or electrospray (ESI) source with purine and HP-0921 as internal calibrants.

(±)-2-methoxy-*N*-(phenylmethoxy)acetamide (128):

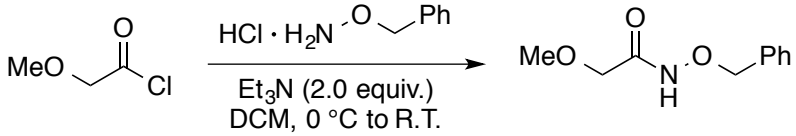

To a stirred suspension of *O*-benzylhydroxylamine hydrochloride (46.1 mmol, 7.35 g) in dichloromethane (184 mL, 0.25 M) and triethylamine (92.2 mmol, 12.9 mL) in an ice bath at 0 °C was added methoxyacetyl chloride (46.1 mmol, 4.2 mL) dropwise, followed by removal of the ice bath and warming of the reaction mixture to room temperature for 1 hour. The solvent was

removed under reduced pressure and the crude solid was purified by column chromatography (3:1 to 2:1 hexanes:ethyl acetate) to afford 8.84 g of amide **124** as a white crystalline solid (45.3 mmol, 94% yield). R_f = 0.3 (1:1 hexanes:ethyl acetate); M.P. = 41.4 – 42.8 °C; ^{1}H NMR (500 MHz, $CDCl_3$): δ 8.83 (br s, 1H), 7.45 – 7.33 (m, 5H), 4.95 (s, 2H), 3.95 (s, 2H), and 3.33 (s, 3H); ^{13}C NMR (101 MHz, $CDCl_3$): δ 166.67, 135.08, 129.13, 128.72, 128.54, 78.34, 71.44, and 59.34 IR (neat) 3193 (br), 3060, 3031, 2995, 2945, 2919, 2875, 2830, 1661 (st), 1496, 1478, 1451, 1360, 1269, 1230, 1198, 1110 (st), 1065, 1003, 986, 953, 909, 841, and 744 cm^{-1}; HR-ESIMS requires for $C_{10}H_{13}NO_3$ $(M+H)^+$ 196.0968, found 196.0969.

(±)-2-(*N*-phthalyl)-*N*-(phenylmethoxy)acetamide (130):

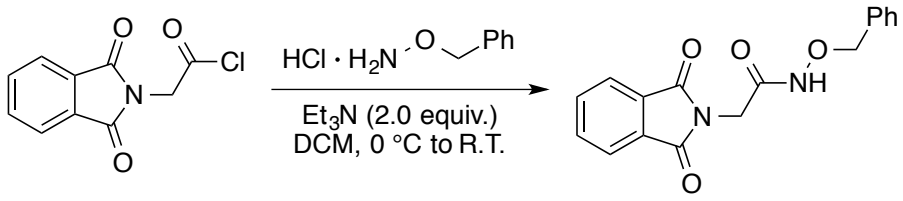

To a stirred suspension of *O*-benzylhydroxylamine hydrochloride (4.1 mmol, 650 mg) in dichloromethane (16 mL, 0.25 M) and triethylamine (8.2 mmol, 1.1 mL) in an ice bath at 0 °C was added phthalylglycyl chloride (4.1 mmol, 910.1 mg) in small portions, followed by removal of the ice bath and warming of the reaction mixture to room temperature for 1 hour. The solvent was removed under reduced pressure and the crude solid was purified by column chromatography (2:1 hexanes:ethyl acetate) to afford 602 mg of amide **130** as a white crystalline solid (1.9 mmol, 50% yield). R_f = 0.2 (2:1 hexanes:ethyl acetate); M.P. = 167.0 – 168.1 °C; ^{1}H NMR (500 MHz, CD_3OD): δ 7.93 – 7.76 (m, 3H), 7.47 – 7.30 (m, 4H), 4.84 (s, 1H), 4.23 (s, 1H), and 3.29 (dd, *J* = 2.9, 1.6 Hz, 2H); ^{13}C (121 MHz, CD_3OD): δ 167.66, 166.69, 135.32, 134.14, 132.01, 129.13, 128.31, 128.09, 122.94, 77.73, and 37.56; IR (neat) 3152 (br), 3060, 2972, 2939, 2854, 1773,

1682 (st), 1684 (st), 1613, 1493, 1463, 1451, 1413, 1389, 1360, 1319, 1248, 1233, 1192, 1113, 1086, 1045, 1012, 971, 947, 897, 756, and 738 cm^{-1}; HR-ESIMS requires for $C_{17}H_{14}N_2O_4$

5.4 References

1. Anumandla, D.A.; Littlefield, R.; Jeffrey, C.S. *Org. Lett.* **2014**, *16*, 5112.
2. Wardrop, D.J.; Bowen, E.G. Synthetic Applications of Nitrenium Ions. In *Nitrenes and Nitrenium Ions*; Falvey, D.E., Gudmundsdottir, A.D., Eds.; Wiley: Weinhiem, 2013; pp 347−449.
3. Kikugawa, Y. *Heterocycles* **2009**, *78*, 571 and references cited therein.
4. TFP is a solvent that can be purchased from SynQuest Laboratories for $ 0.07/g and has been demonstrated to be the optimal solvent of other [4 + 3] reactions, see: Föhlisch, B.; Gehrlach, E.; Geywitz, B. *Chem. Ber*. **1987**, *120*, 1815.

Chapter 6: Conclusions and Future Work

6.1 Conclusions and Future Work

Historically, the aza-oxyallylic cation intermediate was proposed in order to rationalize the selectivity behind the nucleophilic ring opening of α-lactams. Despite proposals of the aza-oxyallylic cation's involvement in a variety of processes, experimental and theoretical evidence had largely ruled out its existence. A key solvolysis experiment by Kikugawa coupled with our own theoretical investigations led us to believe that placement of an electron donating alkoxy group on the nitrogen atom could provide a necessary stabilization to the intermediate.[1-3] Inspired by the large comprehensive body of work on [4+3] cycloadditions of oxyallylic cations, we demonstrated that α-halo hydroxamates react with cyclic dienes under basic conditions in fluorinated solvents, providing the first experimental evidence of an aza-oxyallylic cation. Most of the substrates in the aza-[4+3] cycloaddition demonstrated a selectivity for the *endo* diastereoisomer (≥19:1 *endo*:*exo*). The exception was α-chloro cycloadduct **66f**, with the diastereoisomeric ratio being high at 40% conversion ((≥19:1 *endo*:*exo*); but equilibrated to a 2:1 *endo*:*exo* ratio upon reaction completion. When the purified *endo*-adduct was re-subjected to the reaction conditions the product was observed to have isomerized to a 1:1 mixture of diastereoisomers. In light of this result, we believe that there is some sort of kinetic preference for the *endo*-cycloadduct, however additional investigations aimed at better understanding the exact nature of this selectivity could prove worthwhile. Our initial report focused on demonstrating the viability of our method toward constructing seven-membered heterocycles, with little exploration of the actual reaction mechanism. Another project that could stem from this work would include comprehensive mechanistic studies, specifically directed at determining if the reaction was more of a stepwise process or concerted.

Recently, our methodology has found application in the field of polymer chemistry by Fishman and Kiessling, who utilized our heterocyclic scaffold **133** as a starting point to synthesize a new class of degradable polymers.[4] Ring opening metathesis polymerization (ROMP) using Grubbs' catalyst **134** was found to readily occur on monomer **133** in THF at room temperature. It was demonstrated that several poly-oxazinones **135** were stable over pH values from 4.6 to 9.1; however decomposition to β-hydroxy amide **136** and enal **137** readily occurred upon subjection to pH 2.5 or highly basic conditions. The flexibility of our method allows for the incorporation of a wide variety of side chains both at the C- and N-terminus, permitting extensive derivatization in this new class of degradable polymer. In a special case, Kiessling showed that an azide functional group is tolerant to the aza-[4+3] cycloaddition and could be used as a linker to glycosides via a click reaction with a propargylated sugar. Subsequent polymerization of this glycosidic monomer demonstrated that biomolecules could be incorporated into the degradable backbone, which could allow applications in a number of biomedical applications. Additional projects in this field could include applying our method toward the construction of a library of polymers for biological testing and application exploration.

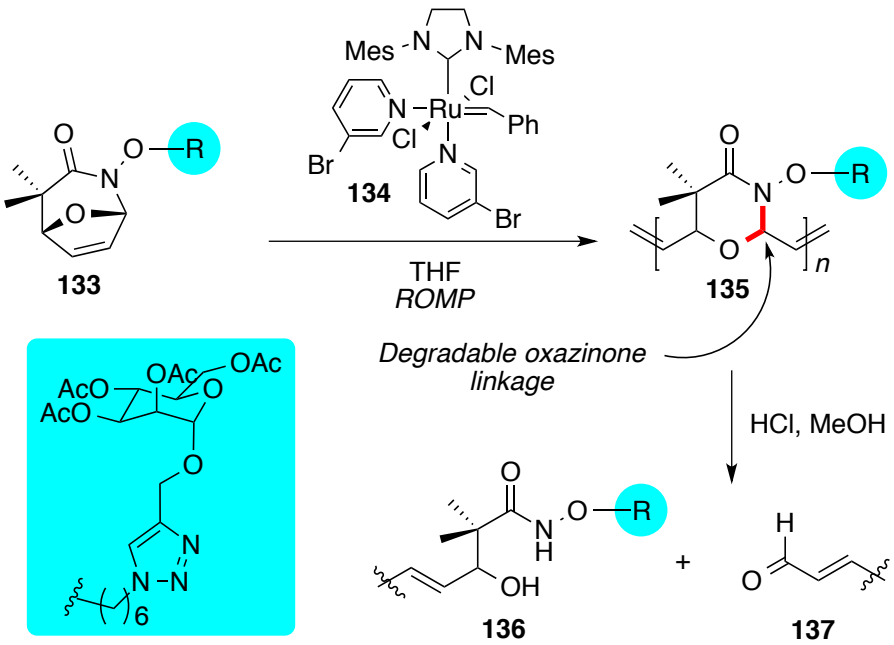

Scheme 6.1.1. [3.2.1]-Aza-bicyclononenes as new monomers for the synthesis of a new class of biodegradable ROMP polymers.

A six-membered piperidine analogue of balanol was synthesized in good yield and high diastereoselectivity, and although the desired target was not realized, we nonetheless demonstrated the feasibility of our approach if the ring contraction problem can be solved. Our method has the advantages of being diastereoselective and stems from commercially available starting materials, as well as the reactions being relatively simple and scalable for large amounts of material. On the other hand, it might be worthwhile to study the effect of shrinking the nitrogen-containing ring size and determine how this affects the biological activity. A seven-membered iminosugar derivative was achieved in only five short synthetic steps from commercially available starting materials and through an aza-[4+3] cycloaddition reaction. The reactions are high yielding, diastereoselective, and have the capability of incorporating a wide variety of side chains at the three-position. Further extensions of this project could involve synthesizing a variety of analogues for biological testing and the construction of a library of compounds.

A concise approach to the stereoselective synthesis of polyhydroxylated *N*-alkoxypiperidines from common seven-membered azacyclic cores was developed. The strategy hinged on the rich functionality that is provided through aza-[4+3] cycloaddition reactions of putative aza-oxyallylic cation intermediates with furan. A chemoselective double reduction using alane provided the prefunctionalized azepines. Silver acetate promoted ring contraction and subsequent acetate hydrolysis with potassium carbonate provided a novel method for the construction of tetrahydropyridine cores in good yield and high diastereoselectivity. Finally, stereoselective catalytic dihydroxylation mediated by osmium tetroxide gave the final polyhydroxylated products in high yields. This method represents a versatile approach to tetrahydropyridine cores and iminosugar derivatives that is only five steps from furan and 1,1-dichloroacetyl chloride. Other directions from this work are being focused on better understanding the ring contraction mechanism and elaborating the tetrahydropyridine scaffolds to other piperidine natural products of interest to our group.

Since our initial report, this new class of heterocycloaddition reactions has been applied to the selective 1,4-diamination of alkenes and the synthesis of polyheterocyclic scaffolds via an intramolecular aza-[4+3] cycloaddition.[5-7] The advances described in this dissertation provide tremendous potential for organic synthesis and method development. The high degree of selectivity contained in the aza-[4+3] cycloaddition and the bold array of functionality provided in the resulting adducts presents adequate opportunities in target-directed synthesis, and has already found application toward the development of a new ROMP degradable polymer. Moving forward, it is expected that the development of new approaches to generating aza-oxyallylic cation intermediates will be realized, leading to heteroatomic analogs that delivers selective 1,4-difunctionalization of dienes. Along with these new methods of generation, the ambivalent reactivity of this versatile intermediate can be taken advantage of in non-cycloaddition reactions. An increased understanding of the mechanistic pathway of these reactions will pave the way for

enantioselective reactions of aza-oxyallylic cations and enable researchers to take full advantage of their use in organic synthesis.

6.2 References

1. Kikugawa, Y. *Heterocycles* **2009**, *78*, 571 and references cited therein.
2. Jeffrey, C.S.; Barnes, K.L.; Eickhoff, J.E.; Carson, C.R. *J. Am. Chem. Soc.* **2011**, *133*, 7688.
3. Barnes, K.L.; Koster, A.K.; Jeffrey, C.S. *Tetrahedron Lett.* **2014**, *55*, 4690.
4. Fishman, J.M.; Kiessling, L.L. *Angew. Chem., Int. Ed.* **2013**, *52*, 5061.
5. Jeffrey, C.S.; Anumandla, D.A.; Carson, C.R. *Org. Lett.* **2012**, *14*, 5764.
6. Anumandla, D.A.; Littlefield, R.; Jeffrey, C.S. *Org. Lett.* **2014**, *16*, 5112.
7. Acharya, A.; Eickhoff, J.A.; Jeffrey, C.S. *Synthesis* **2013**, *45*, 1825.

Appendix

A.1 ^{1}H and ^{13}C NMR Spectra

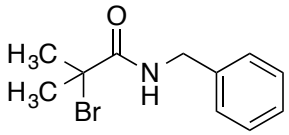

60

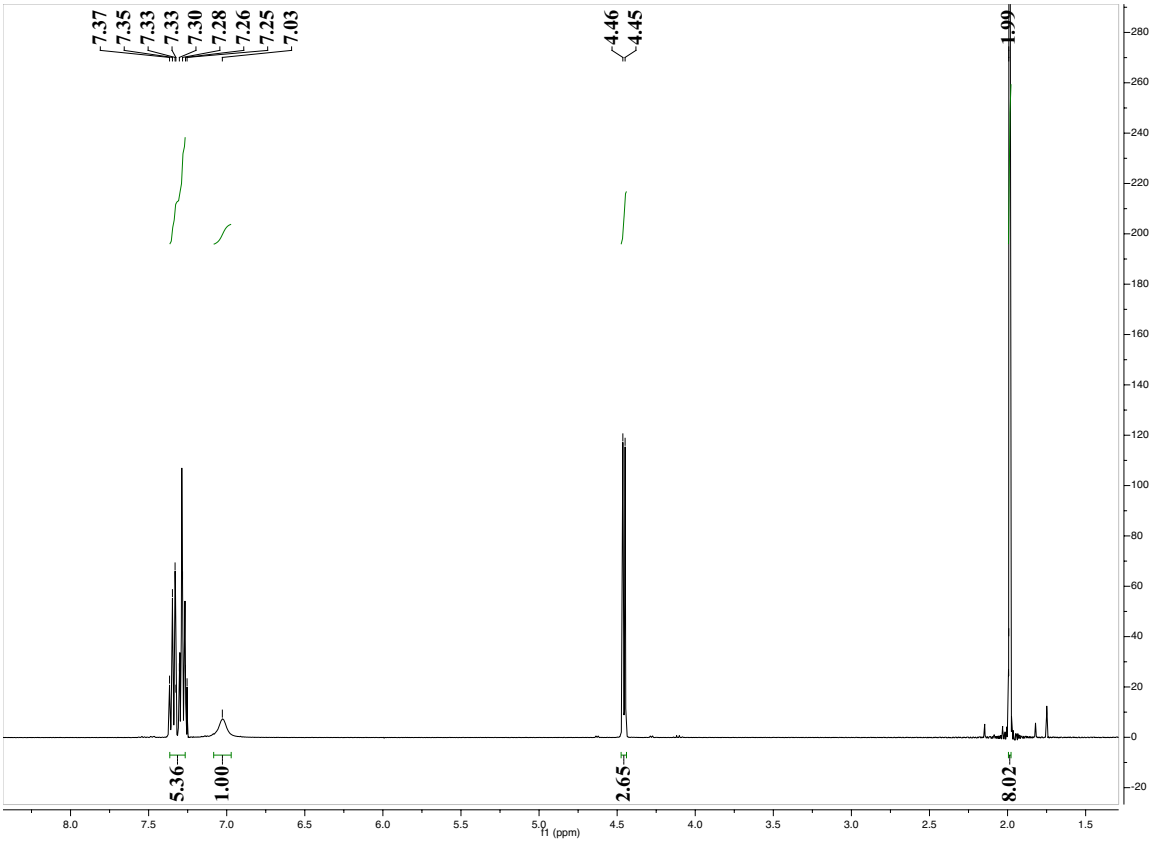

Figure A.1.1 ^{1}H NMR (500 MHz, $CDCl_3$) spectrum of **60**.

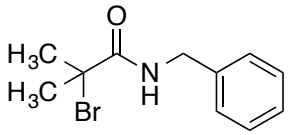

60

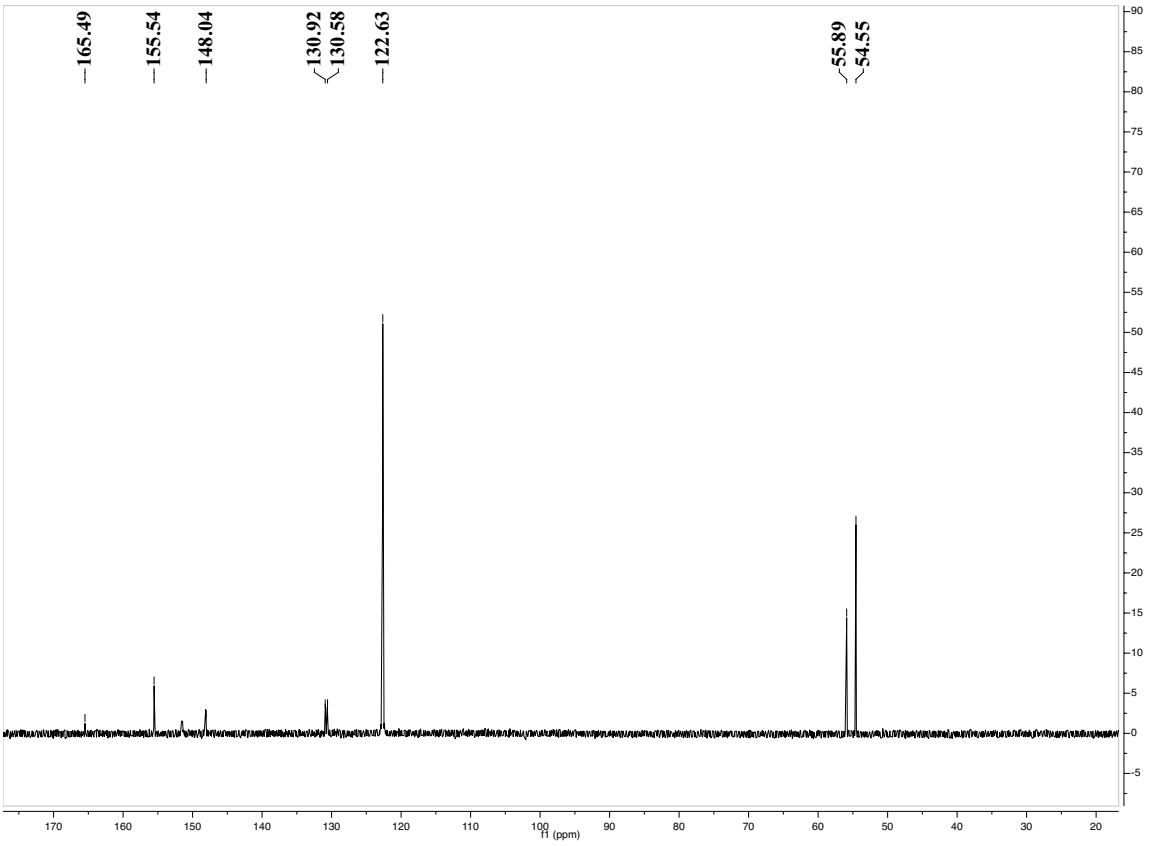

Figure A.1.2 ^{13}C NMR spectrum (126 MHz, CD_3CN) of **60**.

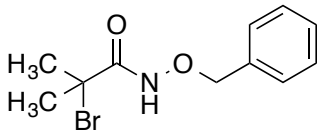

62

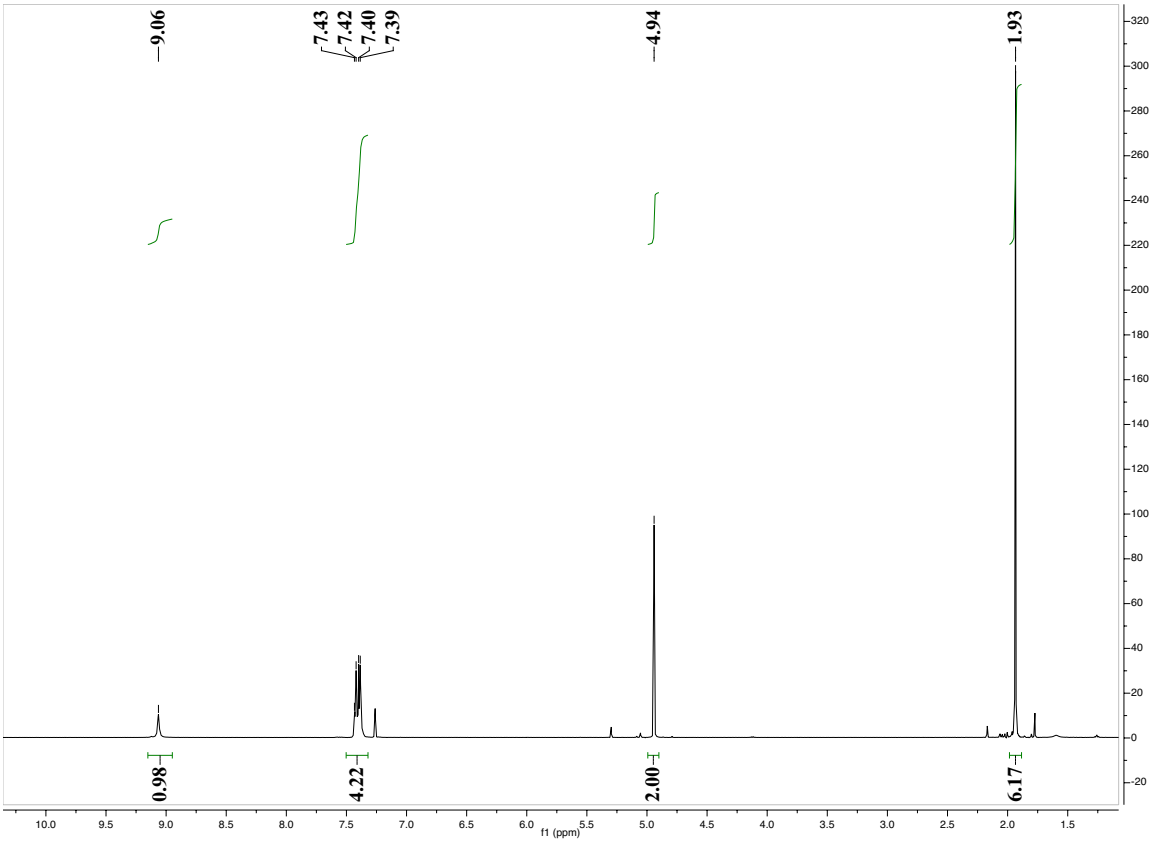

Figure A.1.3 ^{1}H NMR (500 MHz, $CDCl_3$) spectrum of **62**.

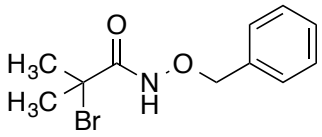

62

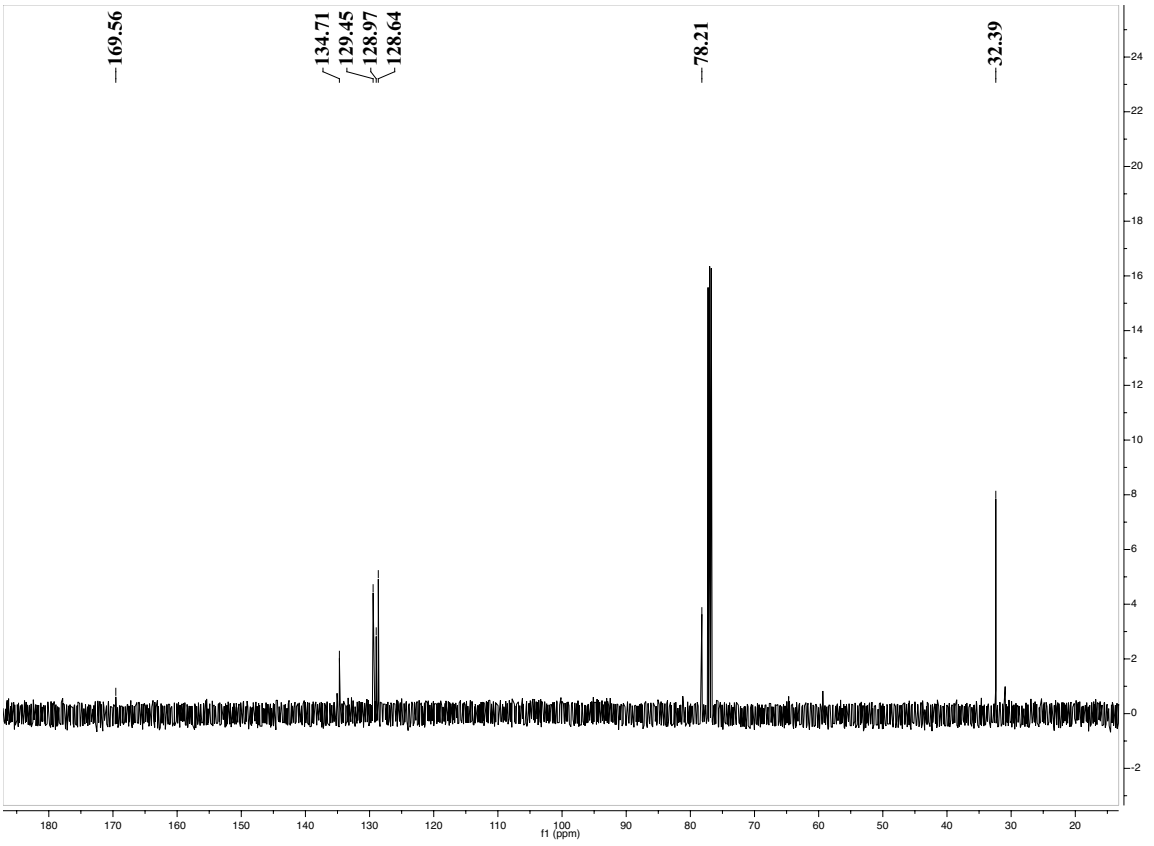

Figure A.1.4 ^{13}C NMR (126 MHz, $CDCl_3$) of **62**.

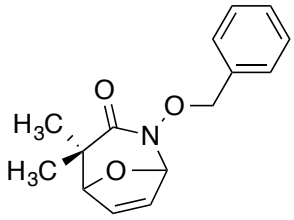

63

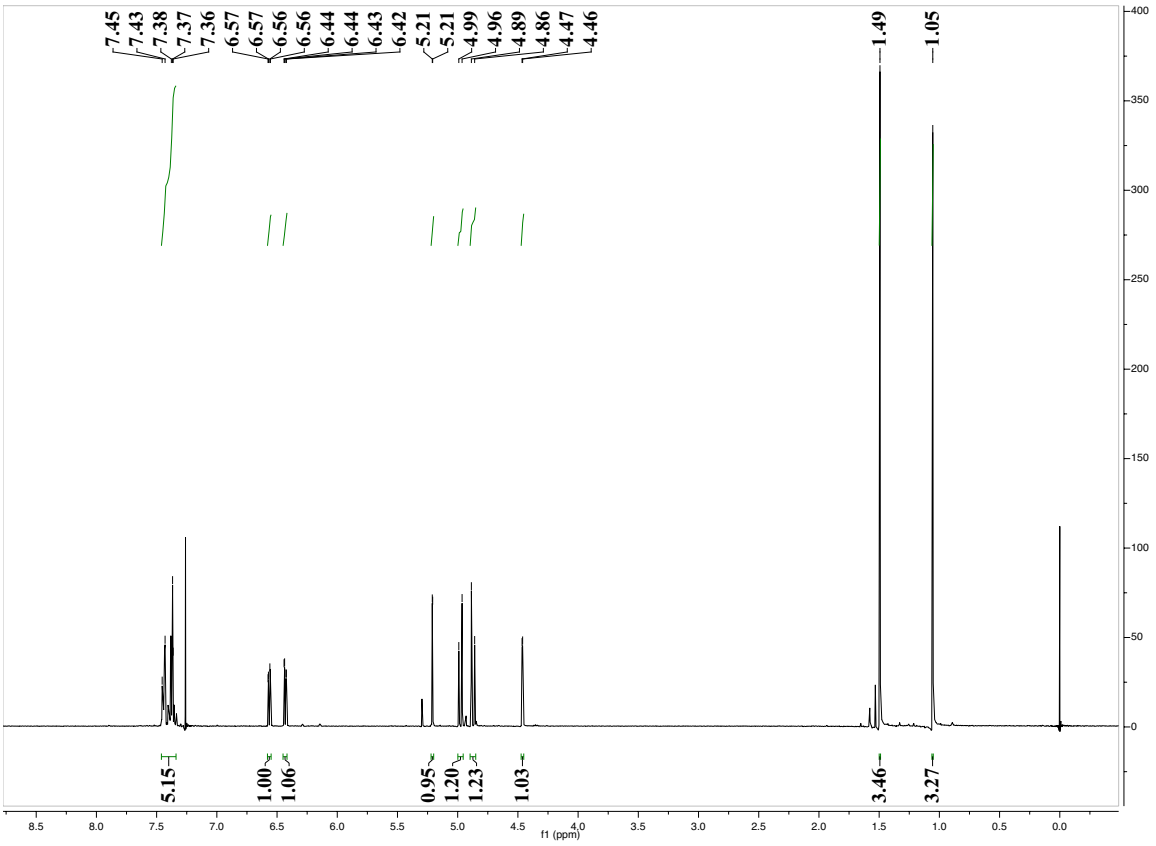

Figure A.1.5 ^{1}H NMR (400 MHz, $CDCl_3$) spectrum of **63**.

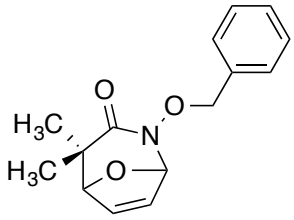

63

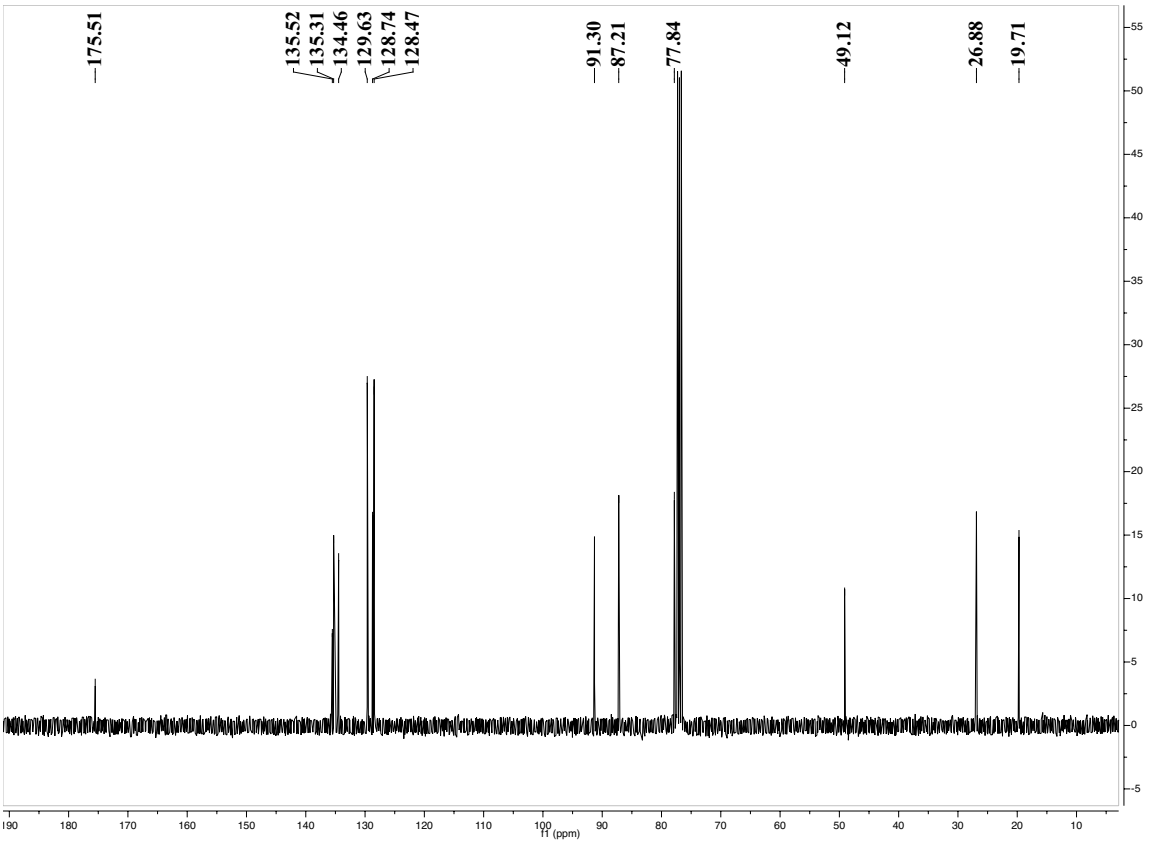

Figure A.1.6 ^{13}C NMR (101 MHz, $CDCl_3$) spectrum of **63**.

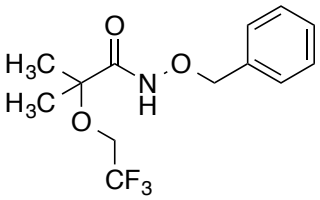

64

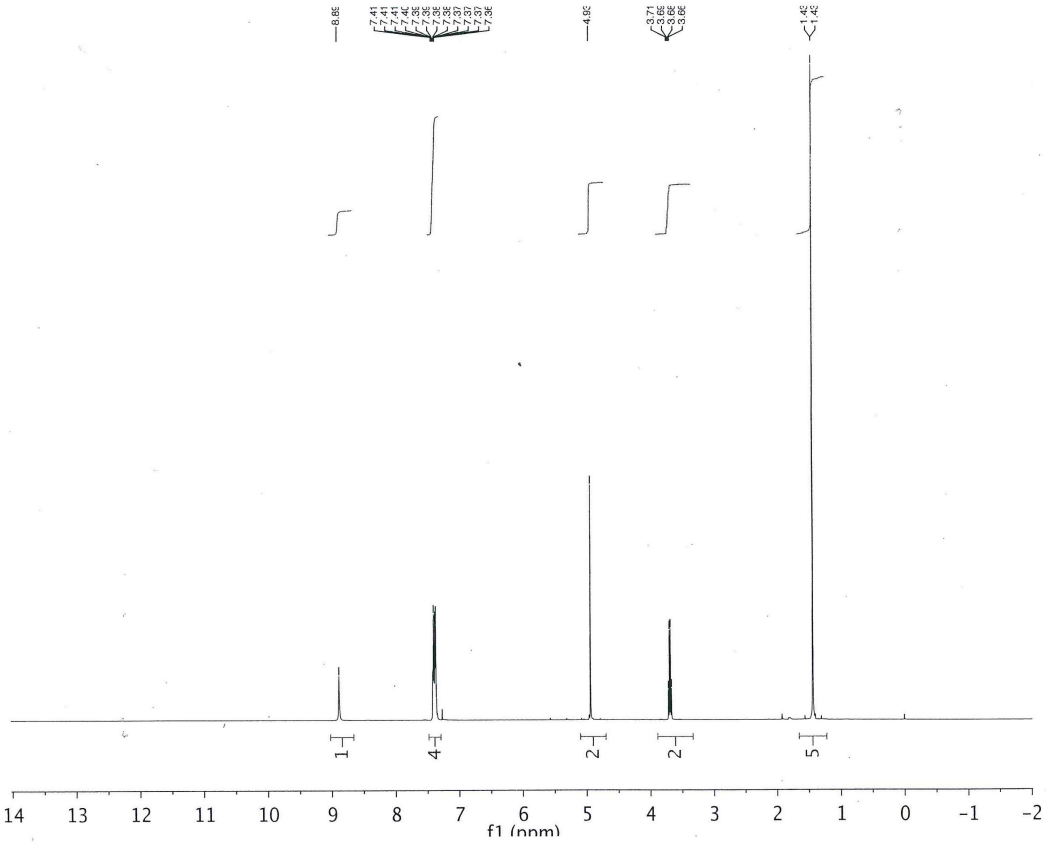

Figure A.1.7 ^{1}H NMR (500 MHz, $CDCl_3$) spectrum of **64**.

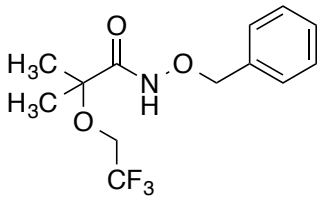

64

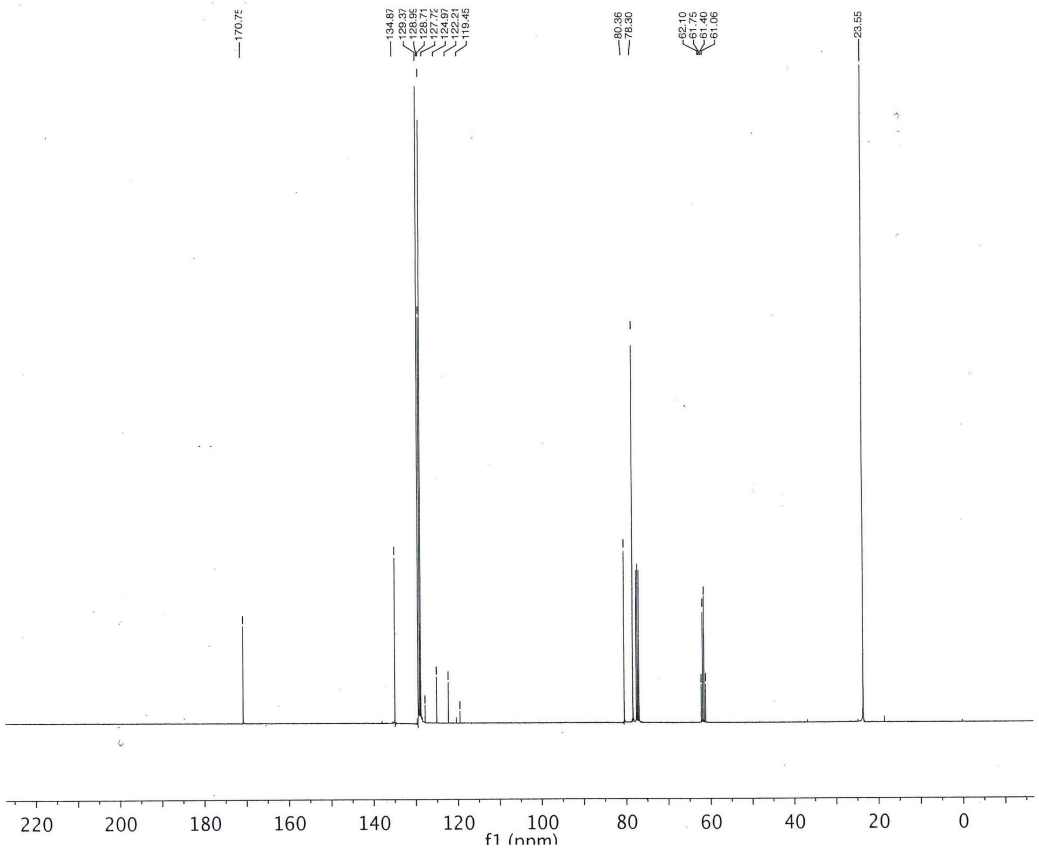

Figure A.1.8 ^{13}C NMR (121 MHz, $CDCl_3$) spectrum of **64**.

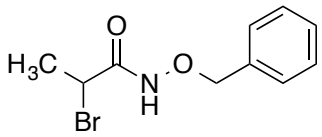

65b

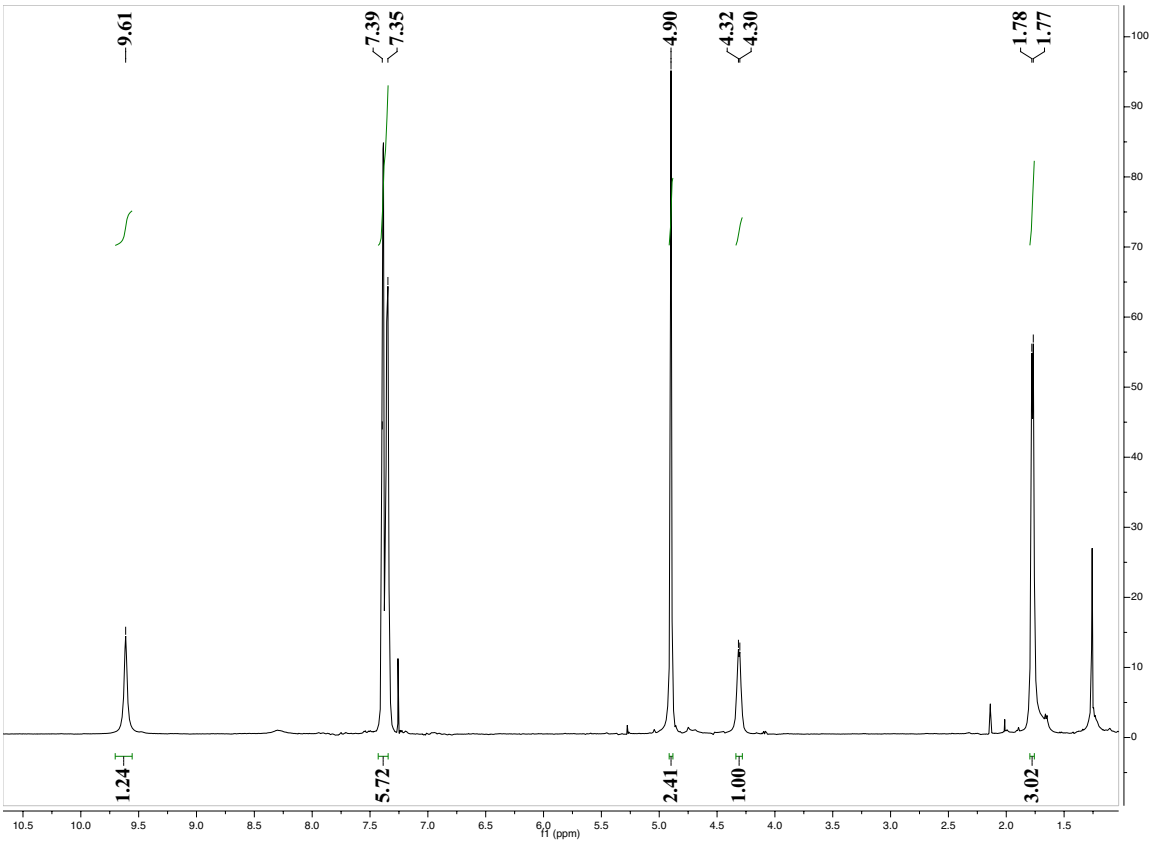

Figure A.1.9 ^{1}H NMR (500 MHz, $CDCl_3$) spectrum of **65b**.

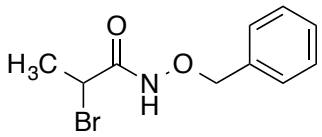

65b

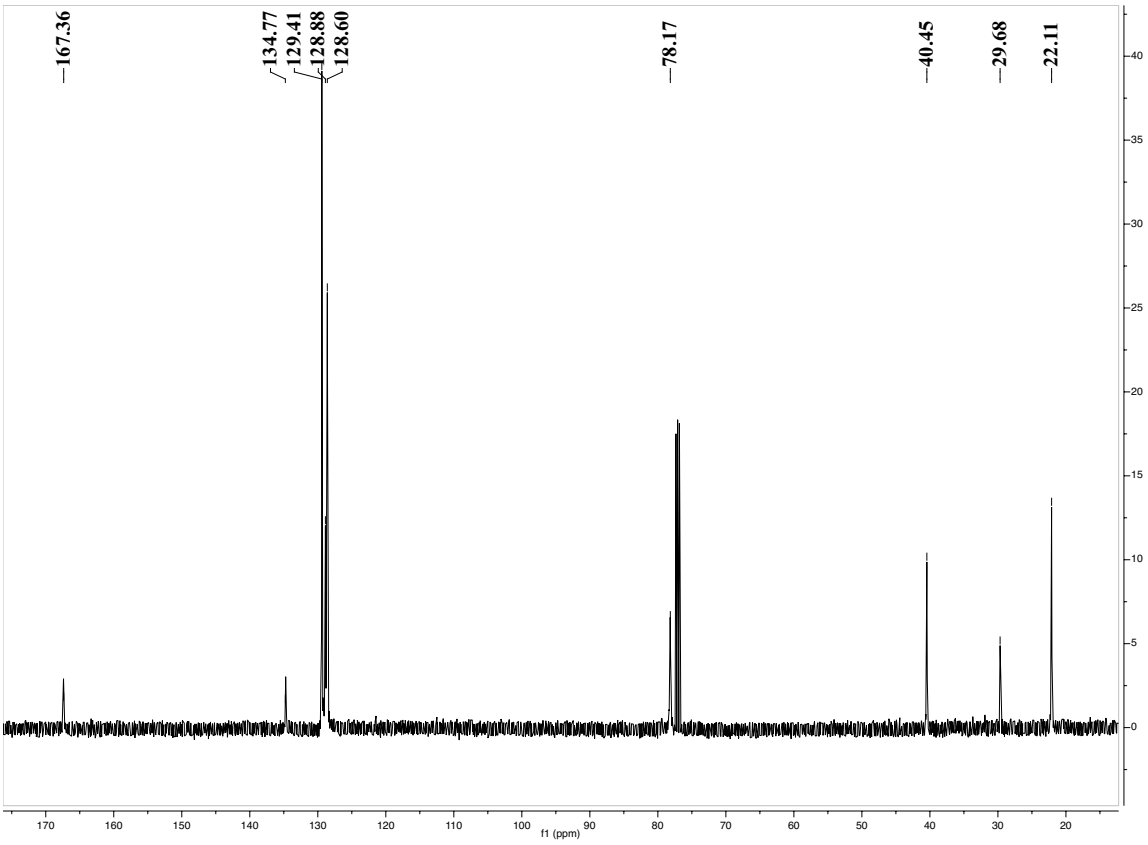

Figure A.1.10 ^{13}C NMR (126 MHz, $CDCl_3$) spectrum of **65b**.

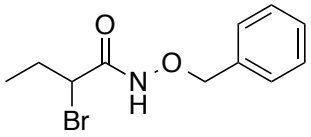

65c

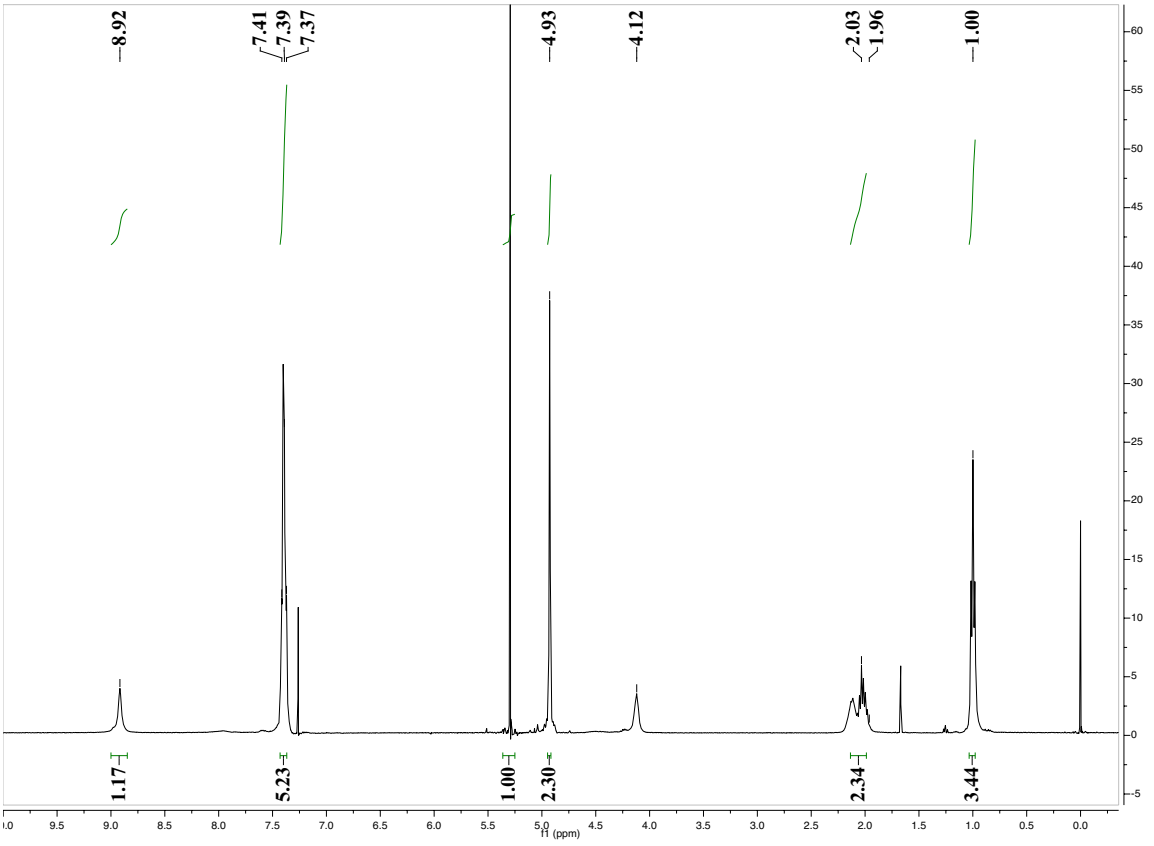

Figure A.1.11 ^{1}H NMR (400 MHz, $CDCl_3$) spectrum of **65c**.

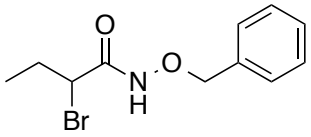

65c

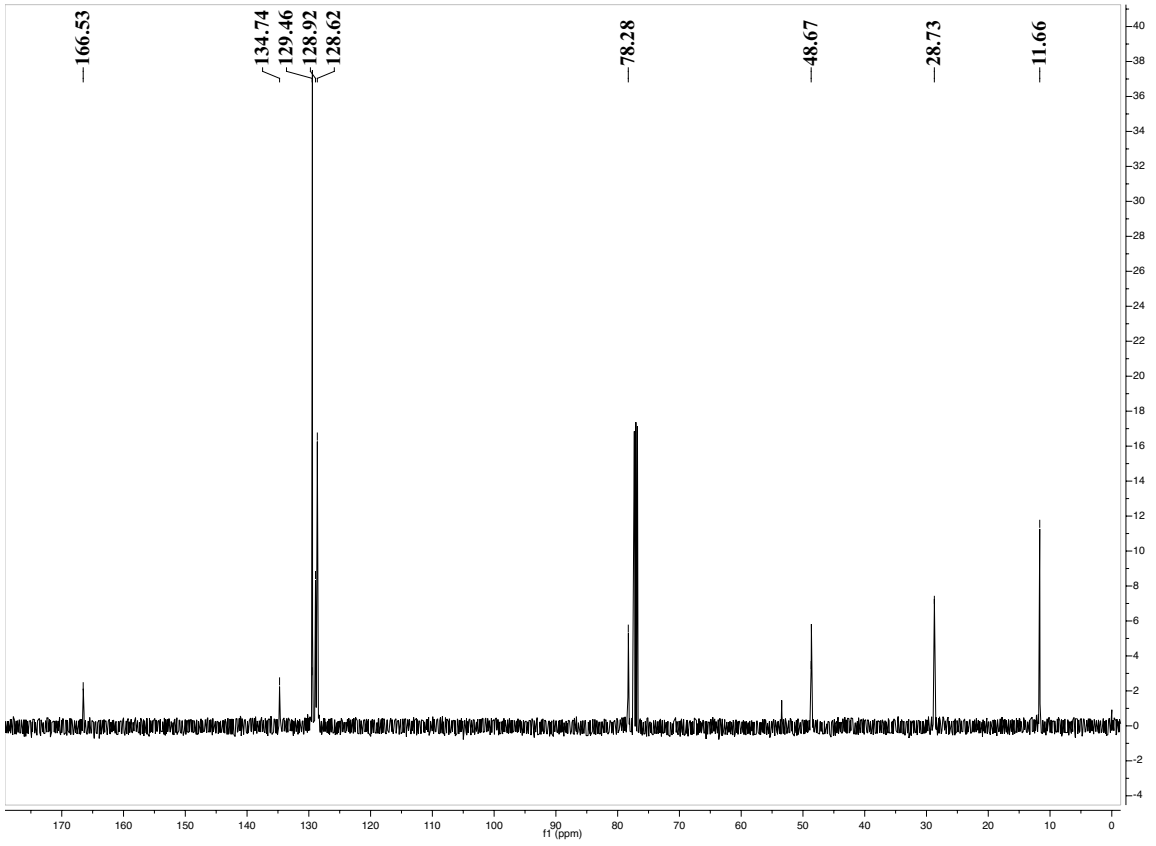

Figure A.1.12 ^{13}C NMR (126 MHz, $CDCl_3$) spectrum of **65c**.

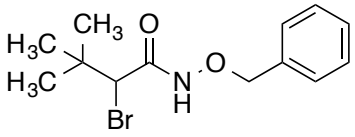

65d

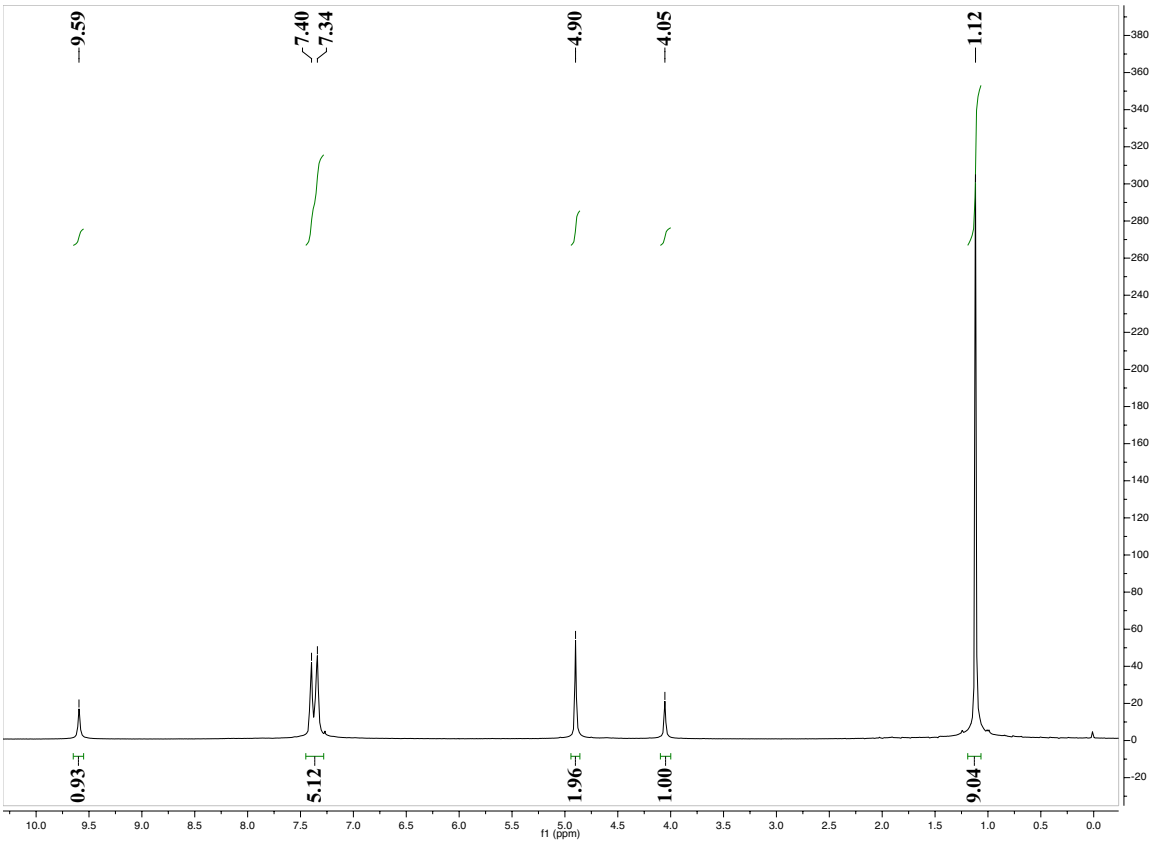

Figure A.1.13 ^{1}H NMR (500 MHz, $CDCl_3$) spectrum of **65d**.

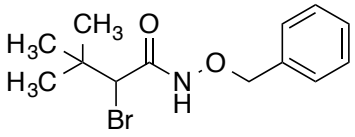

65d

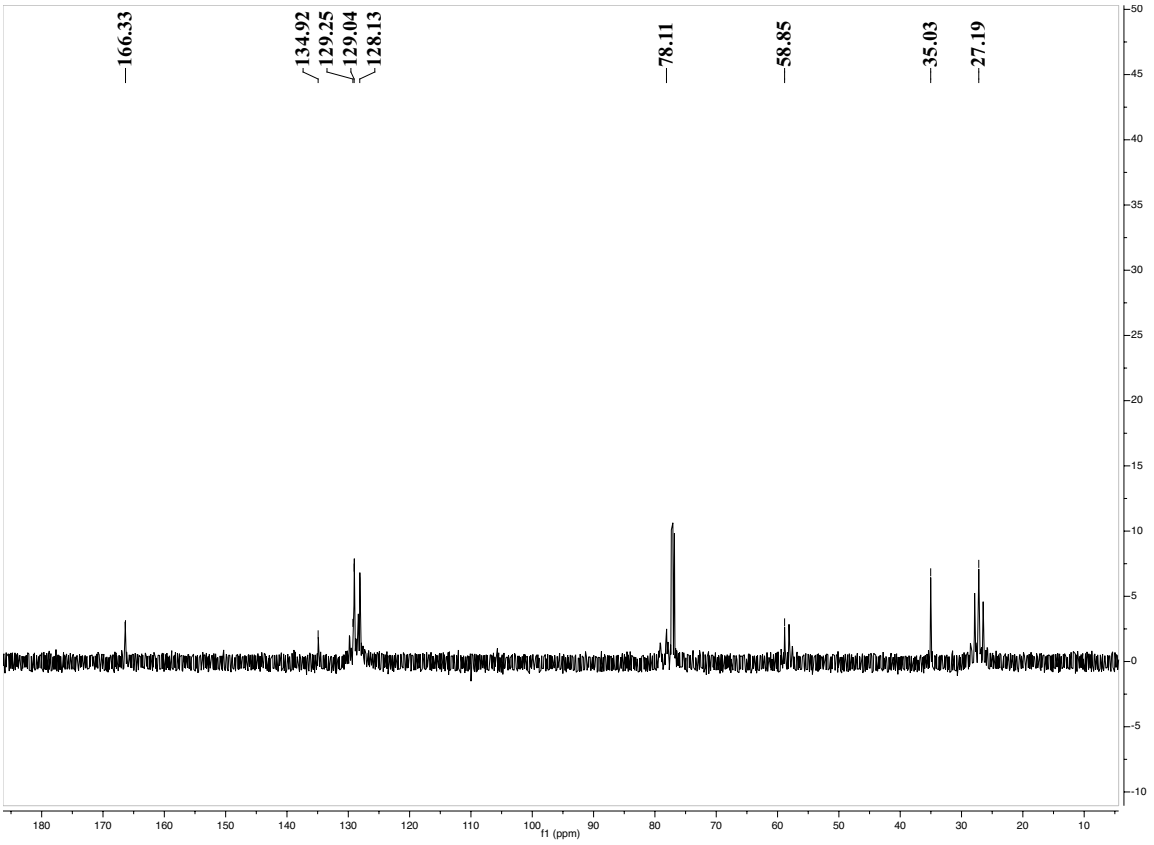

Figure A.1.14 ^{13}C NMR (126 MHz, $CDCl_3$) spectrum of **65d**.

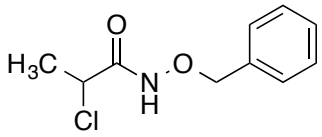

65e

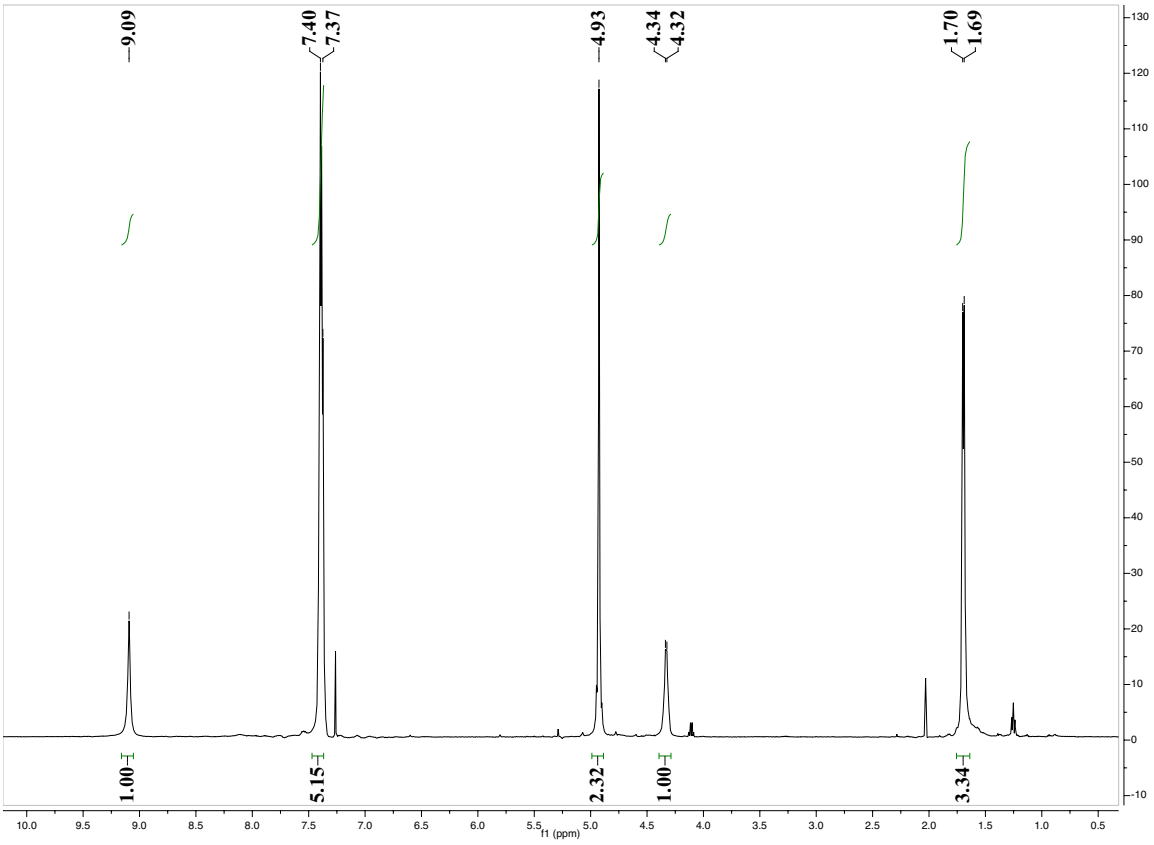

Figure A.1.15 ^{1}H NMR (500 MHz, $CDCl_3$) spectrum of **65e**.

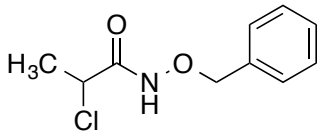

65e

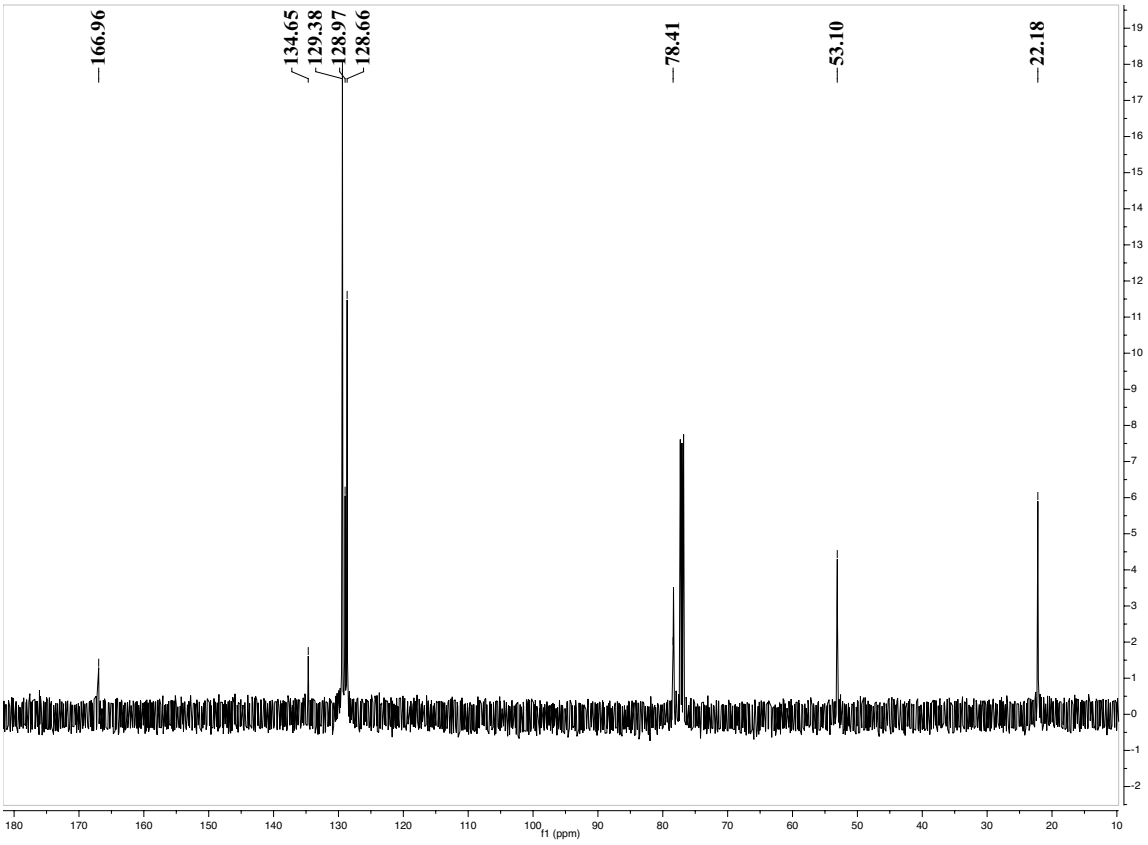

Figure A.1.16 ^{13}C NMR (126 MHz, $CDCl_3$) spectrum of **65e**.

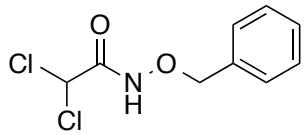

65f

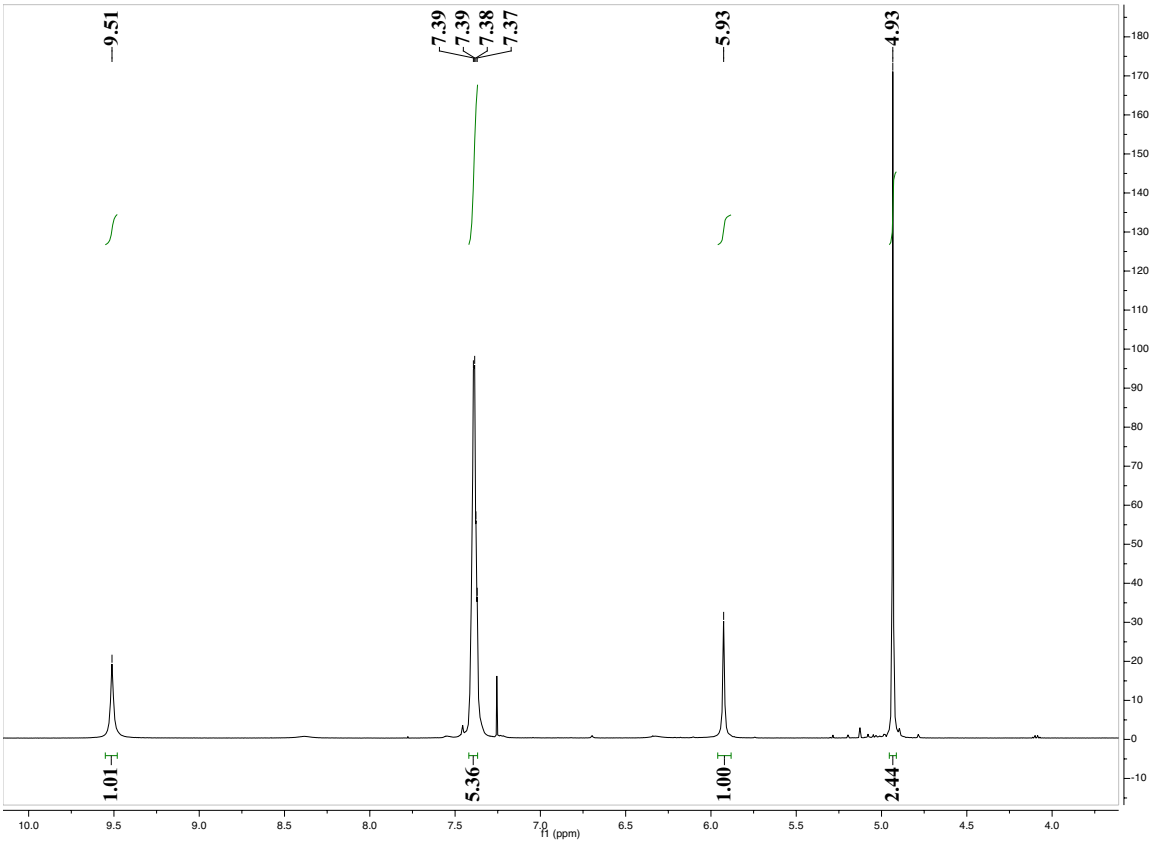

Figure A.1.17 ^{1}H NMR (500 MHz, $CDCl_3$) spectrum of **65f**.

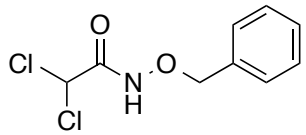

65f

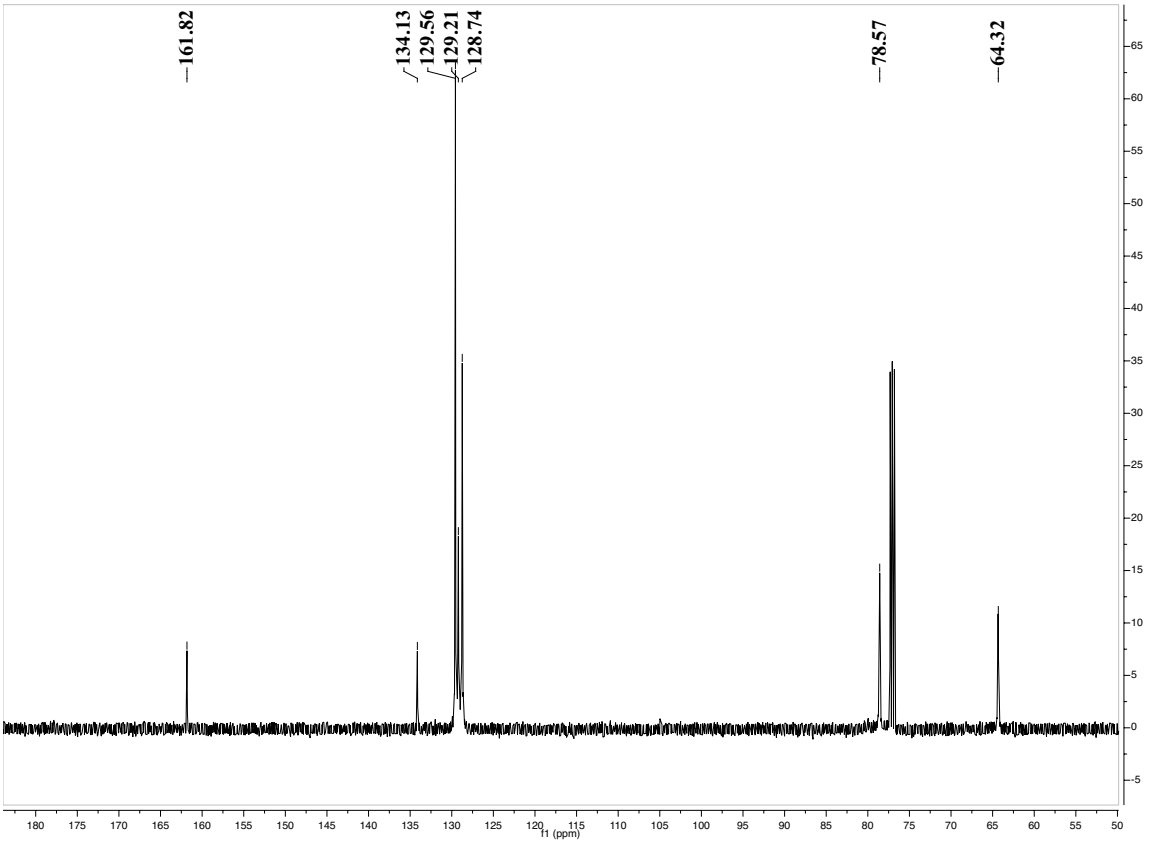

Figure A.1.18 ^{13}C NMR (126 MHz, $CDCl_3$) spectrum of **65f**.

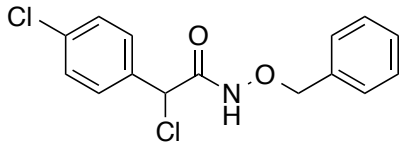

65g

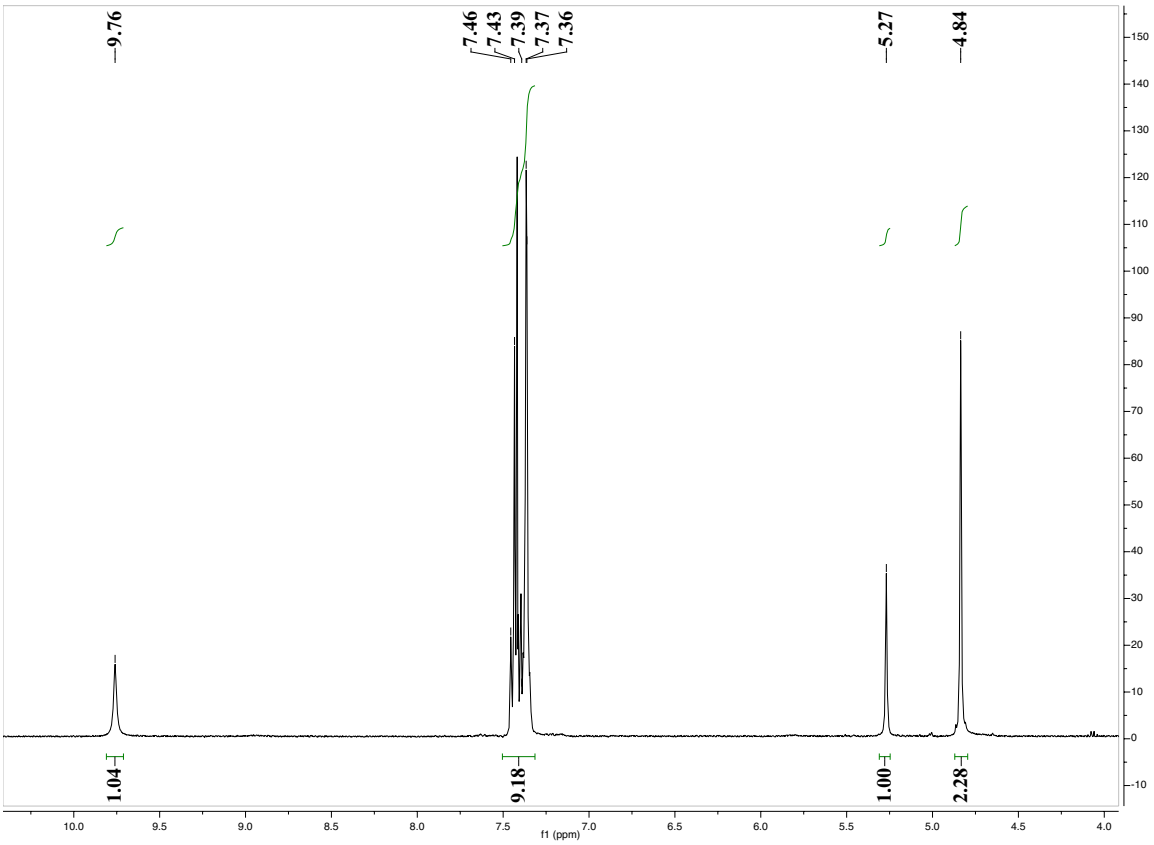

Figure A.1.19 ^{1}H NMR (400 MHz, CD_3CN) spectrum of **65g**.

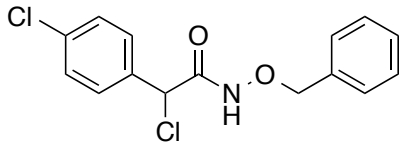

65g

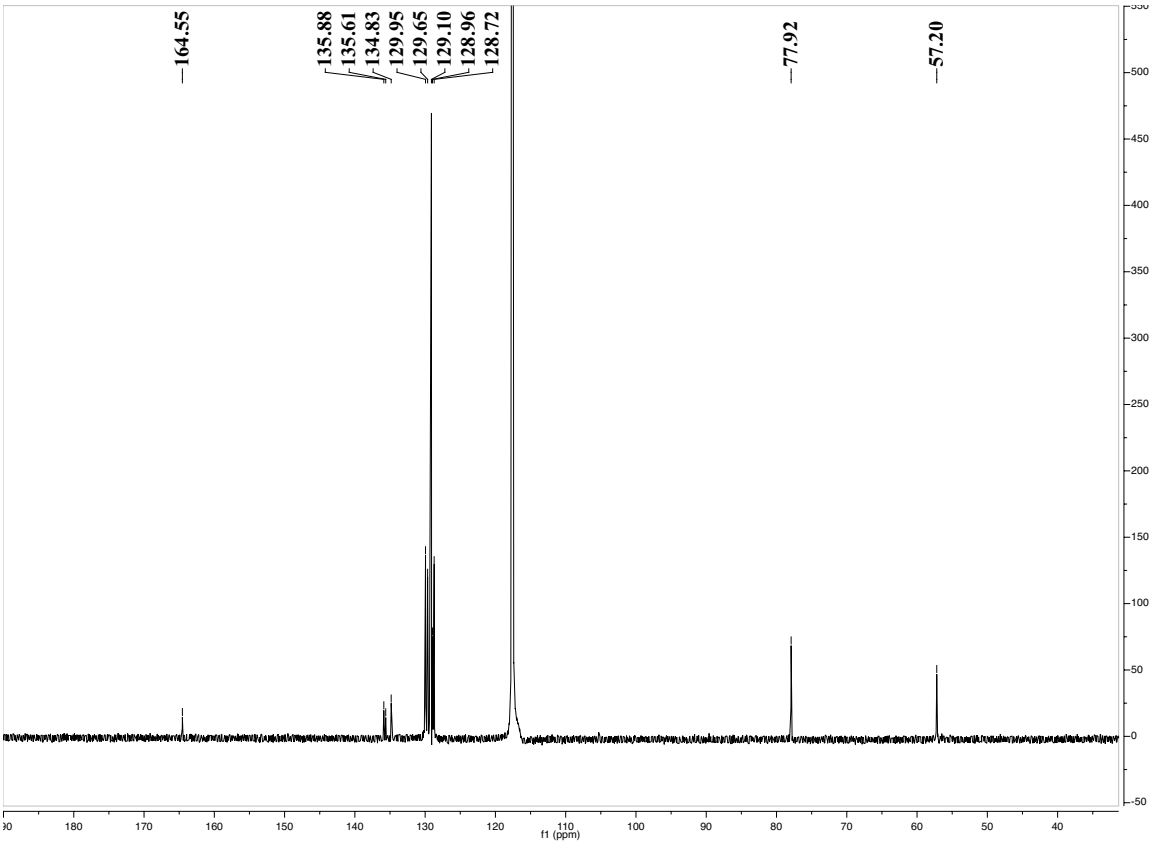

Figure A.1.20 ^{13}C NMR (126 MHz, CD_3CN) spectrum of **65g**.

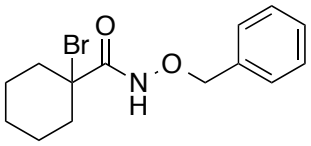

65i, 65l

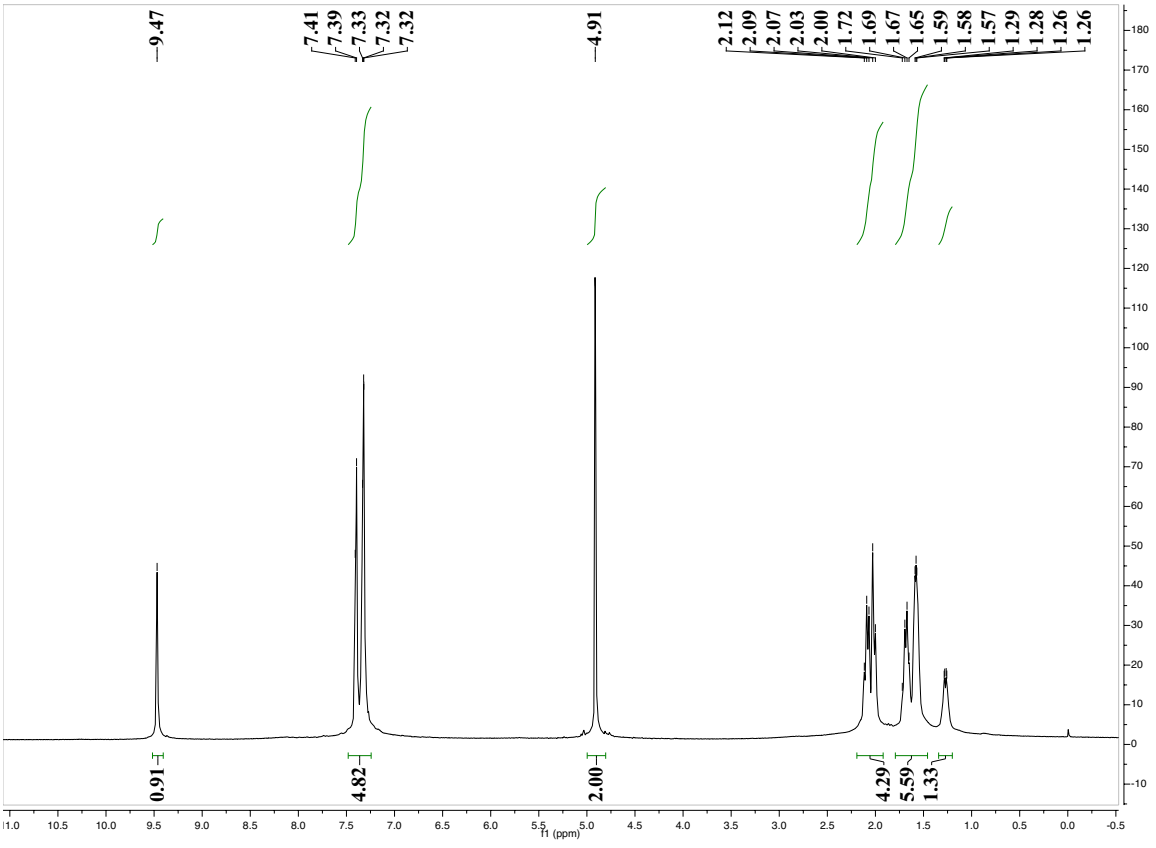

Figure A.1.21 ^{1}H NMR (500 MHz, $CDCl_3$) spectrum of **65i**/**65l**.

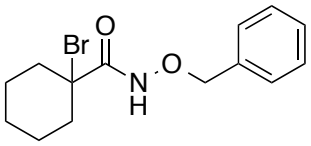

65i, 65l

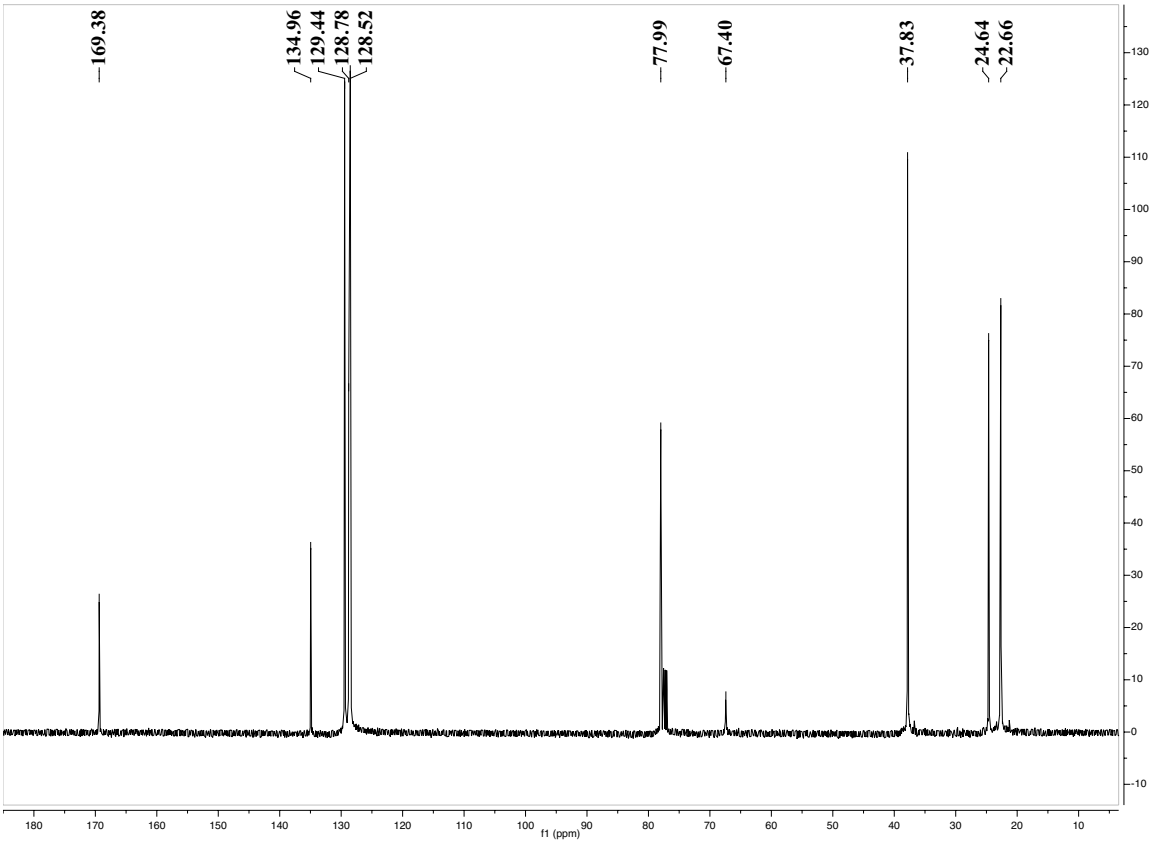

Figure A.1.22 ^{13}C NMR (126 MHz, $CDCl_3$) spectrum of **65i**/**65l**.

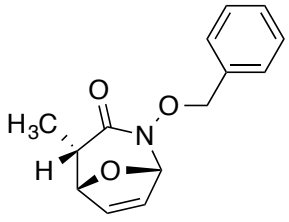

66b

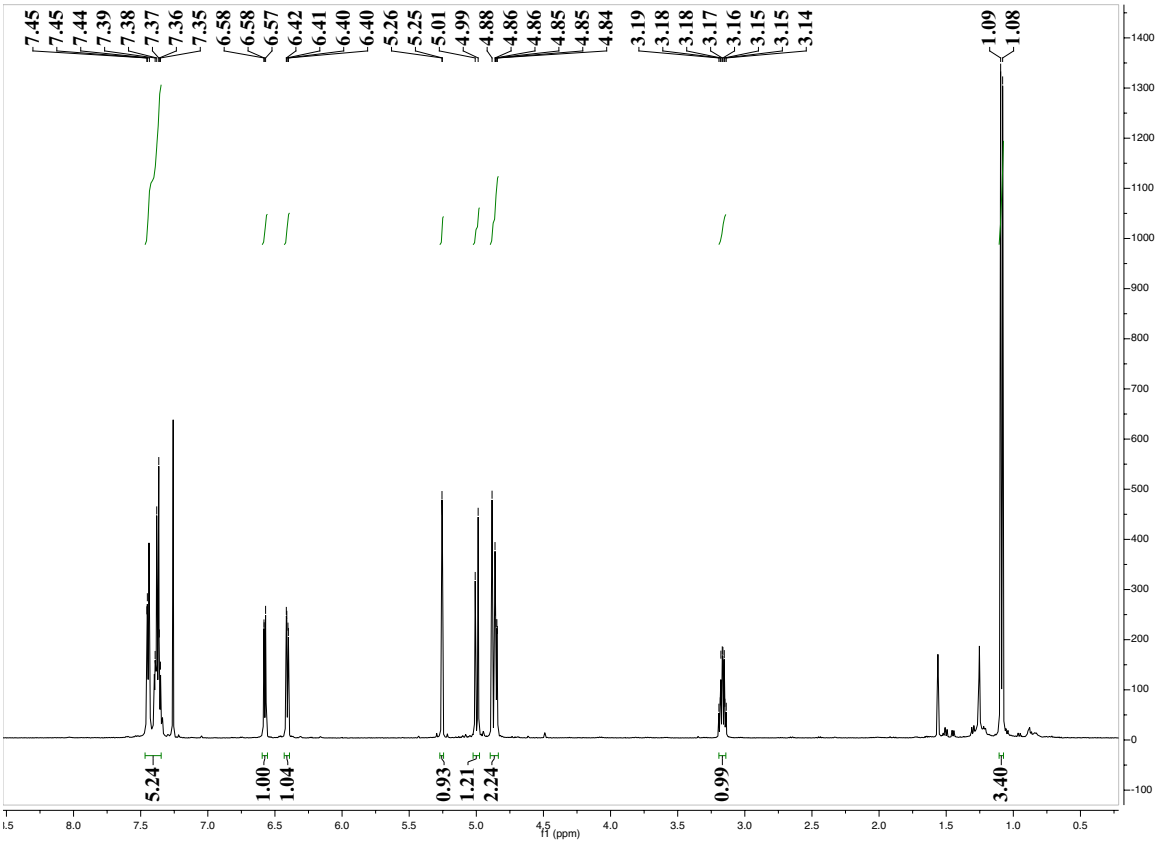

Figure A.1.23 ^{1}H NMR (400 MHz, $CDCl_3$) spectrum of **66b**.

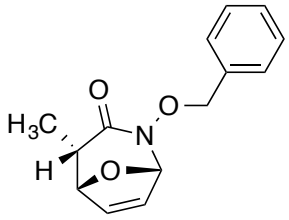

66b

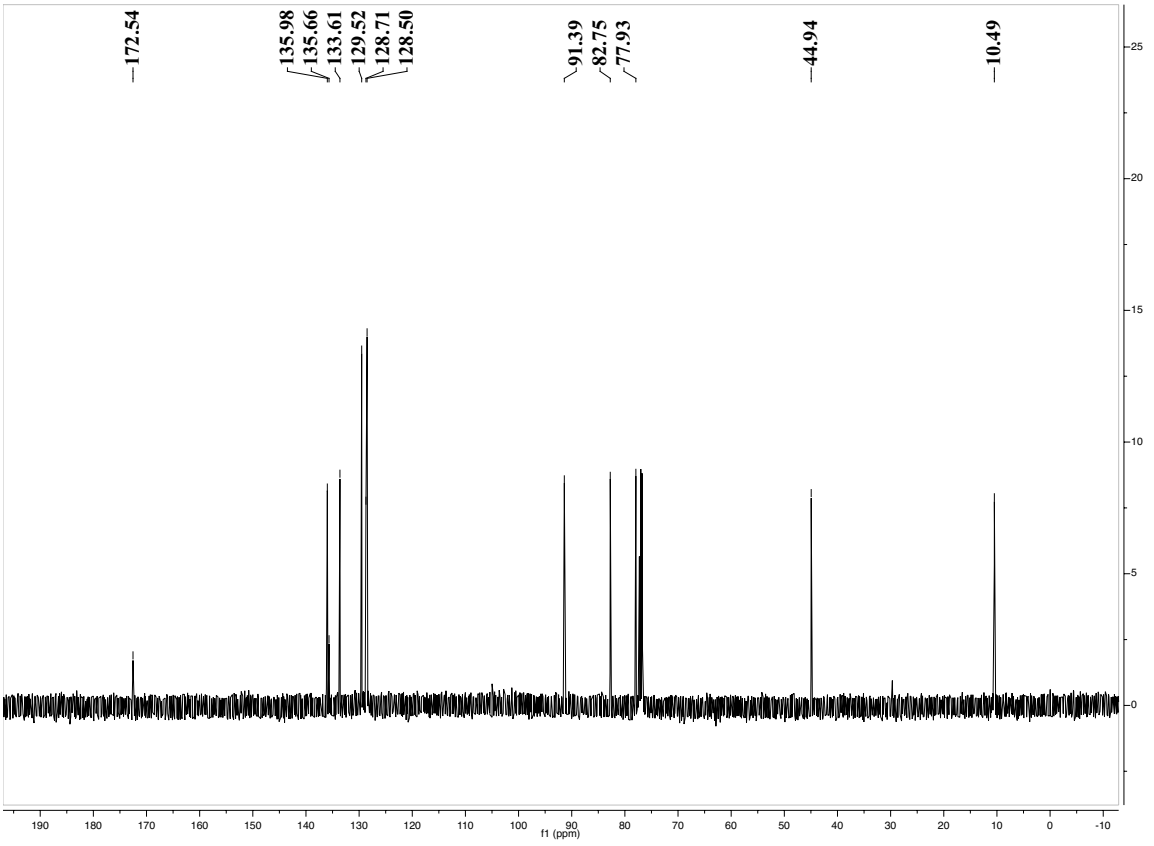

Figure A.1.24 ^{13}C NMR (126 MHz, $CDCl_3$) spectrum of **66b**.

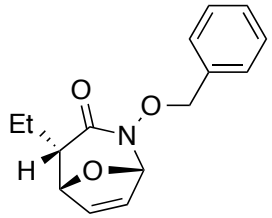

66c

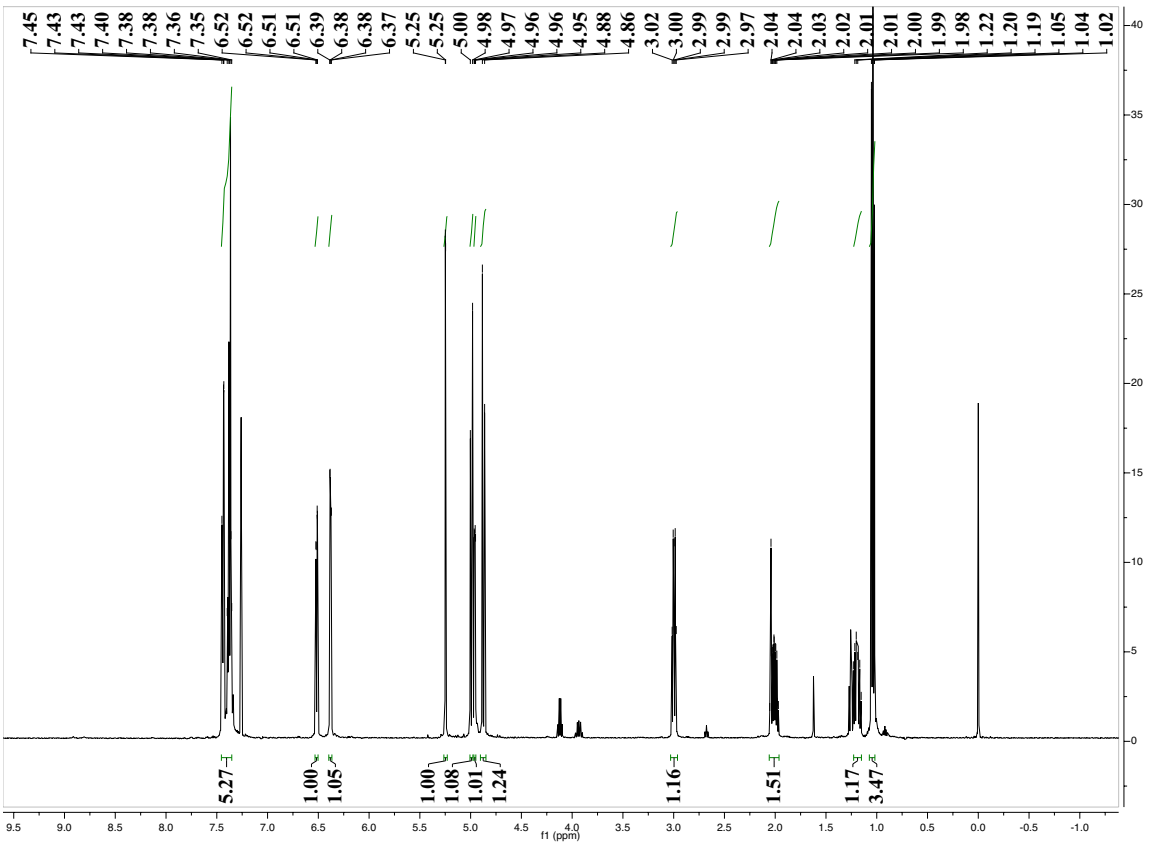

Figure A.1.25 ^{1}H NMR (500 MHz, $CDCl_3$) spectrum of **66c**.

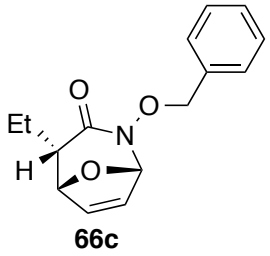

66c

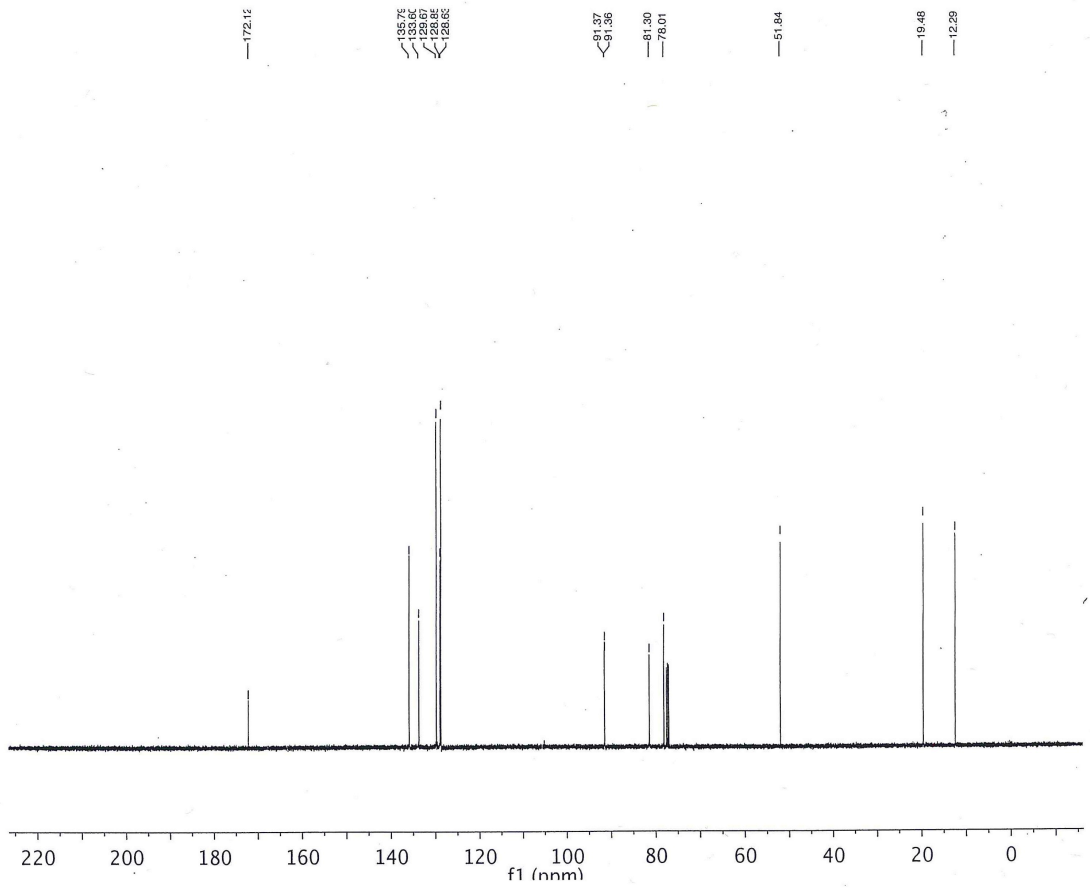

Figure A.1.26 ^{13}C NMR (126 MHz, $CDCl_3$) spectrum of **66c**.

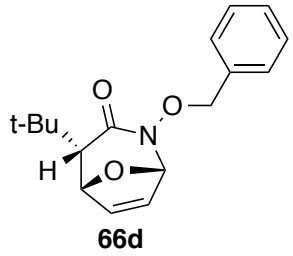

66d

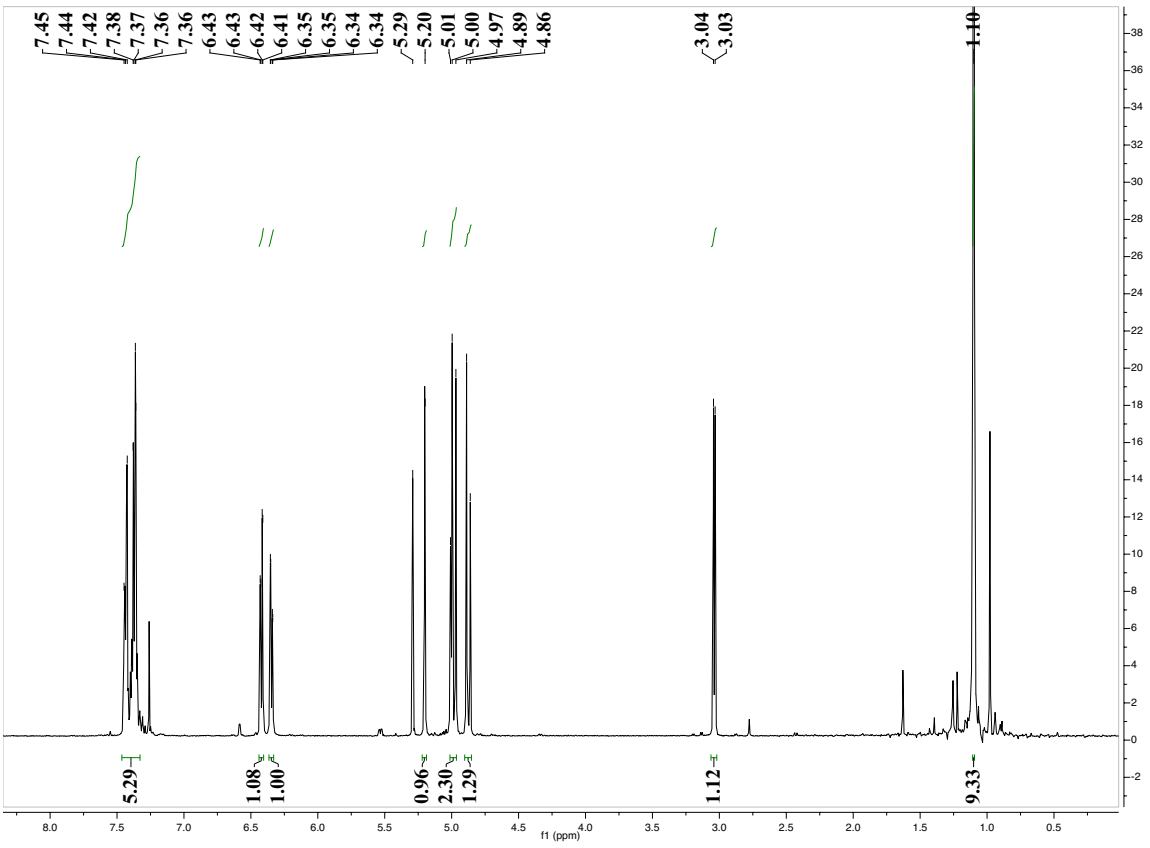

Figure A.1.27 ^{1}H NMR (400 MHz, $CDCl_3$) spectrum of **66d**.

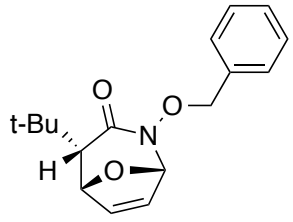

66d

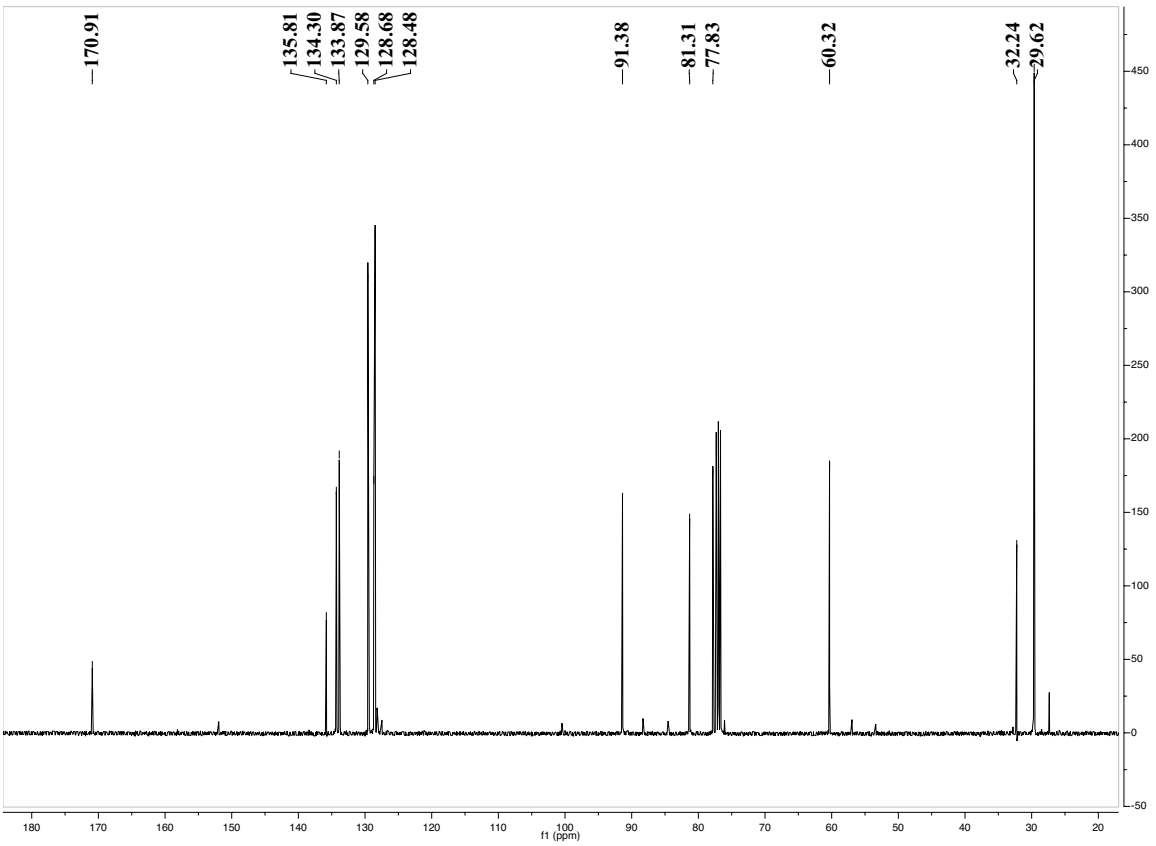

Figure A.1.28 ^{13}C NMR (126 MHz, $CDCl_3$) spectrum of **66d**.

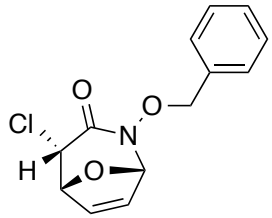

endo **66f**

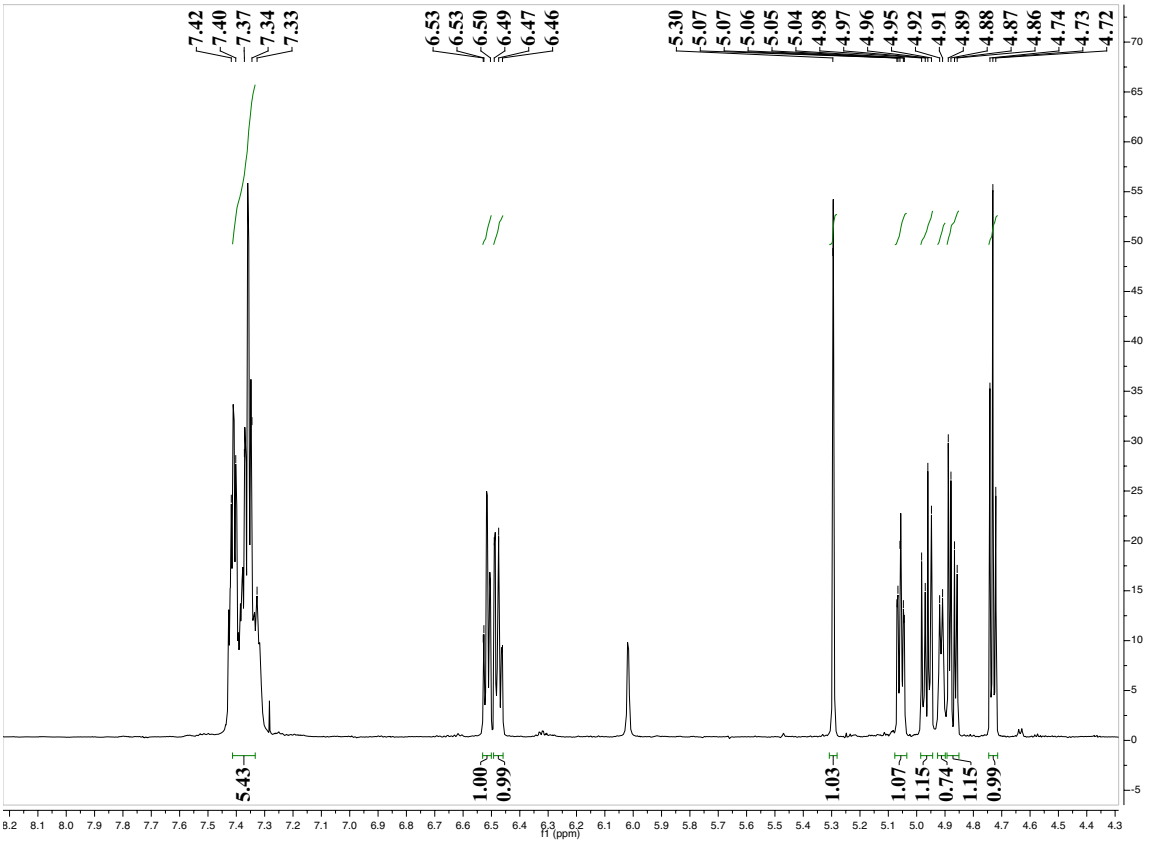

Figure A.1.29 ^{1}H NMR (500 MHz, $CDCl_3$) spectrum of *endo* **66f**.

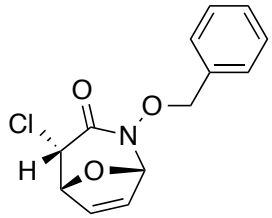

endo **66f**

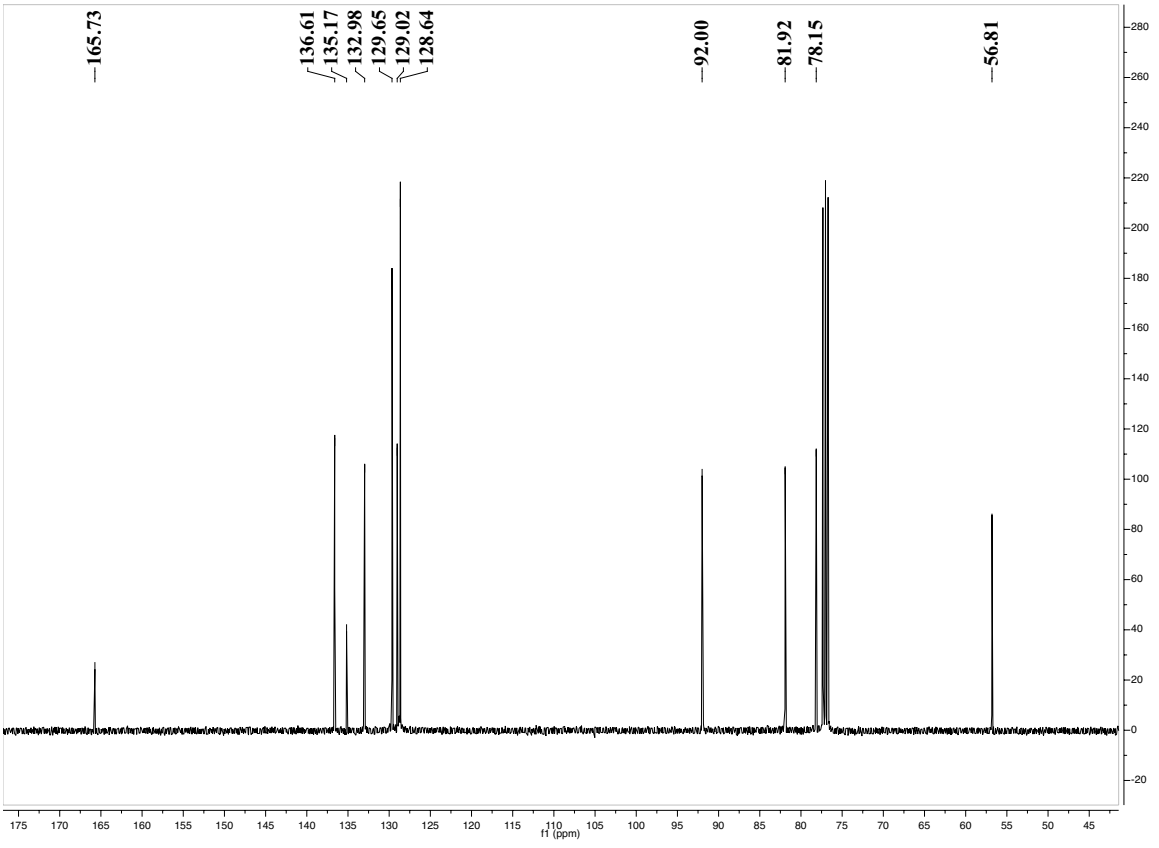

Figure A.1.30 ^{13}C NMR (126 MHz, $CDCl_3$) spectrum of *endo* **66f**.

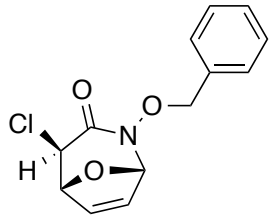

exo **66f**

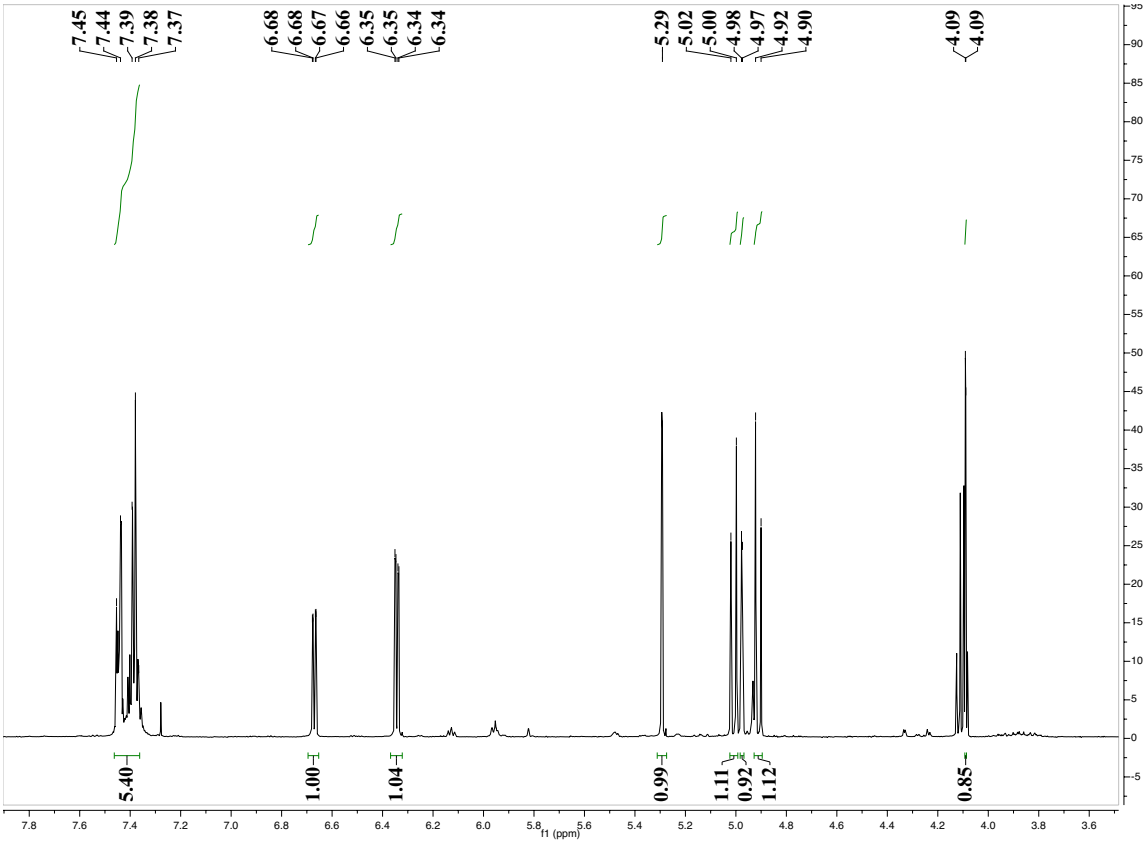

Figure A.1.31 ^{1}H NMR (500 MHz, $CDCl_3$) spectrum of *exo* **66f**.

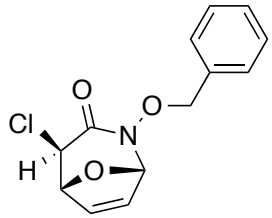

exo **66f**

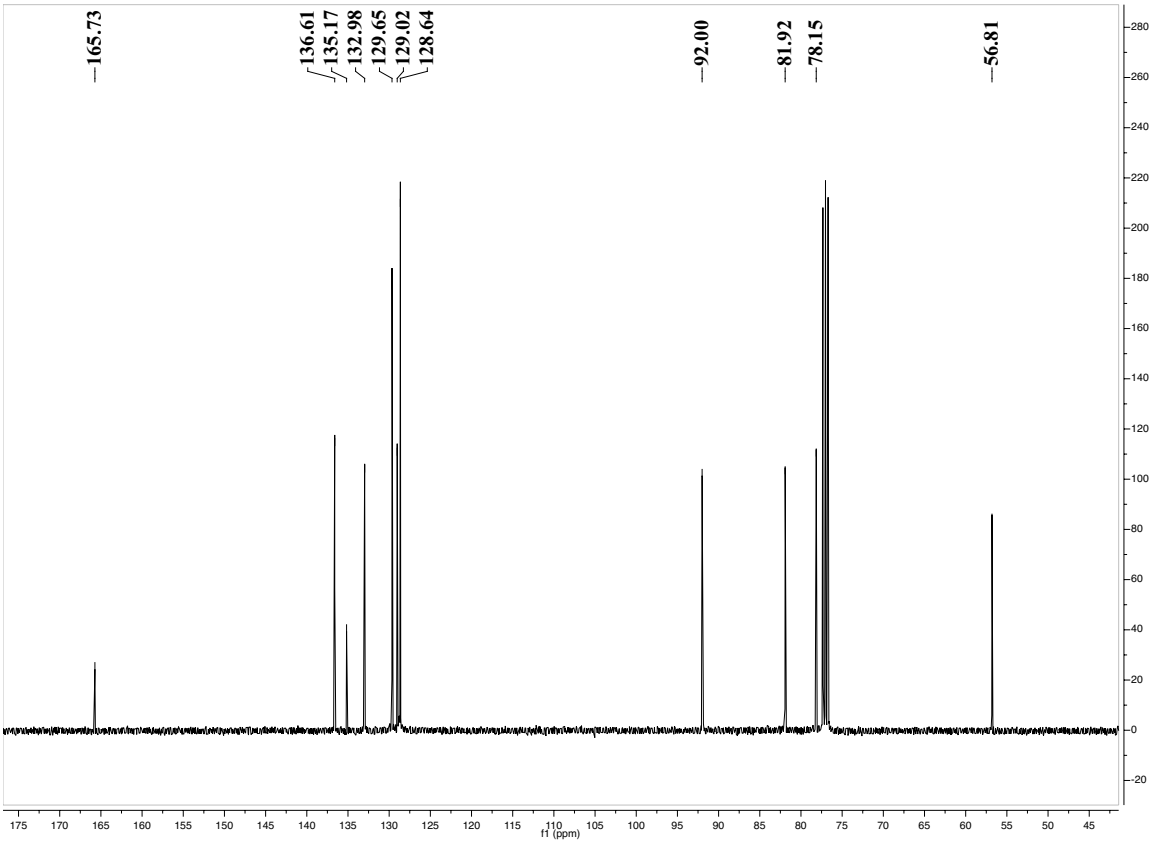

Figure A.1.32 ^{13}C NMR (126 MHz, $CDCl_3$) spectrum of *exo* **66f**.

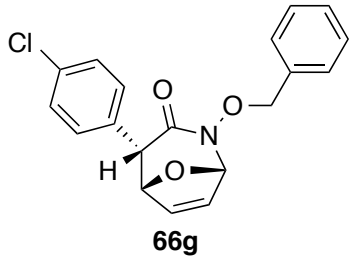

66g

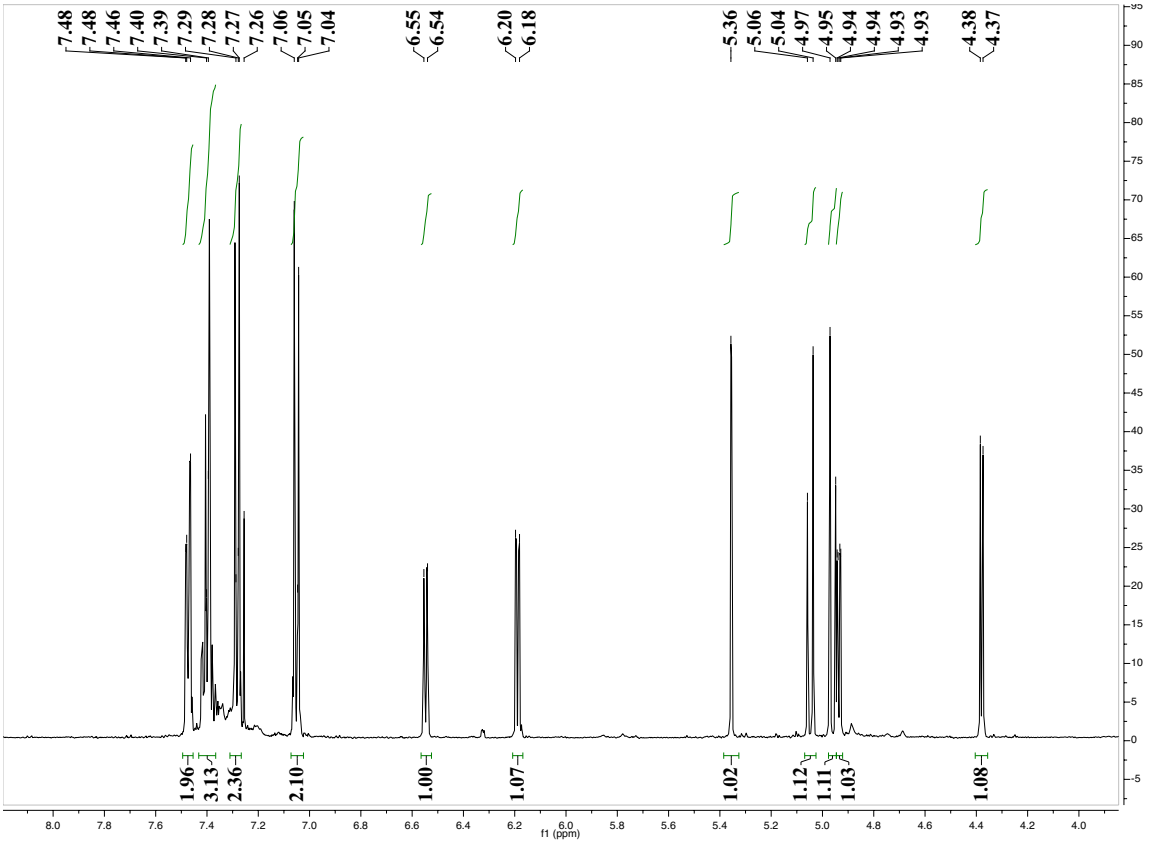

Figure A.1.33 ^{1}H NMR (500 MHz, $CDCl_3$) spectrum of **66g**.

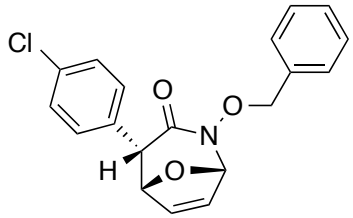

66g

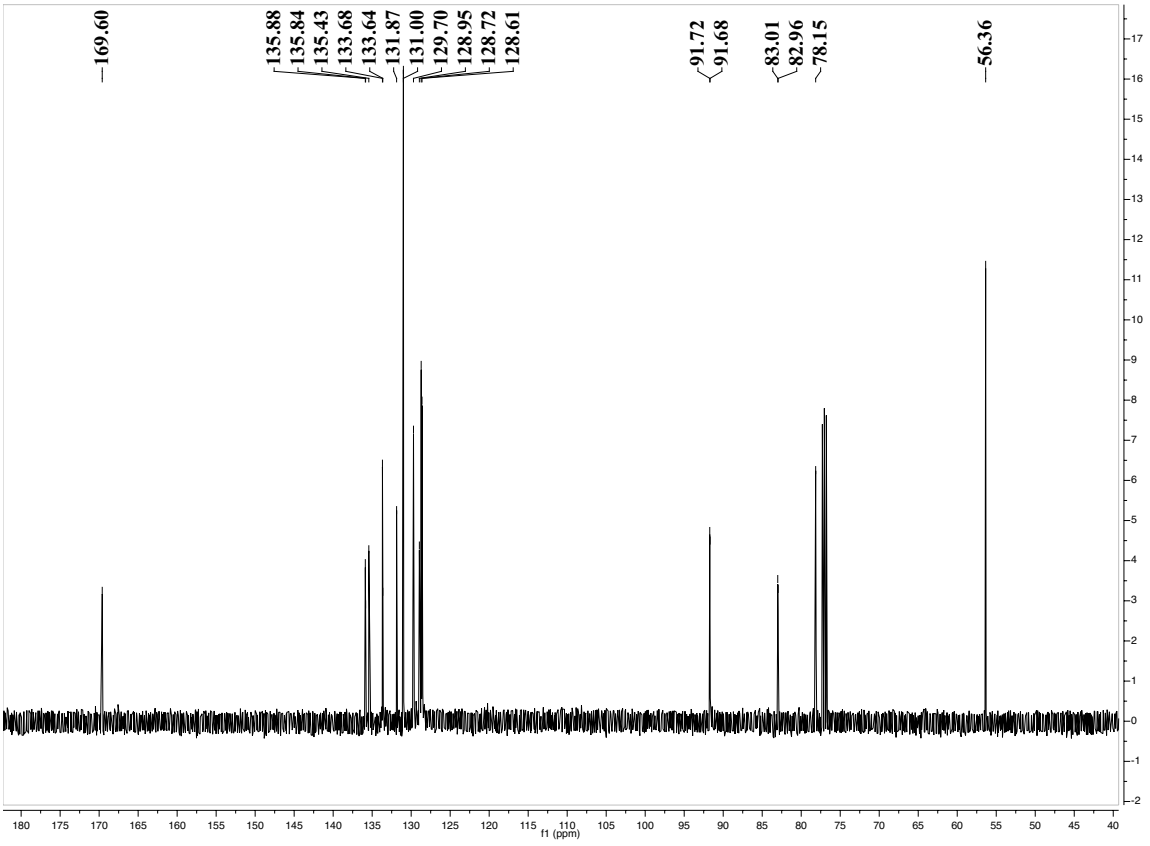

Figure A.1.34 ^{13}C NMR (101 MHz, $CDCl_3$) spectrum of **66g**.

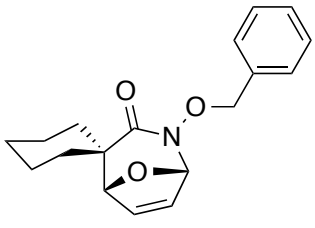

66i

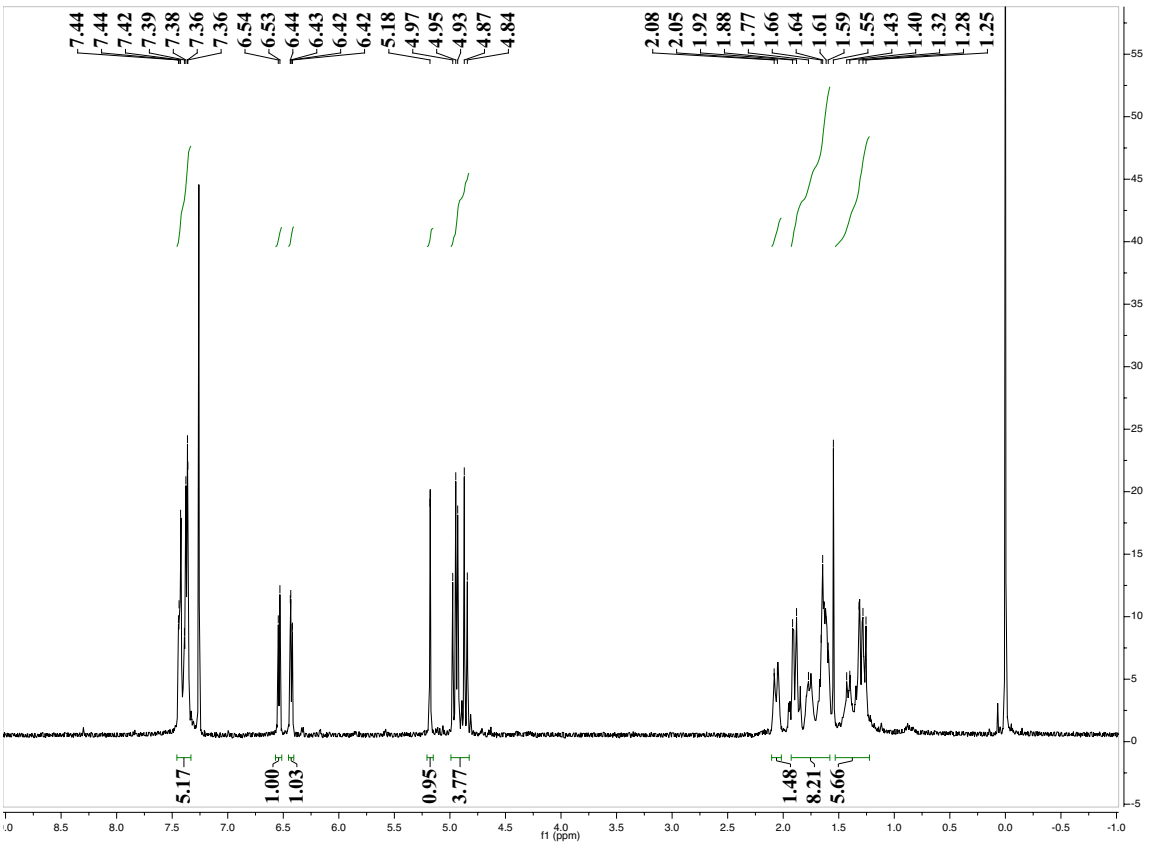

Figure A.1.35 ^{1}H NMR (400 MHz, $CDCl_3$) spectrum of **66i**.

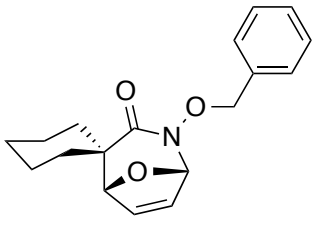

66i

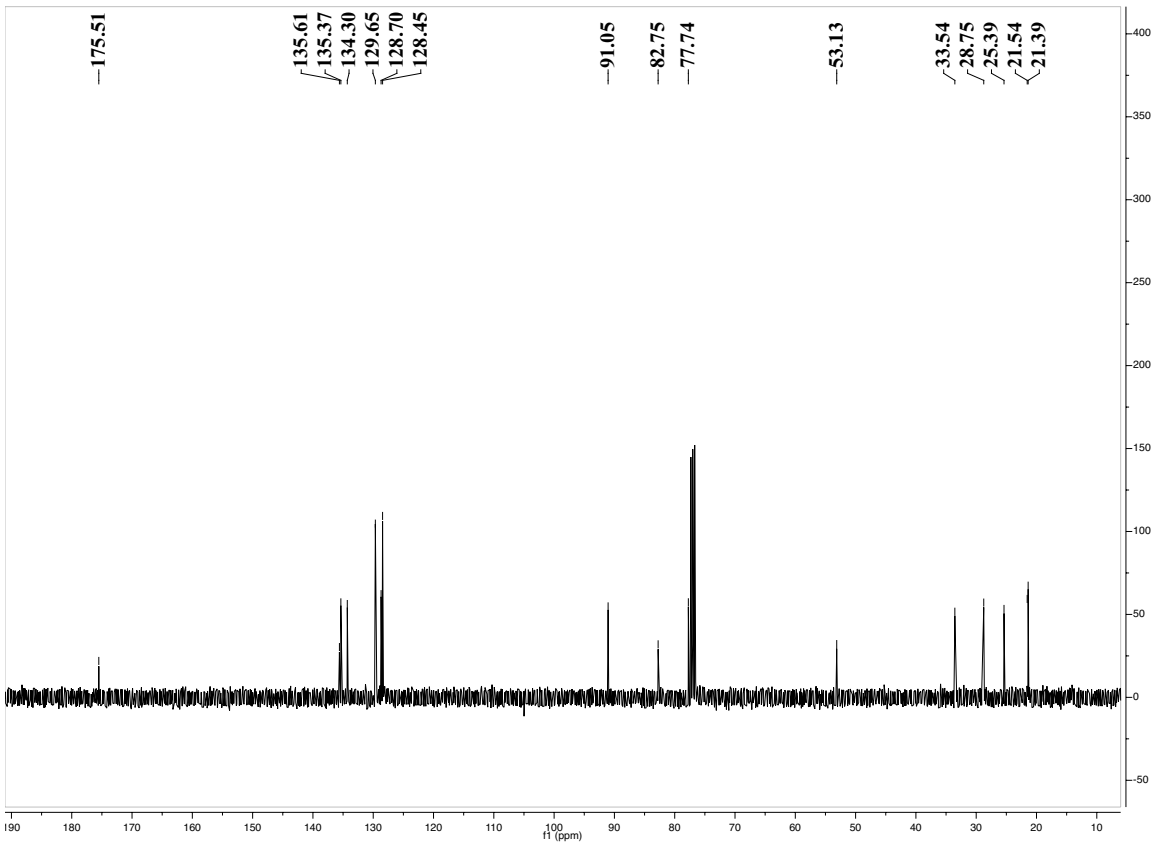

Figure A.1.36 ^{13}C NMR (101 MHz, $CDCl_3$) spectrum of **66i**.

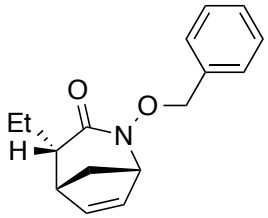

endo **66j**

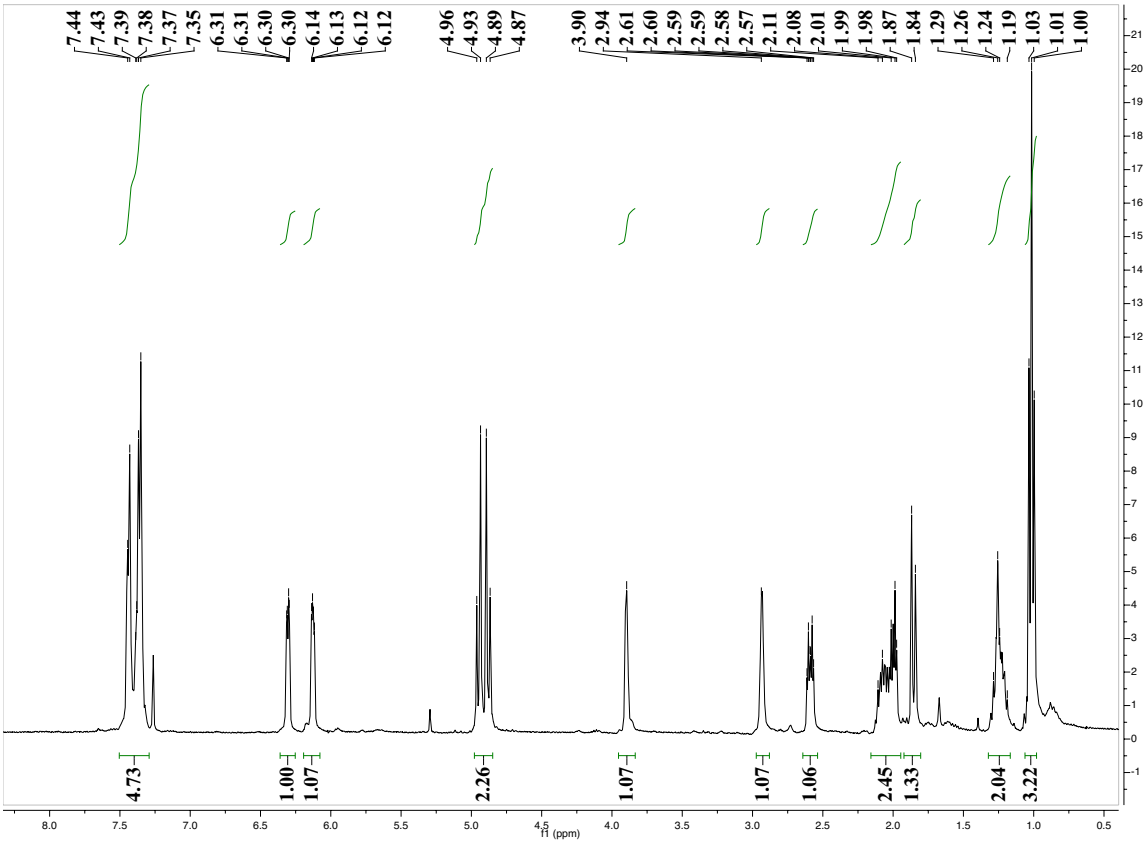

Figure A.1.37 ^{1}H NMR (400 MHz, $CDCl_3$) spectrum of *endo* **66j**.

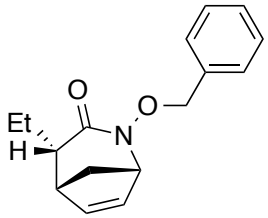

endo **66j**

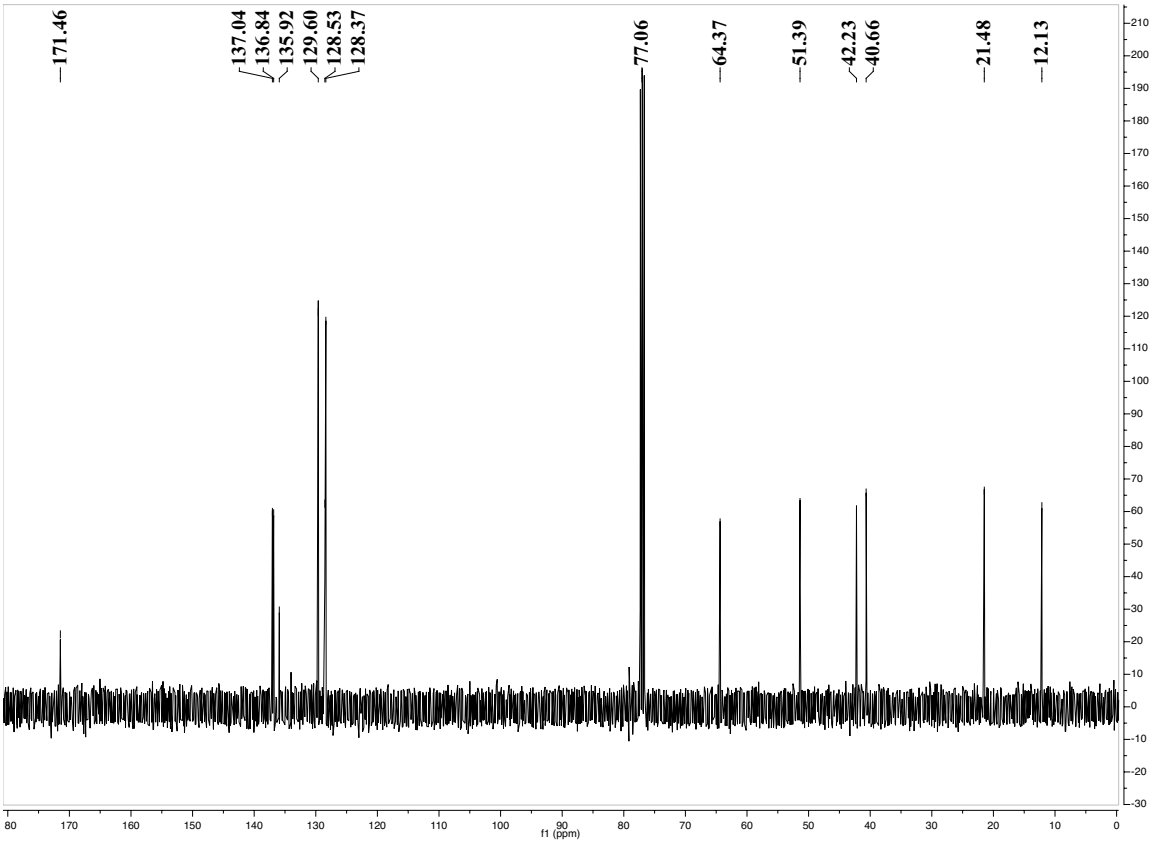

Figure A.1.38 ^{13}C NMR (101 MHz, $CDCl_3$) spectrum of *endo* **66j**.

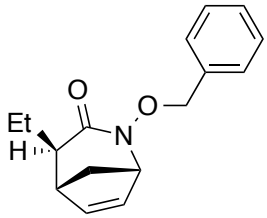

exo **66j**

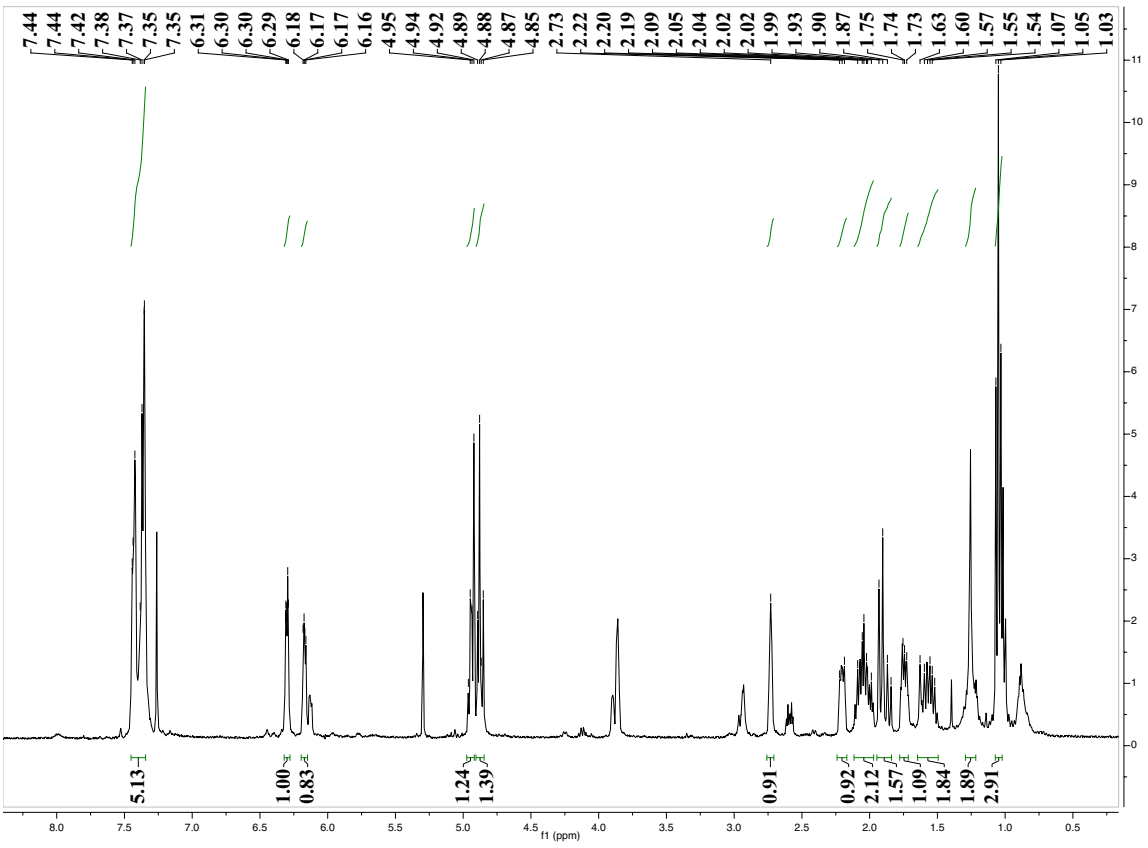

Figure A.1.39 ^{1}H NMR (400 MHz, $CDCl_3$) spectrum of *exo* **66j**.

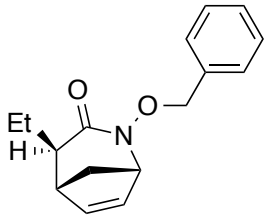

exo **66j**

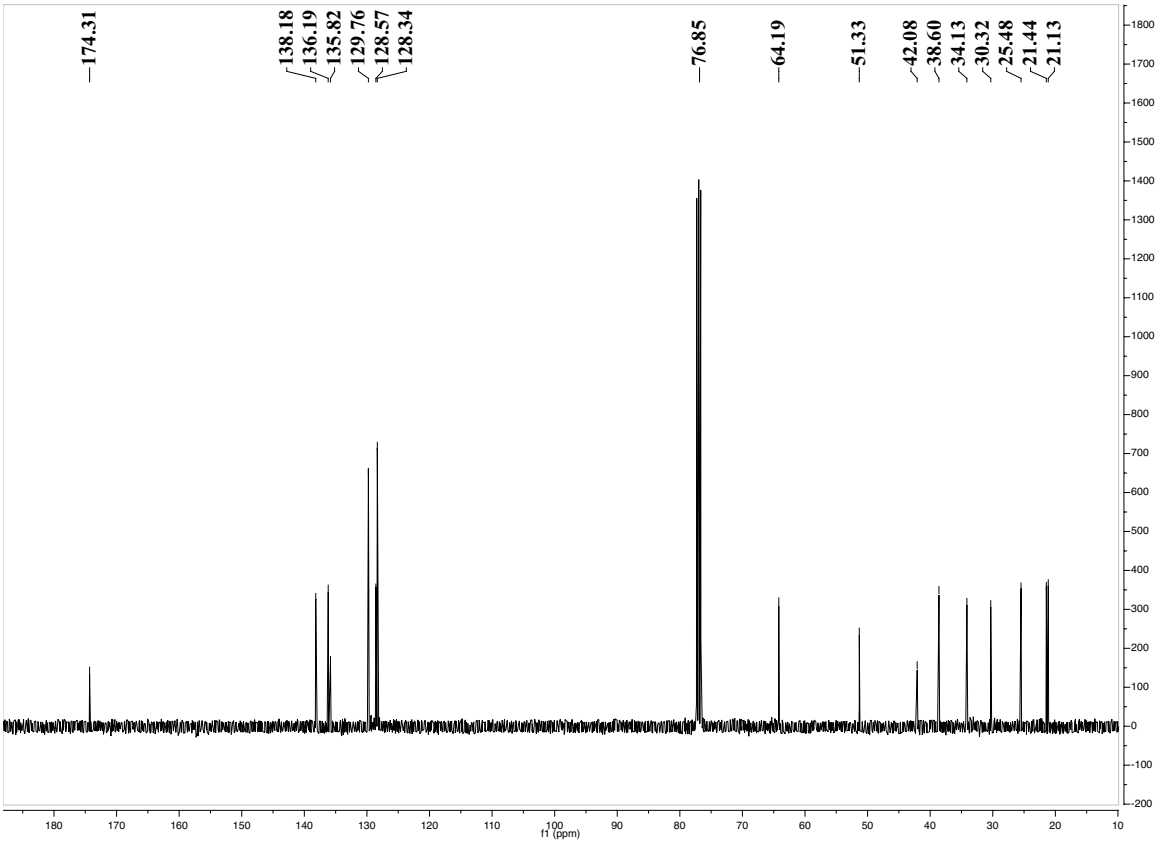

Figure A.1.40 ^{13}C NMR (101 MHz, $CDCl_3$) spectrum of *exo* **66j**.

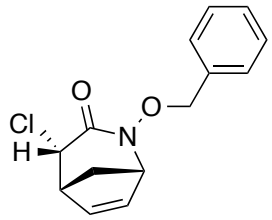

endo **66k**

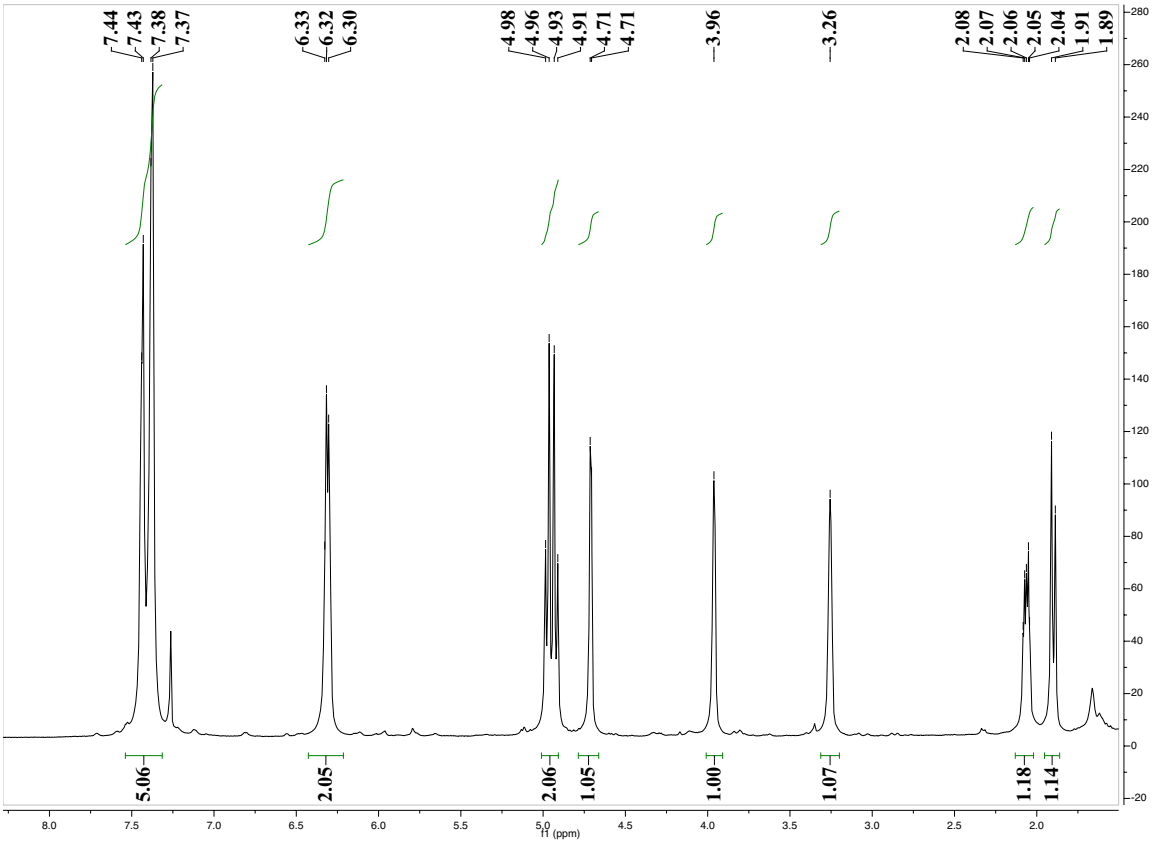

Figure A.1.41 ^{1}H NMR (400 MHz, $CDCl_3$) spectrum of *endo* **66k**.

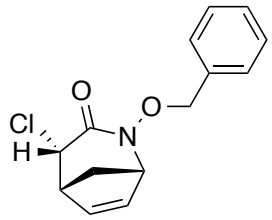

endo **66k**

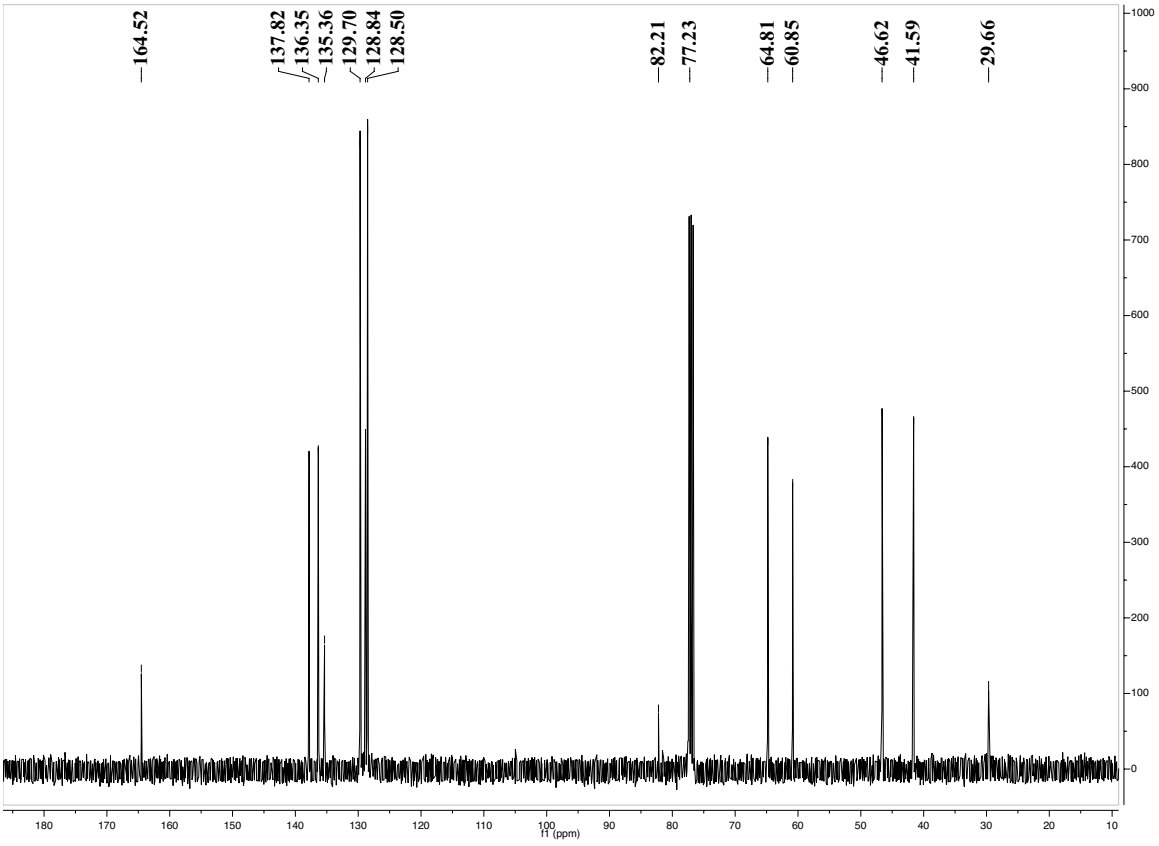

Figure A.1.42 ^{13}C NMR (101 MHz, $CDCl_3$) spectrum of *endo* **66k**.

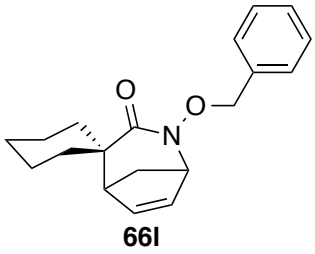

66l

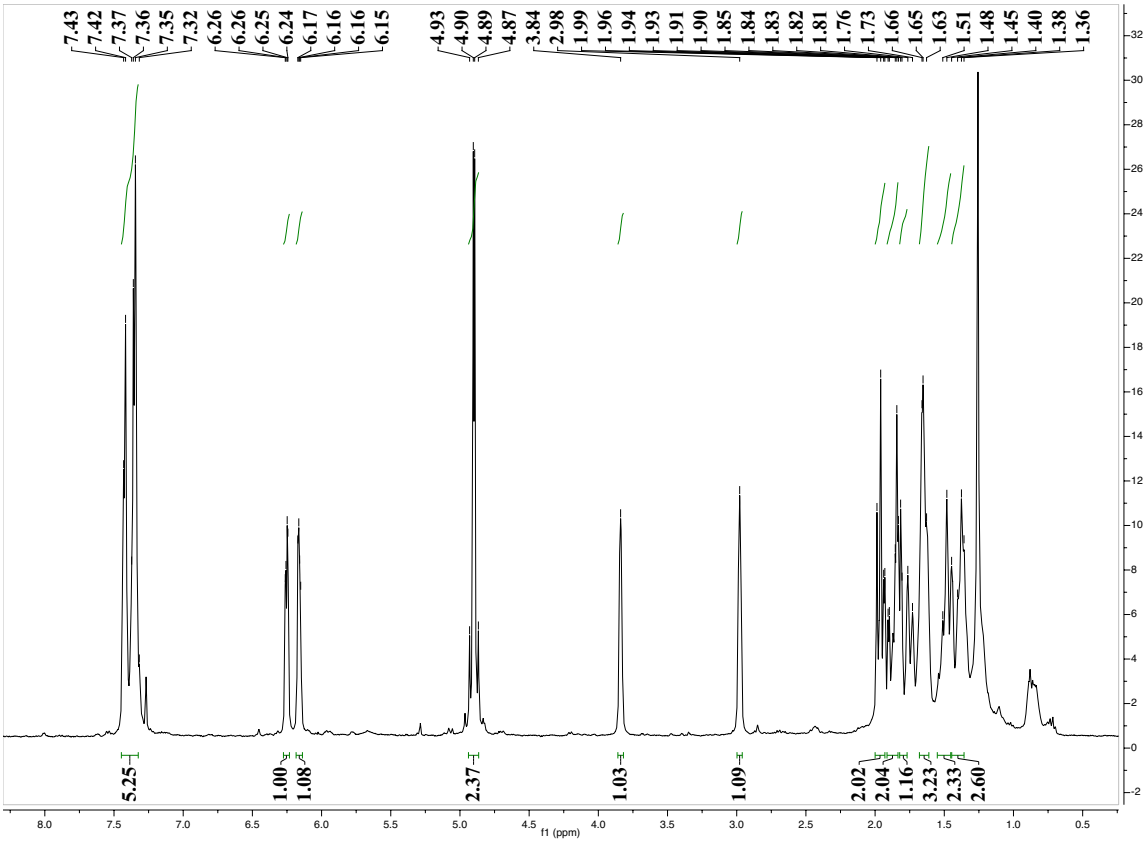

Figure A.1.43 ^{1}H NMR (400 MHz, $CDCl_3$) spectrum of **66l**.

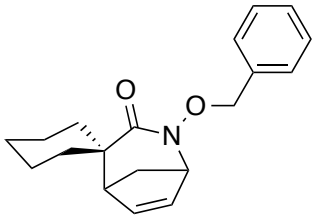

66l

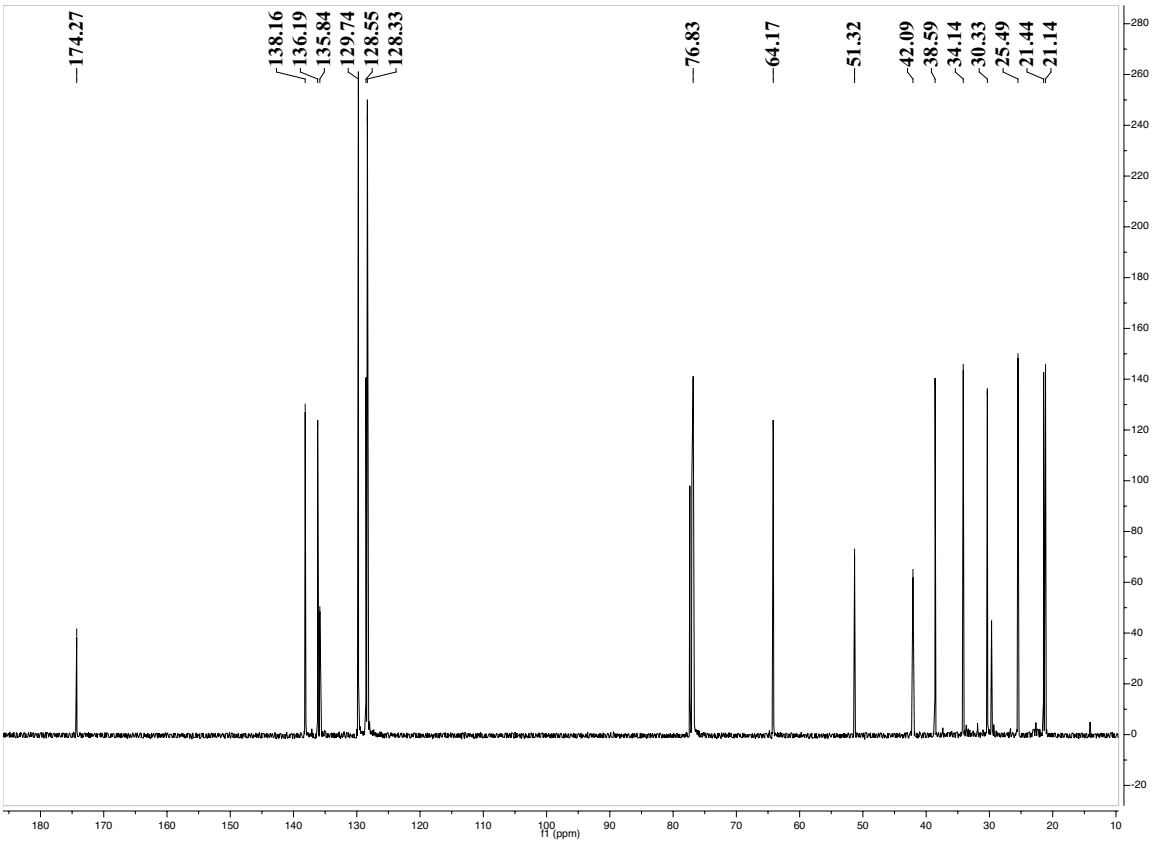

Figure A.1.44 ^{13}C NMR (101 MHz, $CDCl_3$) spectrum of **66l**.

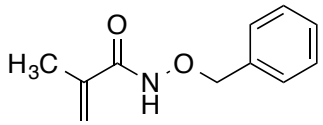

Elimination product from the reaction of attempted cycloaddition of **62** with $LiClO_4/Et_3N$ in diethyl ether

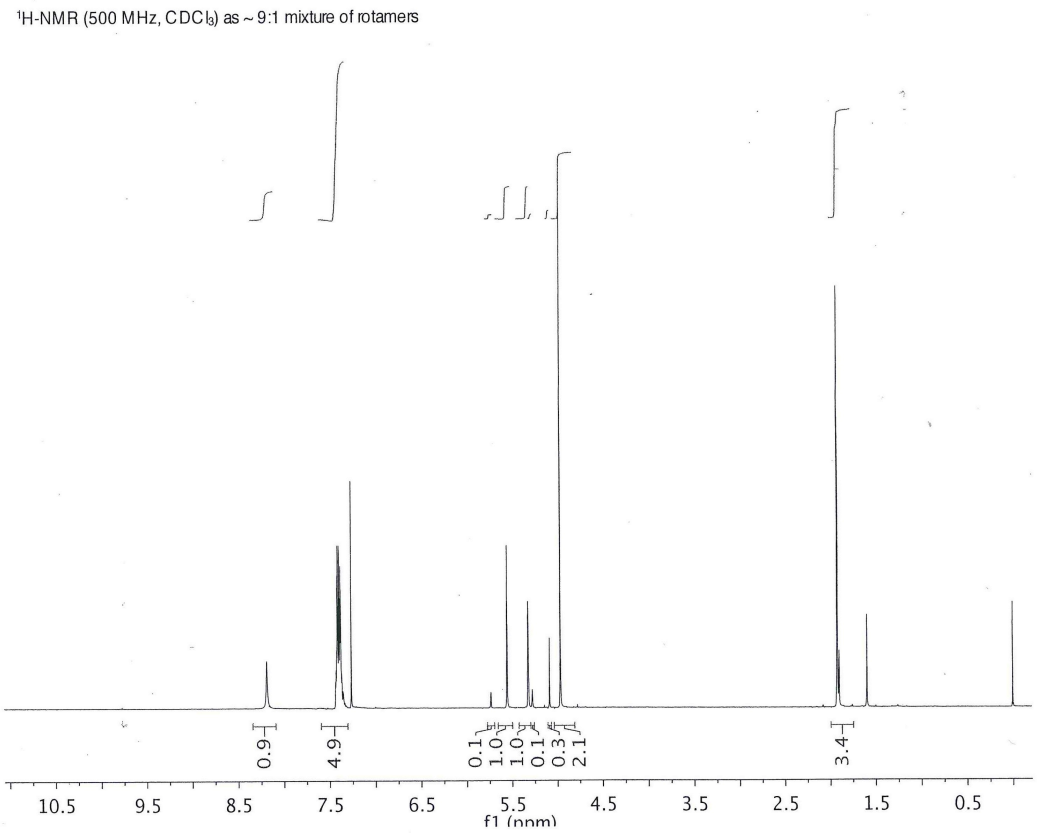

Figure A.1.45 ^1H NMR (400 MHz, $CDCl_3$) spectrum of methacryl amide.

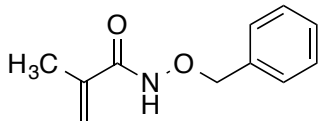

Elimination product from the reaction of attempted cycloaddition of **62** with $LiClO_4/Et_3N$ in diethyl ether

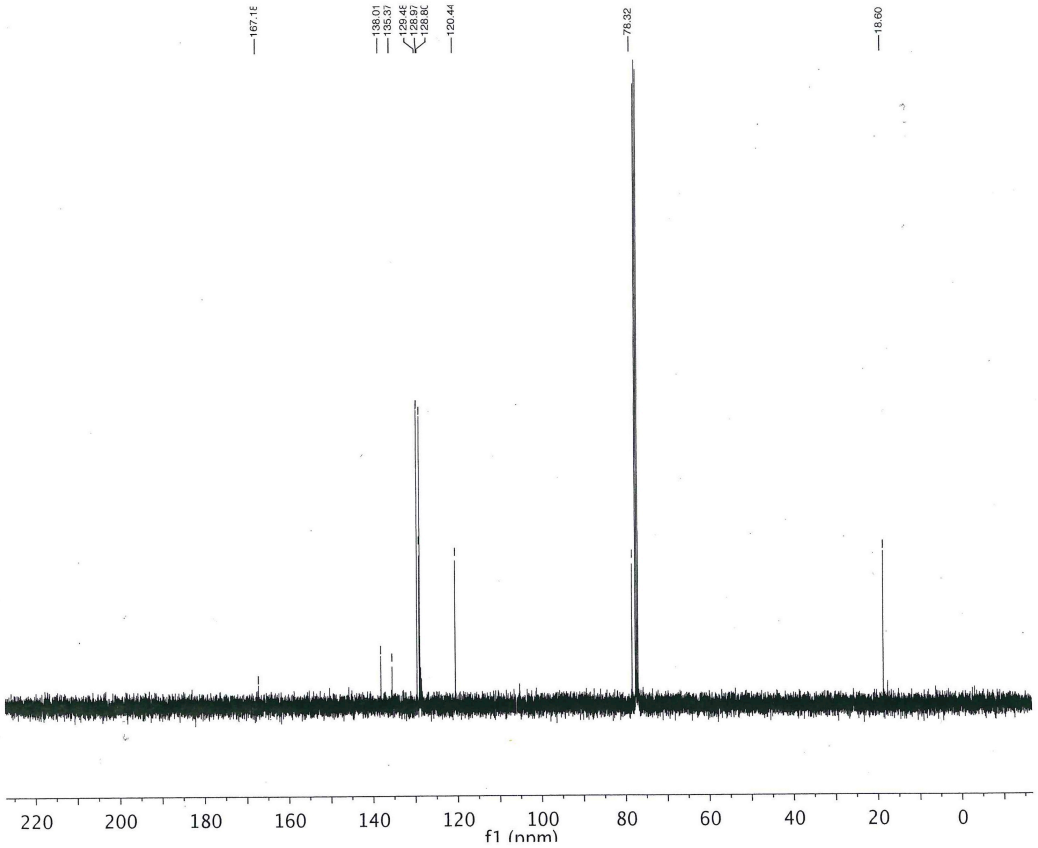

Figure A.1.46 ^{13}C NMR (101 MHz, $CDCl_3$) spectrum of methacrylamide.

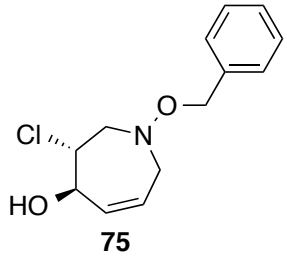

75

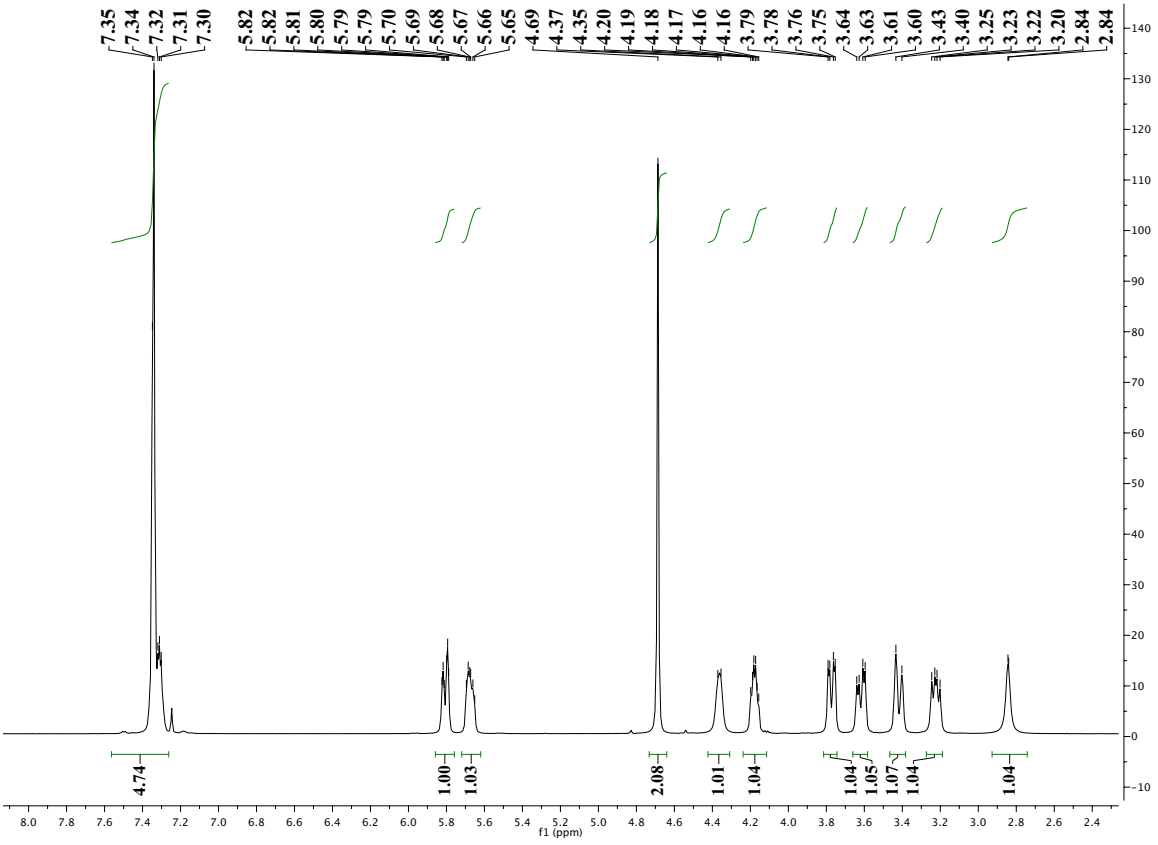

Figure A.1.47 ^{1}H NMR (500 MHz, $CDCl_3$) spectrum of **75**.

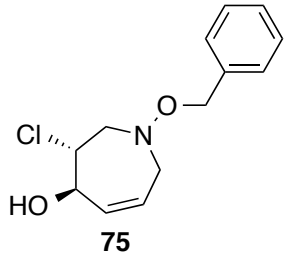

75

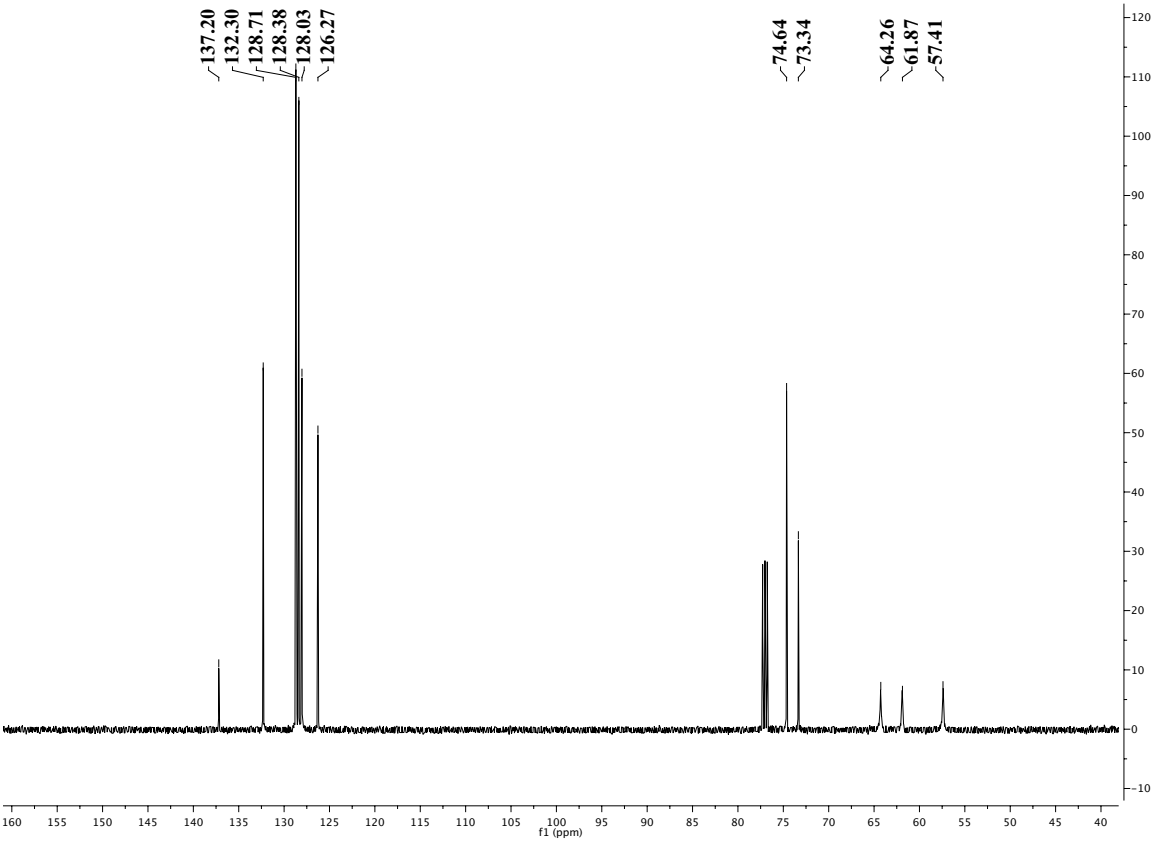

Figure A.1.48 ^{13}C NMR (101 MHz, $CDCl_3$) spectrum of **75**.

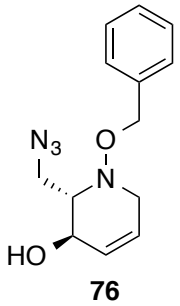

76

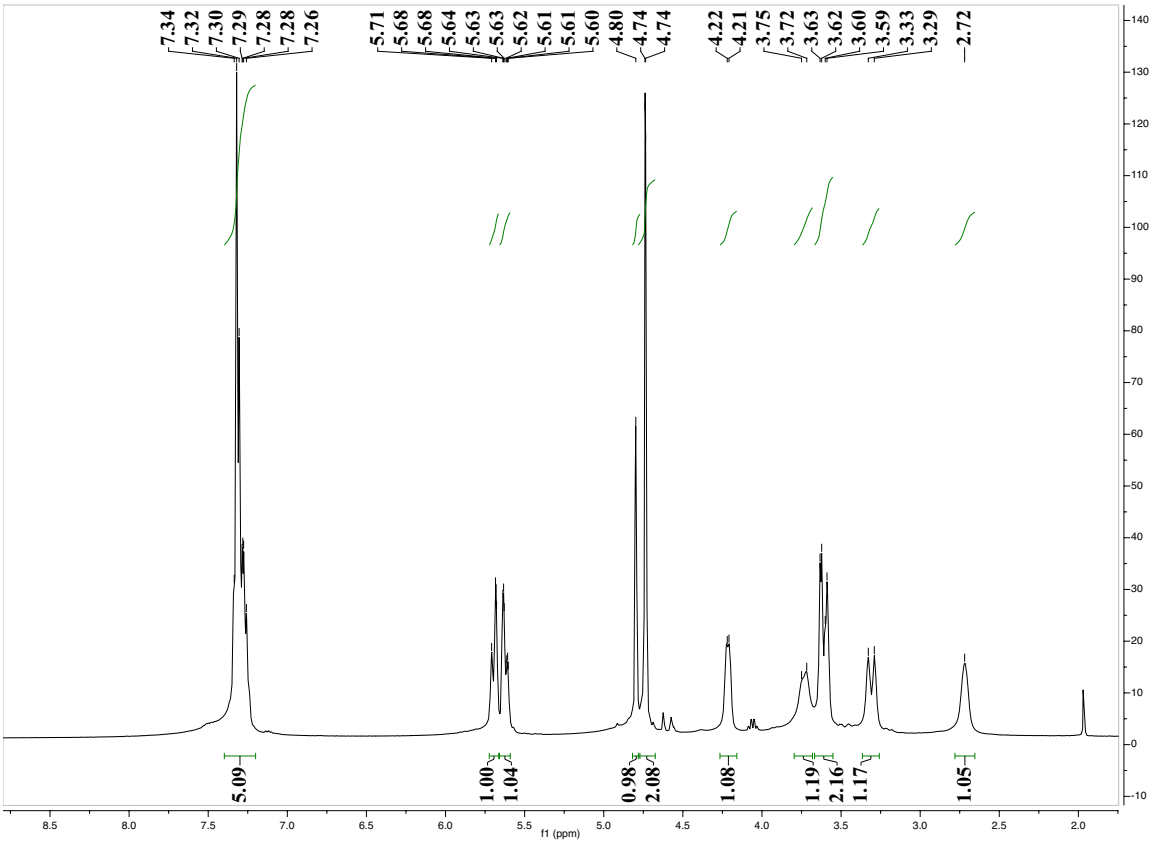

Figure A.1.49 ^{1}H NMR (400 MHz, CD_3OD) spectrum of **76**.

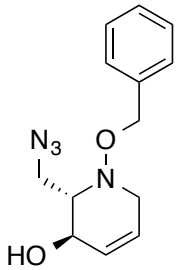

76

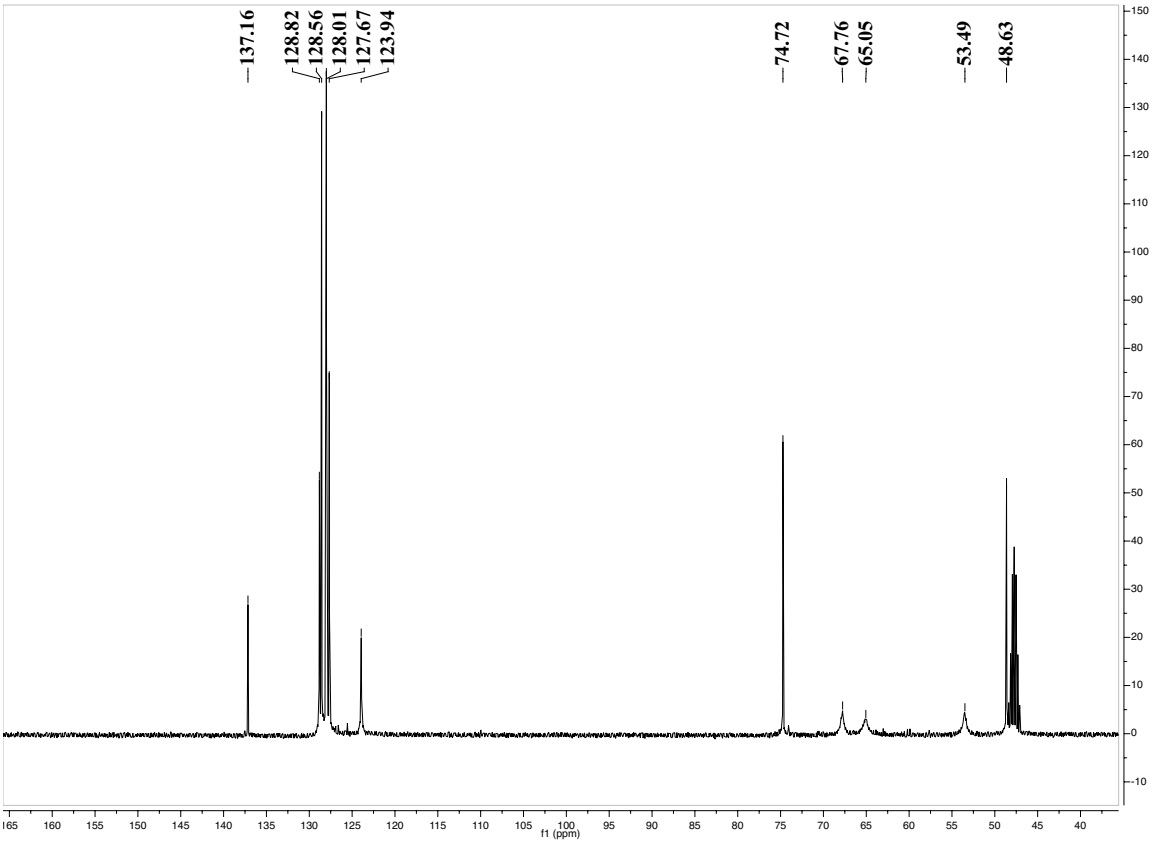

Figure A.1.50 ^{13}C NMR (101 MHz, CD_3OD) spectrum of **76**.

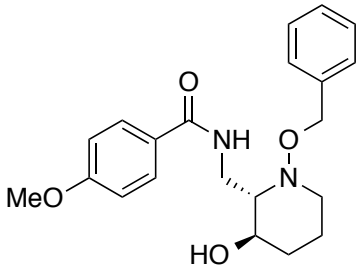

78

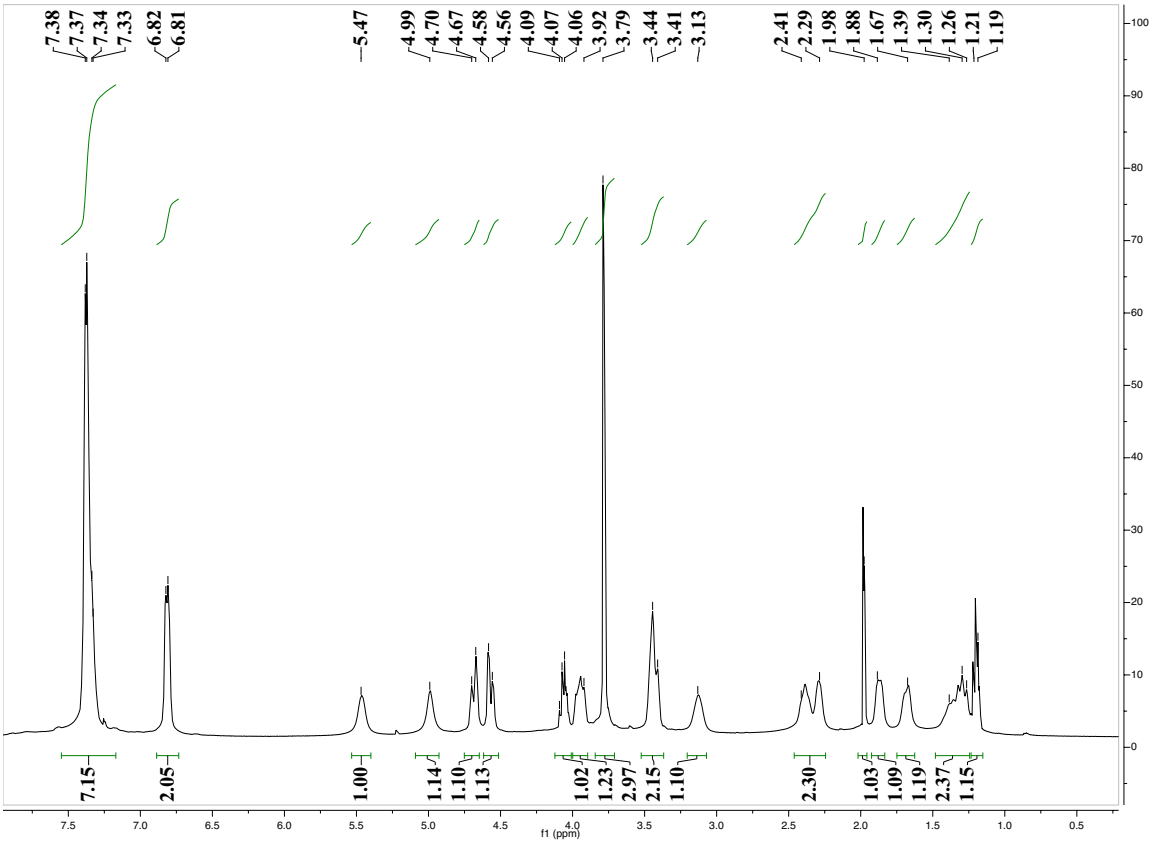

Figure A.1.51 ^{1}H NMR (400 MHz, $CDCl_3$) spectrum of **78**.

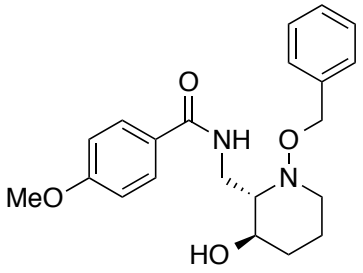

78

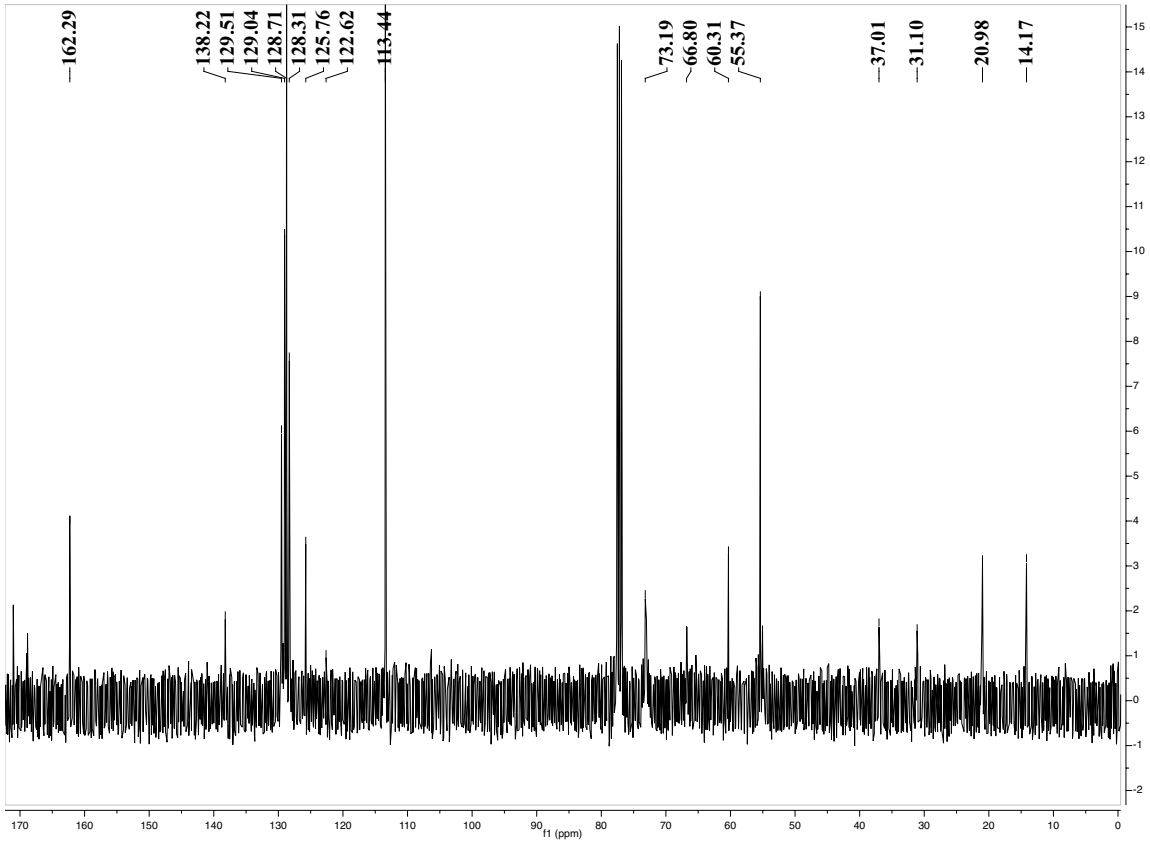

Figure A.1.52 ^{13}C NMR (101 MHz, $CDCl_3$) spectrum of **78**.

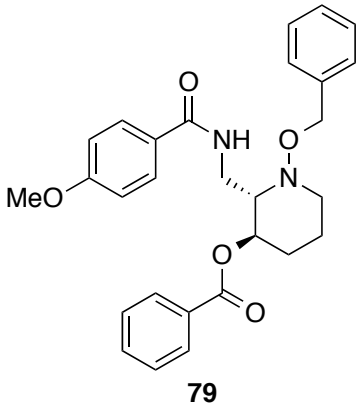

79

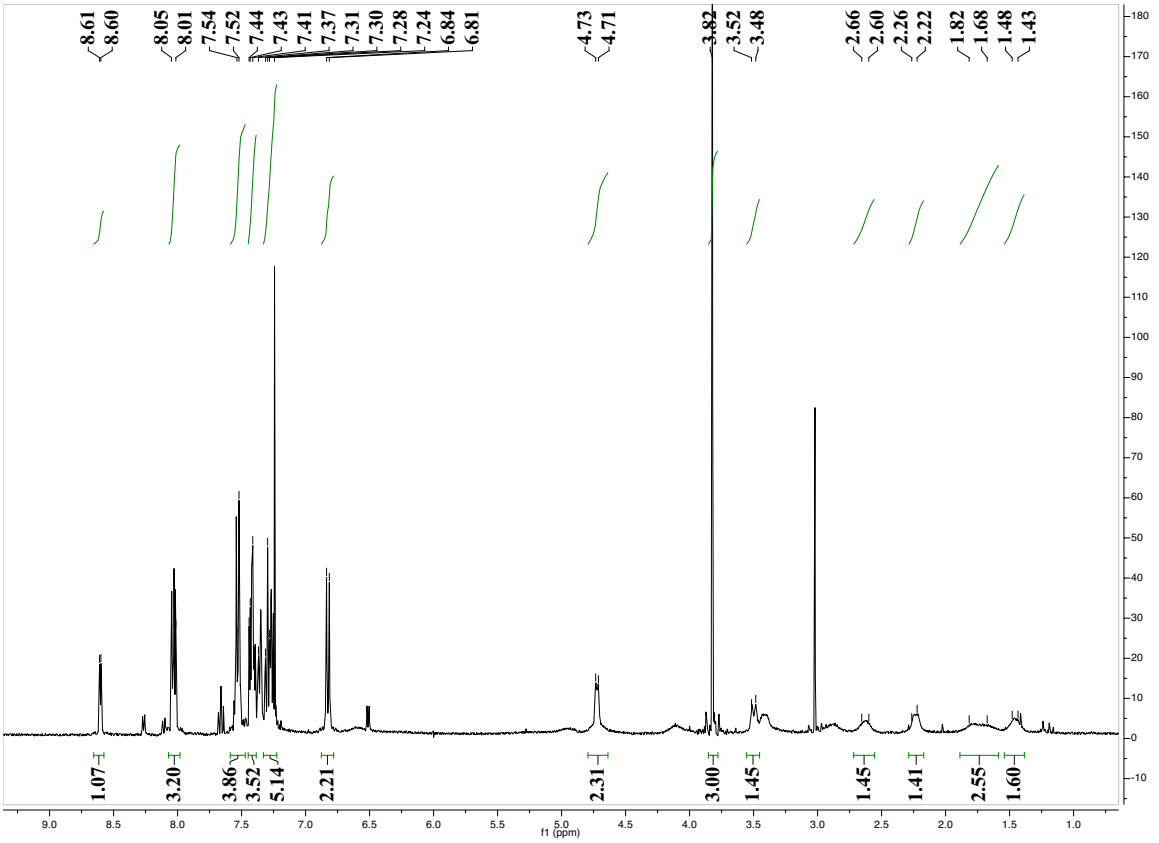

Figure A.1.53 ^{1}H NMR (400 MHz, $CDCl_3$) spectrum of **79**.

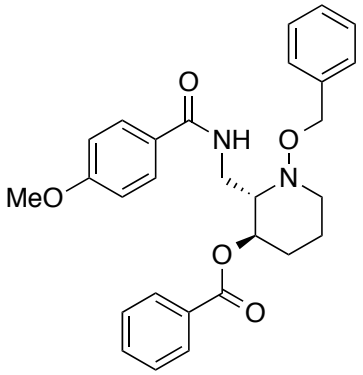

79

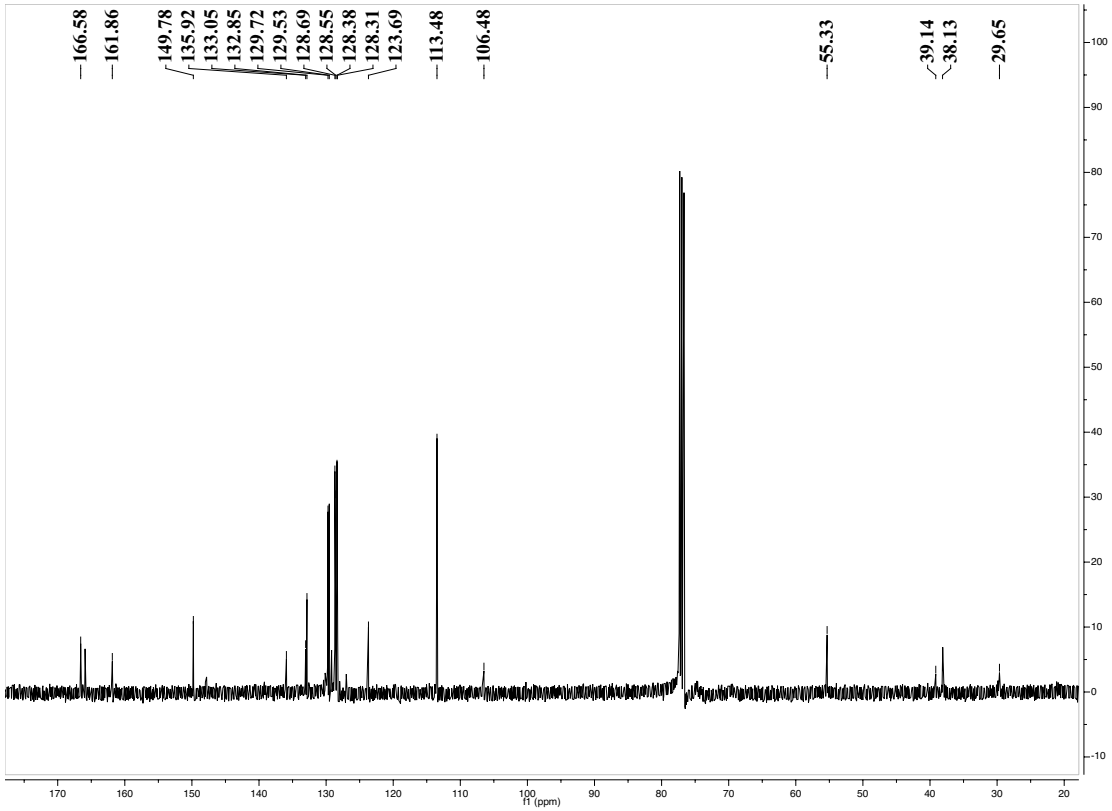

Figure A.1.54 ^{13}C NMR (101 MHz, $CDCl_3$) spectrum of **79**.

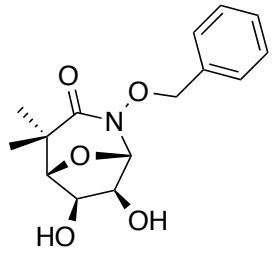

85

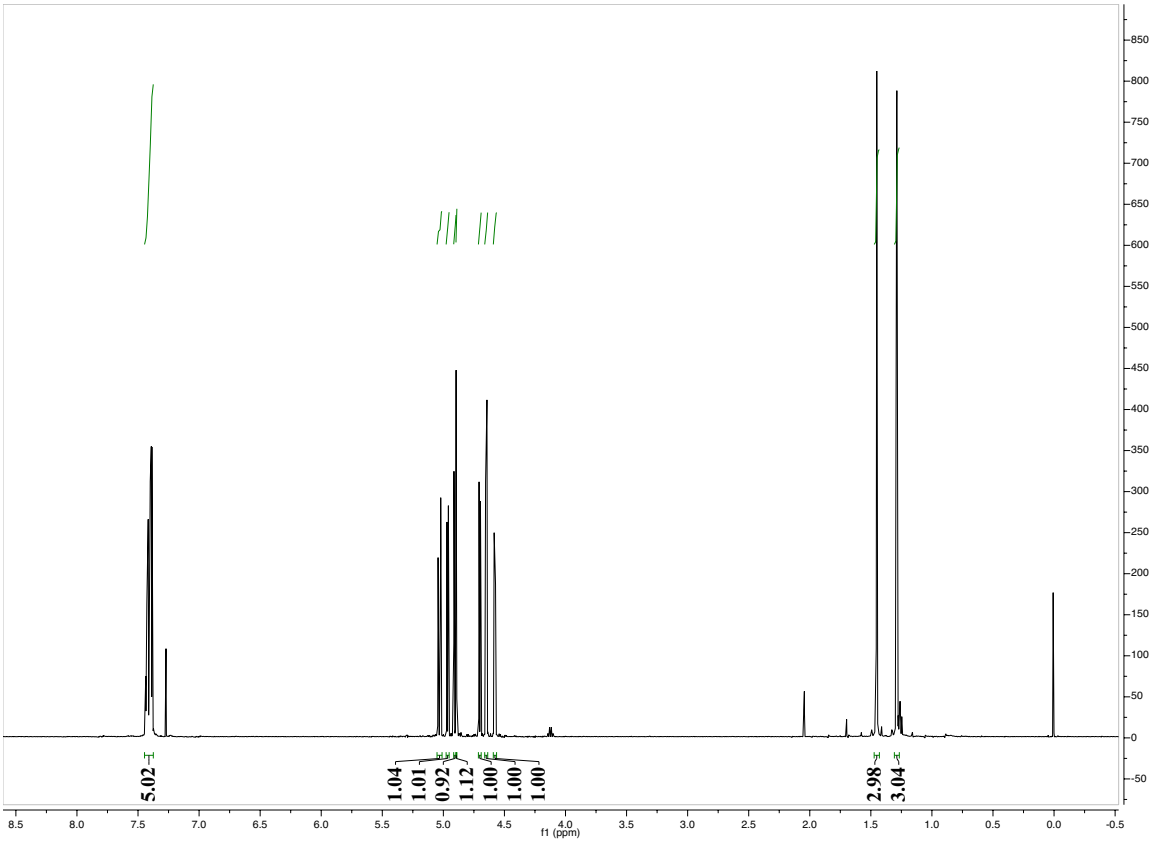

Figure A.1.55 ^{1}H NMR (500 MHz, $CDCl_3$) spectrum of **85**.

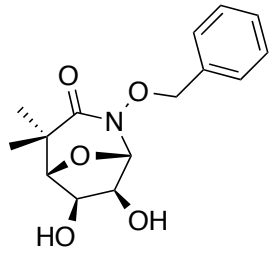

85

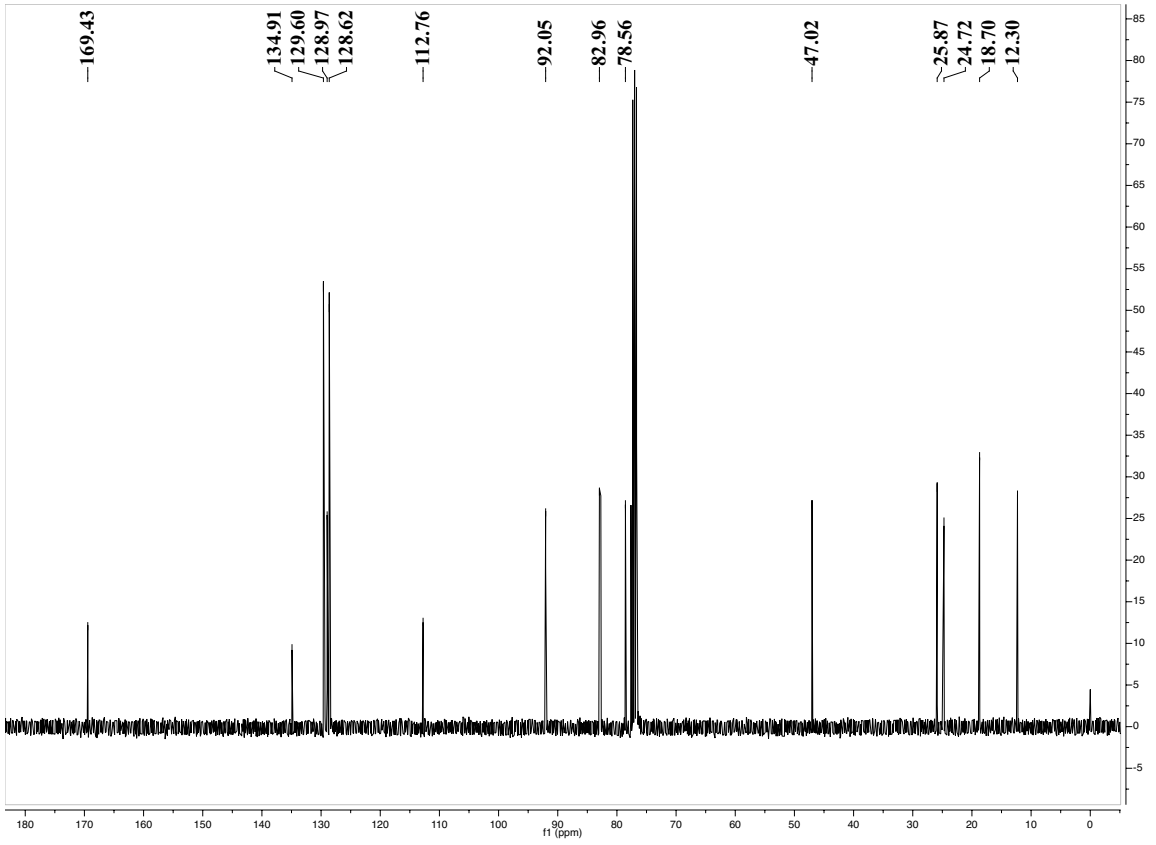

Figure A.1.56 ^{13}C NMR (121 MHz, $CDCl_3$) spectrum of **85**.

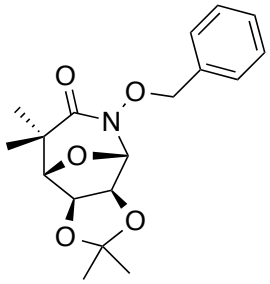

86

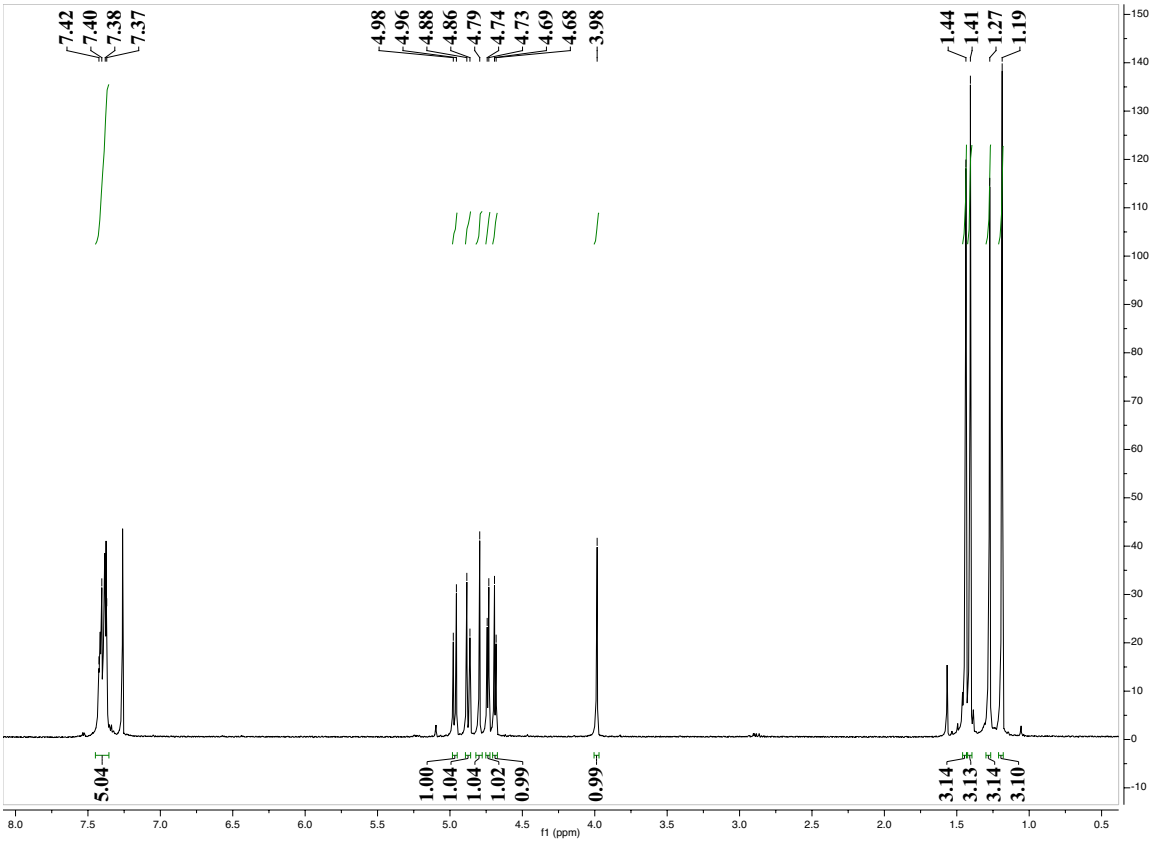

Figure A.1.57 ^{1}H NMR (500 MHz, $CDCl_3$) spectrum of **86**.

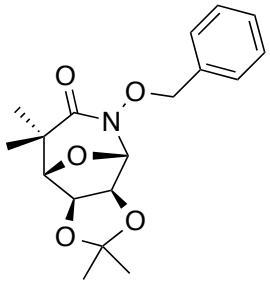

86

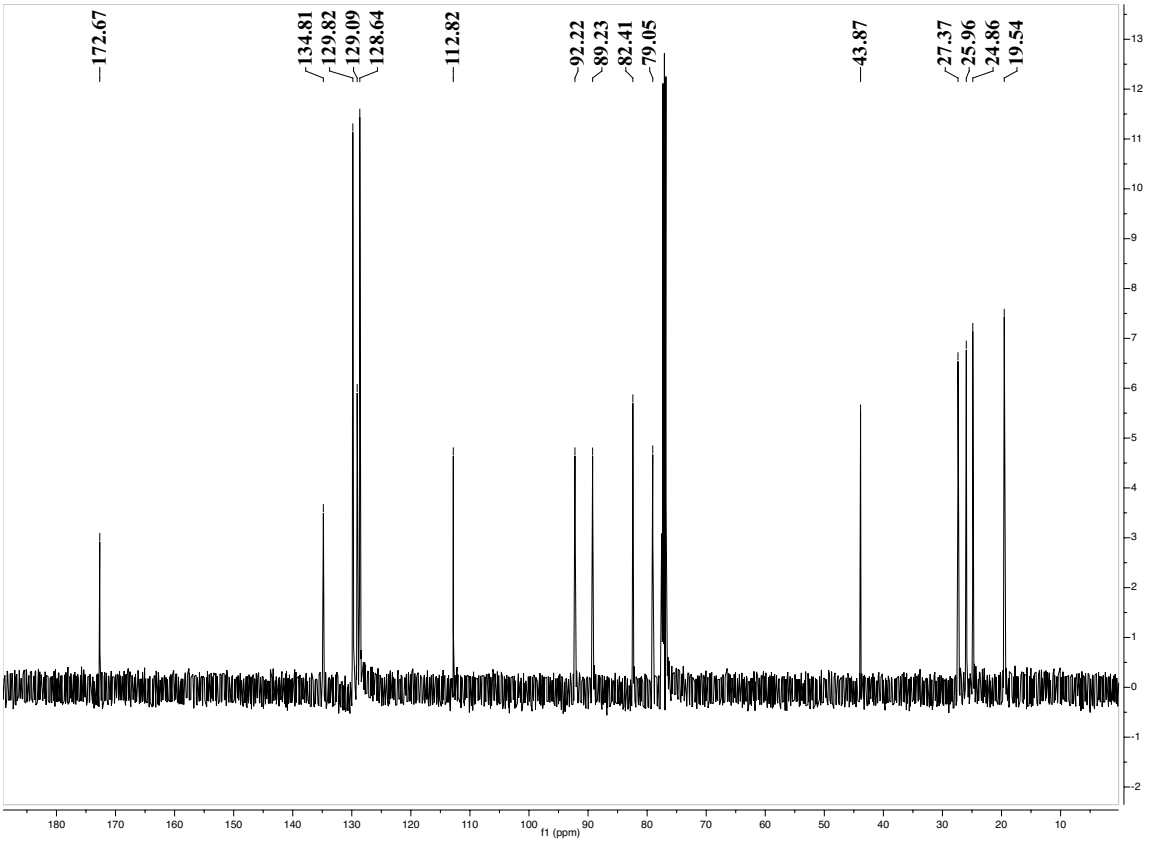

Figure A.1.58 ^{13}C NMR (121 MHz, $CDCl_3$) spectrum of **86**.

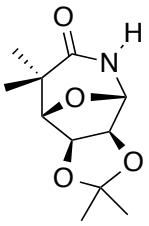

87

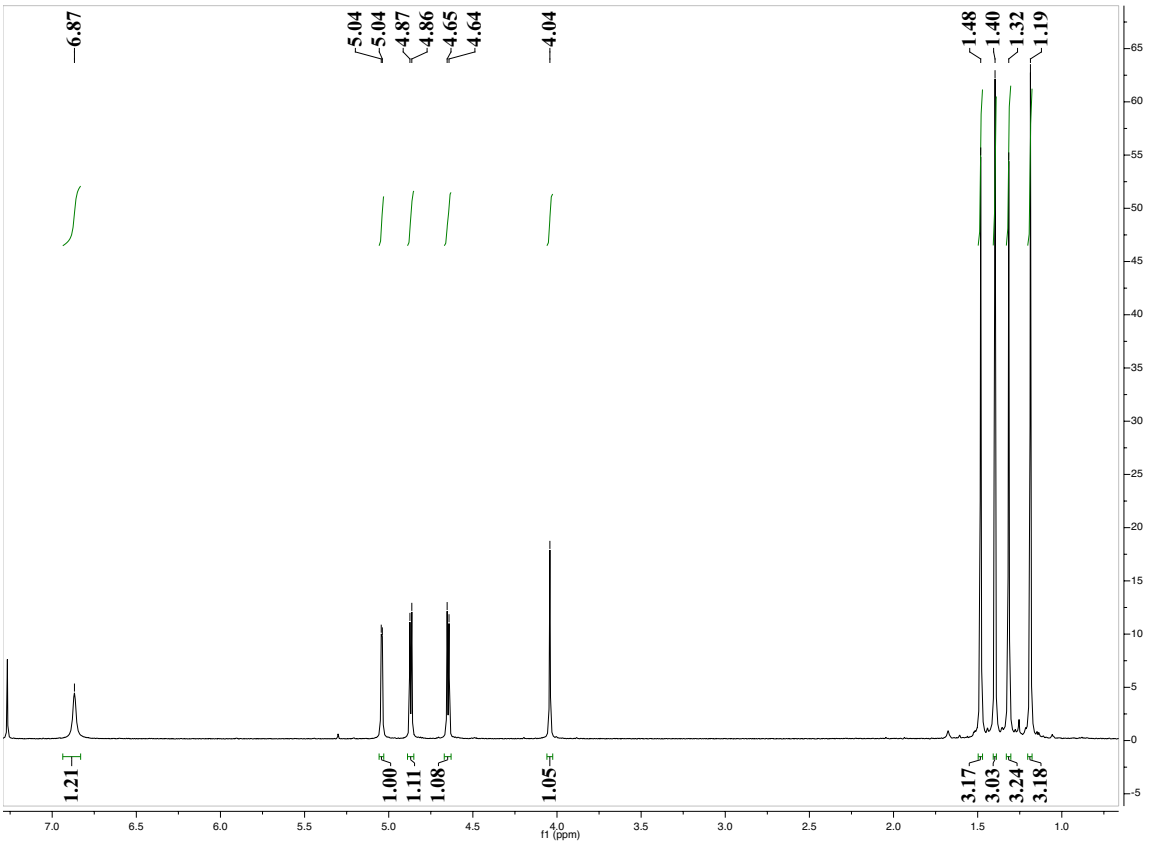

Figure A.1.59 ^{1}H NMR (500 MHz, $CDCl_3$) spectrum of **87**.

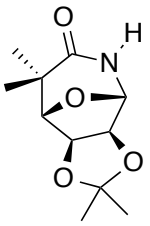

87

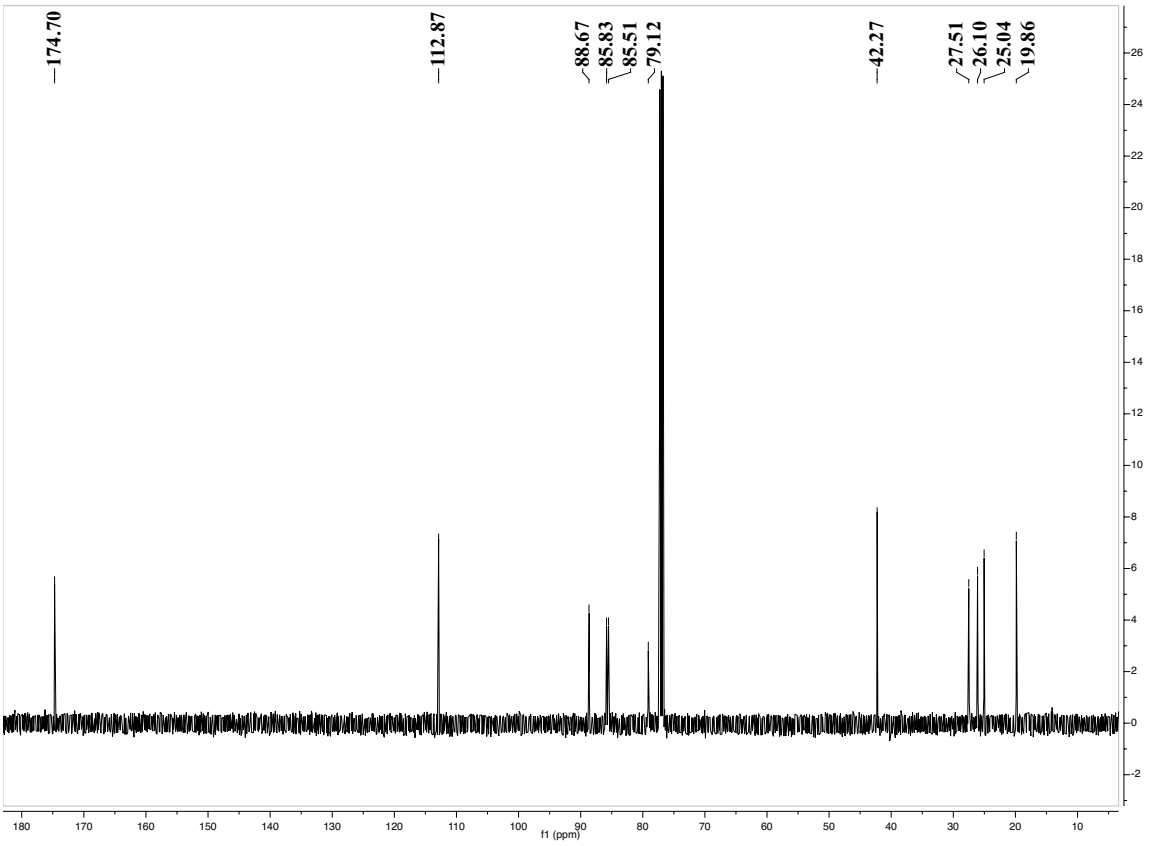

Figure A.1.60 ^{13}C NMR (121 MHz, $CDCl_3$) spectrum of **87**.

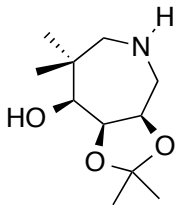

88

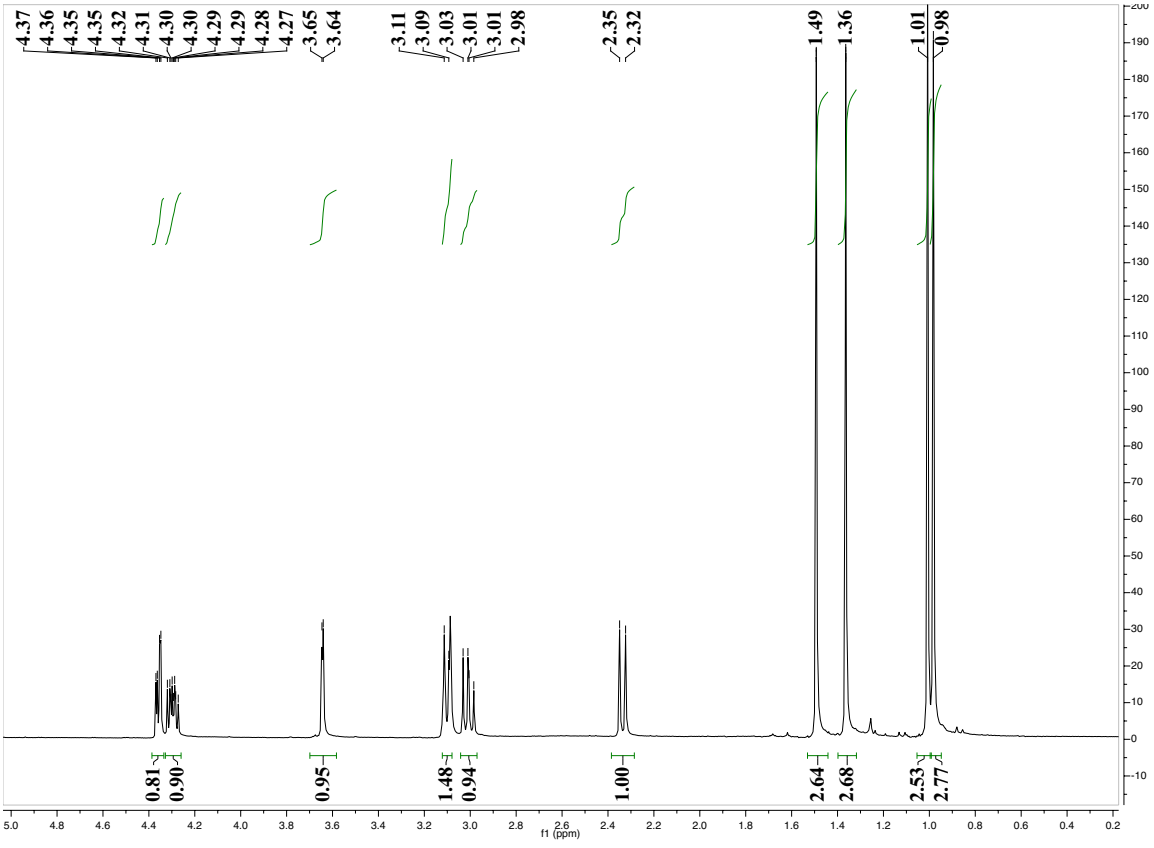

Figure A.1.61 ^{1}H NMR (500 MHz, $CDCl_3$) spectrum of **88**.

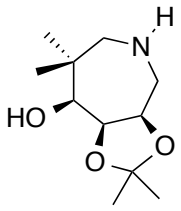

88

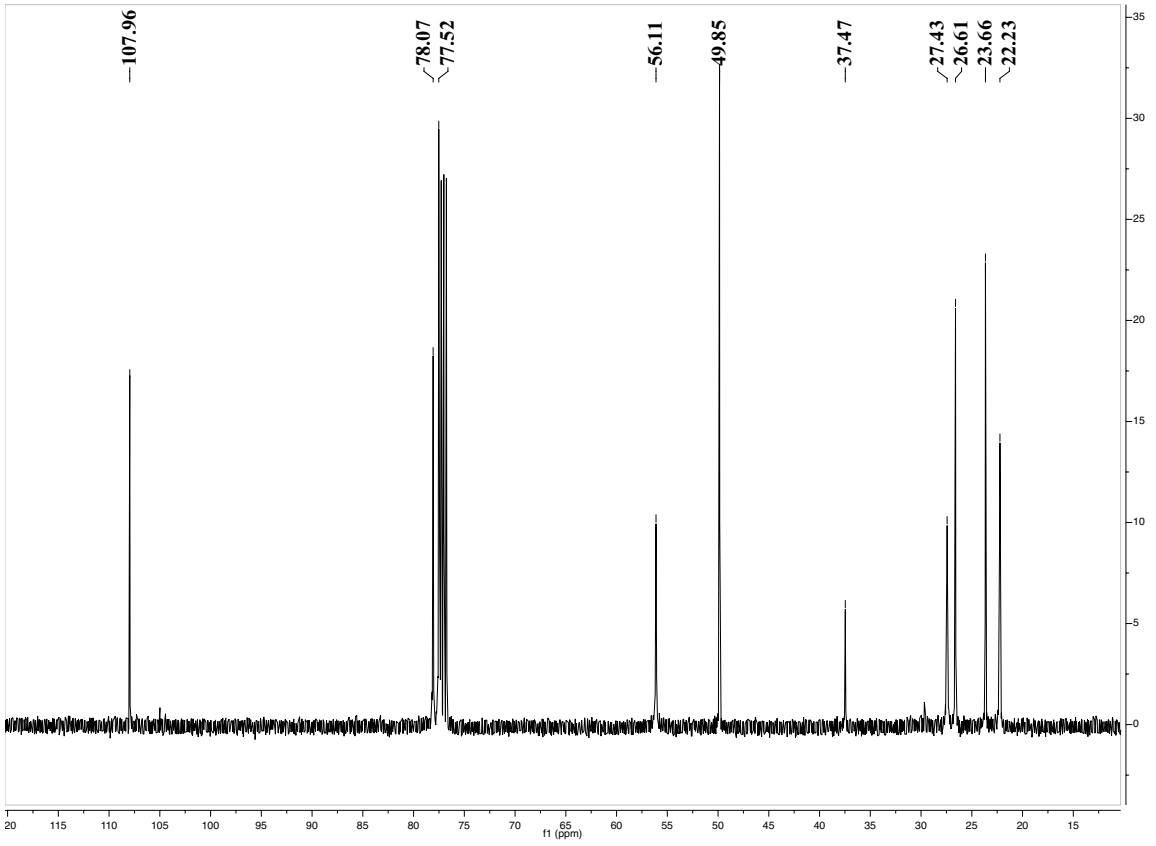

Figure A.1.62 ^{13}C NMR (121 MHz, $CDCl_3$) spectrum of **88**.

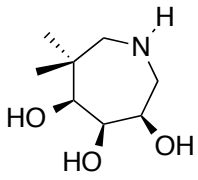

89

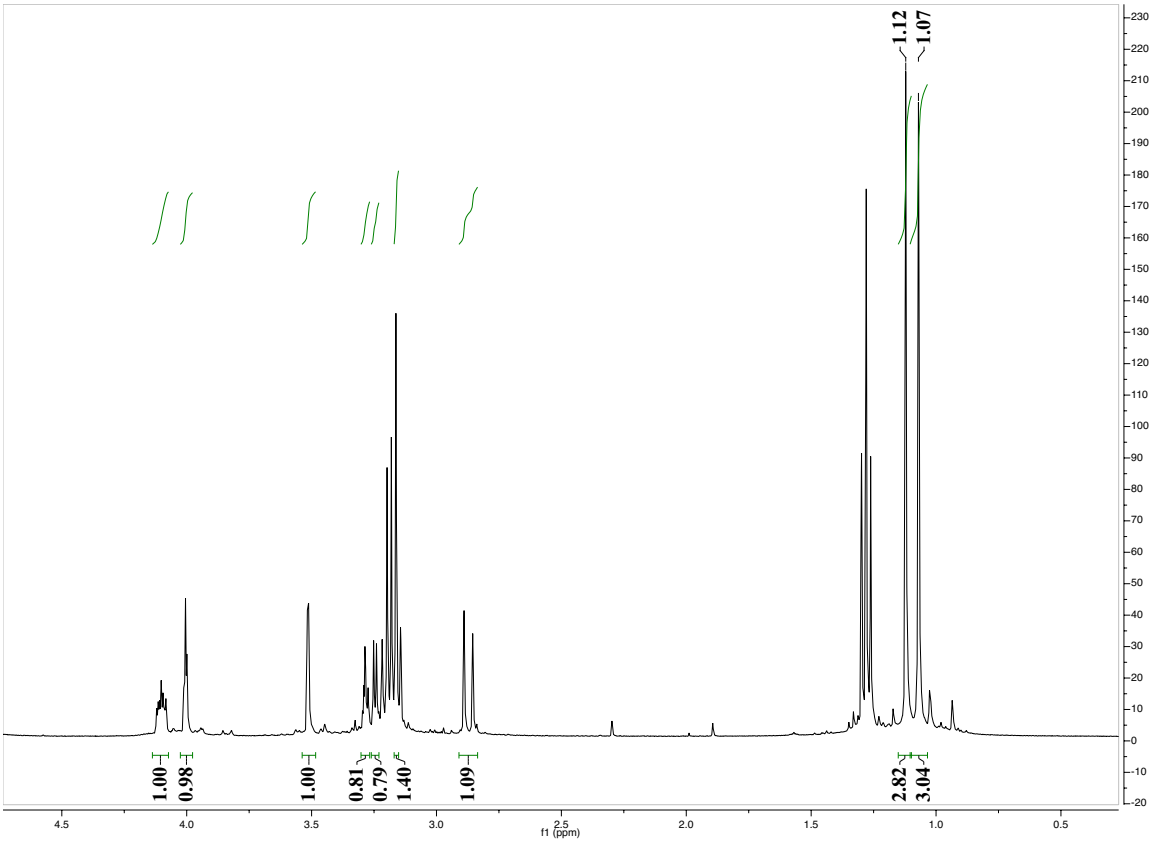

Figure A.1.63 ^{1}H NMR (400 MHz, CD_3OD) spectrum of **89**.

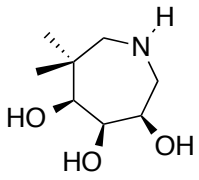

89

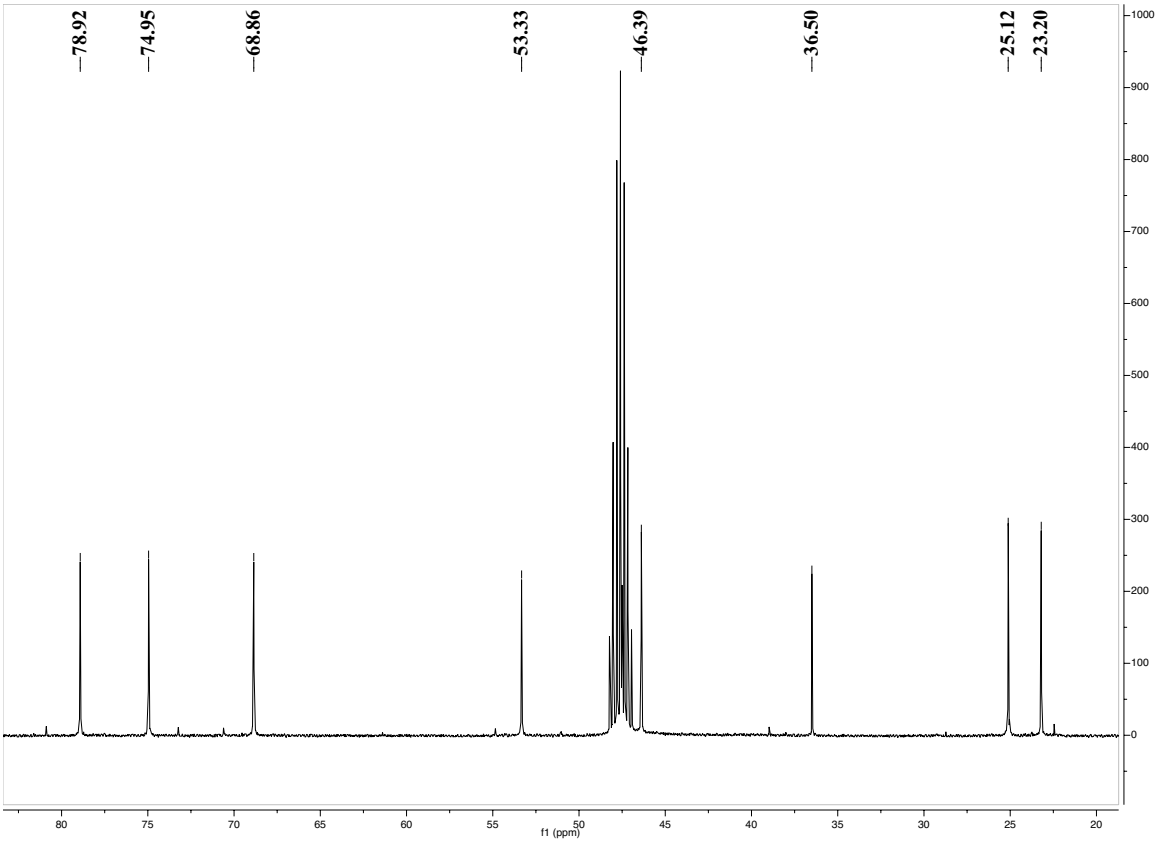

Figure A.1.64 ^{13}C NMR (101 MHz, CD_3OD) spectrum of **89**.

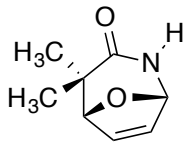

90

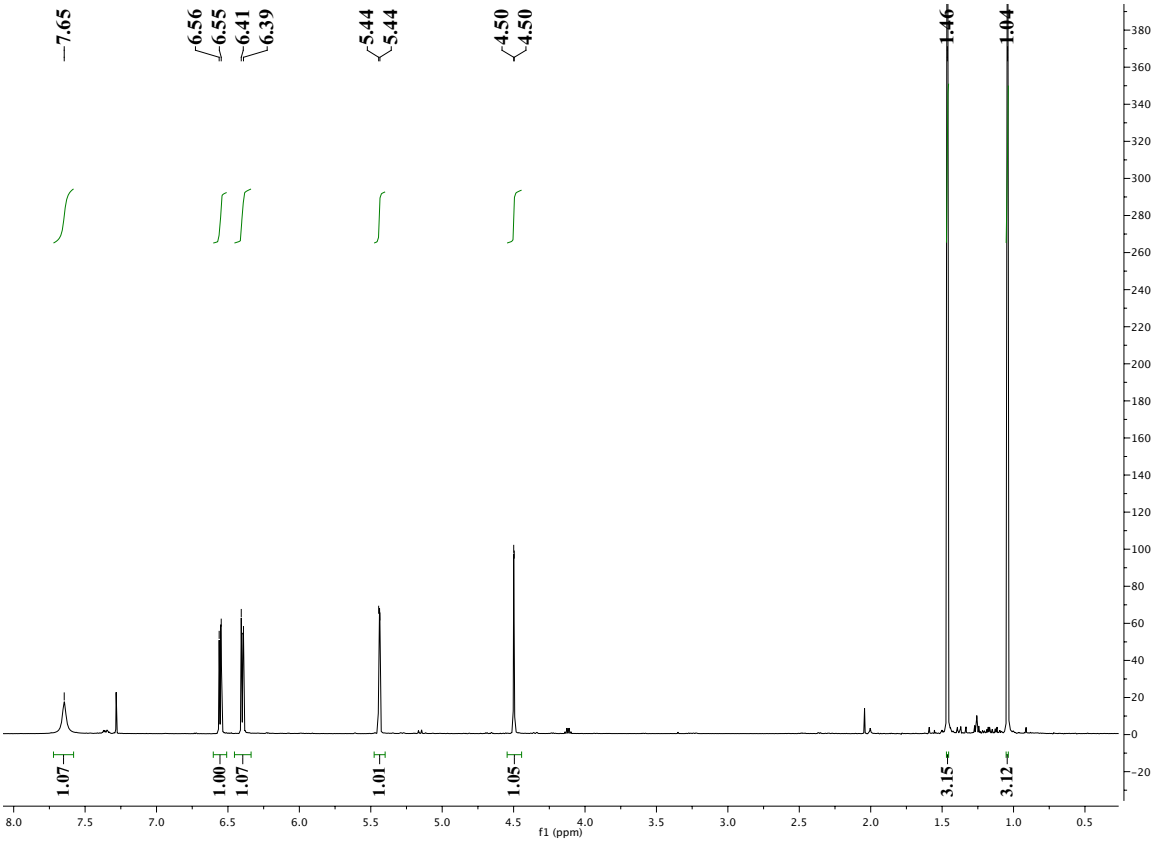

Figure A.1.65 ^{1}H NMR (500 MHz, $CDCl_3$) spectrum of **90**.

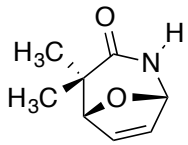

90

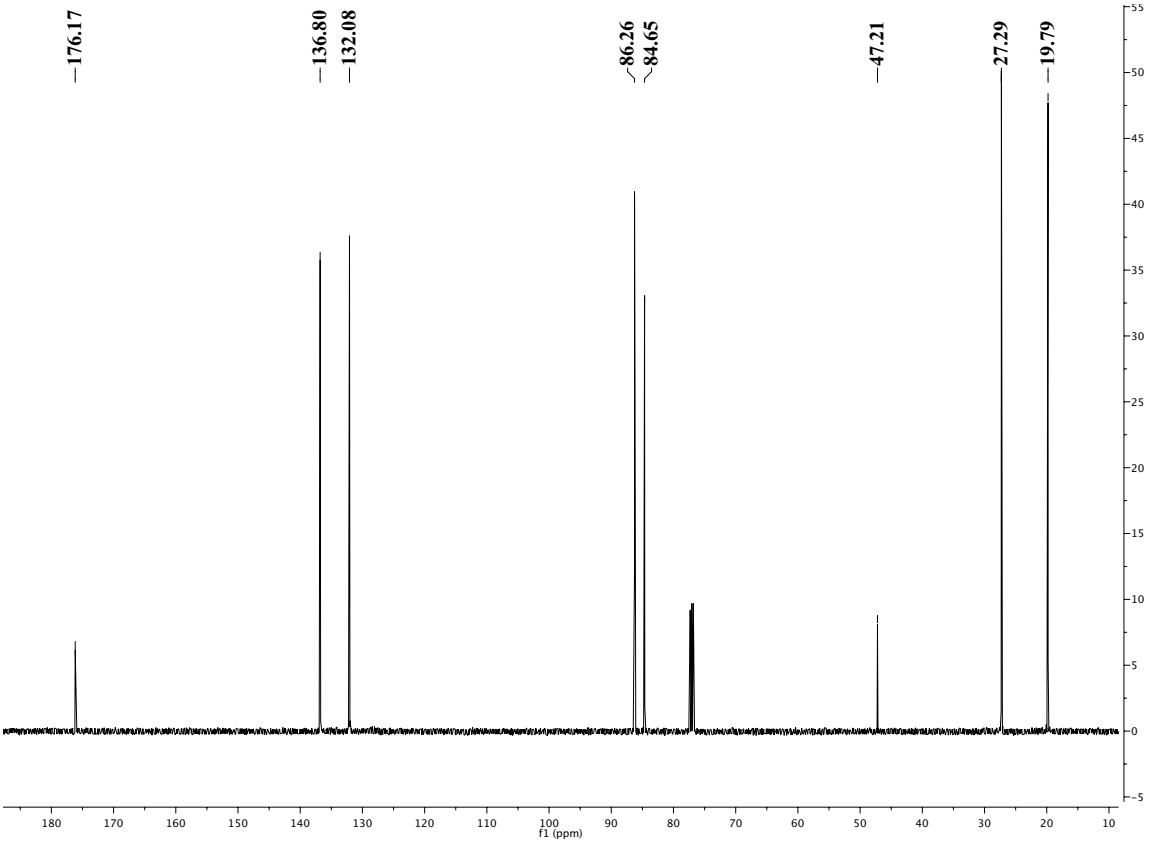

Figure A.1.66 ^{13}C NMR (121 MHz, $CDCl_3$) spectrum of **90**.

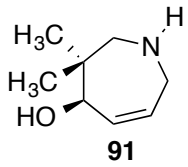

91

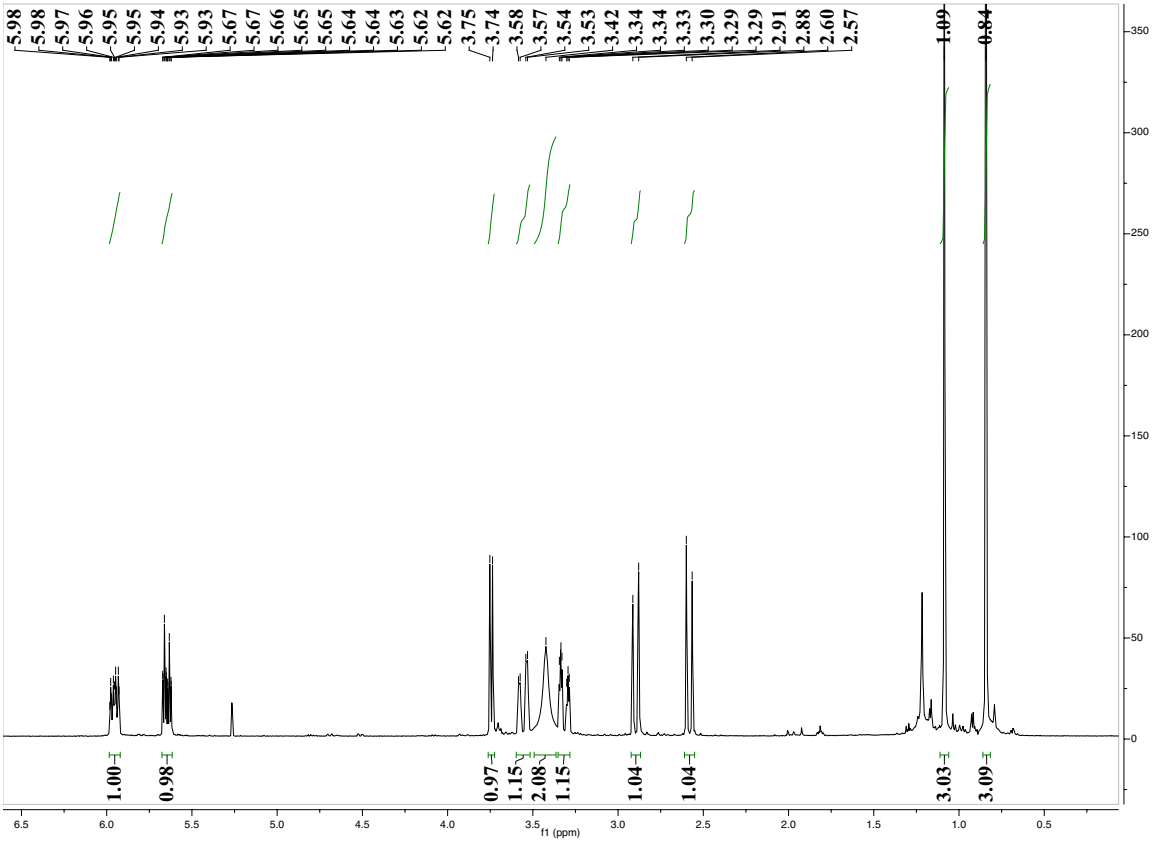

Figure A.1.67 ^{1}H NMR (500 MHz, $CDCl_3$) spectrum of **91**.

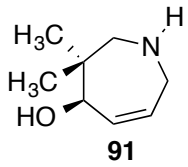

91

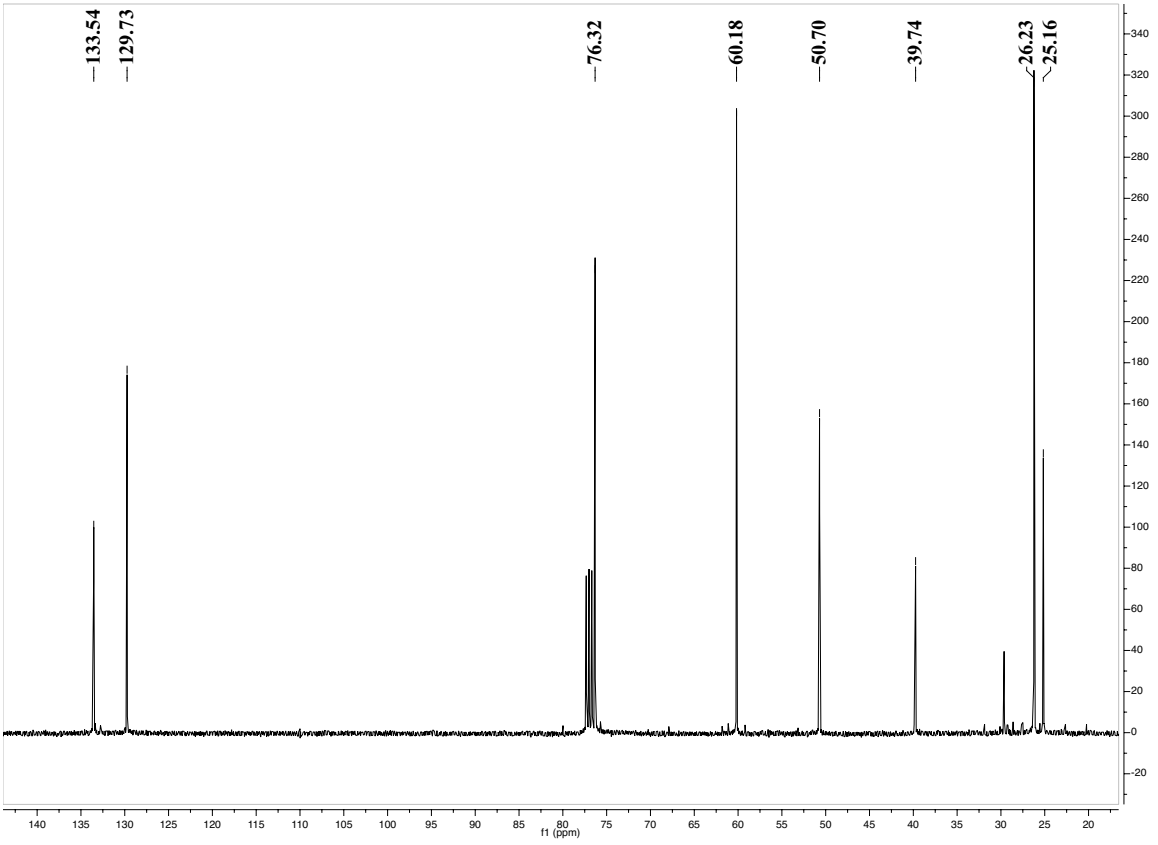

Figure A.1.68 ^{13}C NMR (101 MHz, $CDCl_3$) spectrum of **91**.

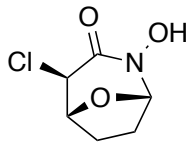

92

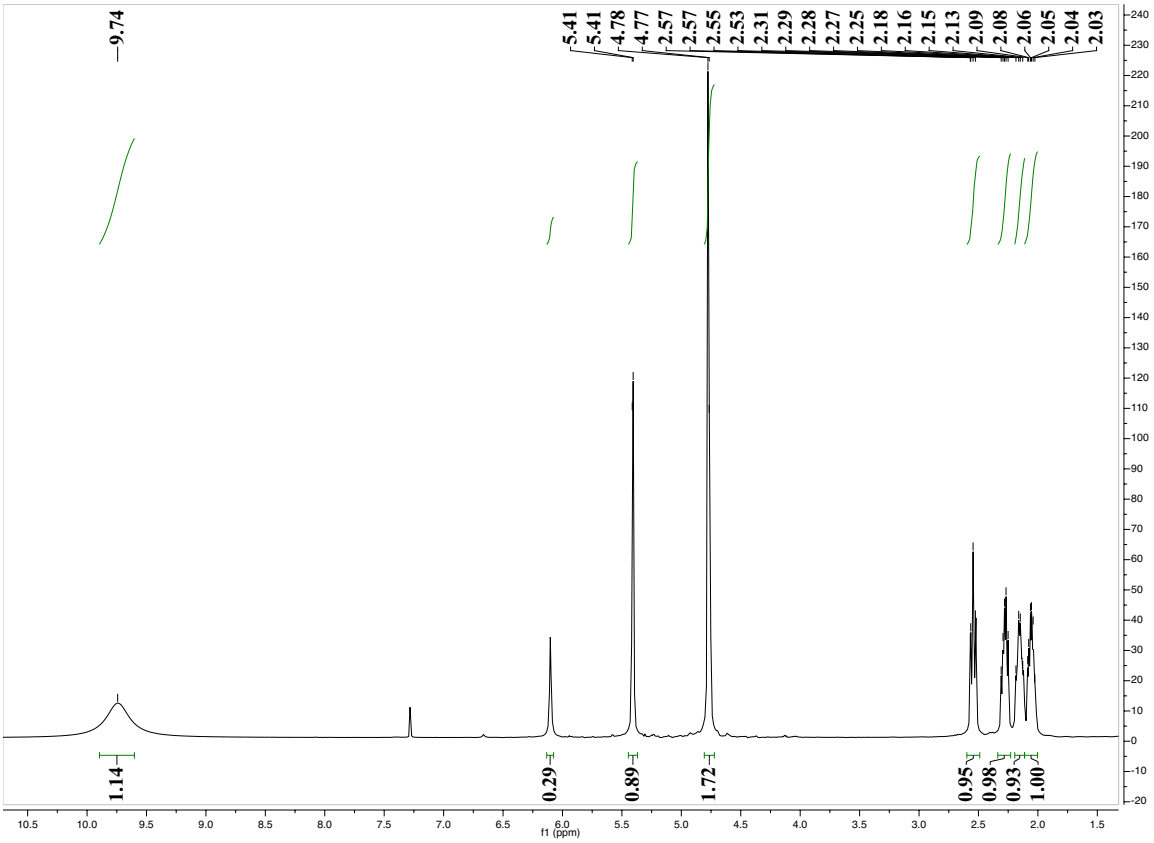

Figure A.1.69 ^{1}H NMR (500 MHz, $CDCl_3$) spectrum of **92**.

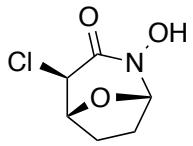

92

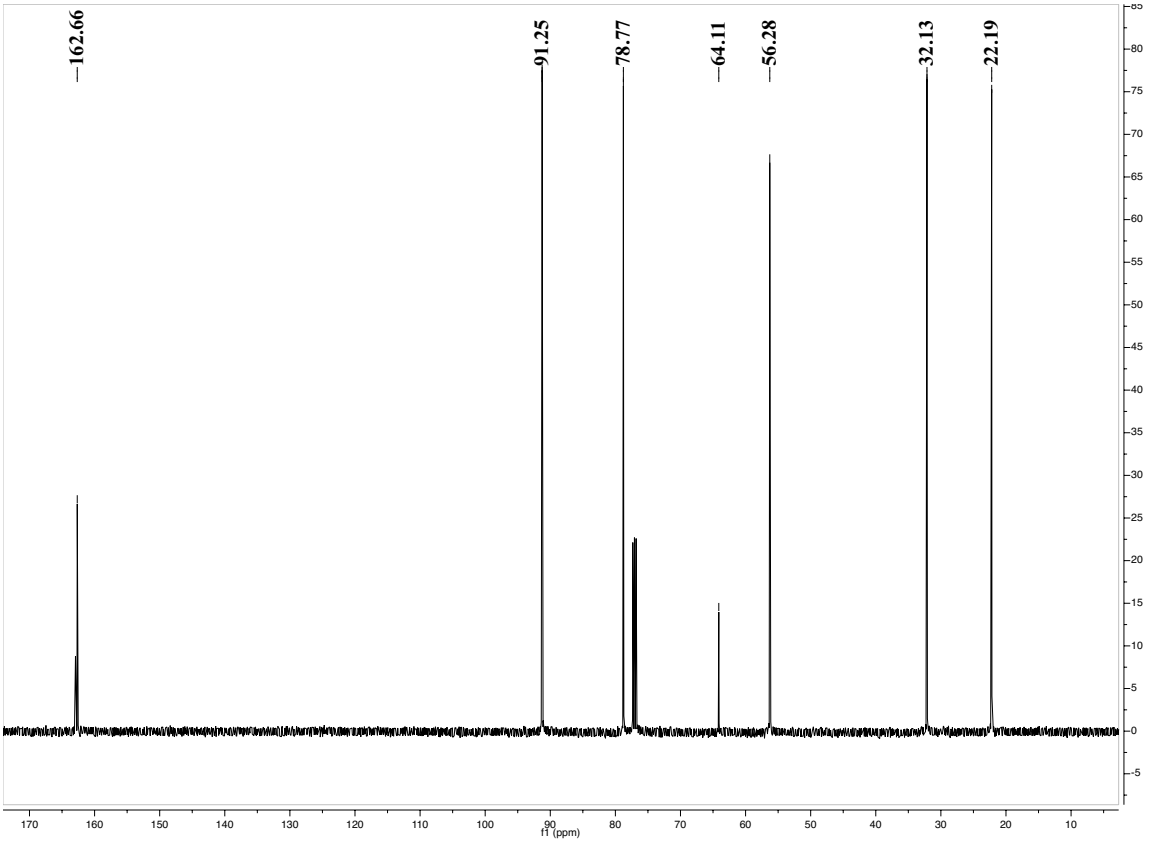

Figure A.1.70 ^{13}C NMR (121 MHz, $CDCl_3$) spectrum of **92**.

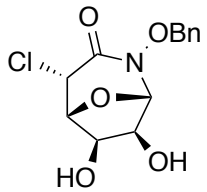

93

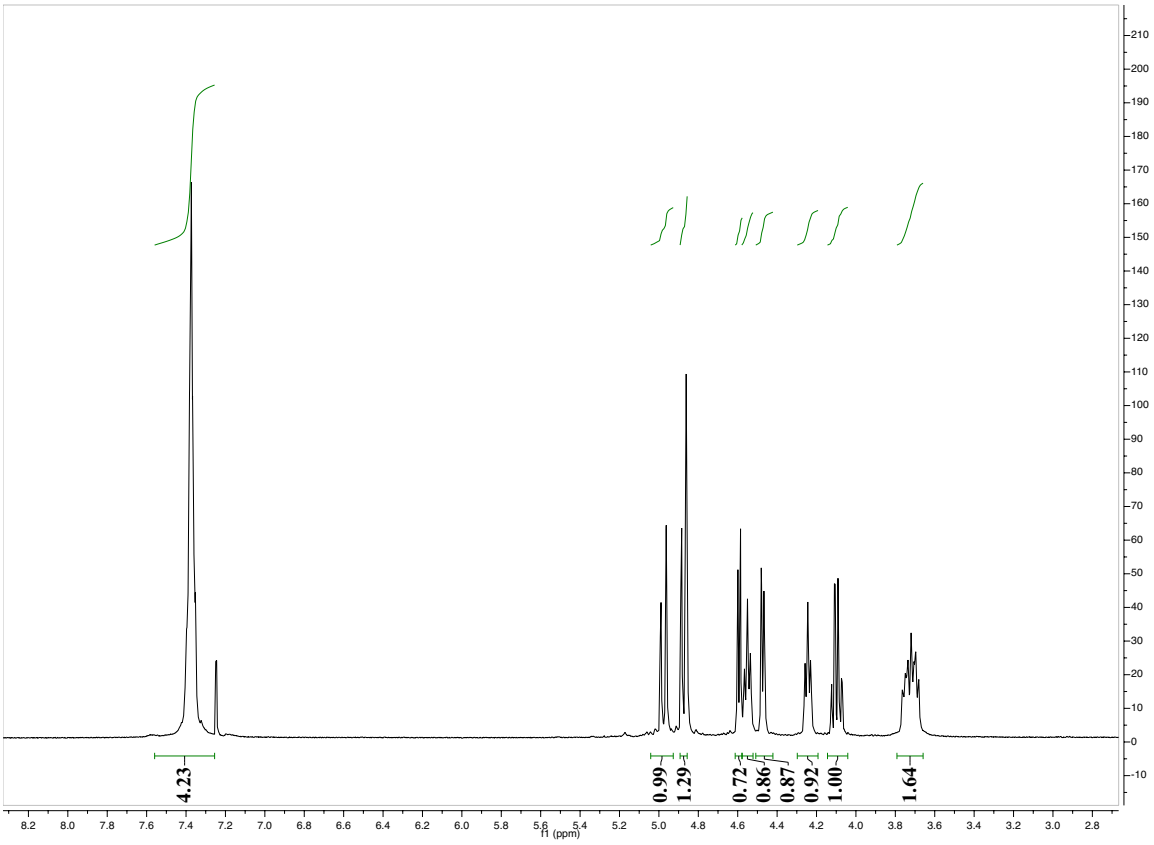

Figure A.1.71 ^{1}H NMR (500 MHz, $CDCl_3$) spectrum of **93**.

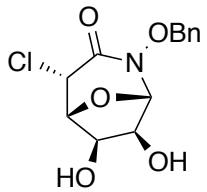

93

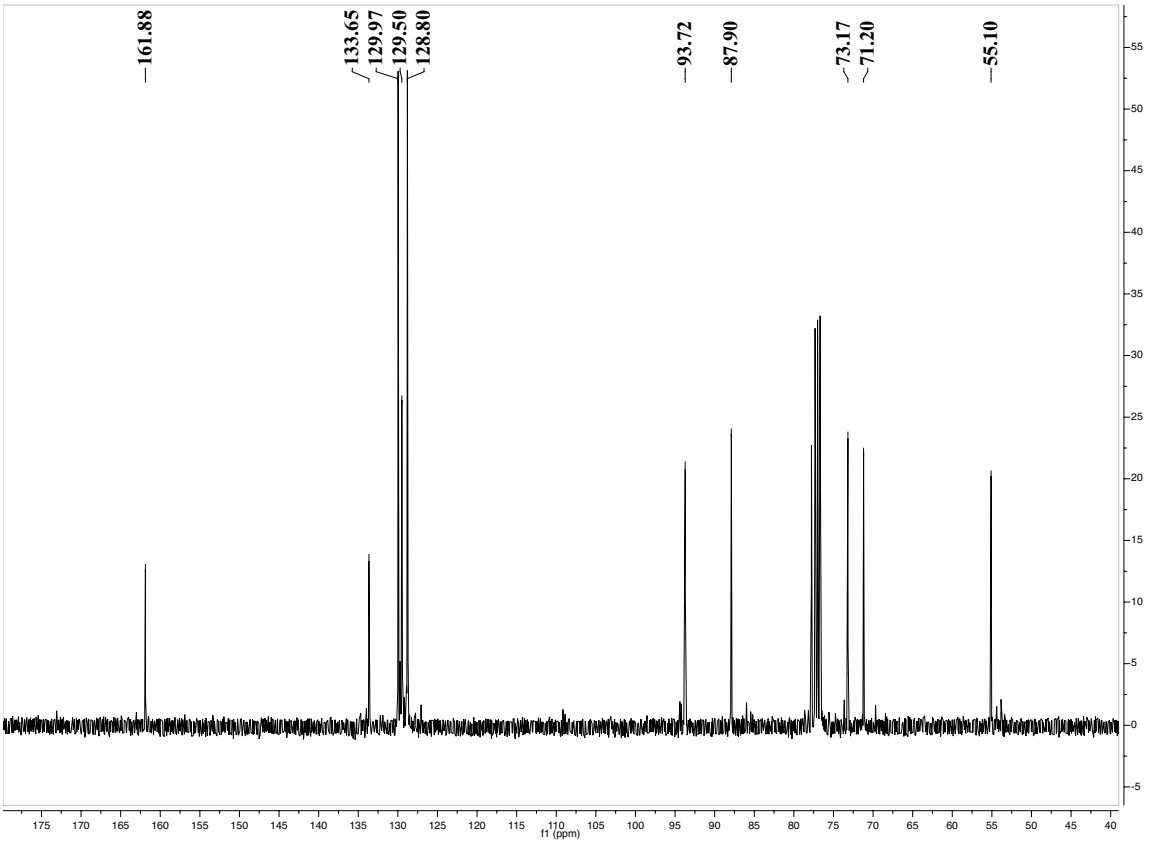

Figure A.1.72 ^{13}C NMR (121 MHz, $CDCl_3$) spectrum of **93**.

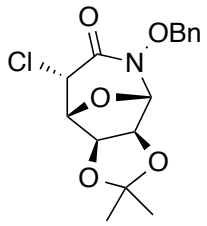

94

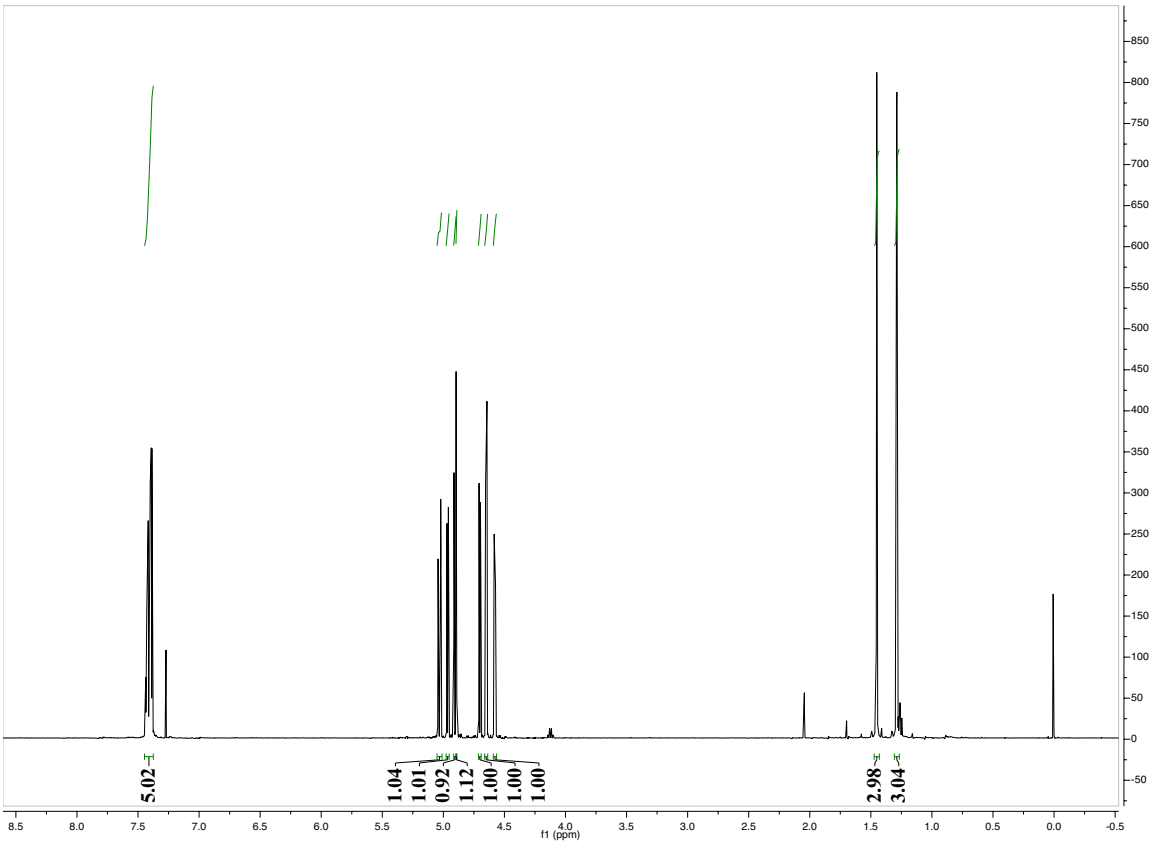

Figure A.1.73 ^{1}H NMR (400 MHz, $CDCl_3$) spectrum of **94**.

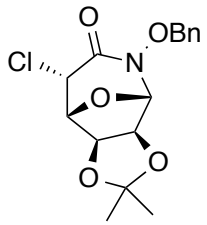

94

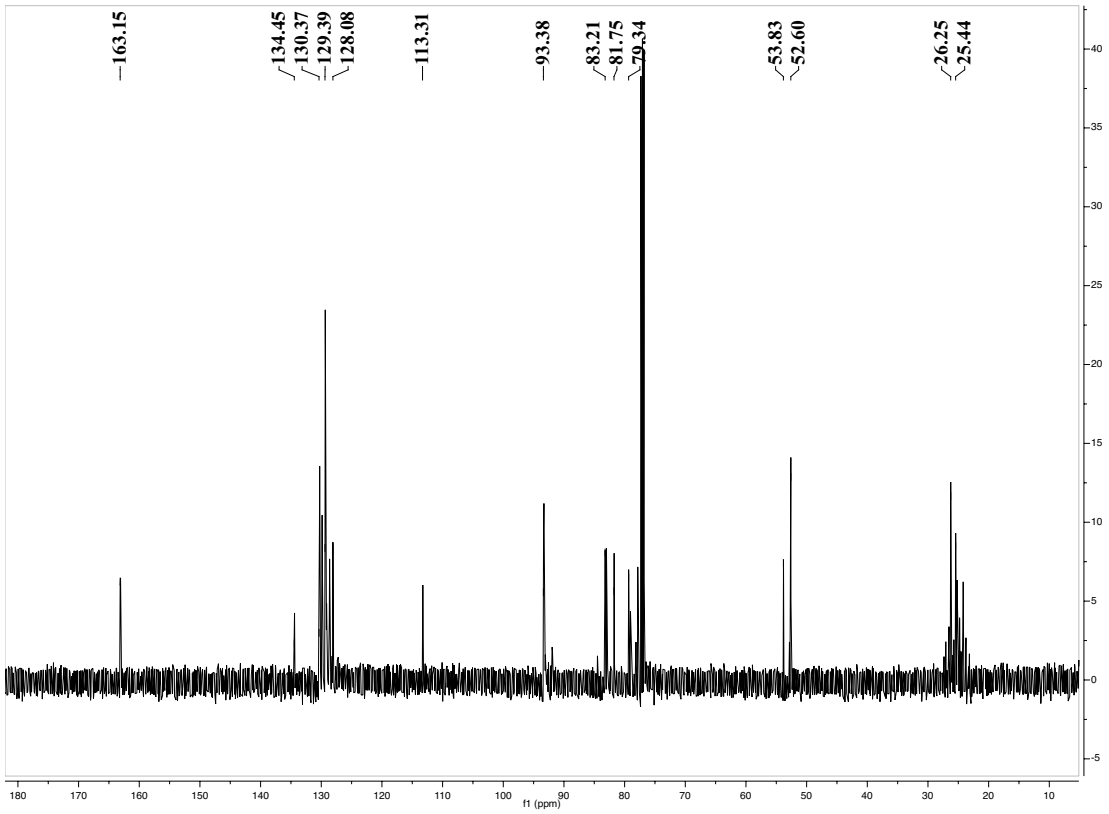

Figure A.1.74 ^{13}C NMR (101 MHz, $CDCl_3$) spectrum of **94**.

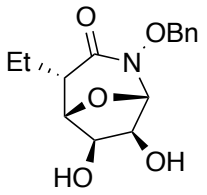

95

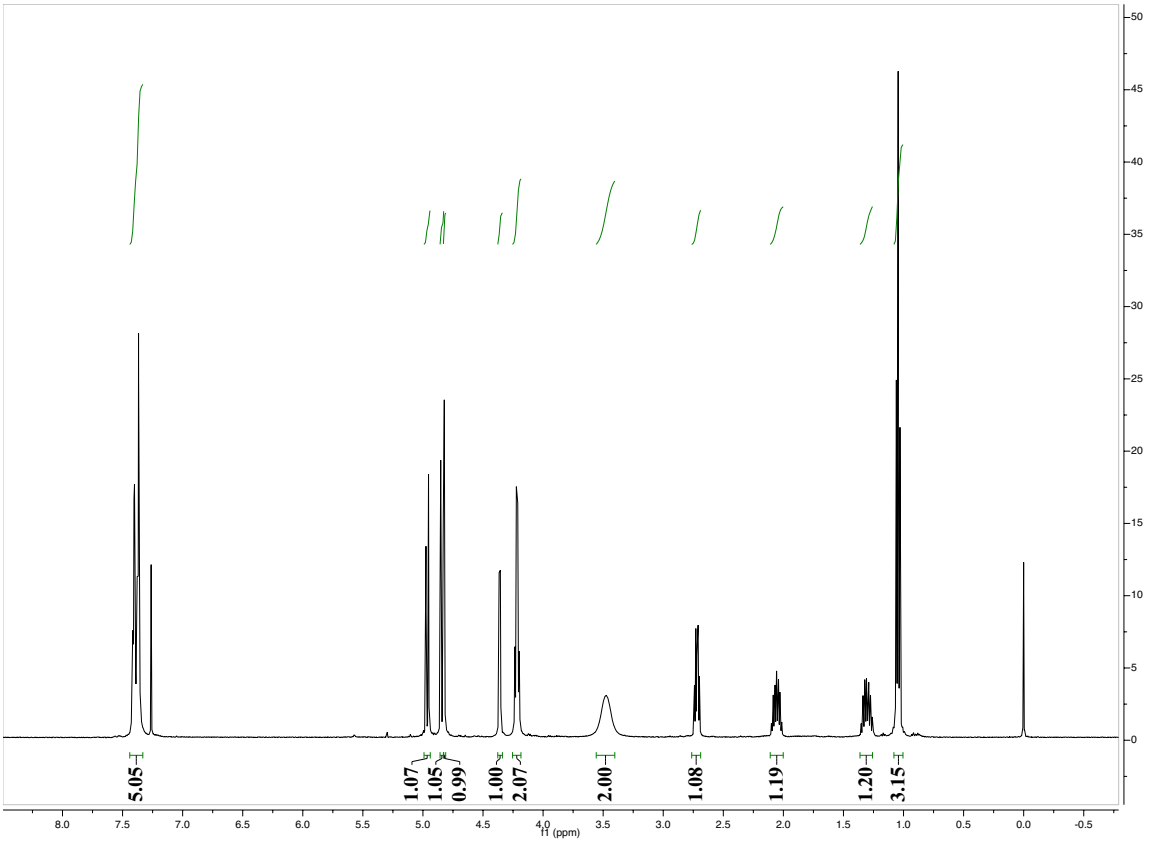

Figure A.1.75 ^{1}H NMR (500 MHz, $CDCl_3$) spectrum of **95**.

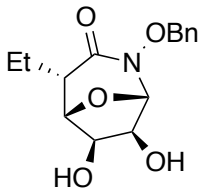

95

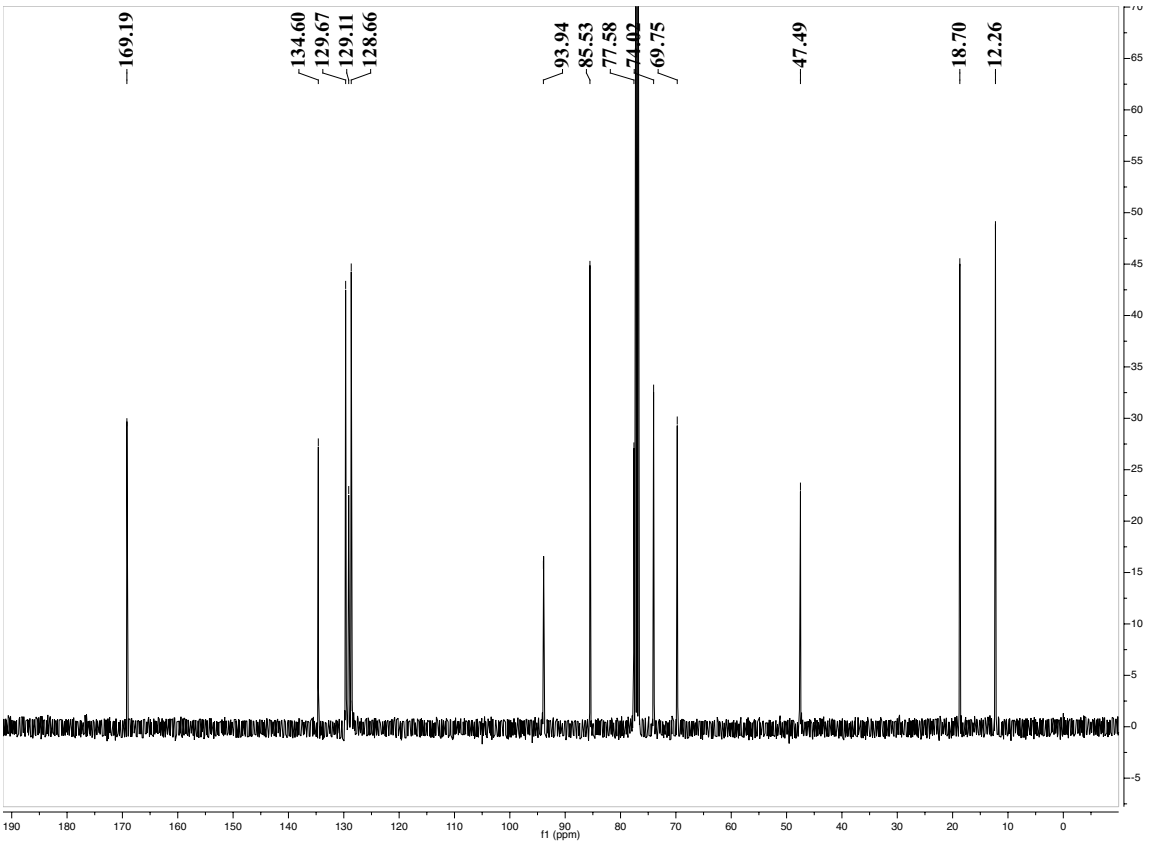

Figure A.1.76 ^{13}C NMR (121 MHz, $CDCl_3$) spectrum of **95**.

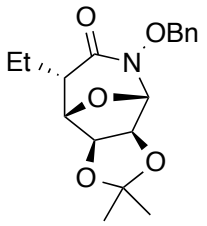

96

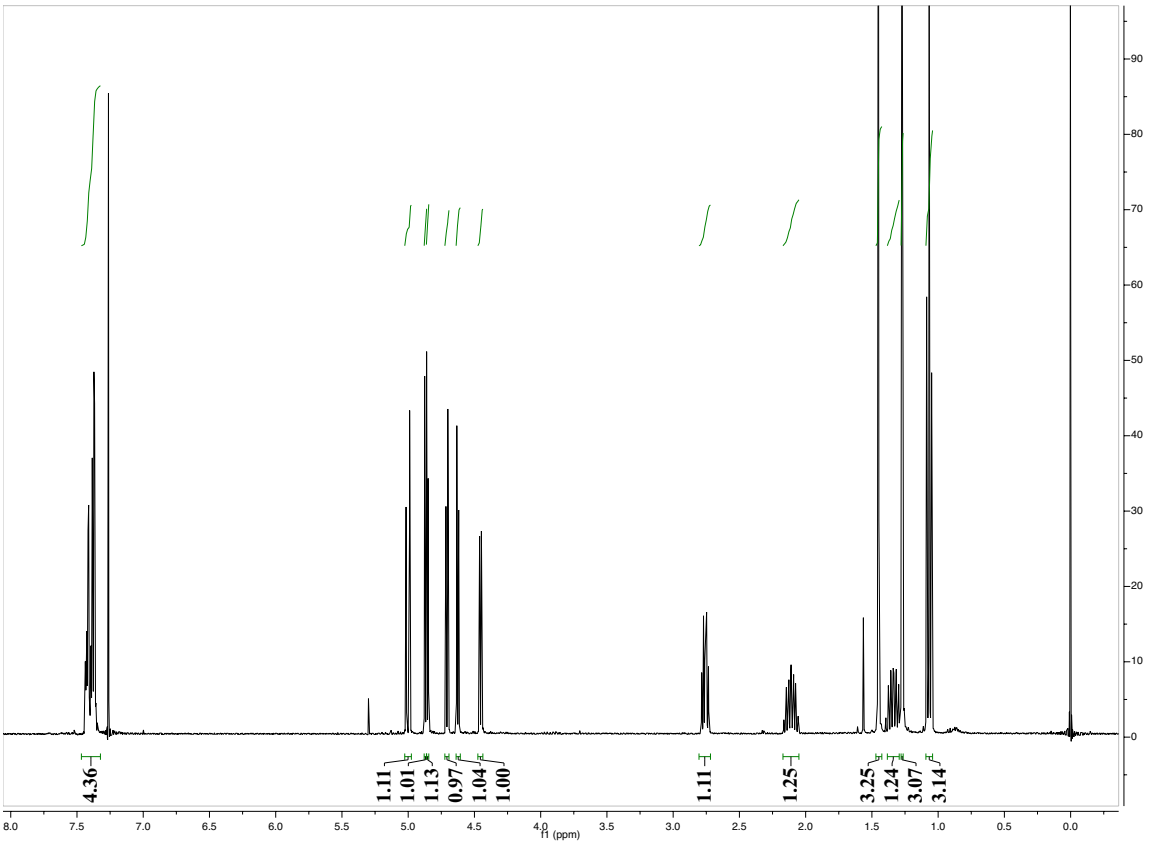

Figure A.1.77 ^{1}H NMR (500 MHz, $CDCl_3$) spectrum of **96**.

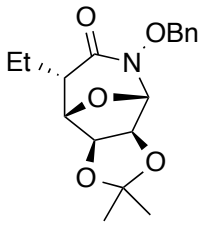

96

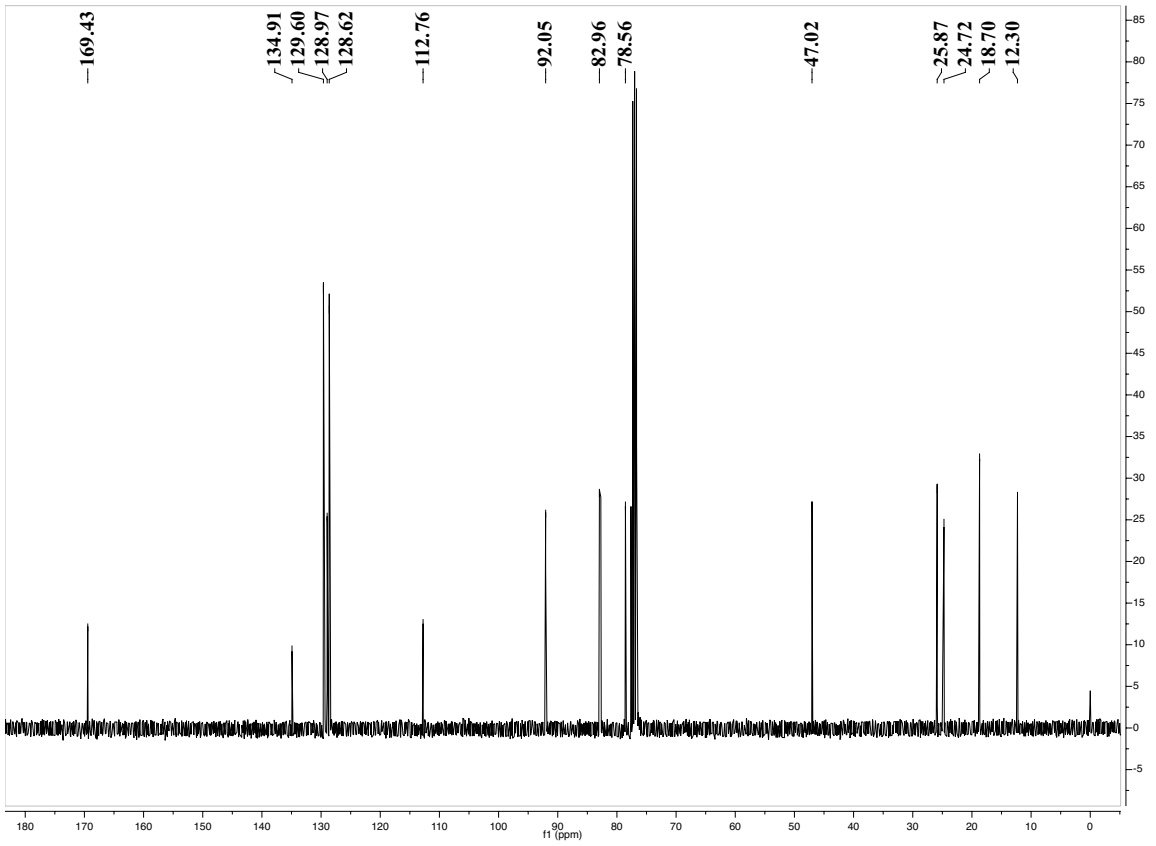

Figure A.1.78 ^{13}C NMR (121 MHz, $CDCl_3$) spectrum of **96**.

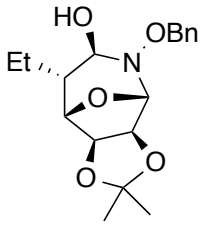

97

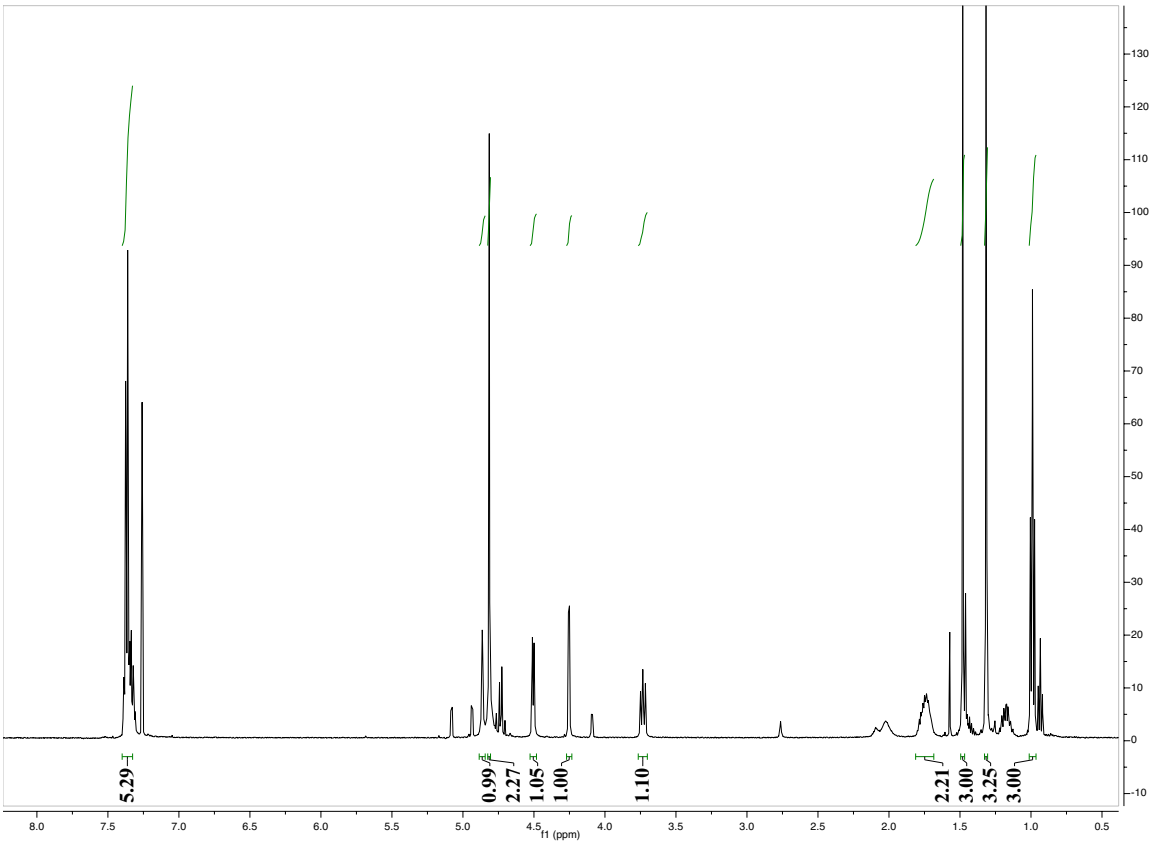

Figure A.1.79 ^{1}H NMR (500 MHz, $CDCl_3$) spectrum of **97**.

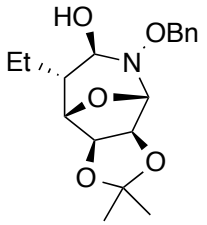

97

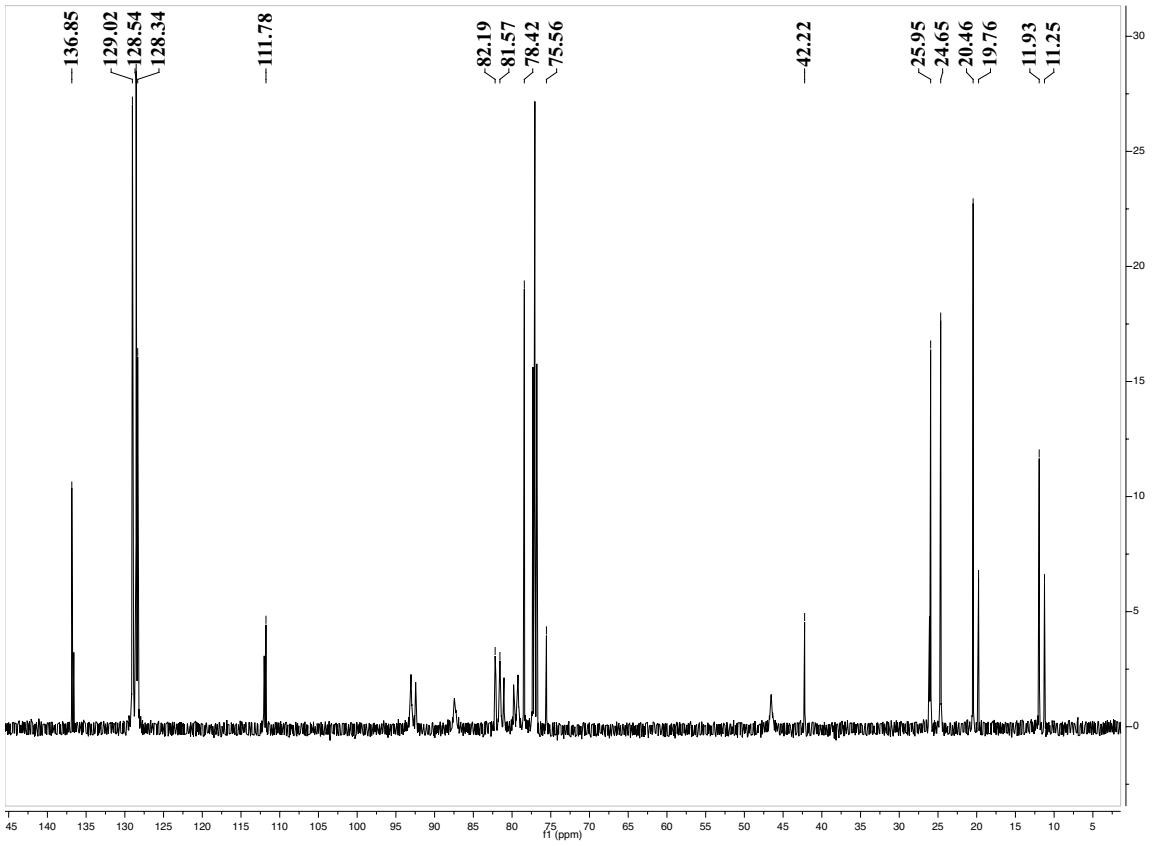

Figure A.1.80 ^{13}C NMR (121 MHz, $CDCl_3$) spectrum of **97**.

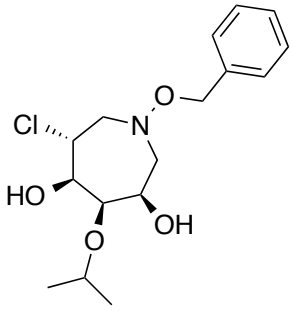

98

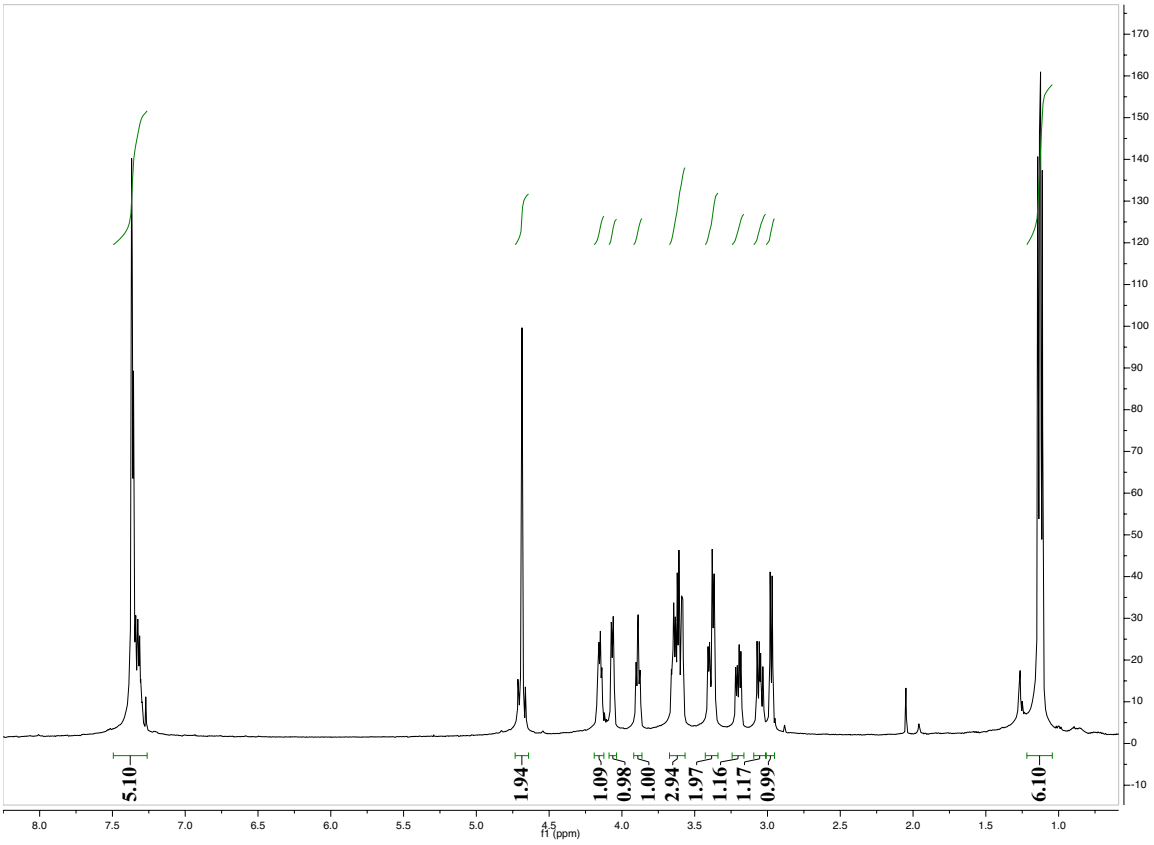

Figure A.1.81 ^{1}H NMR (400 MHz, $CDCl_3$) spectrum of **98**.

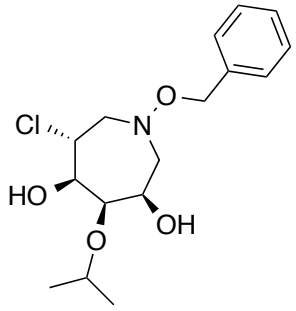

98

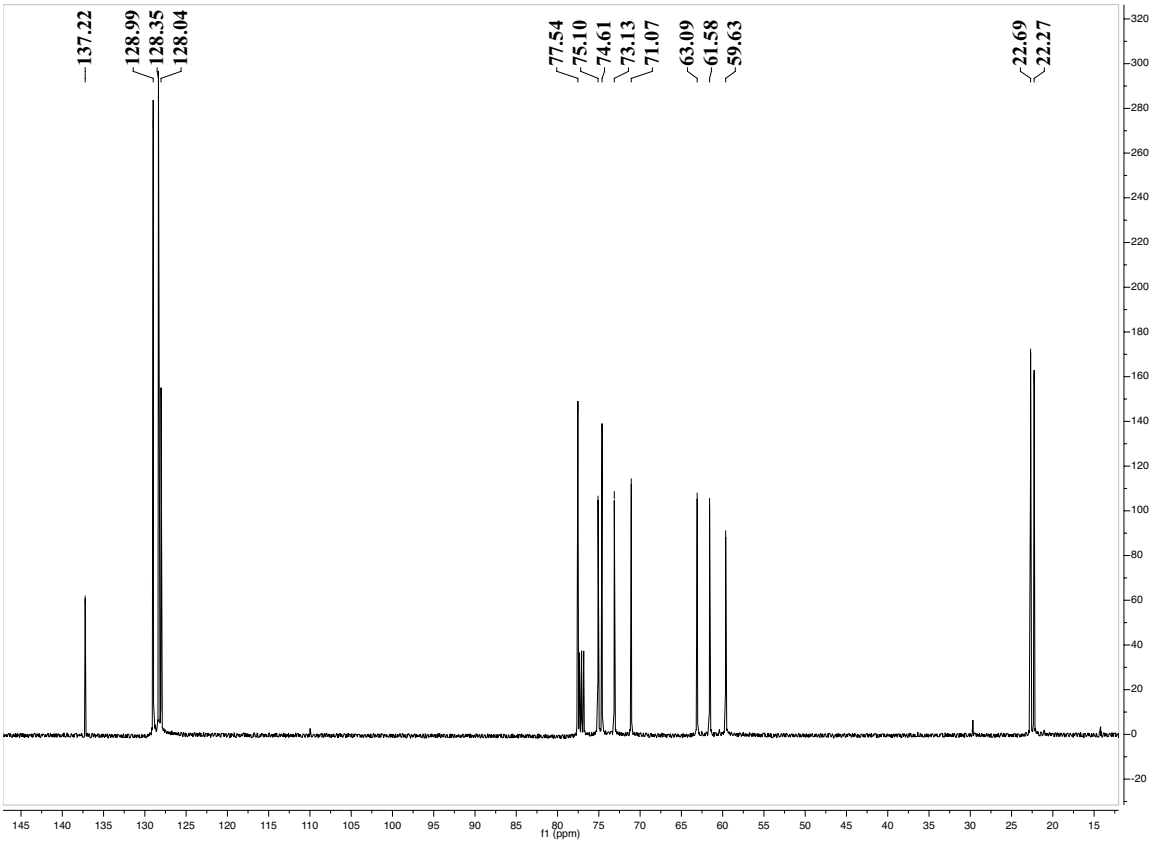

Figure A.1.82 ^{13}C NMR (101 MHz, $CDCl_3$) spectrum of **98**.

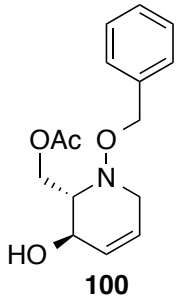

100

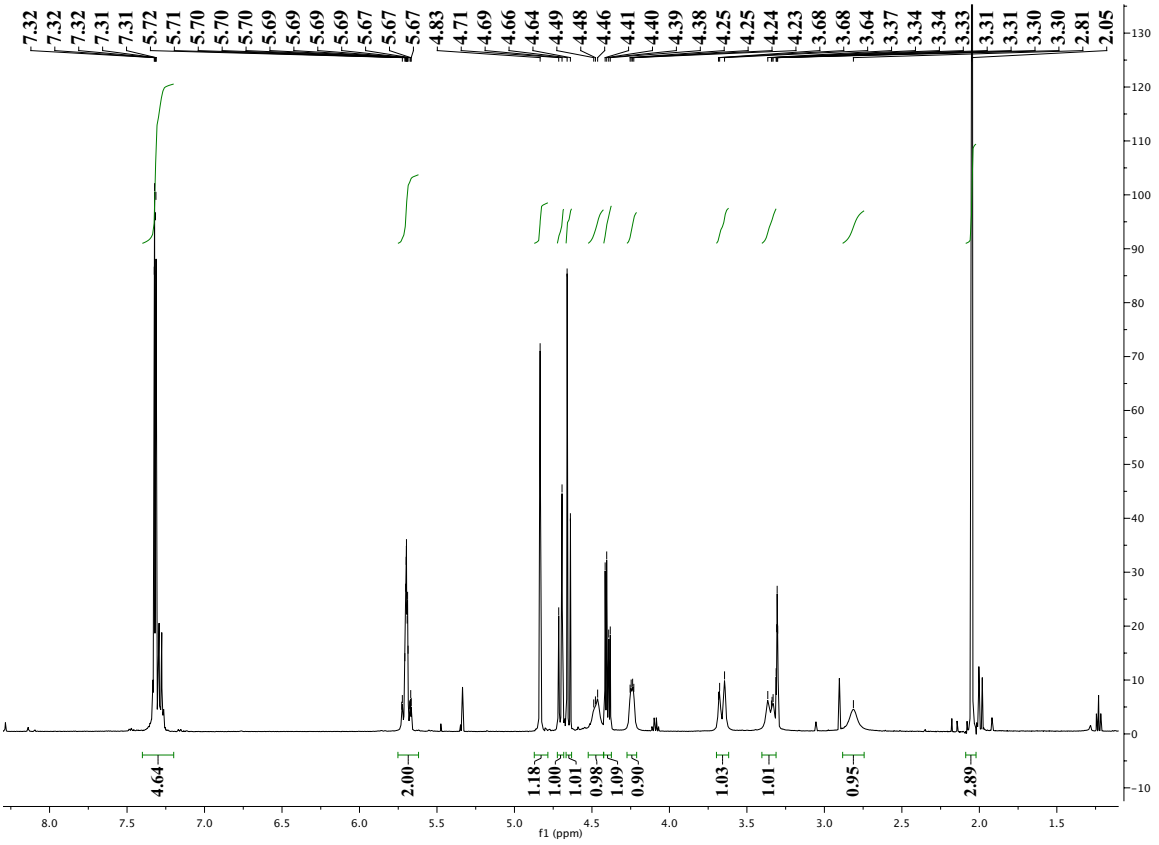

Figure A.1.83 ^{1}H NMR (500 MHz, CD_3OD) spectrum of **100**.

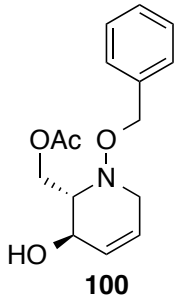

100

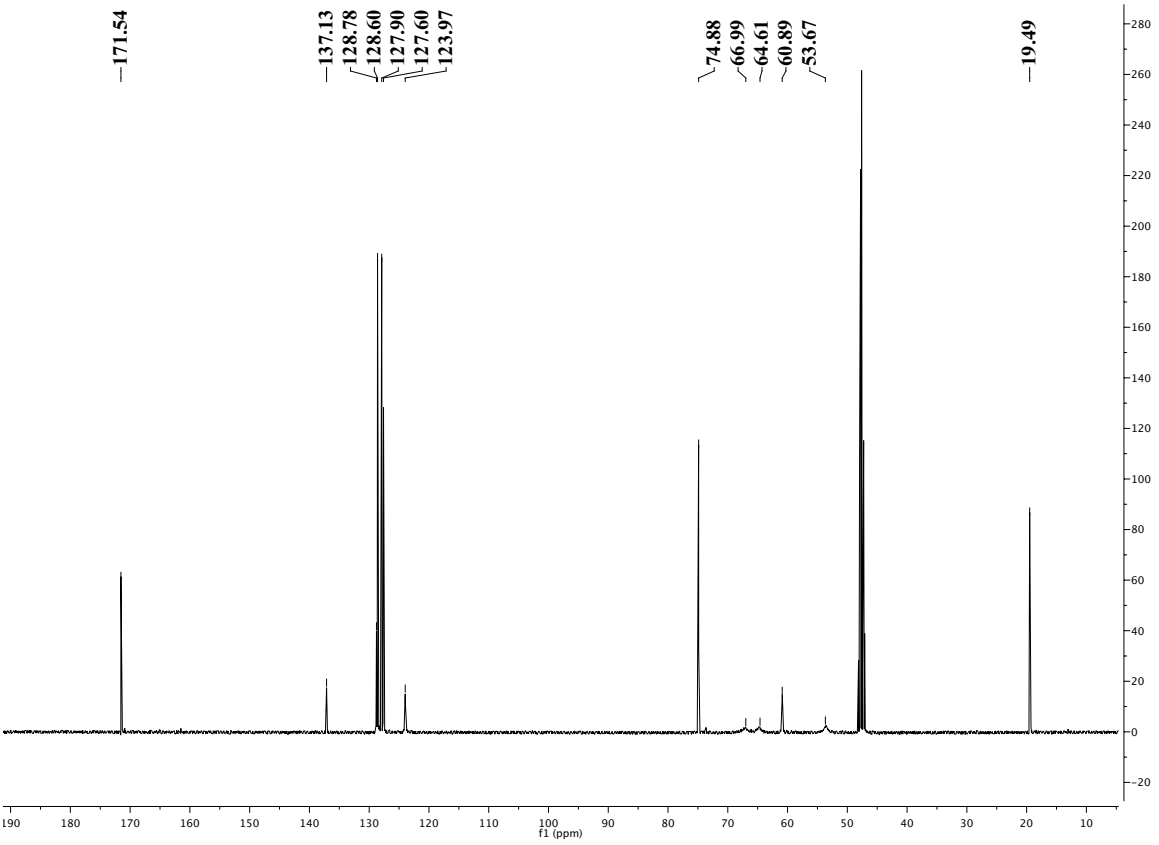

Figure A.1.84 ^{13}C NMR (121 MHz, CD_3OD) spectrum of **100**.

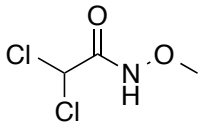

104

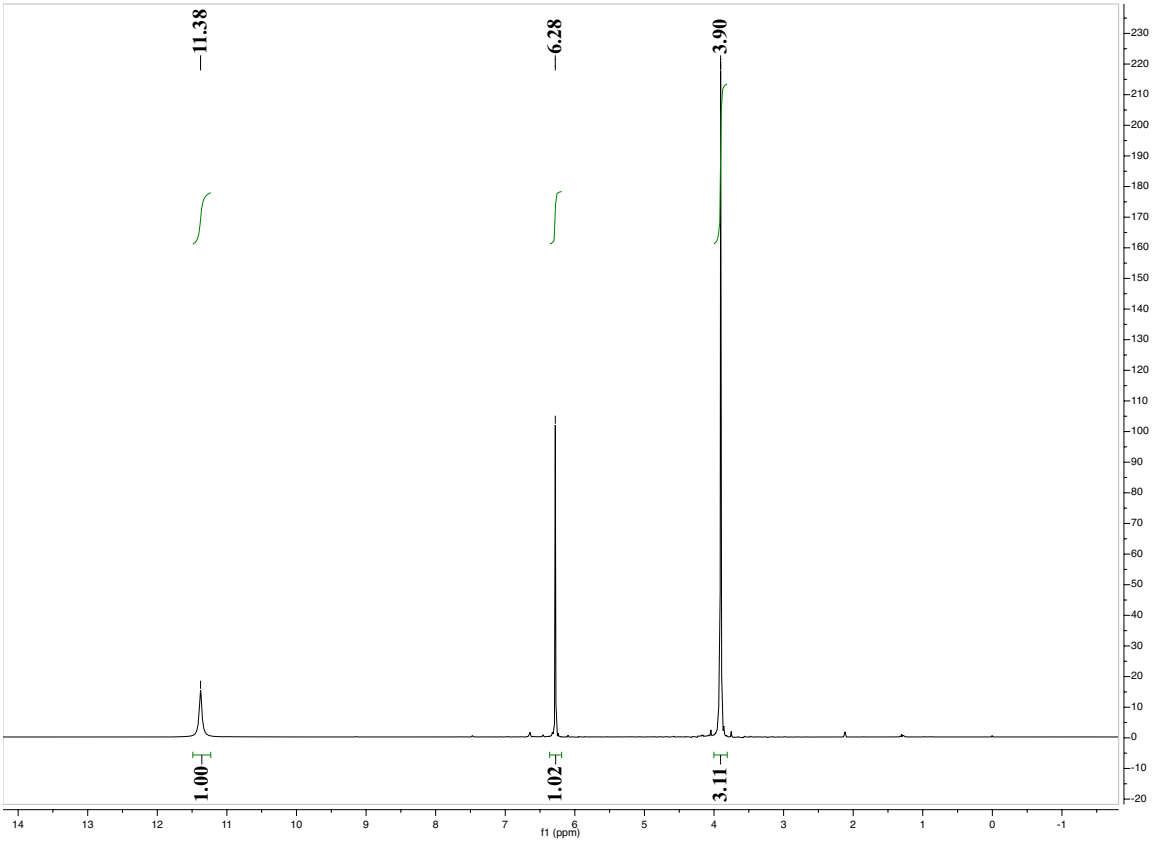

Figure A.1.85 ^{1}H NMR (500 MHz, $CDCl_3$) spectrum of **104**.

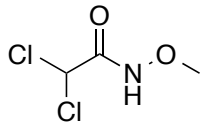

104

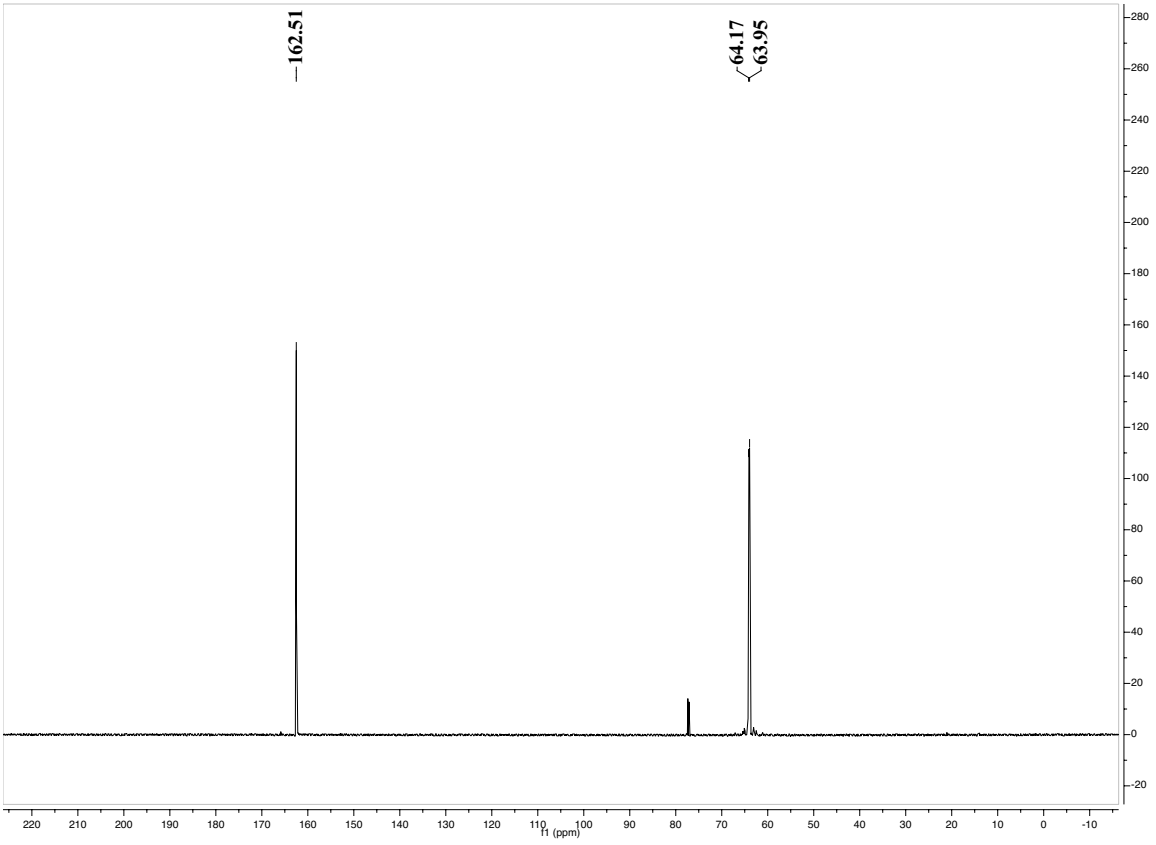

Figure A.1.86 ^{13}C NMR (121 MHz, $CDCl_3$) spectrum of **104**.

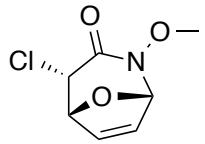

105

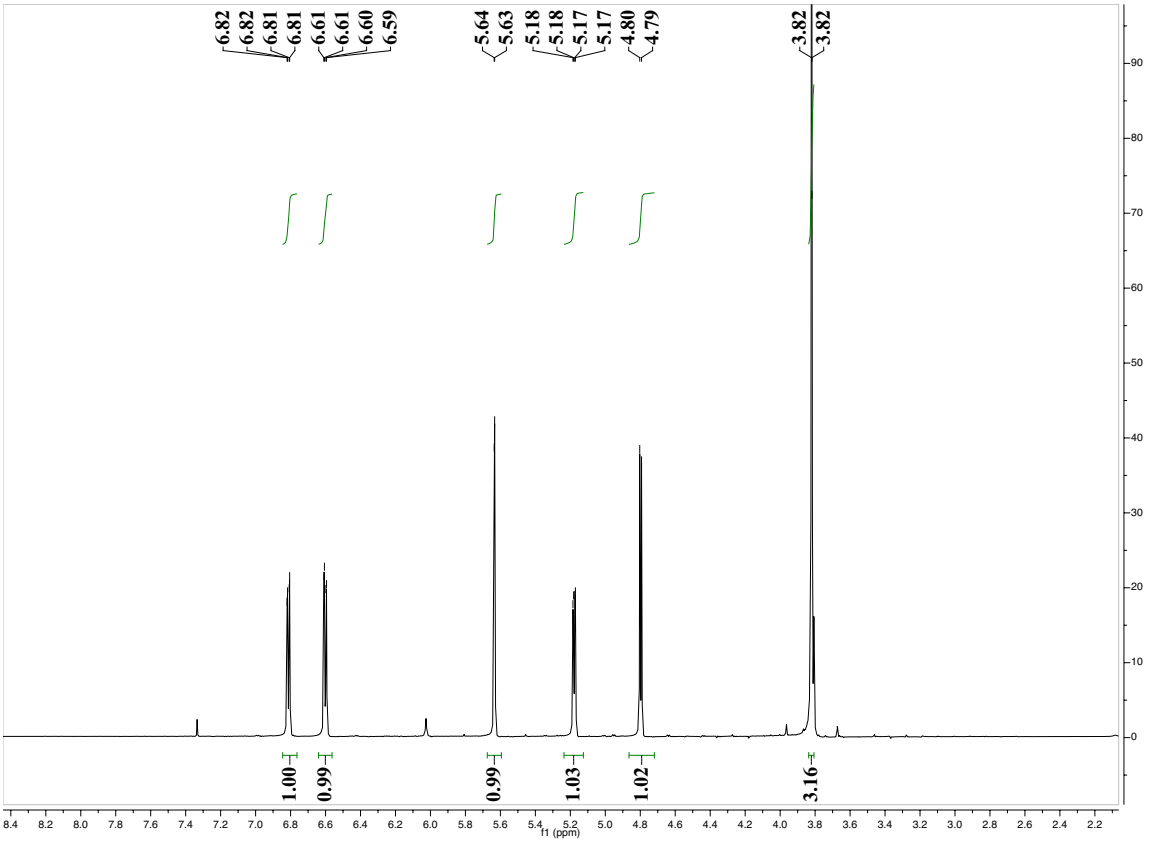

Figure A.1.87 ^{1}H NMR (500 MHz, $CDCl_3$) spectrum of **105**.

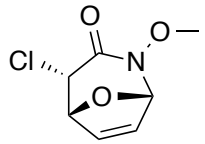

105

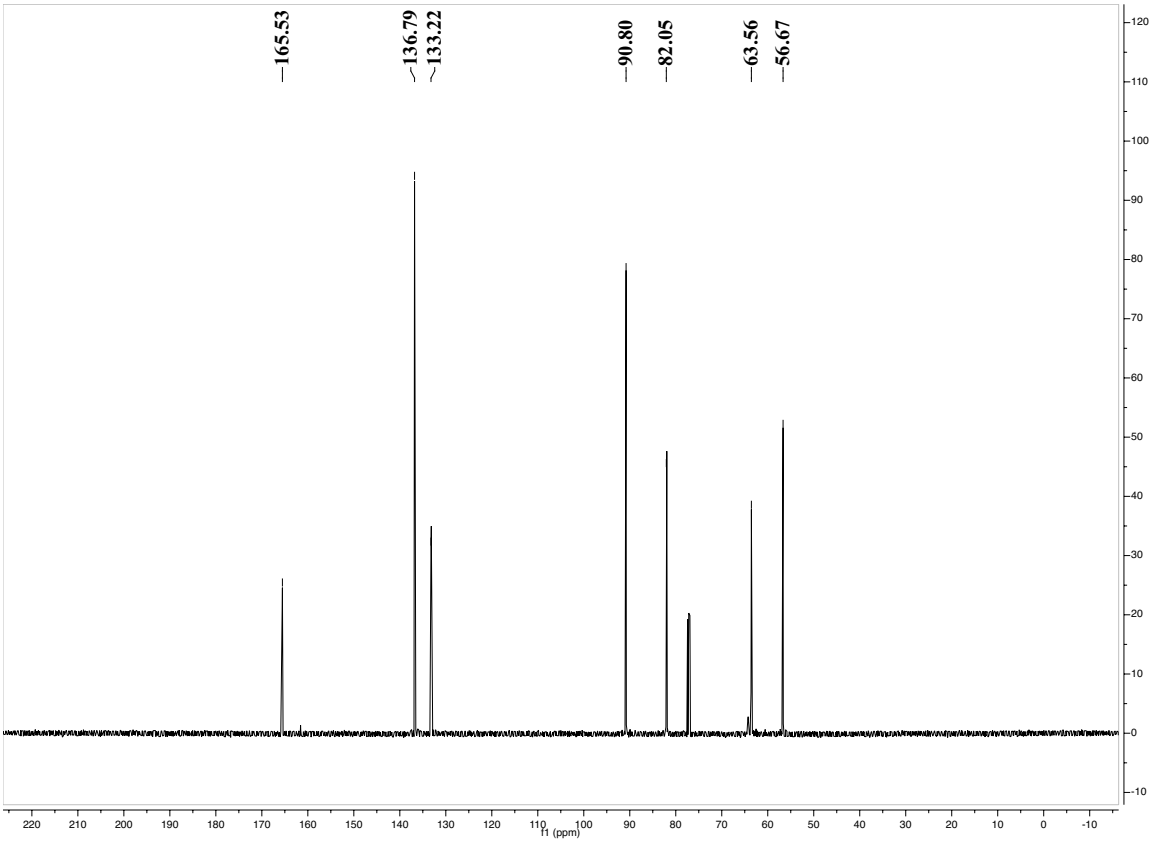

Figure A.1.88 ^{13}C NMR (121 MHz, $CDCl_3$) spectrum of **105**.

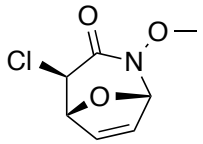

106

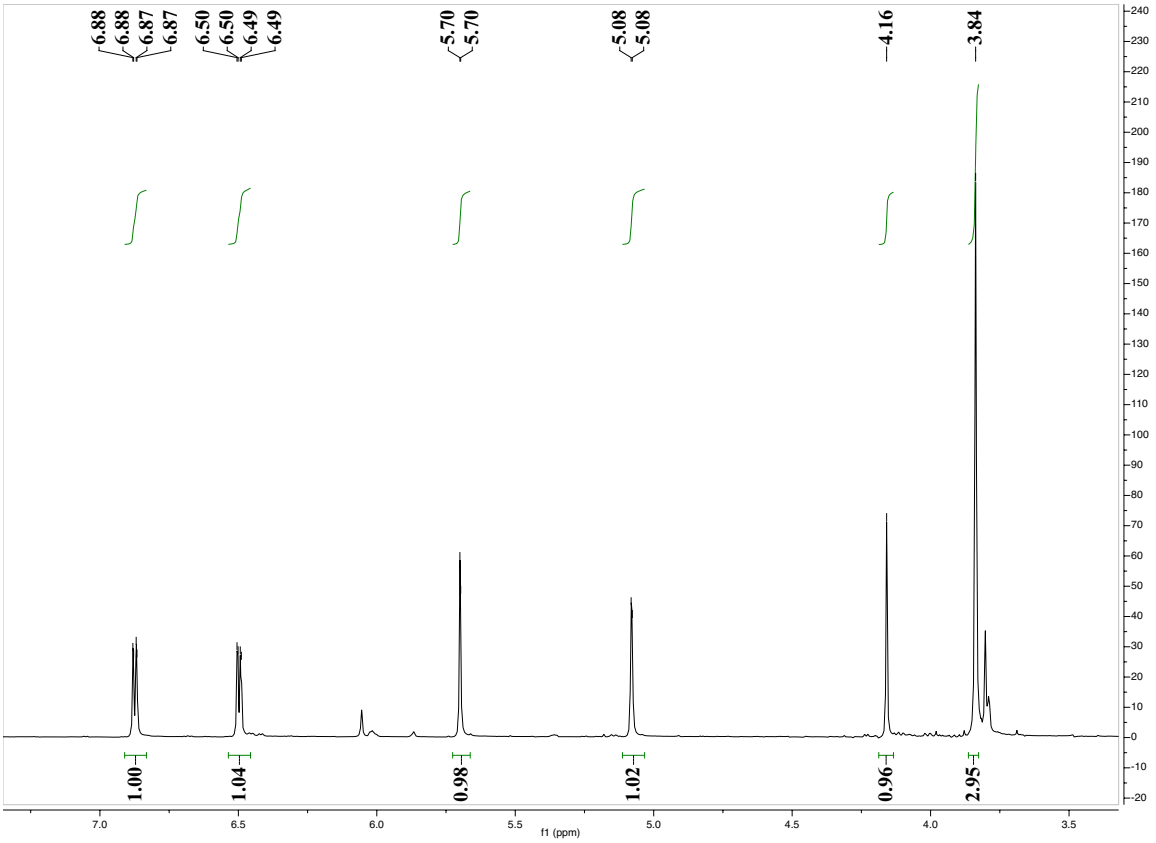

Figure A.1.89 ^{1}H NMR (500 MHz, $CDCl_3$) spectrum of **106**.

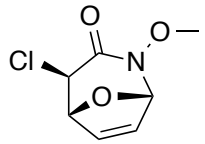

106

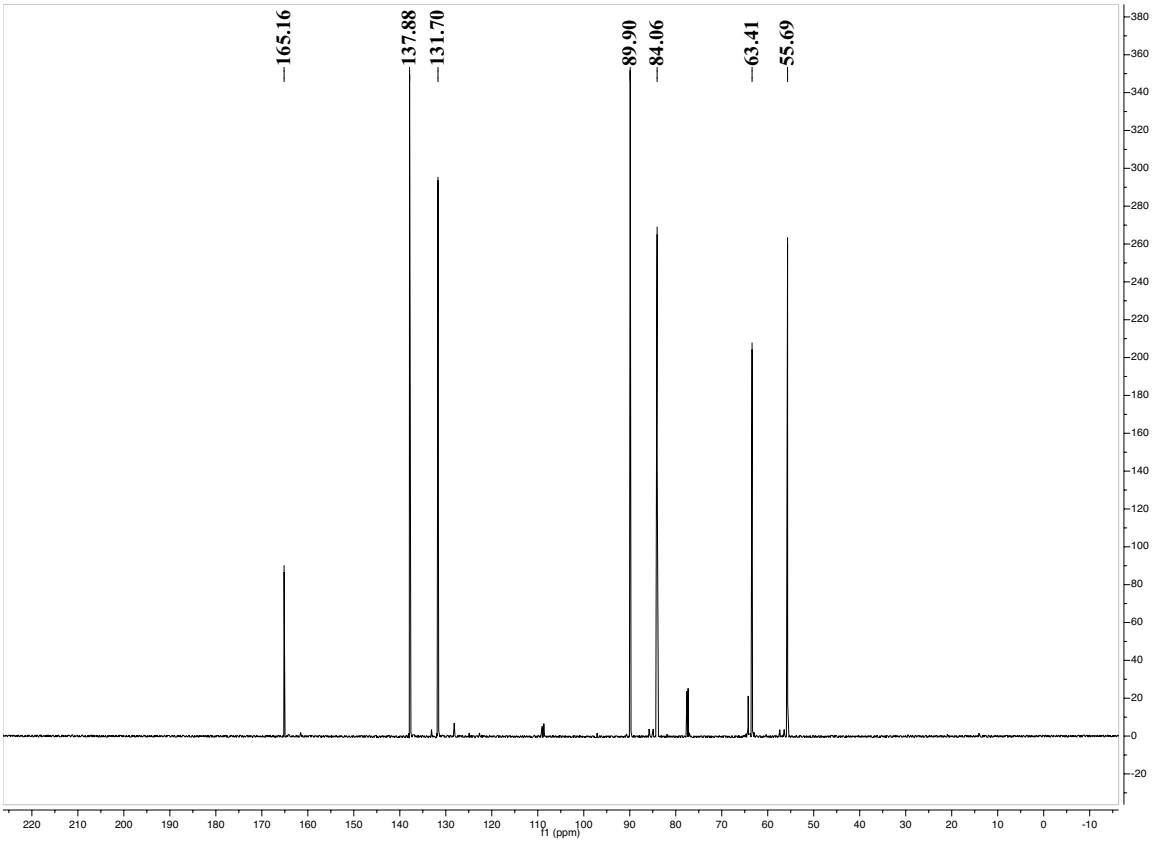

Figure A.1.90 ^{13}C NMR (121 MHz, $CDCl_3$) spectrum of **106**.

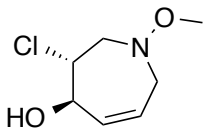

108

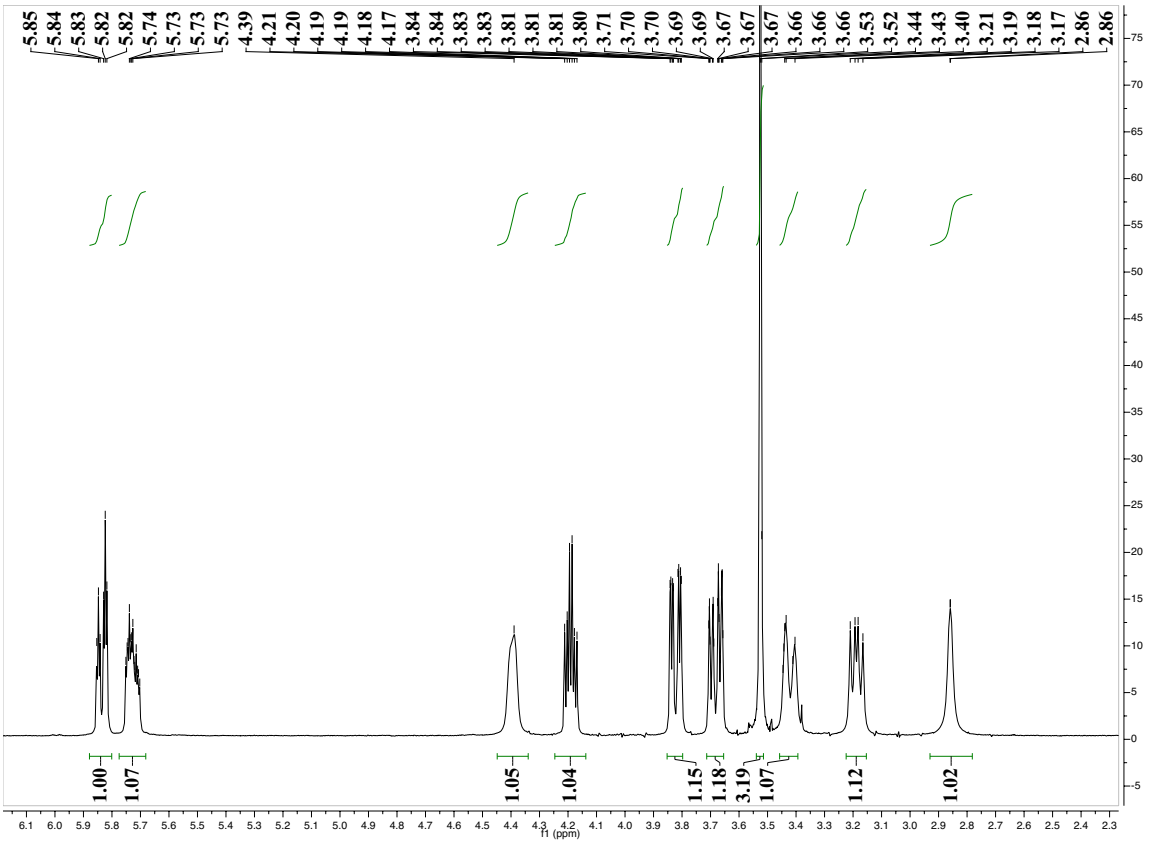

Figure A.1.91 ^{1}H NMR (500 MHz, $CDCl_3$) spectrum of **108**.

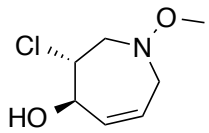

108

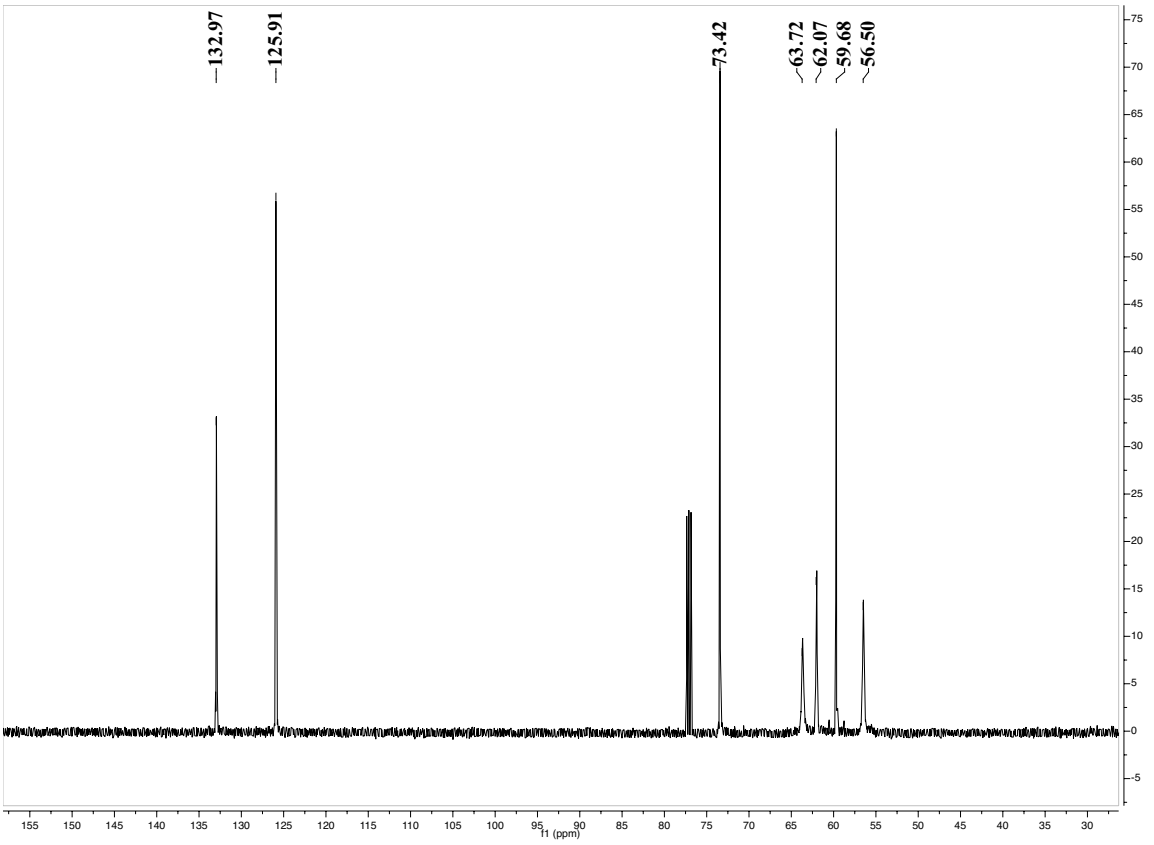

Figure A.1.92 ^{13}C NMR (121 MHz, $CDCl_3$) spectrum of **108**.

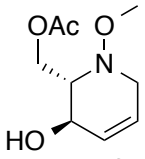

110

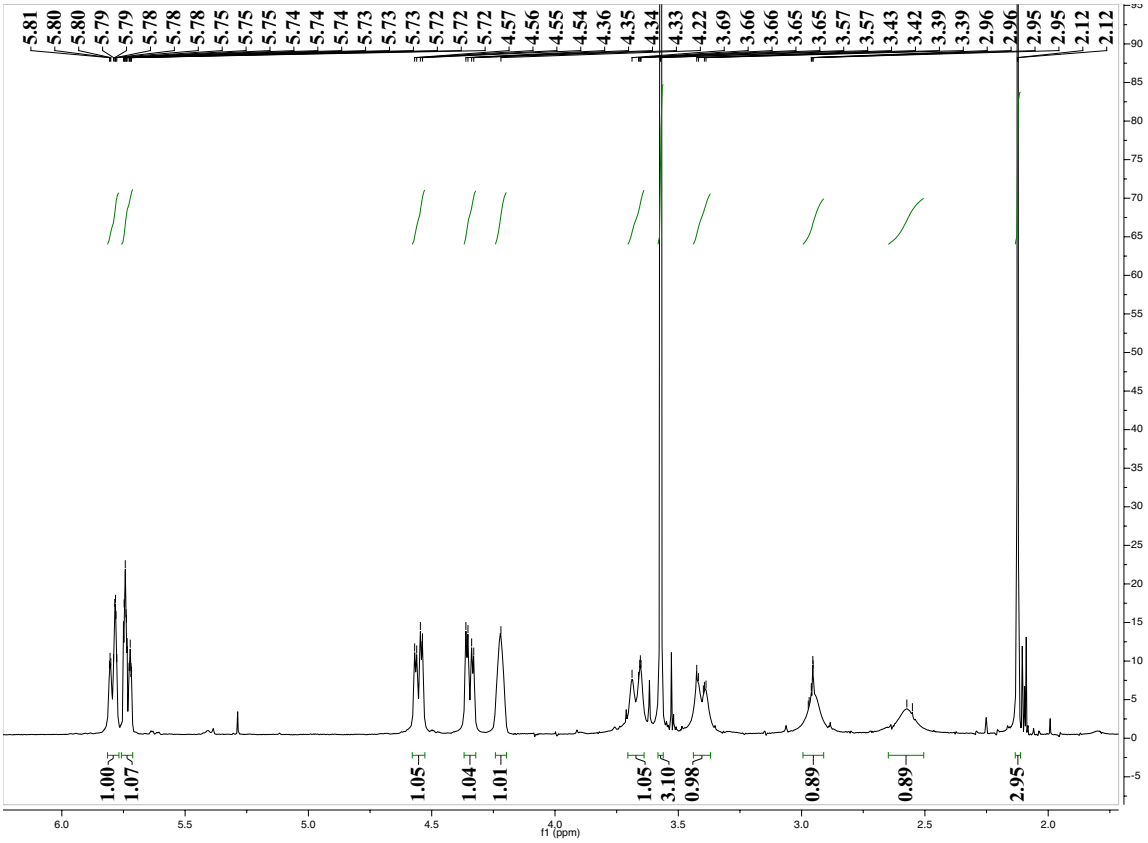

Figure A.1.93 ^{1}H NMR (500 MHz, CD_3OD) spectrum of **110**.

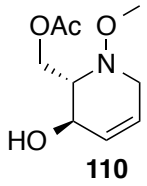

110

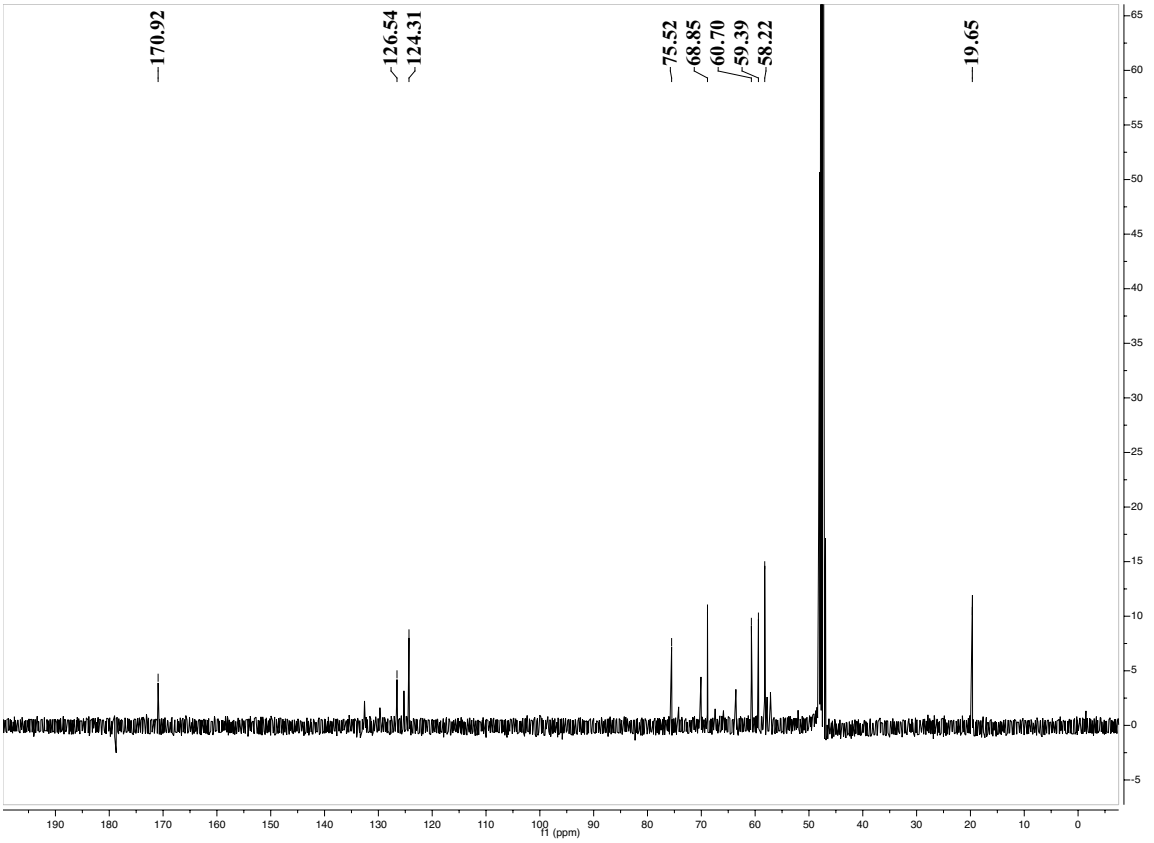

Figure A.1.94 ^{13}C NMR (121 MHz, CD_3OD) spectrum of **110**.

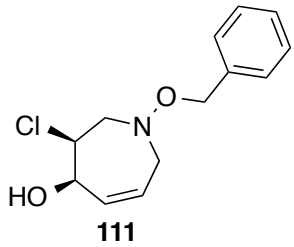

111

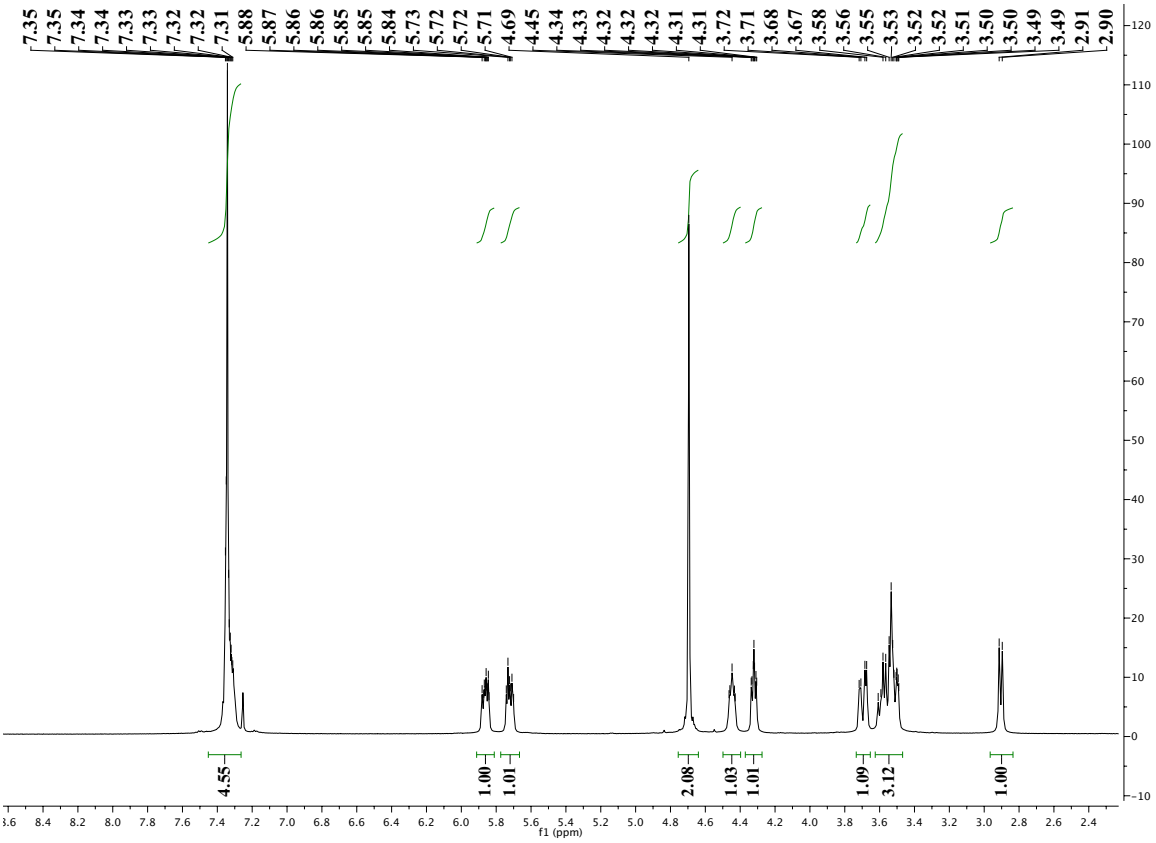

Figure A.1.95 ^{1}H NMR (500 MHz, $CDCl_3$) spectrum of **111**.

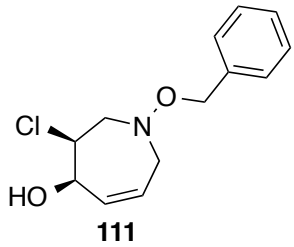

111

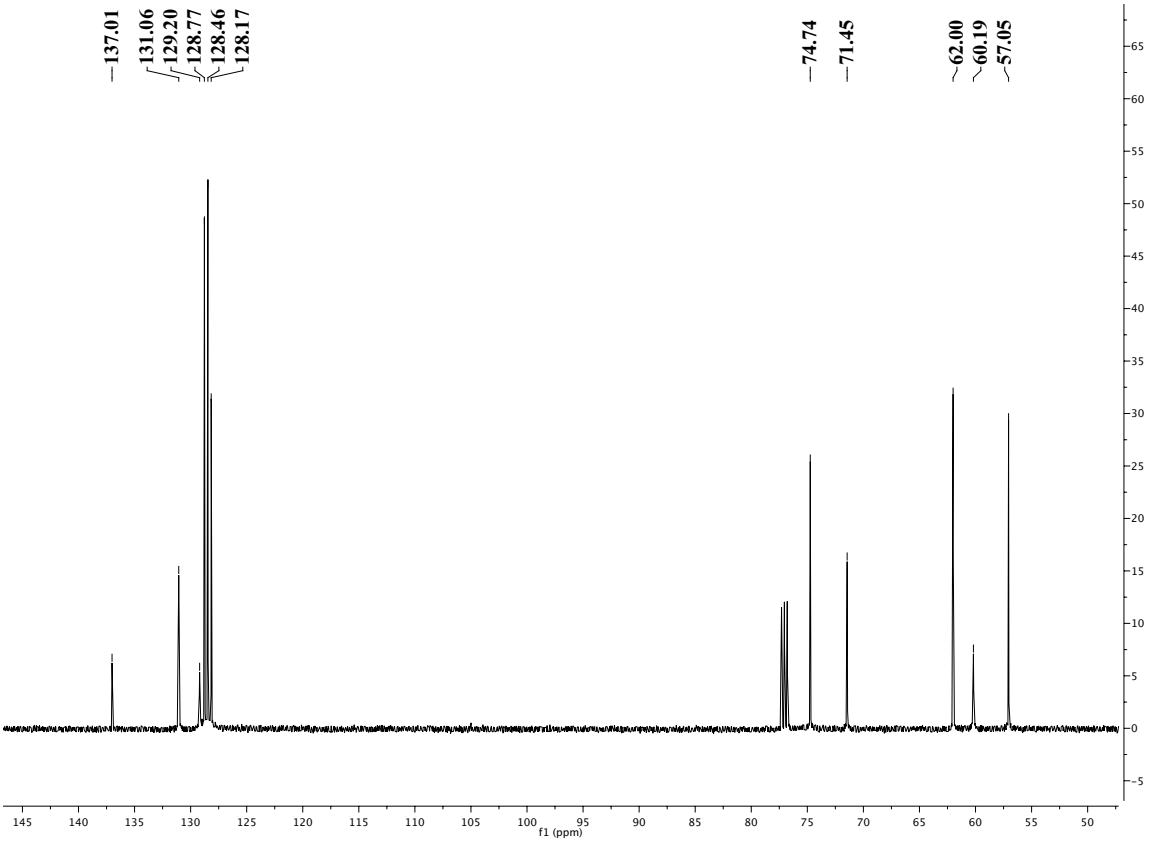

Figure A.1.96 ^{13}C NMR (121 MHz, $CDCl_3$) spectrum of **111**.

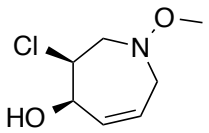

112

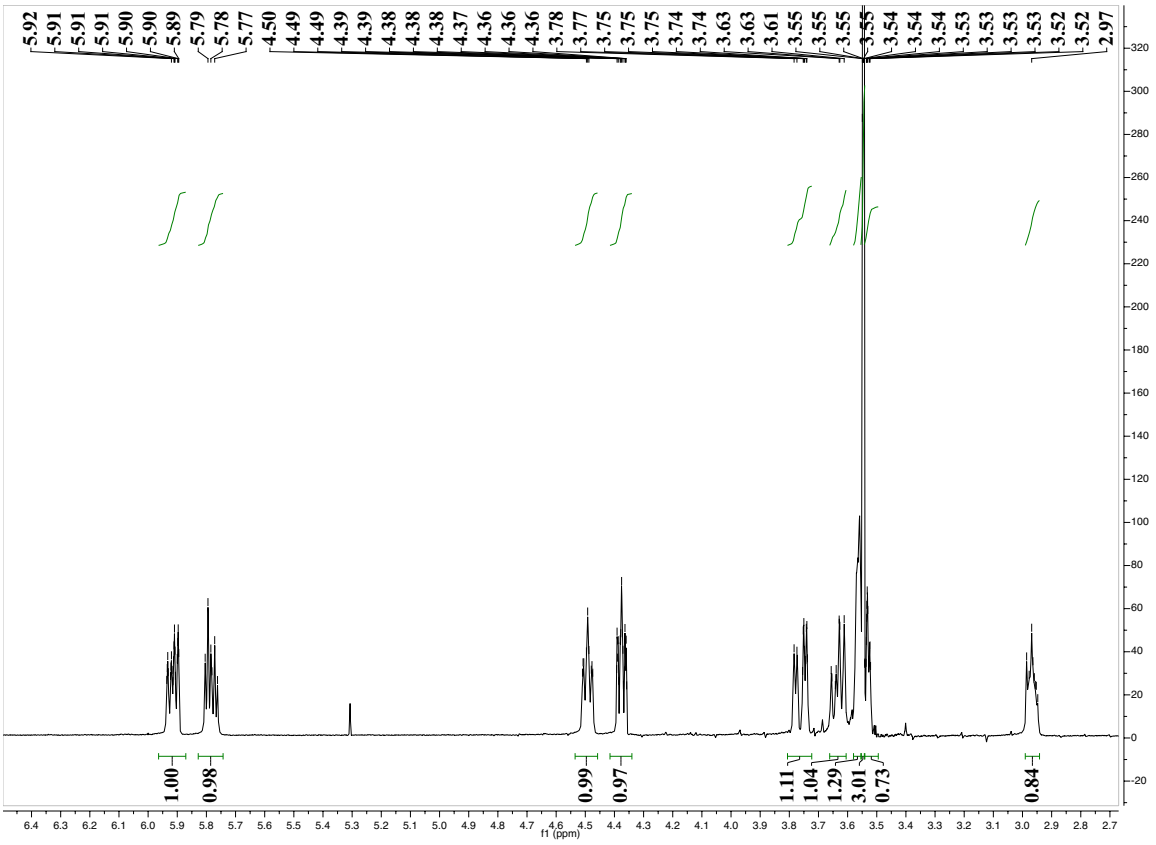

Figure A.1.97 ^{1}H NMR (500 MHz, $CDCl_3$) spectrum of **112**.

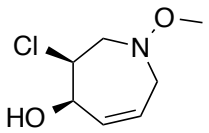

112

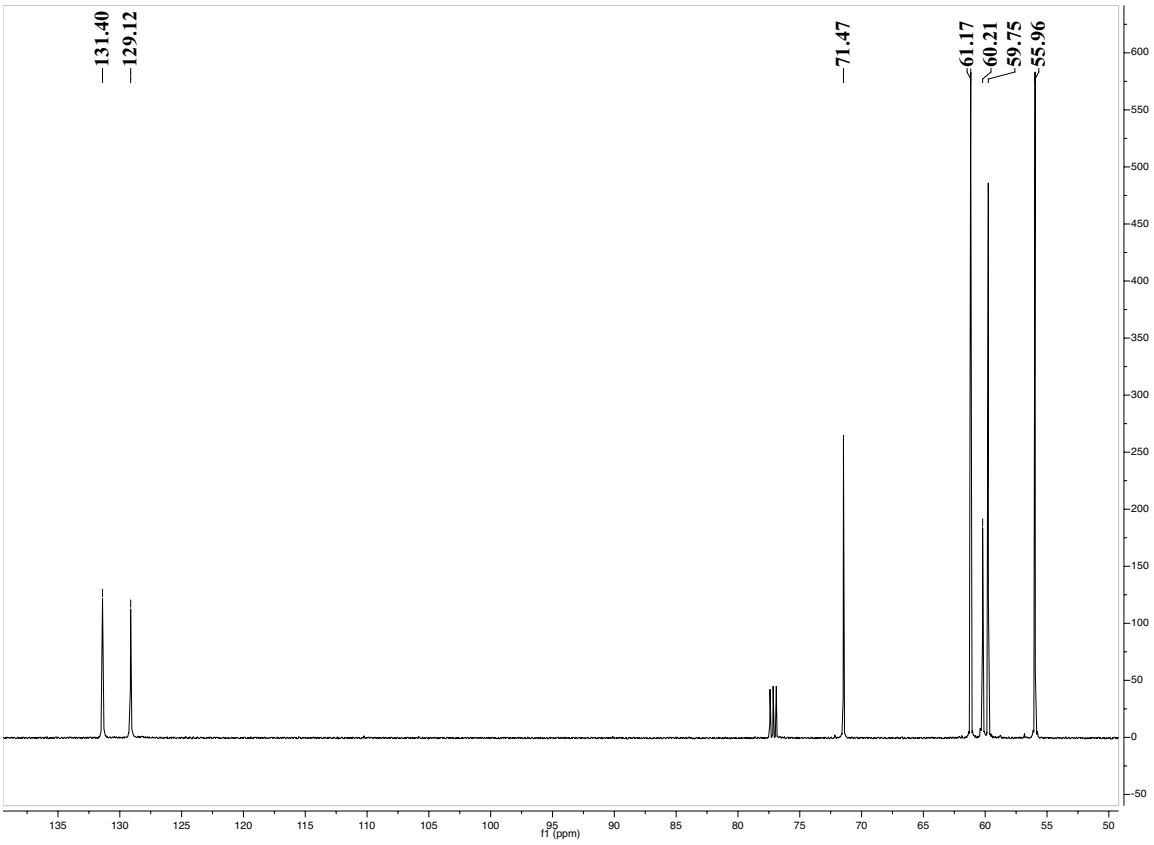

Figure A.1.98 ^{13}C NMR (121 MHz, $CDCl_3$) spectrum of **112**.

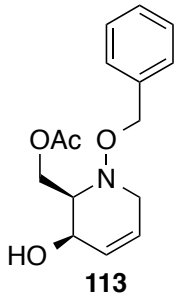

113

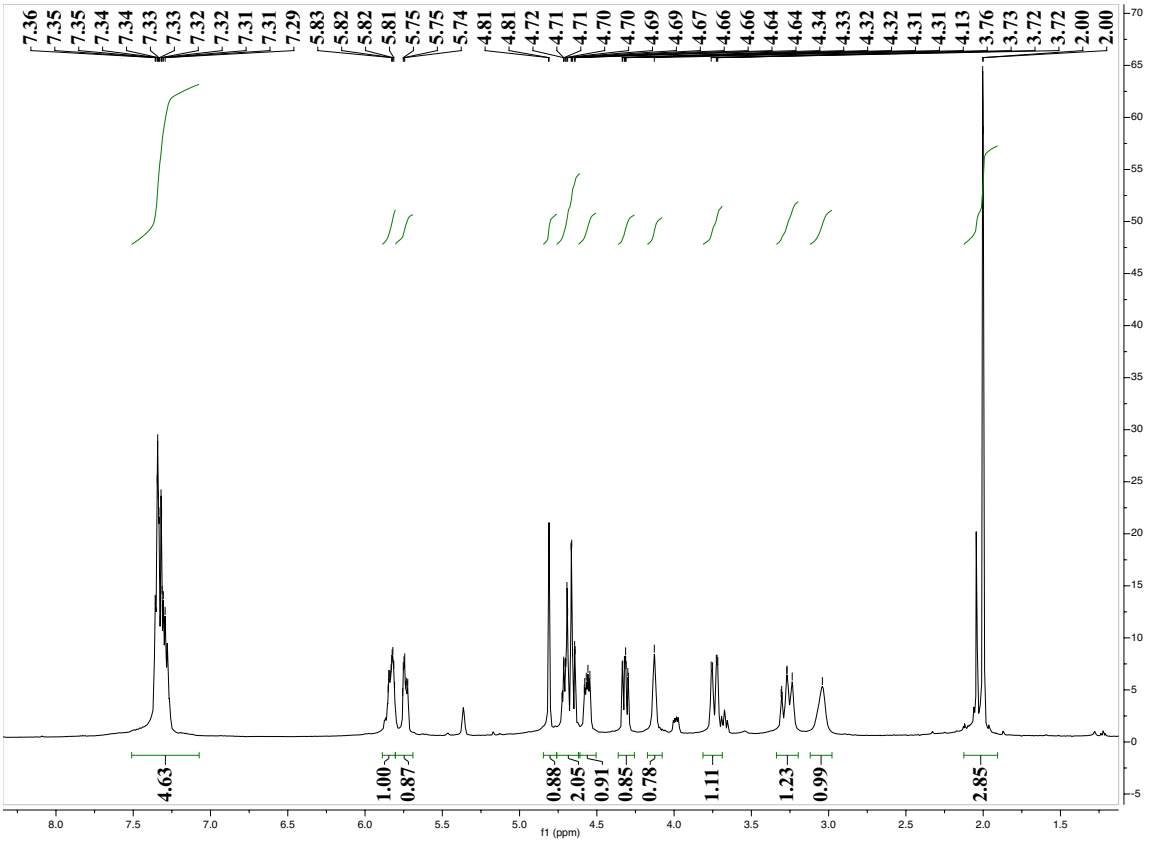

Figure A.1.99 ^{1}H NMR (500 MHz, CD_3OD) spectrum of **113**.

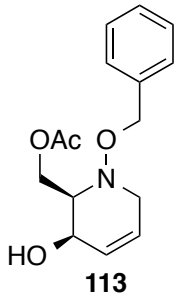

113

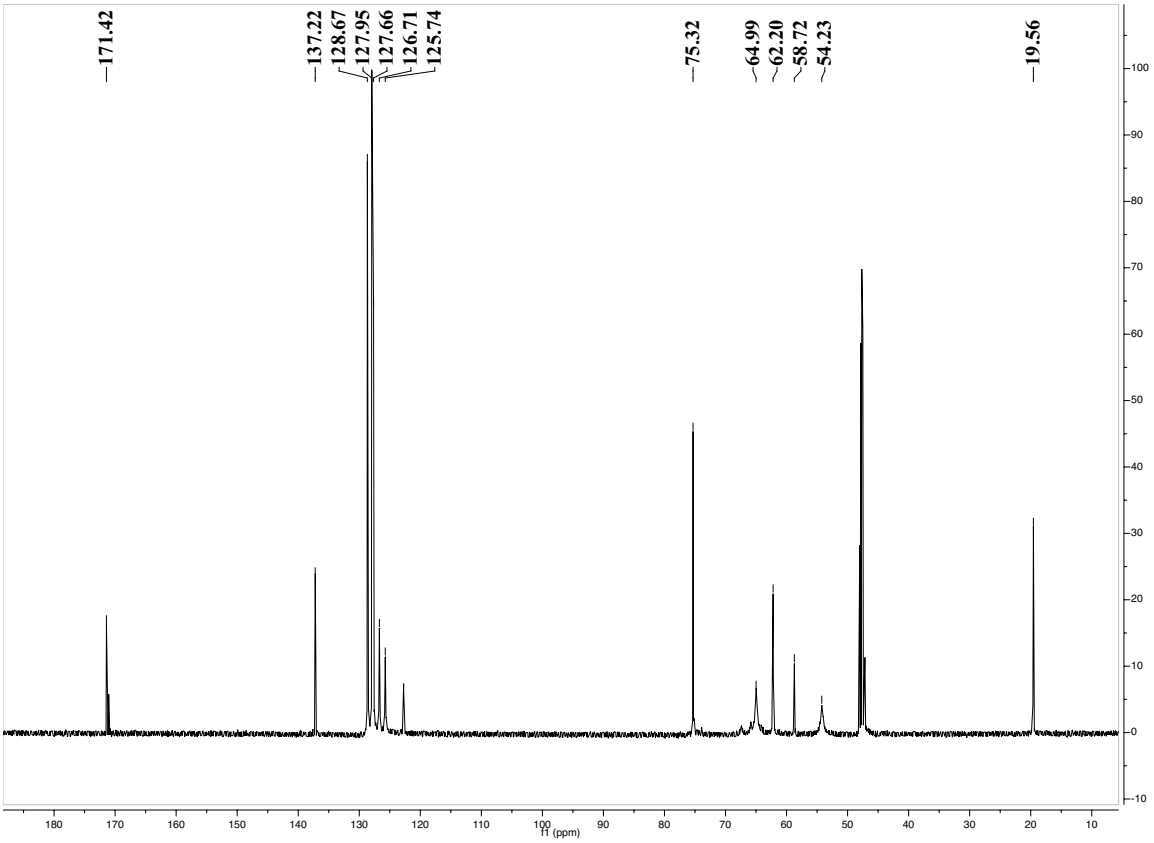

Figure A.1.100 ^{13}C NMR (121 MHz, CD_3OD) spectrum of **113**.

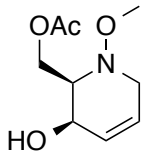

114

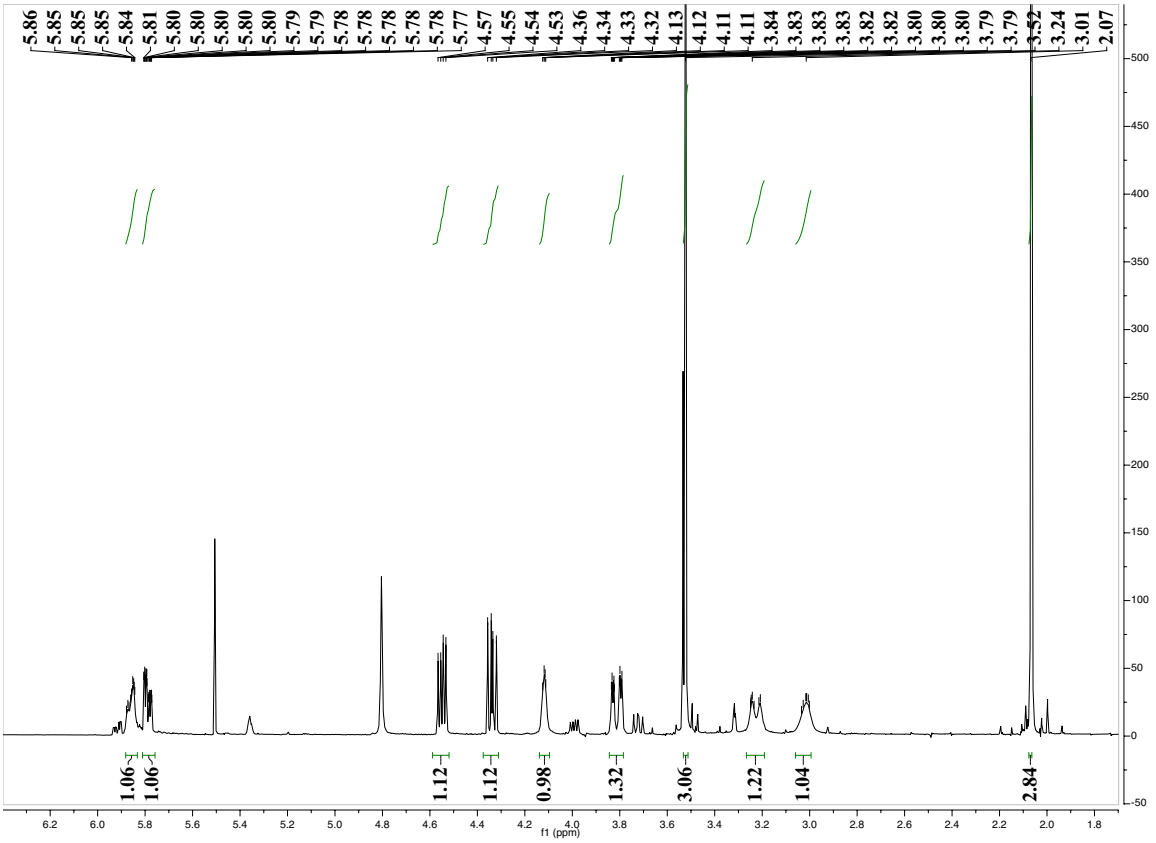

Figure A.1.101 ^{1}H NMR (500 MHz, CD_3OD) spectrum of **114**.

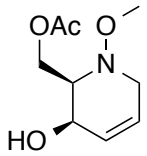

114

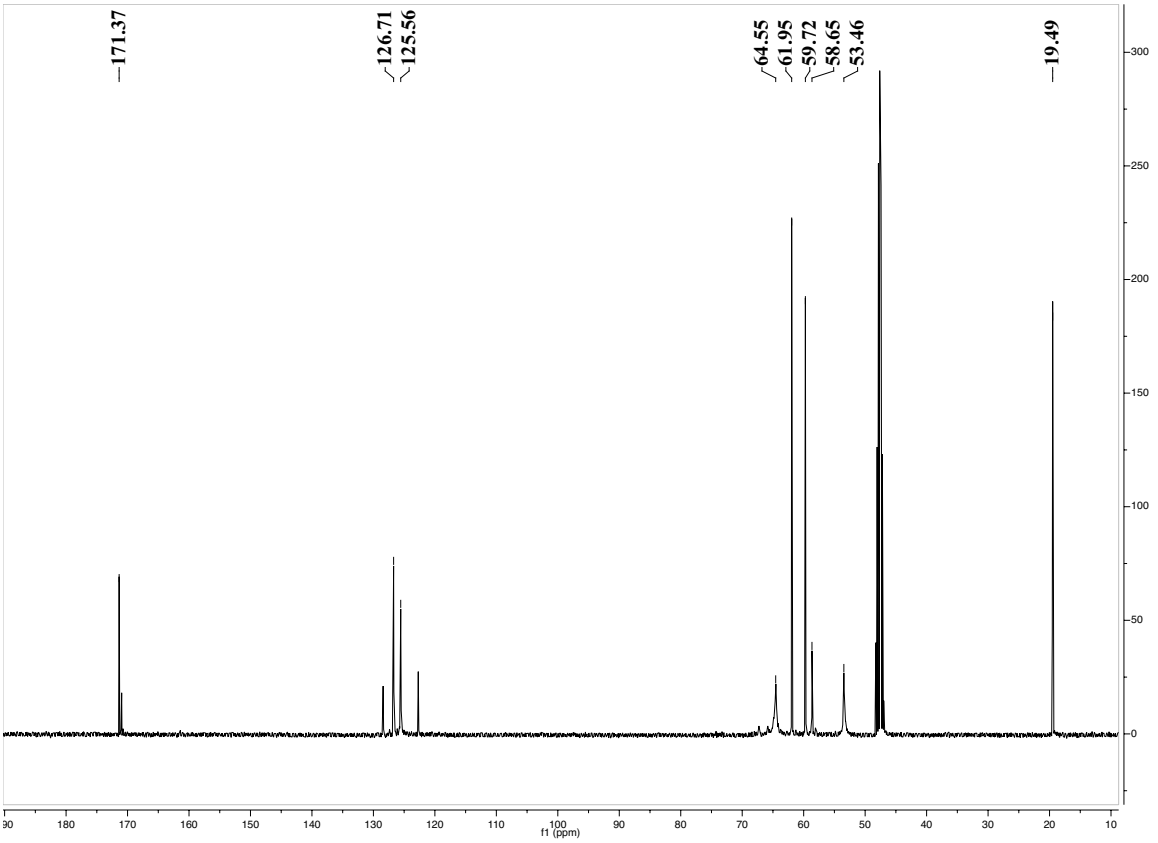

Figure A.1.102 ^{13}C NMR (121 MHz, CD_3OD) spectrum of **114**.

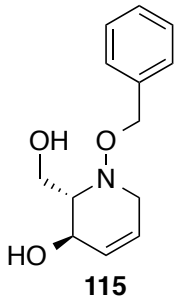

115

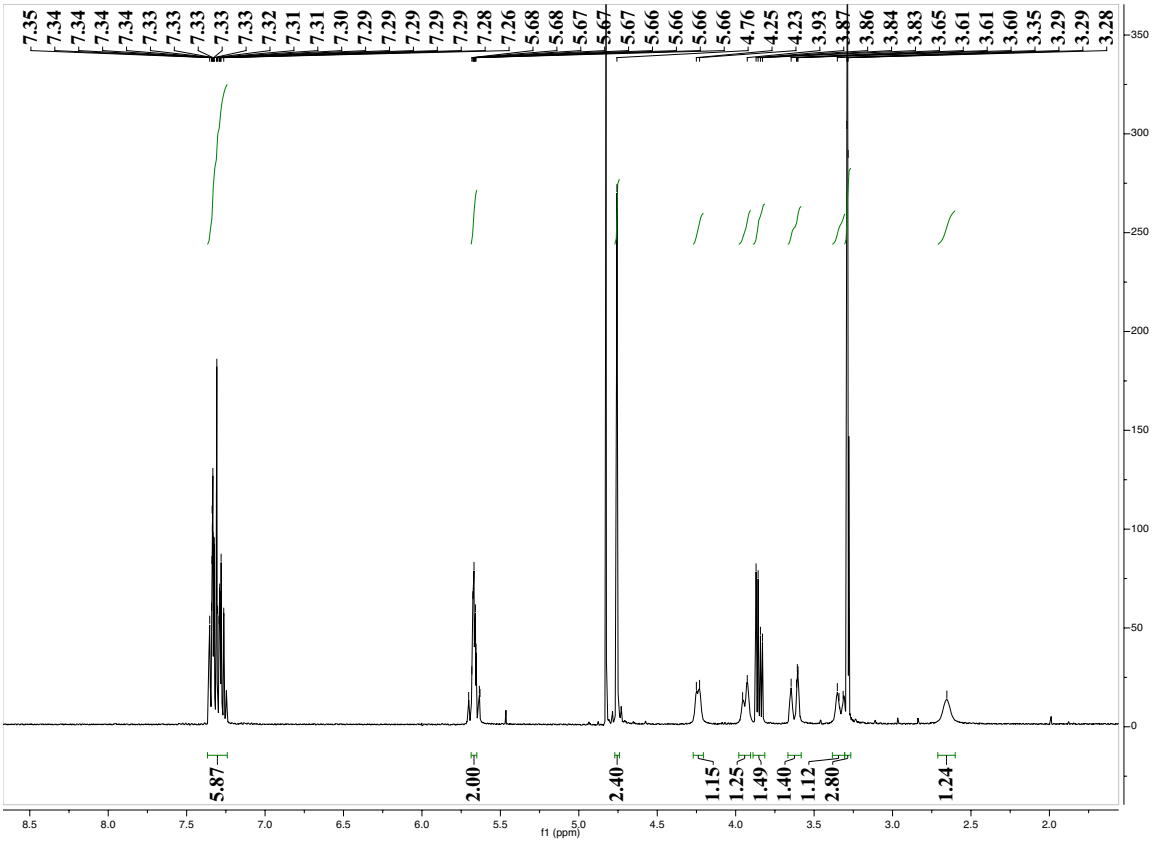

Figure A.1.103 ^{1}H NMR (500 MHz, CD_3OD) spectrum of **115**.

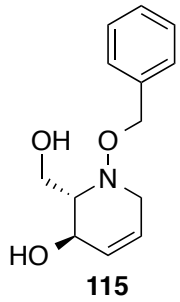

115

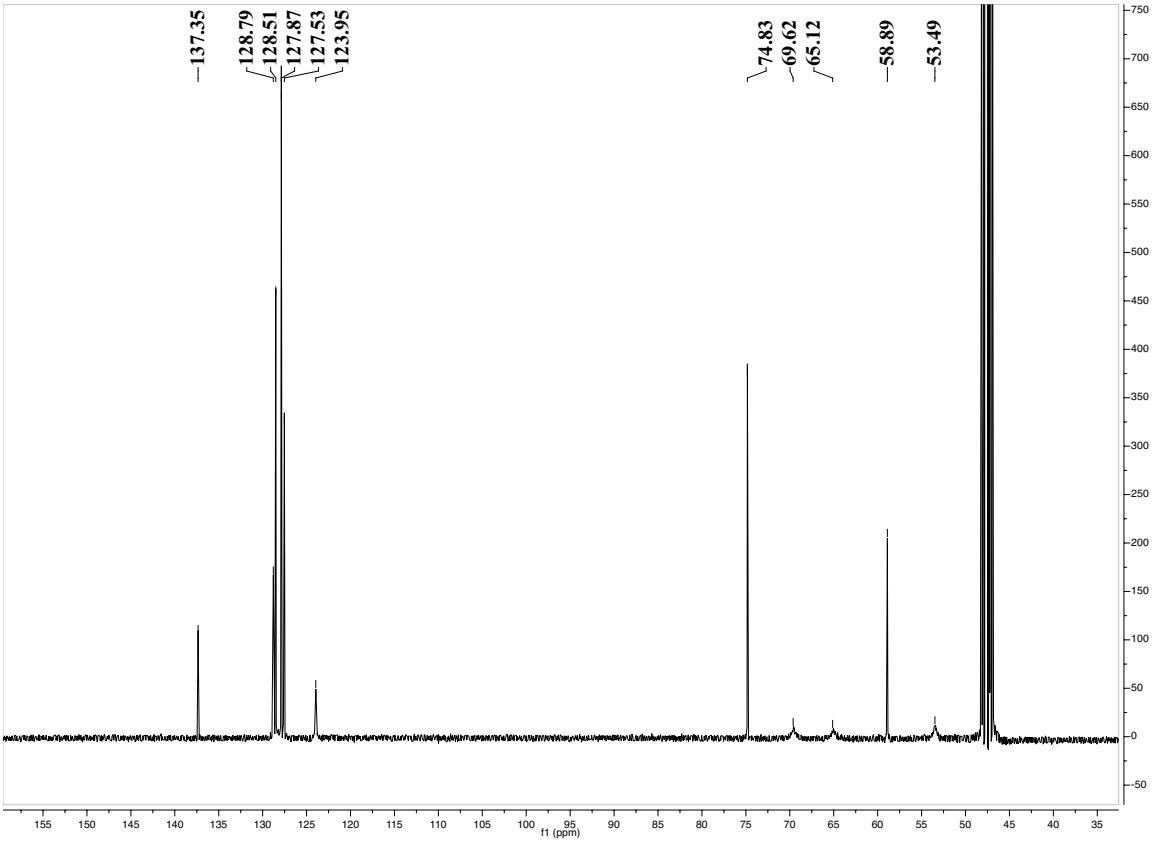

Figure A.1.104 ^{13}C NMR (121 MHz, CD_3OD) spectrum of **115**.

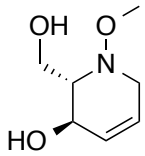

116

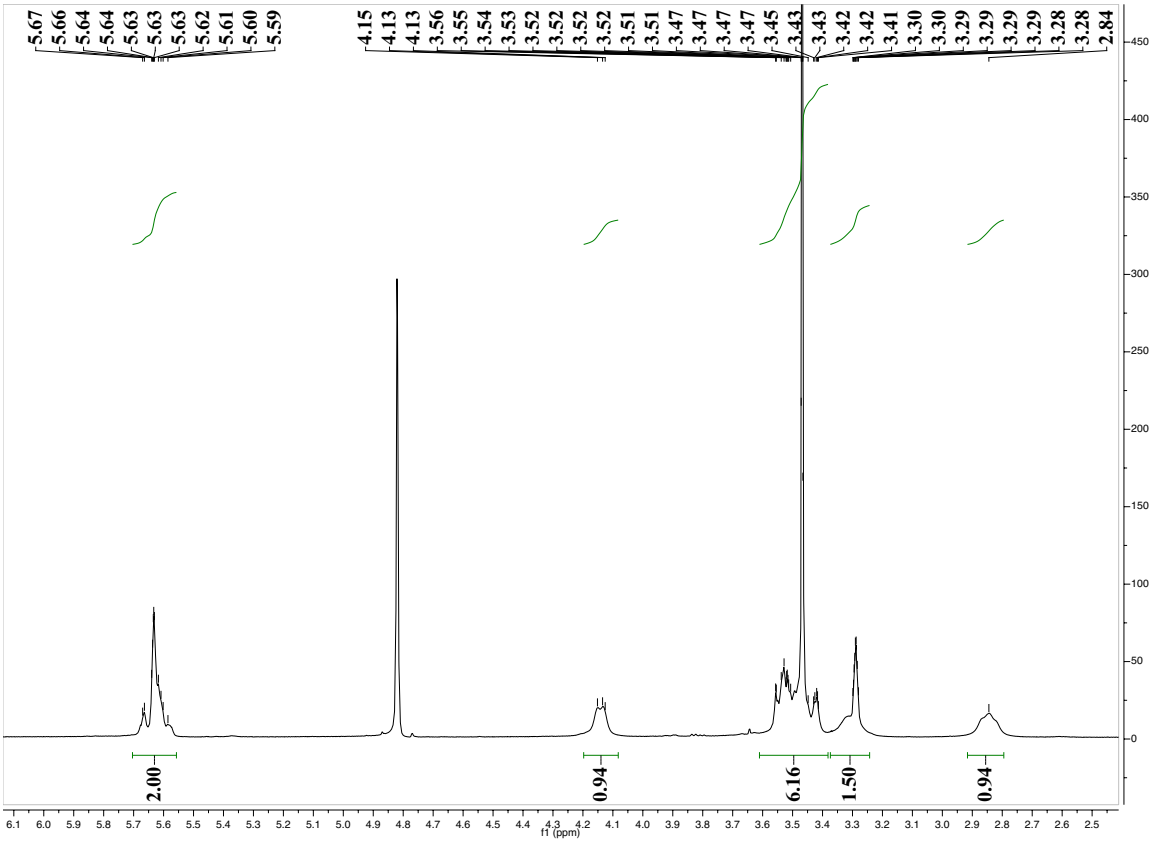

Figure A.1.105 ^{1}H NMR (500 MHz, CD_3OD) spectrum of **116**.

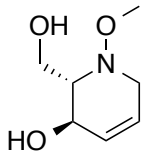

116

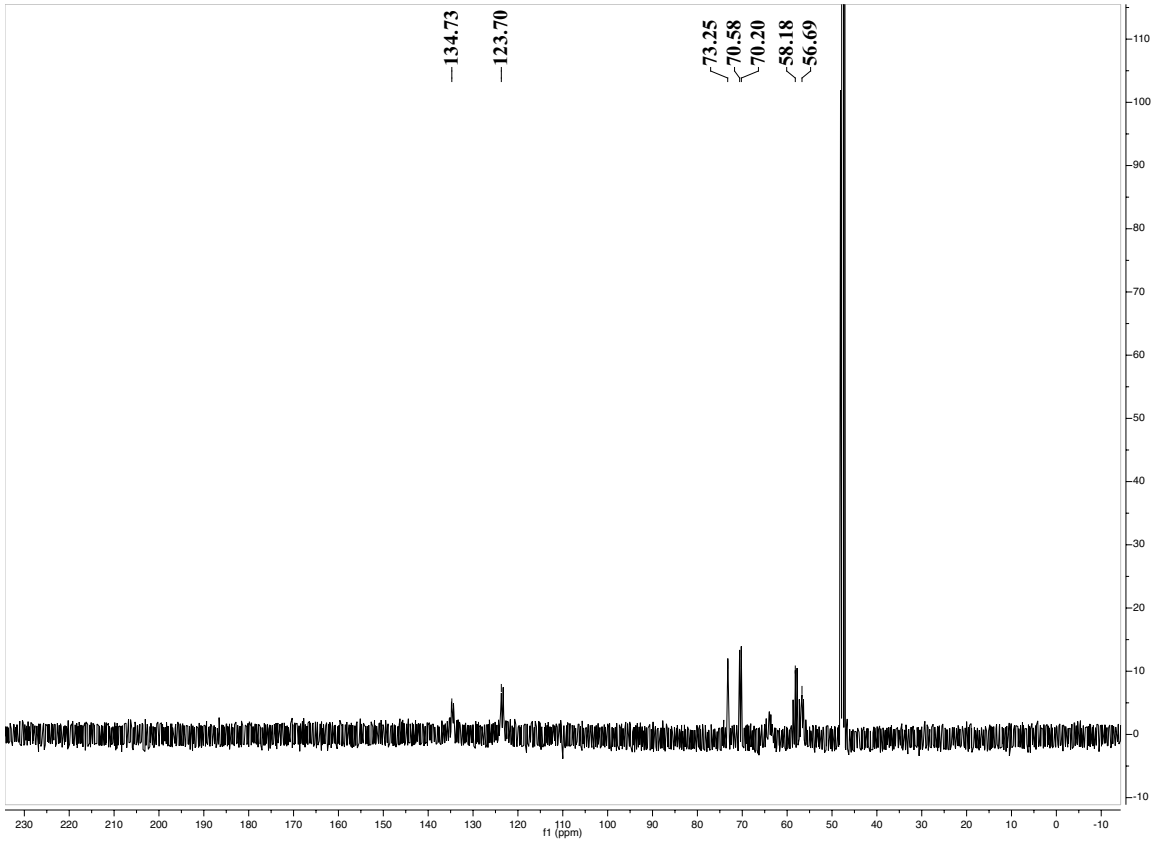

Figure A.1.106 ^{13}C NMR (121 MHz, CD_3OD) spectrum of **116**.

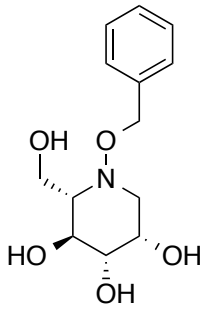

117

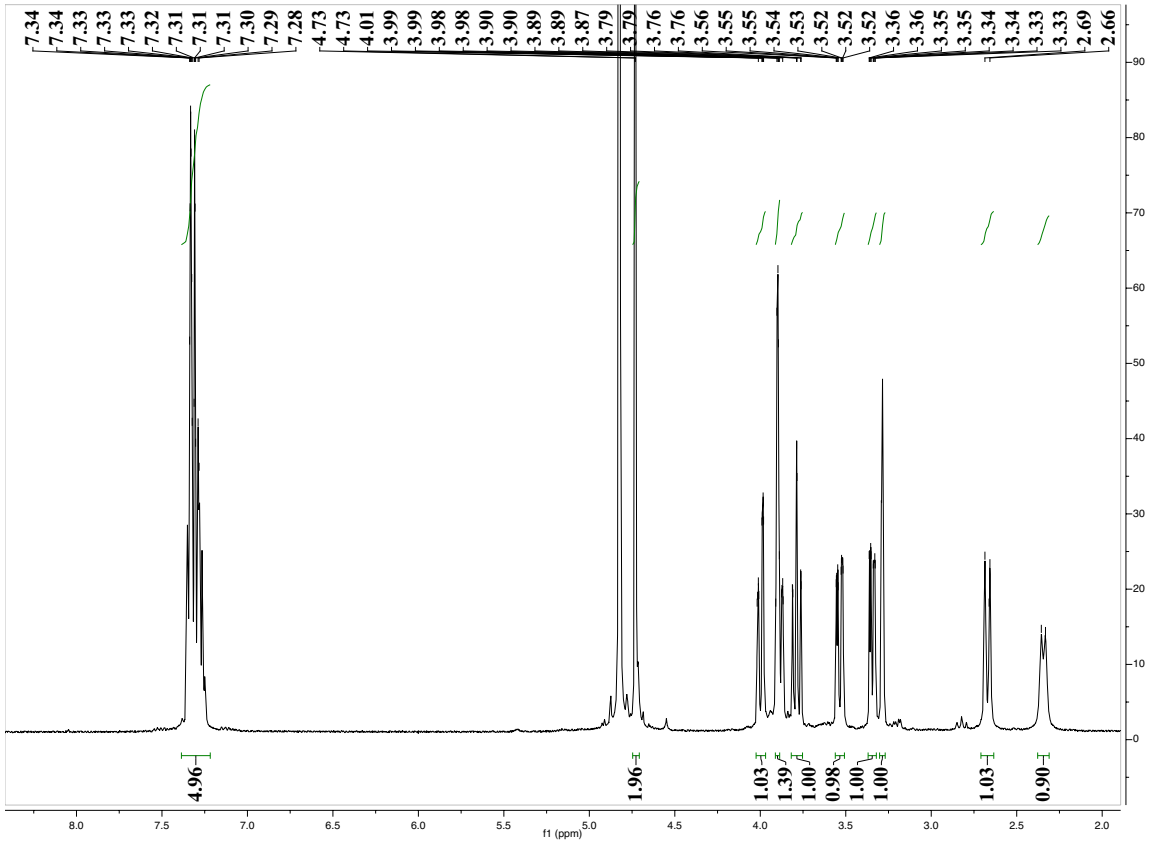

Figure A.1.107 ^{1}H NMR (500 MHz, CD_3OD) spectrum of **117**.

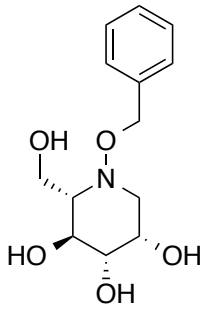

117

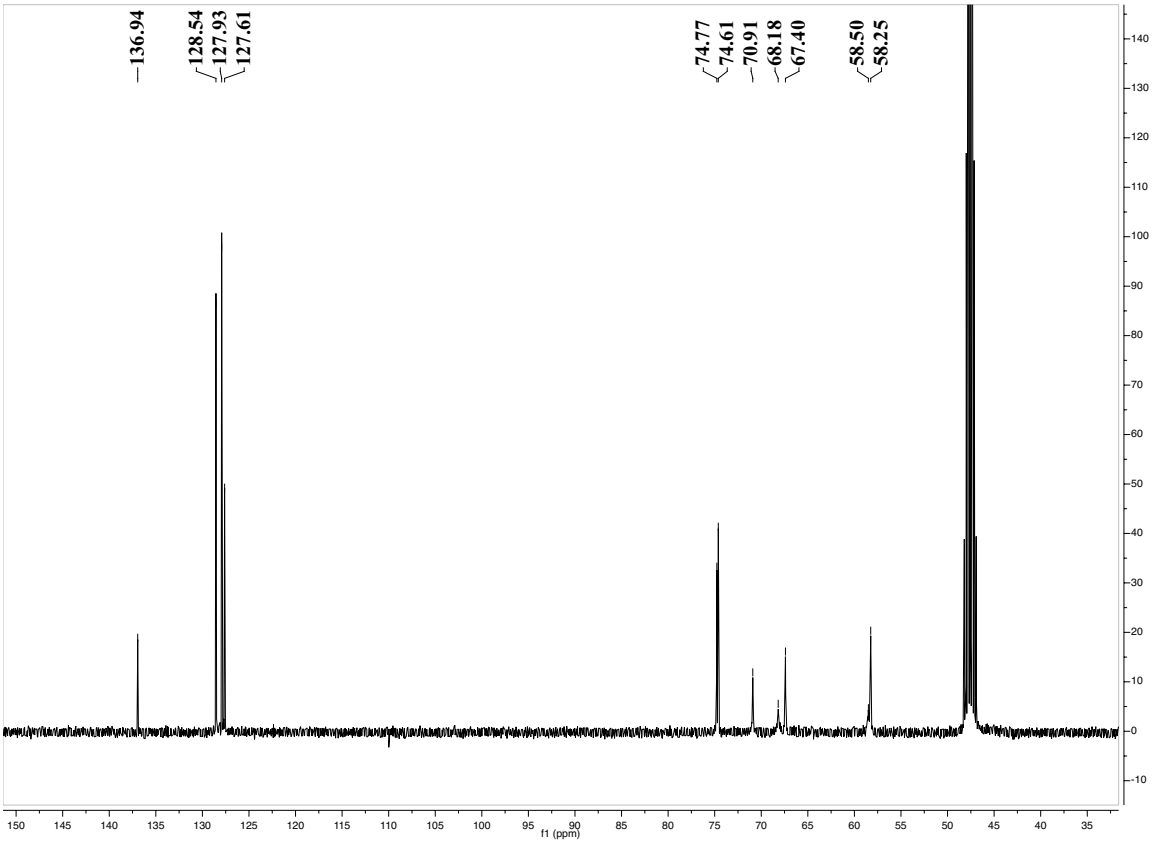

Figure A.1.108 ^{13}C NMR (121 MHz, CD_3OD) spectrum of **117**.

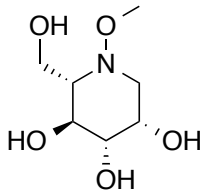

118

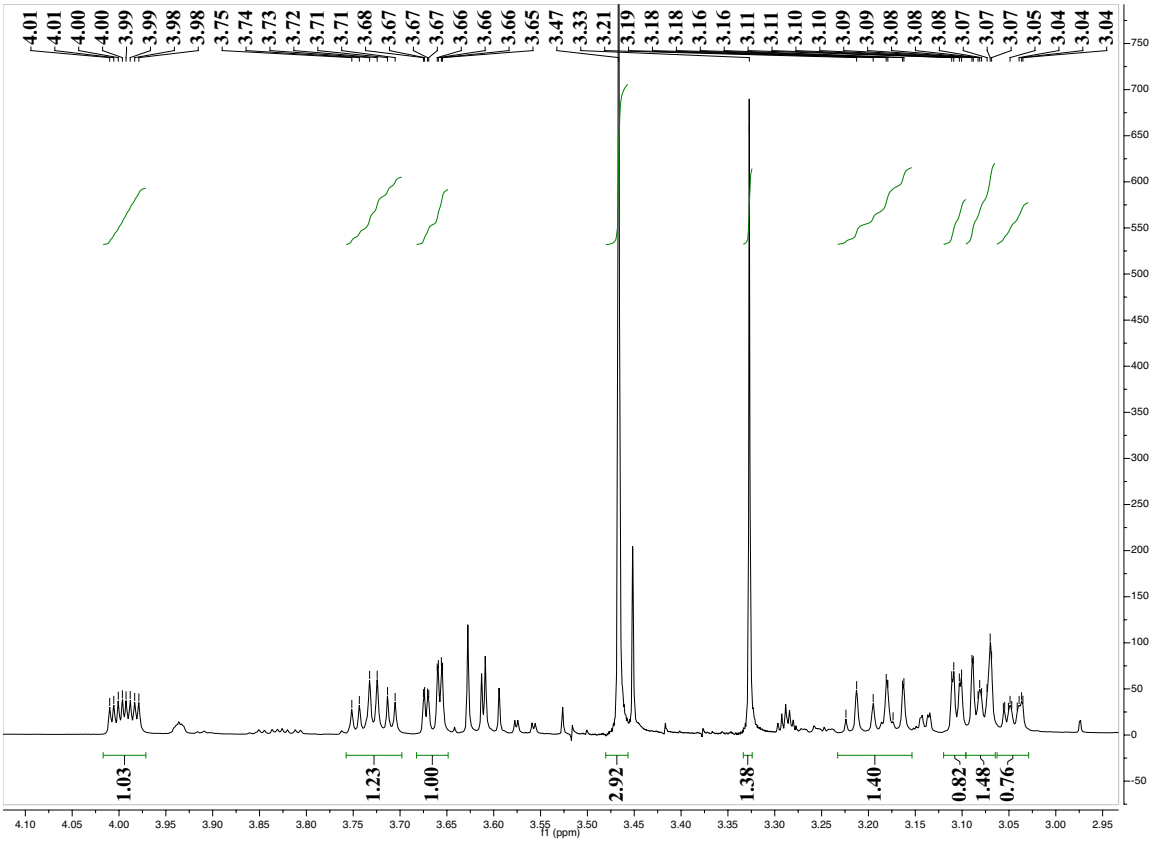

Figure A.1.109 ^{1}H NMR (500 MHz, CD_3OD) spectrum of **118**.

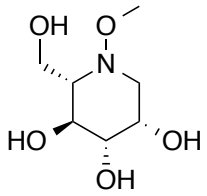

118

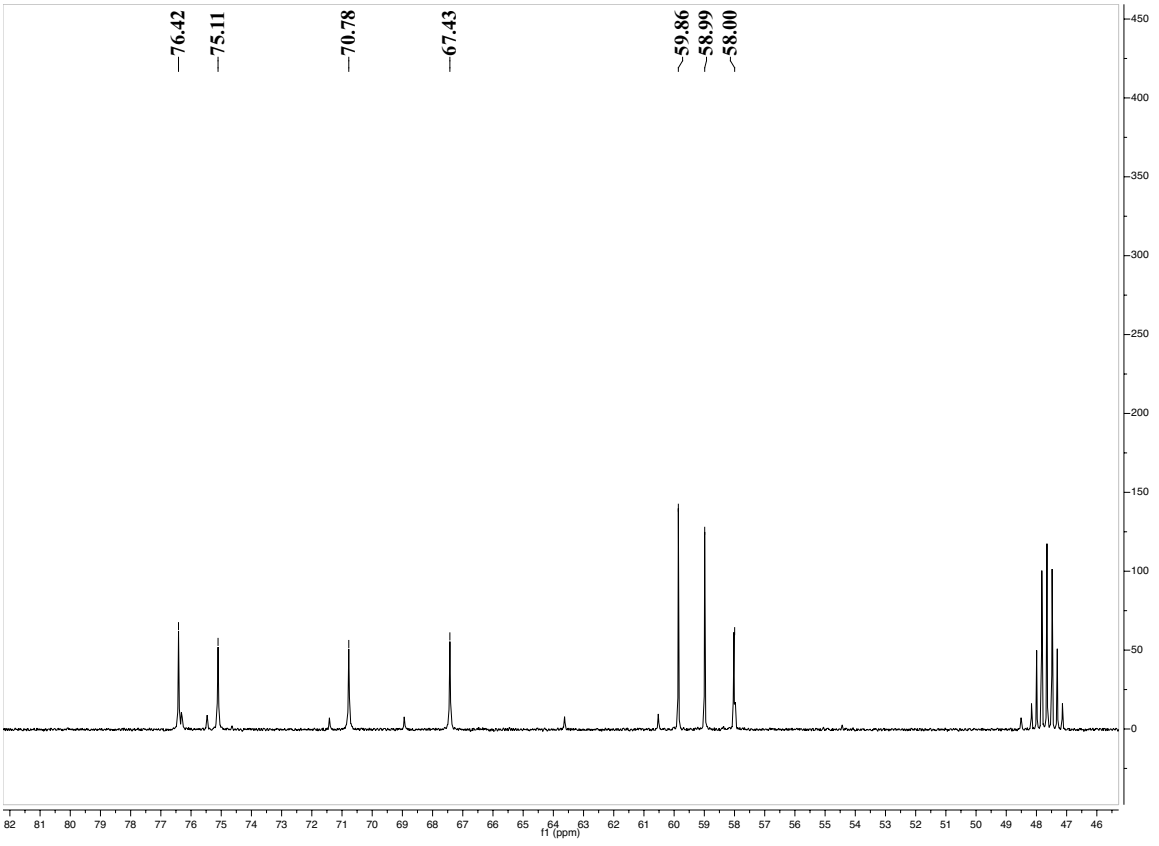

Figure A.1.110 ^{13}C NMR (121 MHz, CD_3OD) spectrum of **118**.

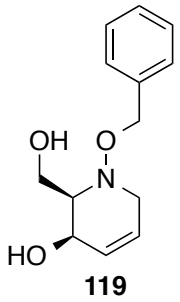

119

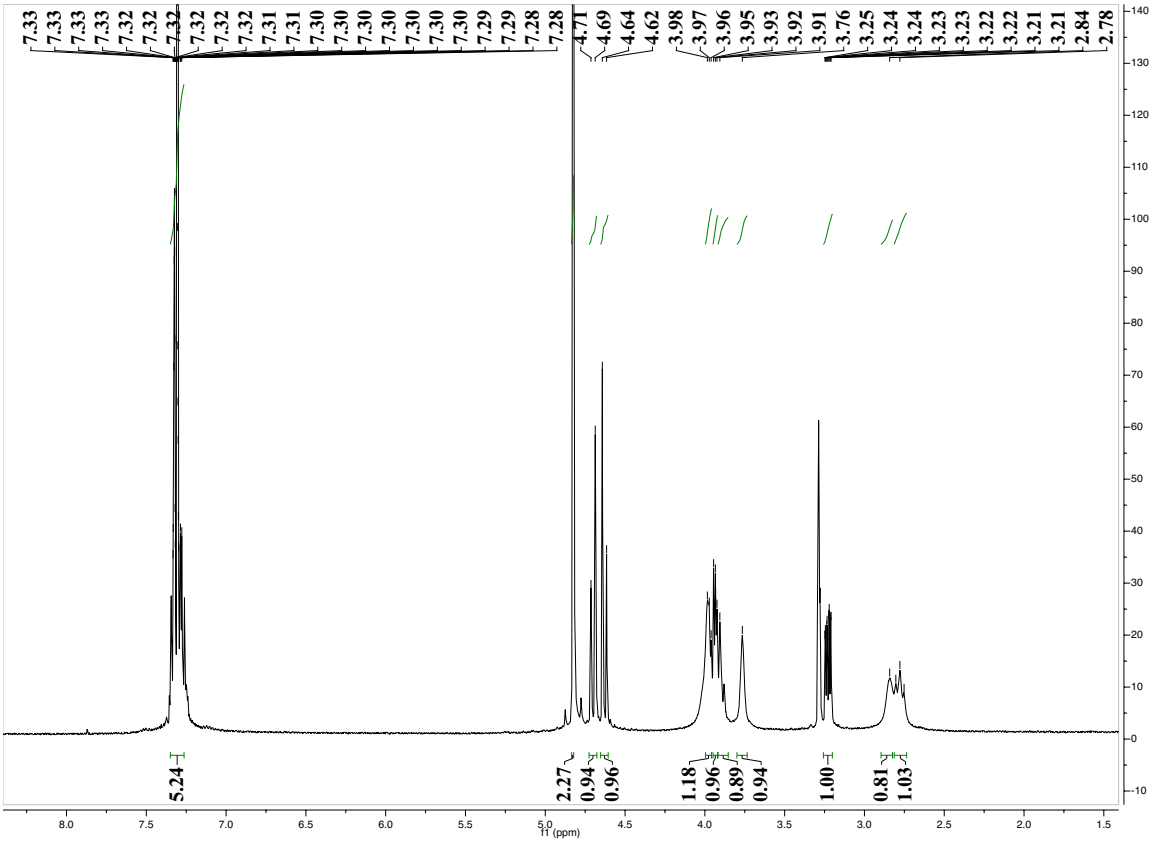

Figure A.1.111 ^{1}H NMR (500 MHz, CD_3OD) spectrum of **119**.

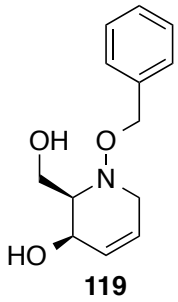

119

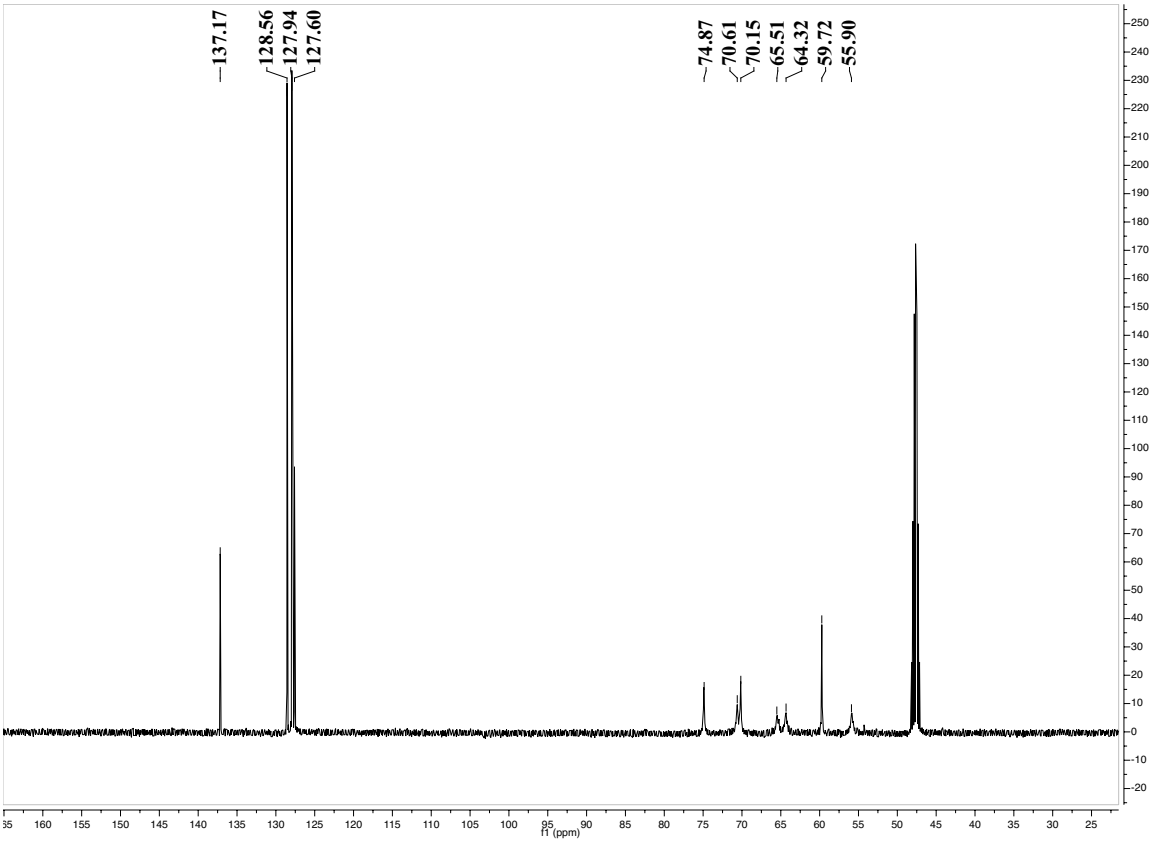

Figure A.1.112 ^{13}C NMR (101 MHz, CD_3OD) spectrum of **119**.

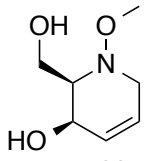

120

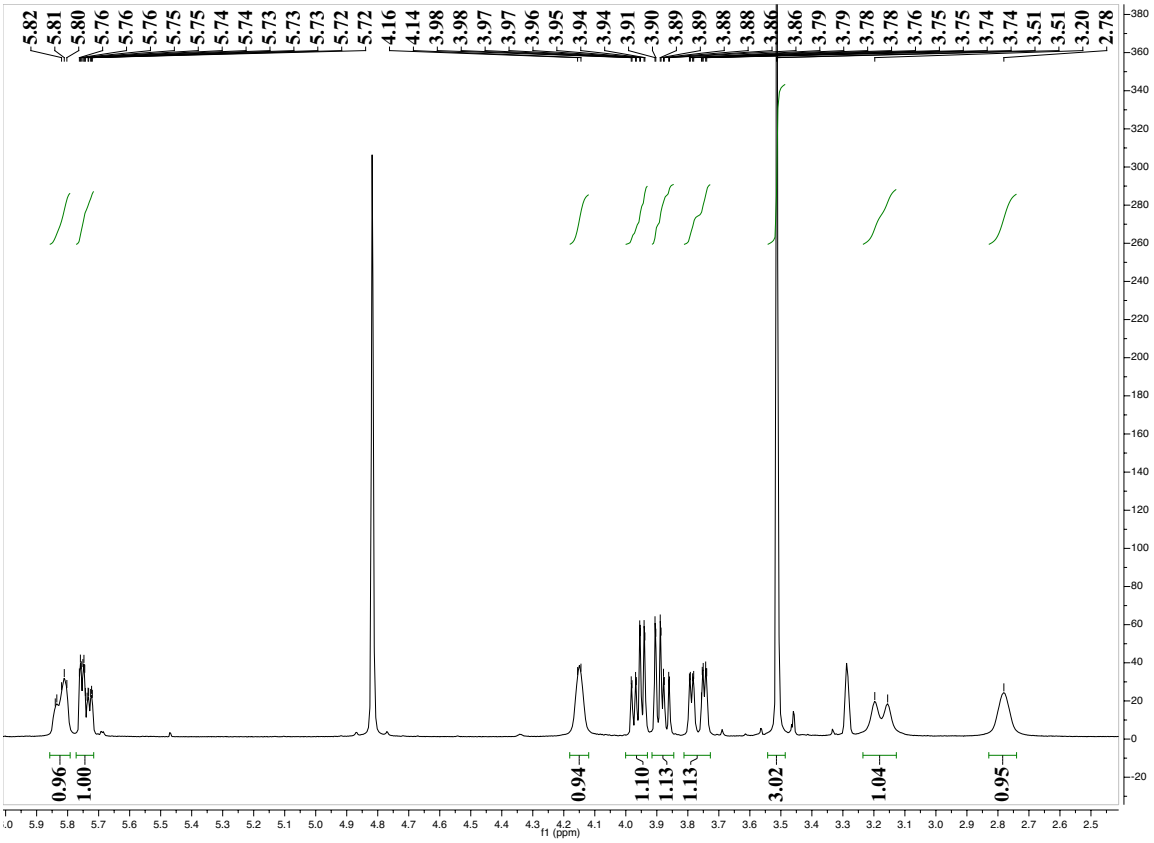

Figure A.1.113 ^{1}H NMR (400 MHz, CD_3OD) spectrum of **120**.

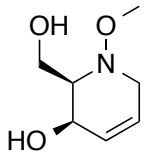

120

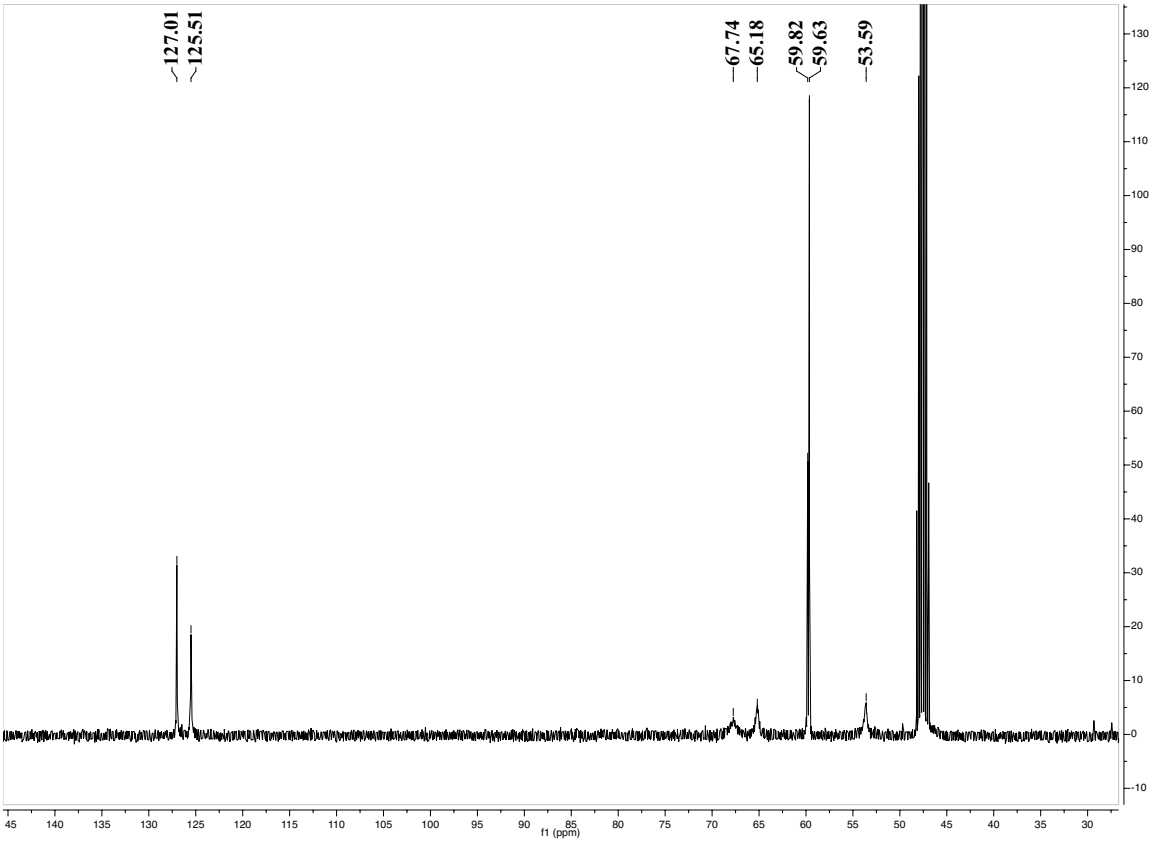

Figure A.1.114 ^{13}C NMR (101 MHz, CD_3OD) spectrum of **120**.

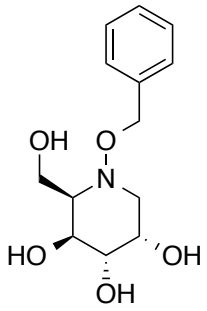

121

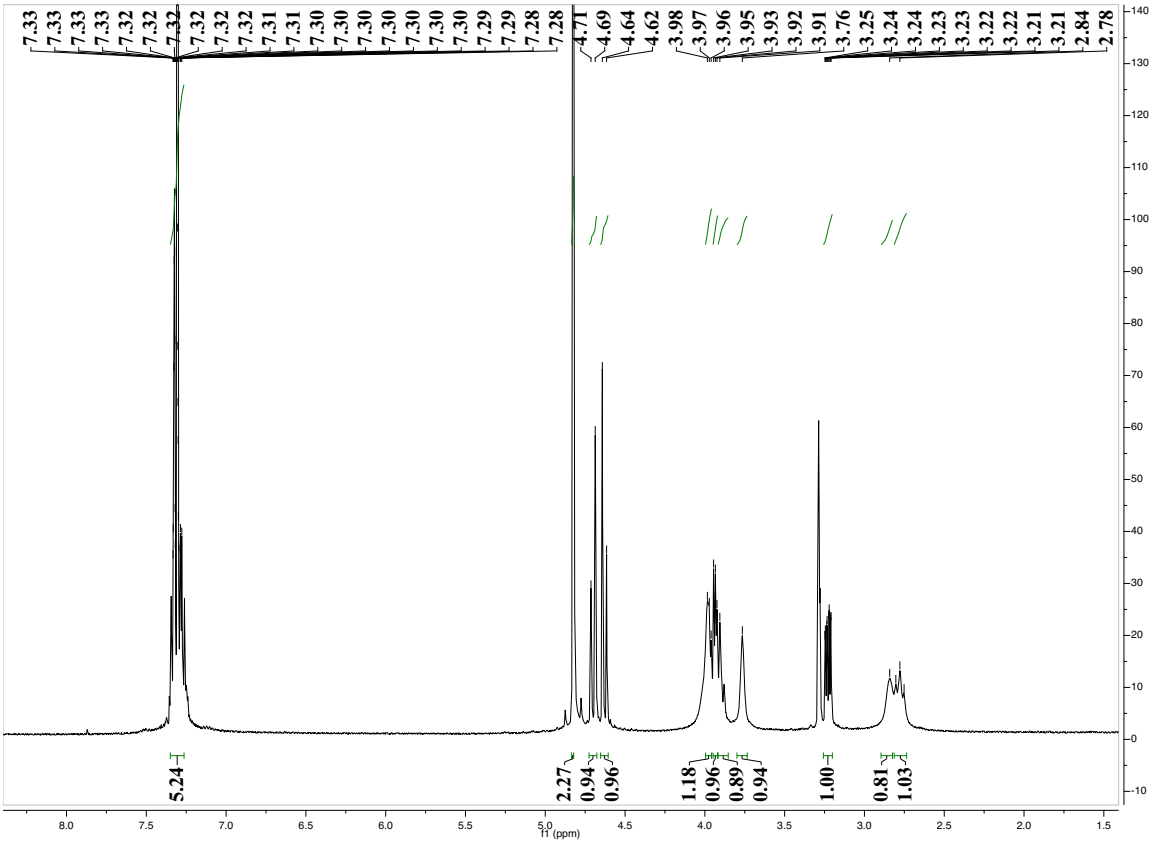

Figure A.1.115 ^{1}H NMR (400 MHz, CD_3OD) spectrum of **121**.

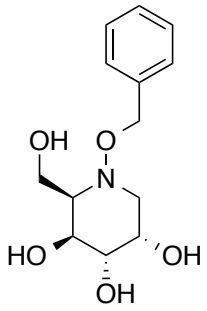

121

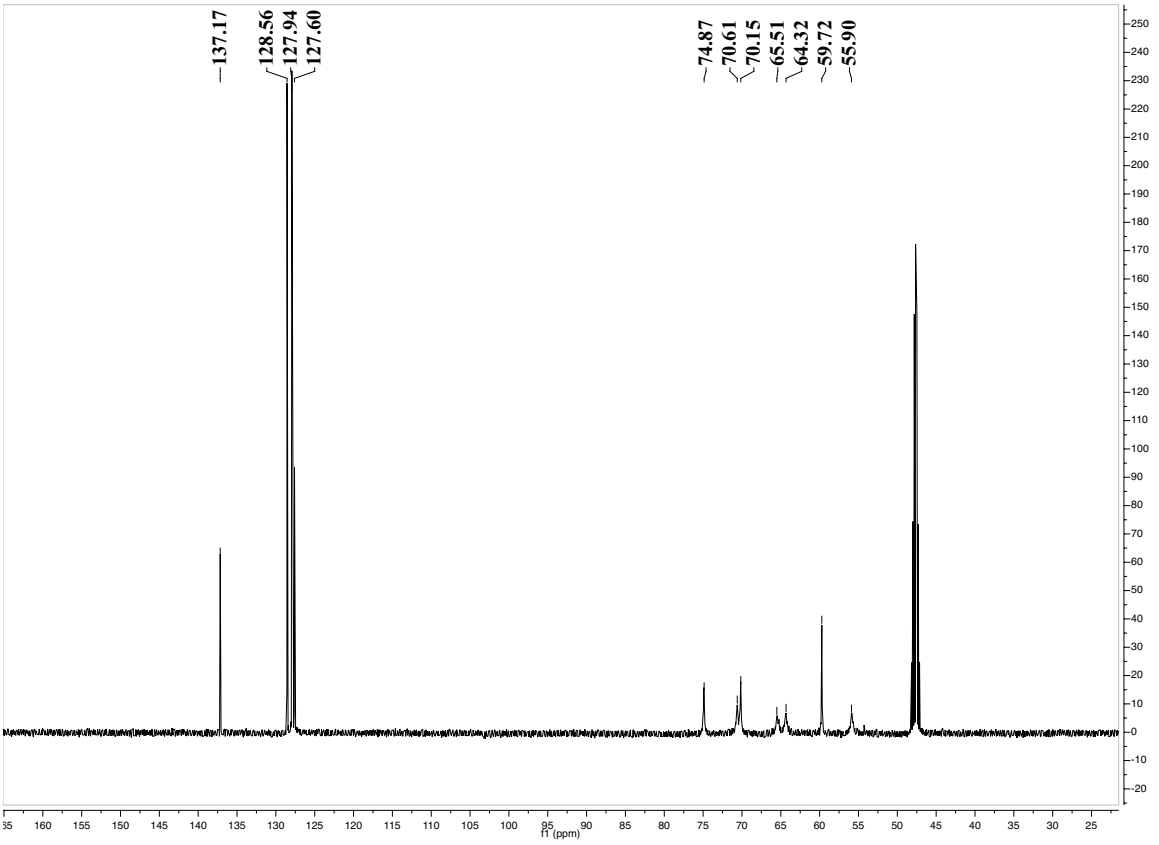

Figure A.1.116 ^{13}C NMR (101 MHz, CD_3OD) spectrum of **121**.

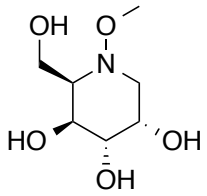

122

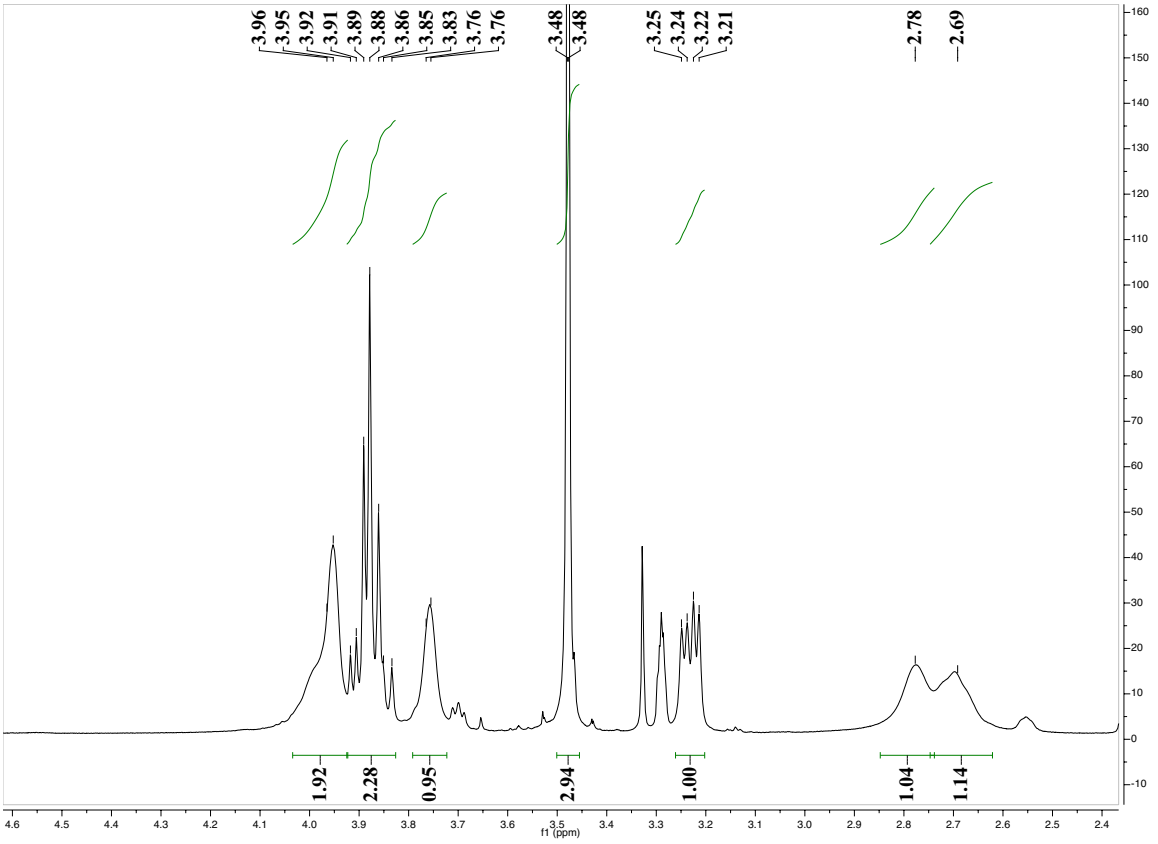

Figure A.1.117 ^{1}H NMR (500 MHz, CD_3OD) spectrum of **122**.

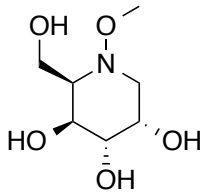

122

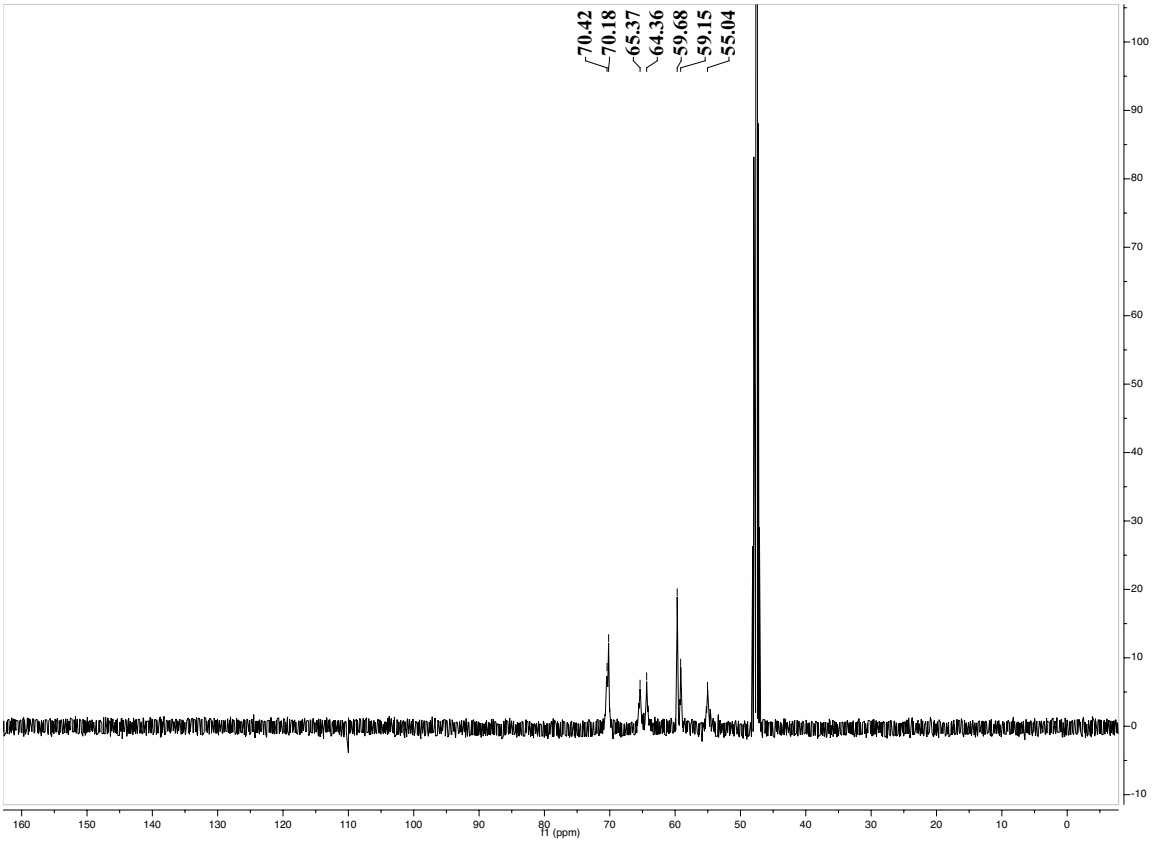

Figure A.1.118 ^{13}C NMR (121 MHz, CD_3OD) spectrum of **122**.

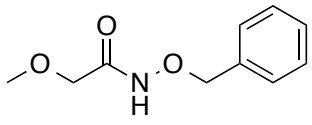

128

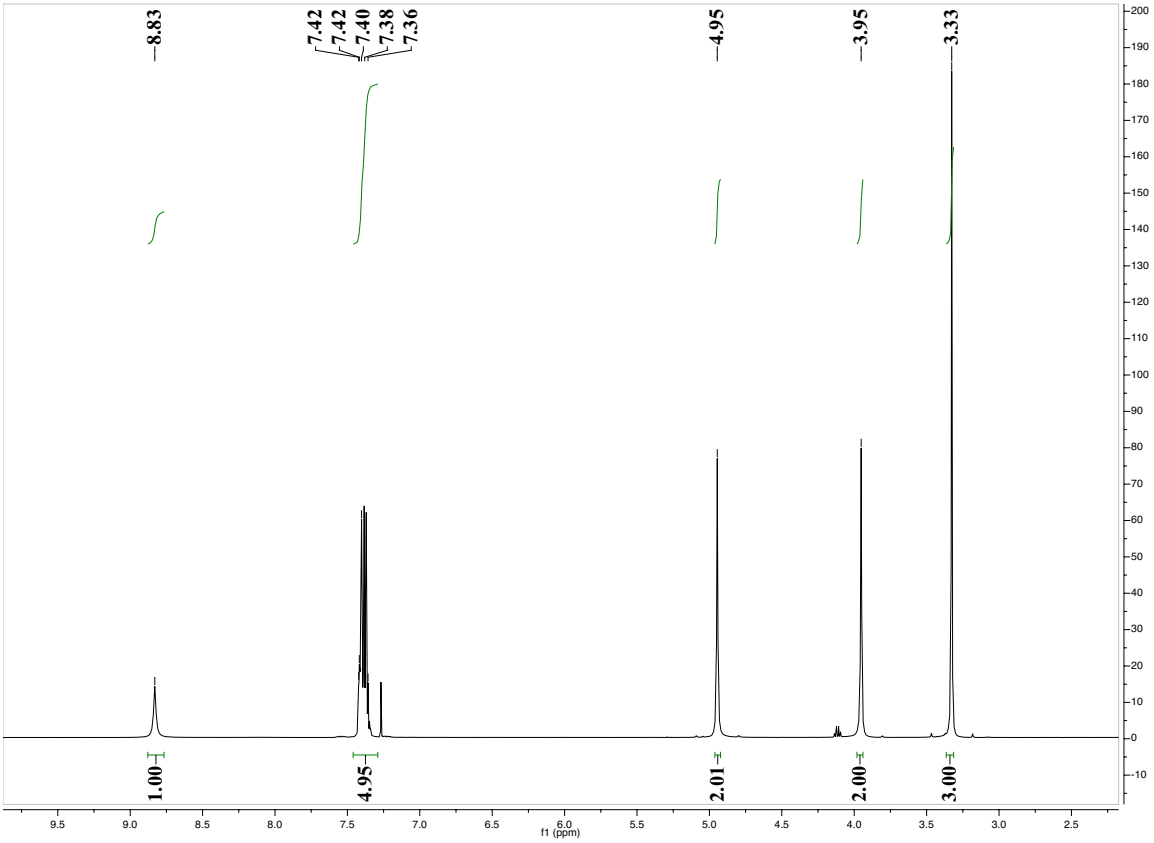

Figure A.1.119 ^{1}H NMR (500 MHz, $CDCl_3$) spectrum of **128**.

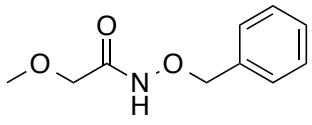

128

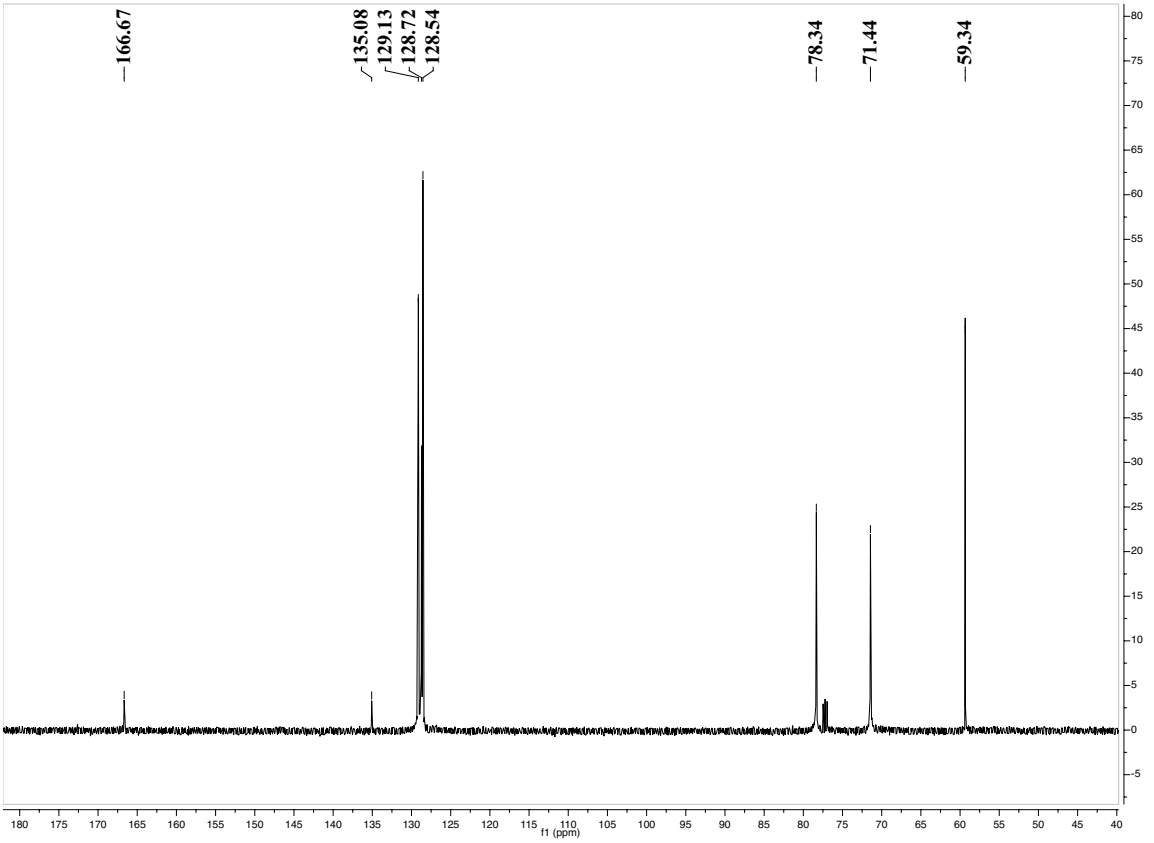

Figure A.1.120 ^{13}C NMR (121 MHz, $CDCl_3$) spectrum of **128**.

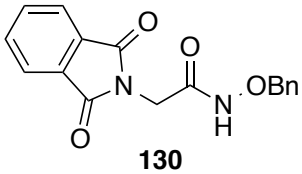

130

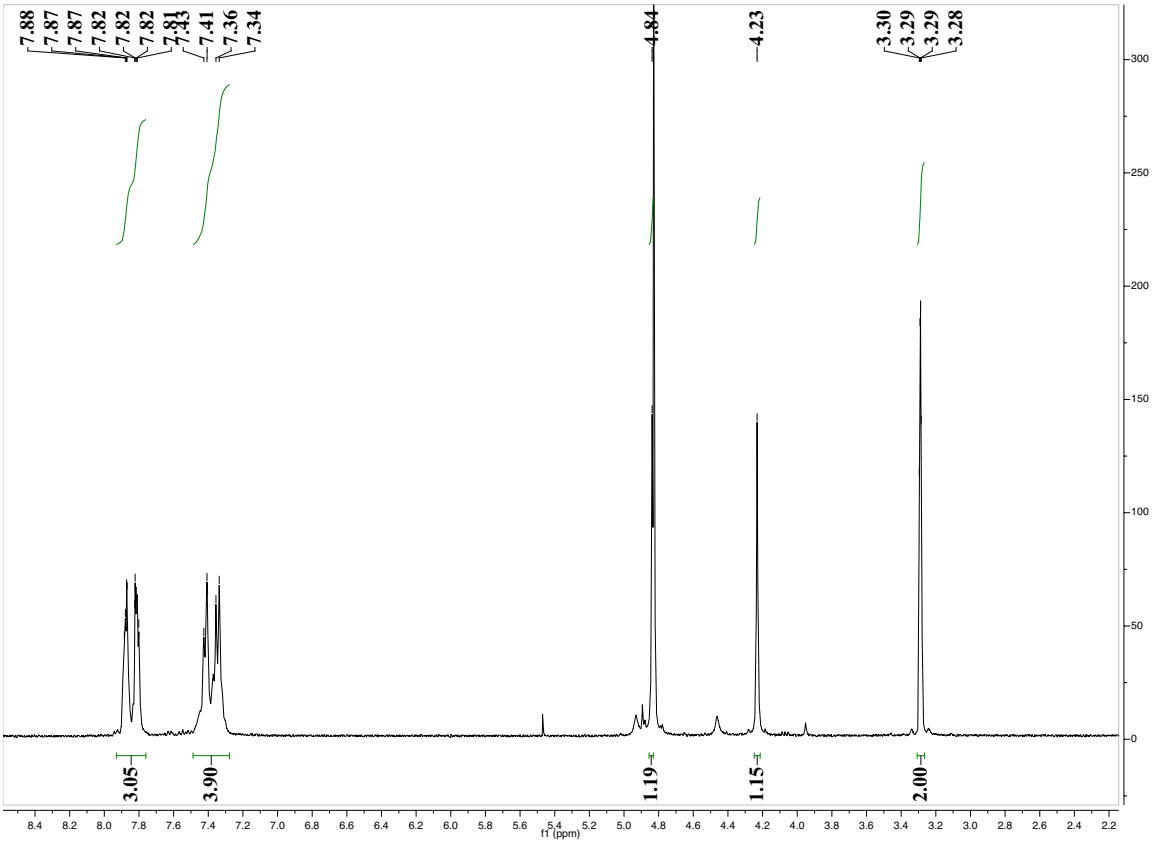

Figure A.1.121 ^{1}H NMR (CD_3OD) spectrum of **130**.

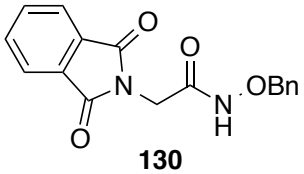

130

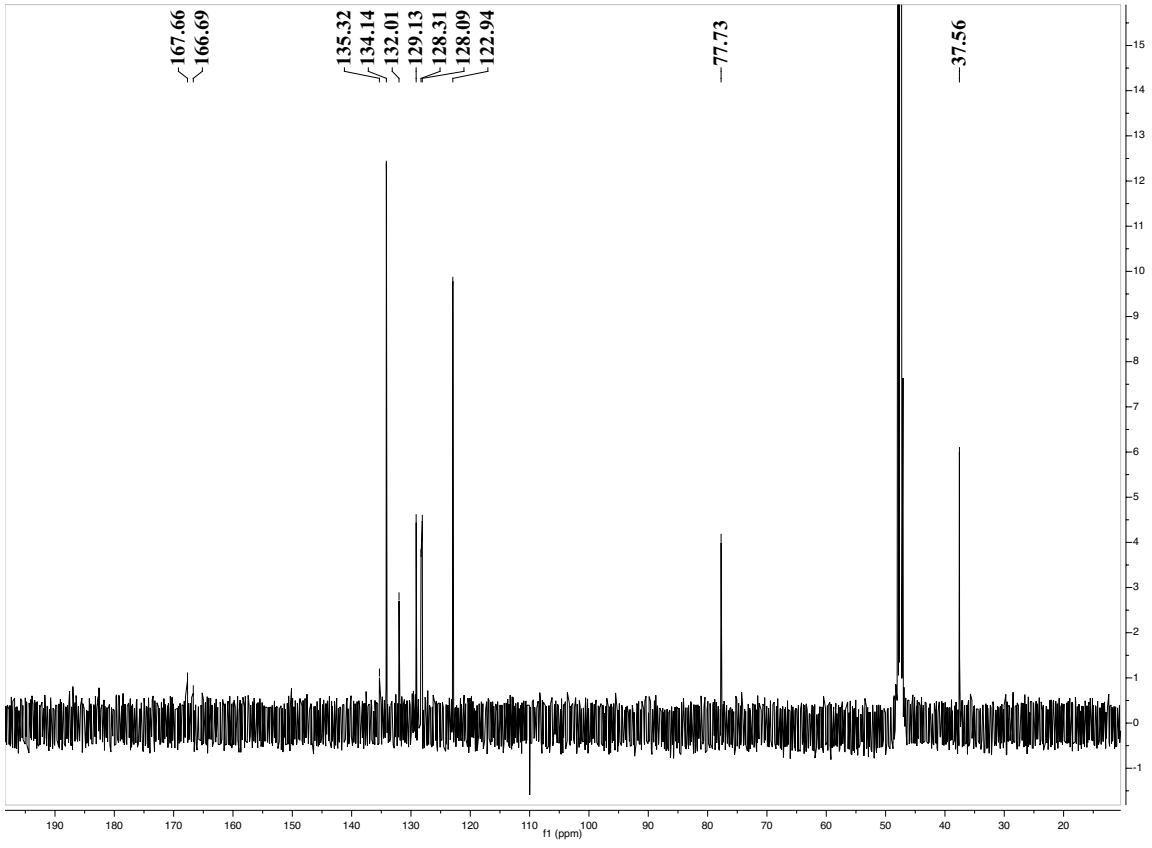

Figure A.1.122 ^{13}C NMR (121 MHz, CD_3OD) spectrum of **130**.

Appendix

A.2 Computational Data

Full Citation for reference 18:

Gaussian 03, Revision C.02, Frisch, M. J.; Trucks, G. W.; Schlegel, H. B.; Scuseria, G. E.; Robb, M. A.; Cheeseman, J. R.; Montgomery, Jr., J. A.; Vreven, T.; Kudin, K. N.; Burant, J. C.; Millam, J. M.; Iyengar, S. S.; Tomasi, J.; Barone, V.; Mennucci, B.; Cossi, M.; Scalmani, G.; Rega, N.; Petersson, G. A.; Nakatsuji, H.; Hada, M.; Ehara, M.; Toyota, K.; Fukuda, R.; Hasegawa, J.; Ishida, M.; Nakajima, T.; Honda, Y.; Kitao, O.; Nakai, H.; Klene, M.; Li, X.; Knox, J. E.; Hratchian, H. P.; Cross, J. B.; Bakken, V.; Adamo, C.; Jaramillo, J.; Gomperts, R.; Stratmann, R. E.; Yazyev, O.; Austin, A. J.; Cammi, R.; Pomelli, C.; Ochterski, J. W.; Ayala, P. Y.; Morokuma, K.; Voth, G. A.; Salvador, P.; Dannenberg, J. J.; Zakrzewski, V. G.; Dapprich, S.; Daniels, A. D.; Strain, M. C.; Farkas, O.; Malick, D. K.; Rabuck, A. D.; Raghavachari, K.; Foresman, J. B.; Ortiz, J. V.; Cui, Q.; Baboul, A. G.; Clifford, S.; Cioslowski, J.; Stefanov, B. B.; Liu, G.; Liashenko, A.; Piskorz, P.; Komaromi, I.; Martin, R. L.; Fox, D. J.; Keith, T.; Al-Laham, M. A.; Peng, C. Y.; Nanayakkara, A.; Challacombe, M.; Gill, P. M. W.; Johnson, B.; Chen, W.; Wong, M. W.; Gonzalez, C.; and Pople, J. A.; Gaussian, Inc., Wallingford CT, 2004.

Example input file for geometry minimization:

%nproc = 2 %

chk = I81a.chk

%mem = 2GB

#n opt b3lyp/6-31G* scrf = (cpcm, solvent = methanol)

azaoxyallylcation dimethyl N-methoxy in methanol

0 1

C	-4.88003	0.59080	0.09215
C	-3.42999	0.96634	0.11274
C	-2.28202	0.01468	0.22341
C	-3.10581	2.42744	0.09334
O	-2.70002	-1.12595	-0.03955
N	-1.10635	0.49900	0.52164
O	-0.13333	-0.51633	0.61433

C	0.67457	-0.47389	-0.55096
H	-5.07804	-0.44975	0.36244
H	-5.29605	0.76899	-0.90482
H	-5.43537	1.20852	0.80640
H	-3.97375	3.02041	-0.21341
H	-2.30051	2.64427	-0.61578
H	-2.80286	2.76539	1.08923
H	1.47902	-1.20579	-0.43945
H	1.11964	0.51840	-0.67446
H	0.08740	-0.73446	-1.43680

RADII = UAKS

Minimization of **57** in methanol

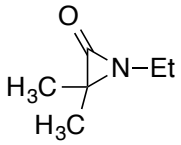

57

Total energy: HF = -365.203694

# of imaginary frequencies = 0

C	1.242187	-1.447664	-1.090548
C	0.858851	-0.470754	0.003783
H	2.315419	-1.667339	-1.041859
H	1.015903	-1.038748	-2.079348
H	0.700982	-2.394891	-0.971560
C	1.087579	-0.957327	1.425543
H	0.514621	-1.872492	1.620938
H	0.804667	-0.205336	2.169912
H	2.148084	-1.192820	1.570807
C	0.783499	1.005041	-0.201236
N	-0.384732	0.368569	-0.276281
C	-1.694176	0.509807	0.363537
C	-2.718991	-0.453803	-0.228050
H	-2.005195	1.550266	0.215570
H	-1.592786	0.347895	1.446185
H	-2.845839	-0.278068	-1.301261
H	-3.688364	-0.317402	0.263722
H	-2.409312	-1.494875	-0.084282
O	1.297656	2.109004	-0.189129

Minimization of **58** in methanol

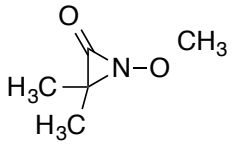

58

Total energy: HF = -401.0423649

# of imaginary frequencies = 0

O	1.588434	0.329171	0.309267
N	0.445852	0.200193	-0.517917
C	-0.607054	1.037141	-0.260671
C	2.595168	-0.586460	-0.137260
O	-0.864133	2.205941	-0.085492
C	-0.912870	-0.384018	0.004522
C	-1.036489	-0.732292	1.476619
C	-1.554857	-1.338884	-0.976441
H	3.447981	-0.411489	0.523435
H	2.875855	-0.383357	-1.176313
H	2.257351	-1.624665	-0.038985
H	-2.089747	-0.697991	1.776208
H	-0.472381	-0.042091	2.110054
H	-0.666626	-1.749140	1.652835
H	-2.640724	-1.349860	-0.824034
H	-1.178294	-2.356619	-0.820480
H	-1.352168	-1.039947	-2.008116

Minimization of **59** in methanol

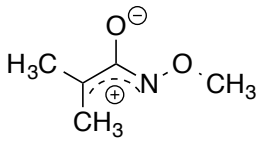

59

Total energy: HF = -401.0345846

# of imaginary frequencies = 0

C	-2.695911	-0.504180	0.120765
C	-1.441931	0.273460	-0.002908
C	-0.224850	-0.509983	-0.066285
C	-1.535903	1.756588	-0.049620
O	-0.209439	-1.762496	-0.055405
N	0.848891	0.339251	-0.073002
O	1.977297	-0.400046	-0.008639
C	3.141014	0.437317	0.094486
H	-2.530096	-1.392175	0.739067
H	-2.954505	-0.893465	-0.881216
H	-3.538843	0.093511	0.480436
H	-2.278890	2.053797	-0.813006
H	-0.578469	2.242337	-0.235723
H	-1.953416	2.113319	0.914036
H	3.988283	-0.249867	0.131122
H	3.095480	1.036168	1.010481
H	3.216119	1.094266	-0.781391

Gas phase minimization of alpha-lactam **58**:

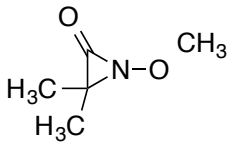

58

Total energy: HF = -401.0342371

# of imaginary frequencies = 0

O	1.571947	0.256103	0.366448
N	0.448985	0.183909	-0.497929
C	-0.595219	1.047510	-0.248904
C	2.619482	-0.549870	-0.169263
O	-0.854227	2.211207	-0.093927
C	-0.914921	-0.378039	0.000856
C	-1.053430	-0.739194	1.469026
C	-1.568331	-1.314718	-0.991597
H	3.454023	-0.428395	0.526268
H	2.911357	-0.205648	-1.167563
H	2.329200	-1.607184	-0.215983
H	-2.106250	-0.686728	1.767145
H	-0.478524	-0.065020	2.109070
H	-0.702310	-1.763623	1.642181
H	-2.655789	-1.312537	-0.850608
H	-1.209128	-2.341162	-0.847177
H	-1.352726	-1.009673	-2.018708

Minimization of aza-oxyallycation **59** in gas phase:

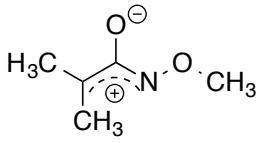

59

Total energy: HF = -401.0189598

# of imaginary frequencies = 0

O	-1.977646	-0.395145	0.021437
N	-0.843699	0.323074	-0.068762
C	0.232680	-0.538518	-0.134537
C	-3.111604	0.470252	0.147429
O	0.238440	-1.775361	-0.195934
C	1.425374	0.274638	0.016439
C	2.672801	-0.485669	0.270198
C	1.508138	1.752423	-0.136451
H	-3.979989	-0.190058	0.172030
H	-3.167494	1.147768	-0.710315
H	-3.046420	1.049363	1.074245
H	2.999455	-0.940704	-0.679718
H	2.464878	-1.339770	0.924677
H	3.486458	0.134881	0.655664
H	2.175132	1.991500	-0.980887
H	1.986477	2.198362	0.748253
H	0.536712	2.212432	-0.305107

Example input file for the relaxed potential energy surface scan:

%nproc = 2

%mem = 4 GB

#N b3lyp/6-31G* opt = modredundant guess = always scrf = (cpcm, solvent = methanol)

a relaxed PES scan

0 1

O	1.588434	0.329171	0.309267
N	0.445852	0.200193	-0.517917
C	-0.607054	1.037141	-0.260671
C	2.595168	-0.586460	-0.137260
O	-0.864133	2.205941	-0.085492
C	-0.912870	-0.384018	0.004522
C	-1.036489	-0.732292	1.476619
C	-1.554857	-1.338884	-0.976441
H	3.447981	-0.411489	0.523435
H	2.875855	-0.383357	-1.176313
H	2.257351	-1.624665	-0.038985
H	-2.089747	-0.697991	1.776208
H	-0.472381	-0.042091	2.110054
H	-0.666626	-1.749140	1.652835
H	-2.640724	-1.349860	-0.824034
H	-1.178294	-2.356619	-0.820480
H	-1.352168	-1.039947	-2.008116

26 + = 0.1 S 100.1

Relaxed PES scan for **57** in methanol

***r*[C(3)-N] Å**	**Total E (Hartees)**
1.42624	-365.200017
1.52624	-365.203694
1.62624	-365.201345
1.72624	-365.196079
1.82624	-365.189784
1.92624	-365.183503
2.02624	-365.178094

2.12624	-365.173891
2.22624	-365.170871
2.32624	-365.168804
2.42624	-365.165683
2.52624	-365.159166

Relaxed PES scan for **58** in methanol

***r*[C(3)-N] Å**	**Total E (Hartees)**
1.46856	-401.0399013
1.56856	-401.0423652
1.66856	-401.0408389
1.76856	-401.0376628
1.86856	-401.0345412
1.96856	-401.0326107
2.06856	-401.0323206
2.16856	-401.0332170
2.26856	-401.0345043
2.36856	-401.0329454
2.46856	-401.0274869
2.28115	-401.0345850

Relaxed PES scan for **59** in the gas phase

***r*[C(3)-N] Å**	**Total E (Hartees)**
1.46856	-401.0321450
1.55718	-401.0342371
1.56856	-401.0342100
1.66856	-401.0321910
1.76856	-401.0283450
1.86856	-401.0241140
1.96856	-401.0208240
2.06856	-401.0191060
2.16856	-401.0187300
2.26856	-401.0189590
2.27110	-401.0189600
2.36856	-401.0173320
2.46856	-401.0119070

Appendix

A.3 X-Ray Crystallography Data

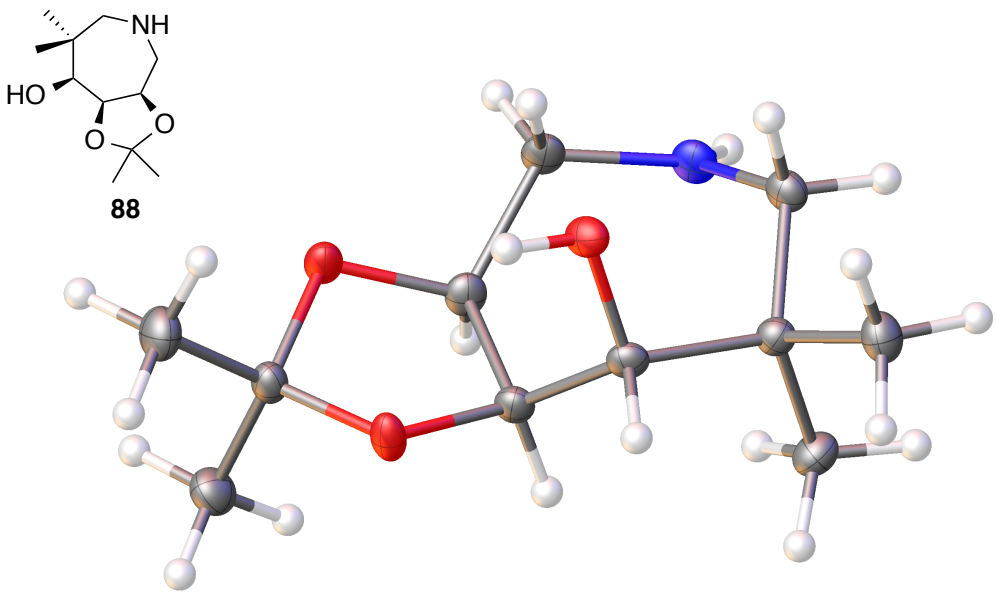

Figure A.3.1. Thermal ellipsoid plot of azepane **88** at 50% probability. Hydrogen atoms are represented as spheres of arbitrary radius. Grey = carbon, red = oxygen, blue = nitrogen.

Table A.3.1. Crystal data and structure refinement for **88**.

Identification code	kb005_0m	
Empirical formula	$C_{11}H_{20}NO_3$	
Formula weight	214.28	
Temperature	100(2) K	
Wavelength	0.71073 Å	
Crystal system	Monoclinic	
Space group	P2(1)/c	
Unit cell dimensions	a = 5.9830(4) Å	α = 90°.
	b = 11.0773(7) Å	β = 98.9630(10)°.
	c = 17.8208(11) Å	γ = 90°.
Volume	1166.66(13) $Å^3$	
Z	4	
Density (calculated)	1.220 Mg/m^3	
Absorption coefficient	0.088 mm^{-1}	
F(000)	468	
Crystal size	0.27 x 0.14 x 0.02 mm^3	
Theta range for data collection	2.17 to 29.14°.	
Index ranges	-8<=h<=8, -15<=k<=15, -24<=l<=24	
Reflections collected	21780	
Independent reflections	3136 [R(int) = 0.0627]	
Completeness to theta = 29.14°	99.9 %	
Absorption correction	sadabs	
Max. and min. transmission	0.9979 and 0.9771	
Refinement method	Full-matrix least-squares on F^2	
Data / restraints / parameters	3136 / 0 / 139	
Goodness-of-fit on F^2	0.903	
Final R indices [I>2sigma(I)]	R1 = 0.0557, wR2 = 0.1427	
R indices (all data)	R1 = 0.0853, wR2 = 0.1638	
Largest diff. peak and hole	0.688 and -0.726 $e.Å^{-3}$	

Table A.3.2. Bond lengths [Å] and angles [°] for **88**.

O(2)-C(7)	1.434(2)
O(2)-C(3)	1.437(2)
O(3)-C(4)	1.420(2)
O(3)-H(3A)	0.8400
O(1)-C(7)	1.424(2)
O(1)-C(2)	1.430(2)
N(1)-C(6)	1.460(2)
N(1)-C(1)	1.465(2)
N(1)-H(1A)	0.8800
C(5)-C(10)	1.530(3)
C(5)-C(11)	1.532(3)
C(5)-C(6)	1.545(2)
C(5)-C(4)	1.547(2)
C(4)-C(3)	1.526(3)
C(4)-H(4A)	1.0000
C(1)-C(2)	1.522(3)
C(1)-H(1B)	0.9900
C(1)-H(1C)	0.9900
C(11)-H(11A)	0.9800
C(11)-H(11B)	0.9800
C(11)-H(11C)	0.9800
C(6)-H(6A)	0.9900
C(6)-H(6B)	0.9900
C(7)-C(8)	1.504(3)
C(7)-C(9)	1.516(3)
C(3)-C(2)	1.552(2)
C(3)-H(3B)	1.0000
C(9)-H(9A)	0.9800
C(9)-H(9B)	0.9800
C(9)-H(9C)	0.9800
C(8)-H(8A)	0.9800
C(8)-H(8B)	0.9800
C(8)-H(8C)	0.9800
C(2)-H(2A)	1.0000
C(10)-H(10A)	0.9800
C(10)-H(10B)	0.9800
C(10)-H(10C)	0.9800
C(7)-O(2)-C(3)	108.52(13)
C(4)-O(3)-H(3A)	109.5
C(7)-O(1)-C(2)	107.31(13)
C(6)-N(1)-C(1)	115.92(14)
C(6)-N(1)-H(1A)	122.0
C(1)-N(1)-H(1A)	122.0
C(10)-C(5)-C(11)	108.65(15)
C(10)-C(5)-C(6)	110.37(15)
C(11)-C(5)-C(6)	107.15(15)

C(10)-C(5)-C(4)	111.79(15)
C(11)-C(5)-C(4)	107.28(14)
C(6)-C(5)-C(4)	111.41(14)
O(3)-C(4)-C(3)	111.36(14)
O(3)-C(4)-C(5)	108.96(14)
C(3)-C(4)-C(5)	114.77(14)
O(3)-C(4)-H(4A)	107.1
C(3)-C(4)-H(4A)	107.1
C(5)-C(4)-H(4A)	107.1
N(1)-C(1)-C(2)	116.02(15)
N(1)-C(1)-H(1B)	108.3
C(2)-C(1)-H(1B)	108.3
N(1)-C(1)-H(1C)	108.3
C(2)-C(1)-H(1C)	108.3
H(1B)-C(1)-H(1C)	107.4
C(5)-C(11)-H(11A)	109.5
C(5)-C(11)-H(11B)	109.5
H(11A)-C(11)-H(11B)	109.5
C(5)-C(11)-H(11C)	109.5
H(11A)-C(11)-H(11C)	109.5
H(11B)-C(11)-H(11C)	109.5
N(1)-C(6)-C(5)	118.35(15)
N(1)-C(6)-H(6A)	107.7
C(5)-C(6)-H(6A)	107.7
N(1)-C(6)-H(6B)	107.7
C(5)-C(6)-H(6B)	107.7
H(6A)-C(6)-H(6B)	107.1
O(1)-C(7)-O(2)	104.48(13)
O(1)-C(7)-C(8)	108.73(15)
O(2)-C(7)-C(8)	108.63(15)
O(1)-C(7)-C(9)	110.89(15)
O(2)-C(7)-C(9)	111.01(15)
C(8)-C(7)-C(9)	112.74(16)
O(2)-C(3)-C(4)	107.84(14)
O(2)-C(3)-C(2)	104.07(14)
C(4)-C(3)-C(2)	117.87(15)
O(2)-C(3)-H(3B)	108.9
C(4)-C(3)-H(3B)	108.9
C(2)-C(3)-H(3B)	108.9
C(7)-C(9)-H(9A)	109.5
C(7)-C(9)-H(9B)	109.5
H(9A)-C(9)-H(9B)	109.5
C(7)-C(9)-H(9C)	109.5
H(9A)-C(9)-H(9C)	109.5
H(9B)-C(9)-H(9C)	109.5
C(7)-C(8)-H(8A)	109.5
C(7)-C(8)-H(8B)	109.5
H(8A)-C(8)-H(8B)	109.5
C(7)-C(8)-H(8C)	109.5

H(8A)-C(8)-H(8C)	109.5
H(8B)-C(8)-H(8C)	109.5
O(1)-C(2)-C(1)	106.59(15)
O(1)-C(2)-C(3)	104.21(13)
C(1)-C(2)-C(3)	118.76(15)
O(1)-C(2)-H(2A)	109.0
C(1)-C(2)-H(2A)	109.0
C(3)-C(2)-H(2A)	109.0
C(5)-C(10)-H(10A)	109.5
C(5)-C(10)-H(10B)	109.5
H(10A)-C(10)-H(10B)	109.5
C(5)-C(10)-H(10C)	109.5
H(10A)-C(10)-H(10C)	109.5
H(10B)-C(10)-H(10C)	109.5

Symmetry transformations used to generate equivalent atoms:

#1 -x+1,-y+1,-z #2 -x+1,-y+1,-z+1

Table A.3.3. Hydrogen coordinates (x 10^4) and isotropic displacement parameters (Å^{2}x 10^3) for **88**.

	x	y	z	U(eq)
H(3A)	4889	1760	2061	26
H(1A)	2610	-2132	2957	22
H(4A)	2905	2246	2961	18
H(1B)	2584	-1747	1700	22
H(1C)	4276	-650	1939	22
H(11A)	5425	769	4579	31
H(11B)	4486	2041	4240	31
H(11C)	6525	1394	3913	31
H(6A)	5933	-489	3220	21
H(6B)	4736	-1068	3872	21
H(3B)	-390	1137	2489	19
H(9A)	-3096	906	1133	35
H(9B)	-2900	879	248	35
H(9C)	-3079	2143	670	35
H(8A)	2817	1981	466	36
H(8B)	645	2833	270	36
H(8C)	753	1577	-166	36
H(2A)	-544	-553	1831	20
H(10A)	1524	68	4349	30
H(10B)	175	-78	3505	30
H(10C)	490	1231	3887	30

Table A.3.4. Torsion angles [°] for **88**.

C(10)-C(5)-C(4)-O(3)	-169.92(14)
C(11)-C(5)-C(4)-O(3)	71.07(17)
C(6)-C(5)-C(4)-O(3)	-45.91(19)
C(10)-C(5)-C(4)-C(3)	-44.3(2)
C(11)-C(5)-C(4)-C(3)	-163.29(15)
C(6)-C(5)-C(4)-C(3)	79.72(18)
C(6)-N(1)-C(1)-C(2)	-82.2(2)
C(1)-N(1)-C(6)-C(5)	66.2(2)
C(10)-C(5)-C(6)-N(1)	62.7(2)
C(11)-C(5)-C(6)-N(1)	-179.15(15)
C(4)-C(5)-C(6)-N(1)	-62.1(2)
C(2)-O(1)-C(7)-O(2)	34.85(18)
C(2)-O(1)-C(7)-C(8)	150.69(15)
C(2)-O(1)-C(7)-C(9)	-84.82(18)
C(3)-O(2)-C(7)-O(1)	-29.83(18)
C(3)-O(2)-C(7)-C(8)	-145.74(15)
C(3)-O(2)-C(7)-C(9)	89.75(17)
C(7)-O(2)-C(3)-C(4)	139.51(14)
C(7)-O(2)-C(3)-C(2)	13.58(18)
O(3)-C(4)-C(3)-O(2)	-61.77(17)
C(5)-C(4)-C(3)-O(2)	173.86(13)
O(3)-C(4)-C(3)-C(2)	55.6(2)
C(5)-C(4)-C(3)-C(2)	-68.8(2)
C(7)-O(1)-C(2)-C(1)	-152.34(15)
C(7)-O(1)-C(2)-C(3)	-25.95(18)
N(1)-C(1)-C(2)-O(1)	176.82(14)
N(1)-C(1)-C(2)-C(3)	59.7(2)
O(2)-C(3)-C(2)-O(1)	7.42(18)
C(4)-C(3)-C(2)-O(1)	-111.91(17)
O(2)-C(3)-C(2)-C(1)	125.78(17)
C(4)-C(3)-C(2)-C(1)	6.4(2)

Symmetry transformations used to generate equivalent atoms:

#1 -x+1,-y+1,-z #2 -x+1,-y+1,-z+1

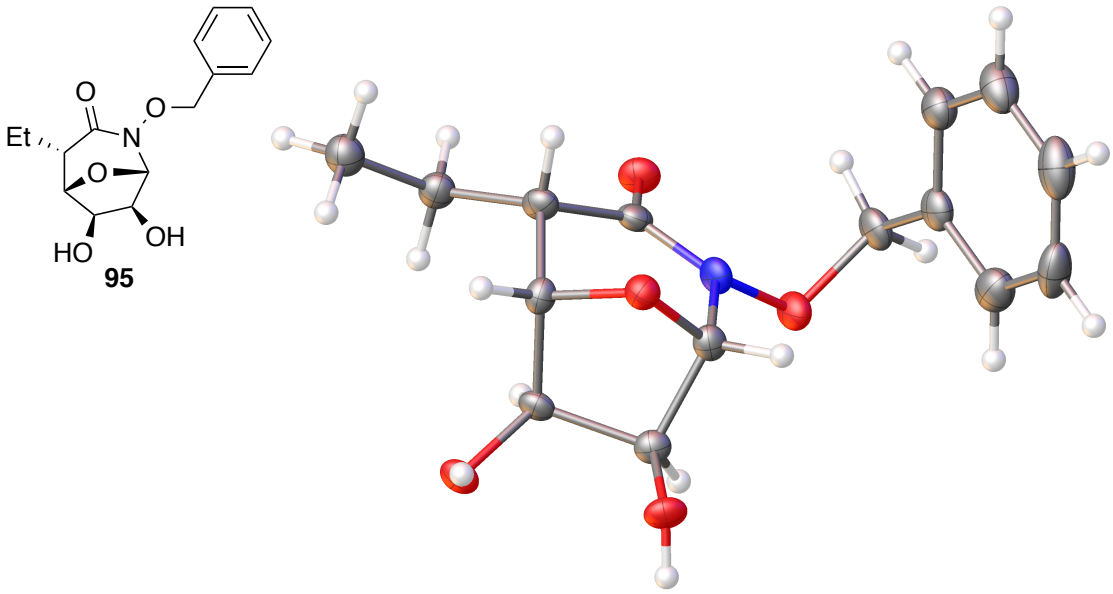

Figure A.3.2. Thermal ellipsoid plot of diol **95** at 50% probability. Hydrogen atoms are represented as spheres of arbitrary radius. Grey = carbon, red = oxygen, blue = nitrogen.

Table A.3.5. Crystal data and structure refinement for **95**.

Identification code	twin5	
Empirical formula	C2.50 H3.17 N0.17 O0.83	
Formula weight	48.89	
Temperature	100(2) K	
Wavelength	0.71073 Å	
Crystal system	Triclinic	
Space group	P-1	
Unit cell dimensions	a = 9.064(3) Å	a= 76.711(5)°.
	b = 11.442(3) Å	b= 85.166(5)°.
	c = 14.671(4) Å	g = 76.139(5)°.
Volume	1437.0(7) $Å^3$	
Z	24	
Density (calculated)	1.356 Mg/m^3	
Absorption coefficient	0.102 mm^{-1}	
F(000)	624	
Crystal size	0.55 x 0.16 x 0.07 mm^3	
Theta range for data collection	1.43 to 25.00°.	
Index ranges	-10<=h<=10, -13<=k<=13, 0<=l<=17	
Reflections collected	5147	
Independent reflections	5149 [R(int) = 0.069]	
Completeness to theta = 25.00°	99.6 %	
Absorption correction	Semi-empirical from equivalents	
Max. and min. transmission	0.9934 and 0.9464	
Refinement method	Full-matrix least-squares on F^2	
Data / restraints / parameters	5149 / 0 / 383	
Goodness-of-fit on F^2	1.017	
Final R indices [I>2sigma(I)]	R1 = 0.0617, wR2 = 0.1300	
R indices (all data)	R1 = 0.1000, wR2 = 0.1434	
Largest diff. peak and hole	0.565 and -0.420 e.$Å^{-3}$	

Table A.3.6. Bond lengths [Å] and angles [°] for **95**.

N(1)-C(1)	1.363(4)	O(7)-C(18)	1.448(3)
N(1)-O(5)	1.402(3)	O(8)-C(19)	1.424(3)
N(1)-C(6)	1.473(4)	O(8)-H(8D)	0.8400
O(1)-C(1)	1.219(4)	O(9)-C(20)	1.421(3)
O(2)-C(6)	1.409(4)	O(9)-H(9C)	0.8400
O(2)-C(3)	1.448(4)	O(10)-C(24)	1.462(4)
O(3)-C(4)	1.418(3)	C(16)-C(17)	1.530(4)
O(3)-H(3A)	0.8400	C(17)-C(22)	1.529(4)
O(4)-C(5)	1.421(3)	C(17)-C(18)	1.528(4)
O(4)-H(4A)	0.8400	C(17)-H(17A)	1.0000
O(5)-C(9)	1.451(4)	C(18)-C(19)	1.540(4)
C(1)-C(2)	1.520(4)	C(18)-H(18A)	1.0000
C(2)-C(3)	1.533(4)	C(19)-C(20)	1.551(4)
C(2)-C(7)	1.540(4)	C(19)-H(19A)	1.0000
C(2)-H(2A)	1.0000	C(20)-C(21)	1.523(4)
C(3)-C(4)	1.538(4)	C(20)-H(20A)	1.0000
C(3)-H(3B)	1.0000	C(21)-H(21A)	1.0000
C(4)-C(5)	1.559(4)	C(22)-C(23)	1.521(4)
C(4)-H(4B)	1.0000	C(22)-H(22A)	0.9900
C(5)-C(6)	1.530(4)	C(22)-H(22B)	0.9900
C(5)-H(5A)	1.0000	C(23)-H(23A)	0.9800
C(6)-H(6A)	1.0000	C(23)-H(23B)	0.9800
C(7)-C(8)	1.512(5)	C(23)-H(23C)	0.9800
C(7)-H(7A)	0.9900	C(24)-C(25)	1.497(4)
C(7)-H(7B)	0.9900	C(24)-H(24A)	0.9900
C(8)-H(8A)	0.9800	C(24)-H(24B)	0.9900
C(8)-H(8B)	0.9800	C(25)-C(30)	1.384(4)
C(8)-H(8C)	0.9800	C(25)-C(26)	1.388(5)
C(9)-C(10)	1.490(5)	C(26)-C(27)	1.387(5)
C(9)-H(9A)	0.9900	C(26)-H(26A)	0.9500
C(9)-H(9B)	0.9900	C(27)-C(28)	1.390(5)
C(10)-C(11)	1.372(5)	C(27)-H(27A)	0.9500
C(10)-C(15)	1.374(5)	C(28)-C(29)	1.372(5)
C(11)-C(12)	1.345(7)	C(28)-H(28A)	0.9500
C(11)-H(11A)	0.9500	C(29)-C(30)	1.391(5)
C(12)-C(13)	1.314(8)	C(29)-H(29A)	0.9500
C(12)-H(12A)	0.9500	C(30)-H(30A)	0.9500
C(13)-C(14)	1.435(8)		
C(13)-H(13A)	0.9500	C(1)-N(1)-O(5)	117.3(2)
C(14)-C(15)	1.423(6)	C(1)-N(1)-C(6)	122.8(3)
C(14)-H(14A)	0.9500	O(5)-N(1)-C(6)	112.4(2)
C(15)-H(15A)	0.9500	C(6)-O(2)-C(3)	102.2(2)
N(2)-C(16)	1.348(4)	C(4)-O(3)-H(3A)	109.5
N(2)-O(10)	1.409(3)	C(5)-O(4)-H(4A)	109.5
N(2)-C(21)	1.468(4)	N(1)-O(5)-C(9)	108.9(2)
O(6)-C(16)	1.231(3)	O(1)-C(1)-N(1)	122.6(3)
O(7)-C(21)	1.404(3)	O(1)-C(1)-C(2)	123.8(3)

N(1)-C(1)-C(2)	113.4(3)	C(11)-C(10)-C(15)	120.6(4)
C(1)-C(2)-C(3)	110.9(3)	C(11)-C(10)-C(9)	119.7(4)
C(1)-C(2)-C(7)	111.7(3)	C(15)-C(10)-C(9)	119.7(3)
C(3)-C(2)-C(7)	113.7(3)	C(12)-C(11)-C(10)	121.7(5)
C(1)-C(2)-H(2A)	106.7	C(12)-C(11)-H(11A)	119.2
C(3)-C(2)-H(2A)	106.7	C(10)-C(11)-H(11A)	119.2
C(7)-C(2)-H(2A)	106.7	C(13)-C(12)-C(11)	120.5(5)
O(2)-C(3)-C(2)	107.2(2)	C(13)-C(12)-H(12A)	119.7
O(2)-C(3)-C(4)	104.9(2)	C(11)-C(12)-H(12A)	119.7
C(2)-C(3)-C(4)	114.3(2)	C(12)-C(13)-C(14)	121.5(5)
O(2)-C(3)-H(3B)	110.1	C(12)-C(13)-H(13A)	119.3
C(2)-C(3)-H(3B)	110.1	C(14)-C(13)-H(13A)	119.3
C(4)-C(3)-H(3B)	110.1	C(15)-C(14)-C(13)	117.4(4)
O(3)-C(4)-C(3)	106.7(2)	C(15)-C(14)-H(14A)	121.3
O(3)-C(4)-C(5)	113.2(2)	C(13)-C(14)-H(14A)	121.3
C(3)-C(4)-C(5)	102.6(2)	C(10)-C(15)-C(14)	118.2(4)
O(3)-C(4)-H(4B)	111.3	C(10)-C(15)-H(15A)	120.9
C(3)-C(4)-H(4B)	111.3	C(14)-C(15)-H(15A)	120.9
C(5)-C(4)-H(4B)	111.3	C(16)-N(2)-O(10)	117.4(2)
O(4)-C(5)-C(6)	111.8(2)	C(16)-N(2)-C(21)	124.8(2)
O(4)-C(5)-C(4)	113.5(2)	O(10)-N(2)-C(21)	112.4(2)
C(6)-C(5)-C(4)	102.2(2)	C(21)-O(7)-C(18)	102.4(2)
O(4)-C(5)-H(5A)	109.7	C(19)-O(8)-H(8D)	109.5
C(6)-C(5)-H(5A)	109.7	C(20)-O(9)-H(9C)	109.5
C(4)-C(5)-H(5A)	109.7	N(2)-O(10)-C(24)	109.7(2)
O(2)-C(6)-N(1)	107.3(2)	O(6)-C(16)-N(2)	122.2(3)
O(2)-C(6)-C(5)	104.5(2)	O(6)-C(16)-C(17)	123.0(3)
N(1)-C(6)-C(5)	111.6(2)	N(2)-C(16)-C(17)	114.8(3)
O(2)-C(6)-H(6A)	111.1	C(22)-C(17)-C(18)	114.8(2)
N(1)-C(6)-H(6A)	111.1	C(22)-C(17)-C(16)	111.0(2)
C(5)-C(6)-H(6A)	111.1	C(18)-C(17)-C(16)	108.7(2)
C(8)-C(7)-C(2)	113.4(3)	C(22)-C(17)-H(17A)	107.3
C(8)-C(7)-H(7A)	108.9	C(18)-C(17)-H(17A)	107.3
C(2)-C(7)-H(7A)	108.9	C(16)-C(17)-H(17A)	107.3
C(8)-C(7)-H(7B)	108.9	O(7)-C(18)-C(17)	106.2(2)
C(2)-C(7)-H(7B)	108.9	O(7)-C(18)-C(19)	105.1(2)
H(7A)-C(7)-H(7B)	107.7	C(17)-C(18)-C(19)	112.8(2)
C(7)-C(8)-H(8A)	109.5	O(7)-C(18)-H(18A)	110.8
C(7)-C(8)-H(8B)	109.5	C(17)-C(18)-H(18A)	110.8
H(8A)-C(8)-H(8B)	109.5	C(19)-C(18)-H(18A)	110.8
C(7)-C(8)-H(8C)	109.5	O(8)-C(19)-C(18)	114.5(2)
H(8A)-C(8)-H(8C)	109.5	O(8)-C(19)-C(20)	113.7(2)
H(8B)-C(8)-H(8C)	109.5	C(18)-C(19)-C(20)	103.5(2)
O(5)-C(9)-C(10)	107.5(3)	O(8)-C(19)-H(19A)	108.3
O(5)-C(9)-H(9A)	110.2	C(18)-C(19)-H(19A)	108.3
C(10)-C(9)-H(9A)	110.2	C(20)-C(19)-H(19A)	108.3
O(5)-C(9)-H(9B)	110.2	O(9)-C(20)-C(21)	107.0(2)
C(10)-C(9)-H(9B)	110.2	O(9)-C(20)-C(19)	111.7(2)
H(9A)-C(9)-H(9B)	108.5	C(21)-C(20)-C(19)	100.0(2)

O(9)-C(20)-H(20A)	112.5	C(25)-C(24)-H(24A)	109.1
C(21)-C(20)-H(20A)	112.5	O(10)-C(24)-H(24B)	109.1
C(19)-C(20)-H(20A)	112.5	C(25)-C(24)-H(24B)	109.1
O(7)-C(21)-N(2)	108.0(2)	H(24A)-C(24)-H(24B)	107.8
O(7)-C(21)-C(20)	103.5(2)	C(30)-C(25)-C(26)	118.9(3)
N(2)-C(21)-C(20)	111.1(2)	C(30)-C(25)-C(24)	119.6(3)
O(7)-C(21)-H(21A)	111.3	C(26)-C(25)-C(24)	121.5(3)
N(2)-C(21)-H(21A)	111.3	C(27)-C(26)-C(25)	121.0(3)
C(20)-C(21)-H(21A)	111.3	C(27)-C(26)-H(26A)	119.5
C(23)-C(22)-C(17)	112.6(3)	C(25)-C(26)-H(26A)	119.5
C(23)-C(22)-H(22A)	109.1	C(26)-C(27)-C(28)	119.4(3)
C(17)-C(22)-H(22A)	109.1	C(26)-C(27)-H(27A)	120.3
C(23)-C(22)-H(22B)	109.1	C(28)-C(27)-H(27A)	120.3
C(17)-C(22)-H(22B)	109.1	C(29)-C(28)-C(27)	120.1(3)
H(22A)-C(22)-H(22B)	107.8	C(29)-C(28)-H(28A)	120.0
C(22)-C(23)-H(23A)	109.5	C(27)-C(28)-H(28A)	120.0
C(22)-C(23)-H(23B)	109.5	C(28)-C(29)-C(30)	120.2(3)
H(23A)-C(23)-H(23B)	109.5	C(28)-C(29)-H(29A)	119.9
C(22)-C(23)-H(23C)	109.5	C(30)-C(29)-H(29A)	119.9
H(23A)-C(23)-H(23C)	109.5	C(25)-C(30)-C(29)	120.5(3)
H(23B)-C(23)-H(23C)	109.5	C(25)-C(30)-H(30A)	119.8
O(10)-C(24)-C(25)	112.6(2)	C(29)-C(30)-H(30A)	119.8
O(10)-C(24)-H(24A)	109.1		

Table A.3.7. Torsion angles [°] for **95**.

C(1)-N(1)-O(5)-C(9)	91.7(3)	C(16)-N(2)-O(10)-C(24)	86.9(3)
C(6)-N(1)-O(5)-C(9)	-117.6(3)	C(21)-N(2)-O(10)-C(24)	-117.7(2)
O(5)-N(1)-C(1)-O(1)	-12.9(4)	O(10)-N(2)-C(16)-O(6)	-16.7(4)
C(6)-N(1)-C(1)-O(1)	-160.3(3)	C(21)-N(2)-C(16)-O(6)	-168.8(3)
O(5)-N(1)-C(1)-C(2)	172.0(2)	O(10)-N(2)-C(16)-C(17)	166.1(2)
C(6)-N(1)-C(1)-C(2)	24.6(4)	C(21)-N(2)-C(16)-C(17)	14.1(4)
O(1)-C(1)-C(2)-C(3)	157.4(3)	O(6)-C(16)-C(17)-C(22)	31.6(4)
N(1)-C(1)-C(2)-C(3)	-27.5(4)	N(2)-C(16)-C(17)-C(22)	-151.3(3)
O(1)-C(1)-C(2)-C(7)	29.5(4)	O(6)-C(16)-C(17)-C(18)	158.8(3)
N(1)-C(1)-C(2)-C(7)	-155.4(3)	N(2)-C(16)-C(17)-C(18)	-24.1(3)
C(6)-O(2)-C(3)-C(2)	-77.2(3)	C(21)-O(7)-C(18)-C(17)	-80.9(3)
C(6)-O(2)-C(3)-C(4)	44.7(3)	C(21)-O(7)-C(18)-C(19)	39.0(3)
C(1)-C(2)-C(3)-O(2)	54.9(3)	C(22)-C(17)-C(18)-O(7)	-177.4(2)
C(7)-C(2)-C(3)-O(2)	-178.3(2)	C(16)-C(17)-C(18)-O(7)	57.5(3)
C(1)-C(2)-C(3)-C(4)	-60.9(3)	C(22)-C(17)-C(18)-C(19)	67.9(3)
C(7)-C(2)-C(3)-C(4)	65.9(3)	C(16)-C(17)-C(18)-C(19)	-57.1(3)
O(2)-C(3)-C(4)-O(3)	96.6(3)	O(7)-C(18)-C(19)-O(8)	112.9(3)
C(2)-C(3)-C(4)-O(3)	-146.2(3)	C(17)-C(18)-C(19)-O(8)	-131.8(3)
O(2)-C(3)-C(4)-C(5)	-22.7(3)	O(7)-C(18)-C(19)-C(20)	-11.3(3)
C(2)-C(3)-C(4)-C(5)	94.5(3)	C(17)-C(18)-C(19)-C(20)	104.0(3)
O(3)-C(4)-C(5)-O(4)	0.3(3)	O(8)-C(19)-C(20)-O(9)	-29.6(3)
C(3)-C(4)-C(5)-O(4)	114.9(3)	C(18)-C(19)-C(20)-O(9)	95.2(3)
O(3)-C(4)-C(5)-C(6)	-120.3(3)	O(8)-C(19)-C(20)-C(21)	-142.6(2)
C(3)-C(4)-C(5)-C(6)	-5.7(3)	C(18)-C(19)-C(20)-C(21)	-17.8(3)
C(3)-O(2)-C(6)-N(1)	69.7(3)	C(18)-O(7)-C(21)-N(2)	66.0(3)
C(3)-O(2)-C(6)-C(5)	-48.9(3)	C(18)-O(7)-C(21)-C(20)	-51.9(3)
C(1)-N(1)-C(6)-O(2)	-46.9(3)	C(16)-N(2)-C(21)-O(7)	-35.7(4)
O(5)-N(1)-C(6)-O(2)	164.3(2)	O(10)-N(2)-C(21)-O(7)	171.0(2)
C(1)-N(1)-C(6)-C(5)	67.0(3)	C(16)-N(2)-C(21)-C(20)	77.1(3)
O(5)-N(1)-C(6)-C(5)	-81.8(3)	O(10)-N(2)-C(21)-C(20)	-76.2(3)
O(4)-C(5)-C(6)-O(2)	-88.5(3)	O(9)-C(20)-C(21)-O(7)	-73.6(3)
C(4)-C(5)-C(6)-O(2)	33.3(3)	C(19)-C(20)-C(21)-O(7)	42.9(3)
O(4)-C(5)-C(6)-N(1)	155.9(2)	O(9)-C(20)-C(21)-N(2)	170.7(2)
C(4)-C(5)-C(6)-N(1)	-82.3(3)	C(19)-C(20)-C(21)-N(2)	-72.8(3)
C(1)-C(2)-C(7)-C(8)	-169.6(3)	C(18)-C(17)-C(22)-C(23)	67.5(3)
C(3)-C(2)-C(7)-C(8)	64.0(4)	C(16)-C(17)-C(22)-C(23)	-168.7(2)
N(1)-O(5)-C(9)-C(10)	-176.1(3)	N(2)-O(10)-C(24)-C(25)	65.3(3)
O(5)-C(9)-C(10)-C(11)	-86.9(4)	O(10)-C(24)-C(25)-C(30)	-122.1(3)
O(5)-C(9)-C(10)-C(15)	92.6(4)	O(10)-C(24)-C(25)-C(26)	60.0(4)
C(15)-C(10)-C(11)-C(12)	0.0(5)	C(30)-C(25)-C(26)-C(27)	-0.3(5)
C(9)-C(10)-C(11)-C(12)	179.5(4)	C(24)-C(25)-C(26)-C(27)	177.6(3)
C(10)-C(11)-C(12)-C(13)	-0.3(7)	C(25)-C(26)-C(27)-C(28)	-0.2(5)
C(11)-C(12)-C(13)-C(14)	0.0(7)	C(26)-C(27)-C(28)-C(29)	0.4(5)
C(12)-C(13)-C(14)-C(15)	0.5(6)	C(27)-C(28)-C(29)-C(30)	-0.1(5)
C(11)-C(10)-C(15)-C(14)	0.6(5)	C(26)-C(25)-C(30)-C(29)	0.6(5)
C(9)-C(10)-C(15)-C(14)	-178.9(3)	C(24)-C(25)-C(30)-C(29)	-177.4(3)
C(13)-C(14)-C(15)-C(10)	-0.8(5)	C(28)-C(29)-C(30)-C(25)	-0.4(5)

Table A.3.8. Hydrogen bonds for **95** [Å and °].

D-H...A	d(D-H)	d(H...A)	d(D...A)	<(DHA)
O(3)-H(3A)...O(9)#1	0.84	2.02	2.829(3)	160.2
O(4)-H(4A)...O(6)#2	0.84	1.97	2.771(3)	160.4
O(8)-H(8D)...O(4)#1	0.84	1.91	2.739(3)	169.1
O(9)-H(9C)...O(8)#3	0.84	1.88	2.706(3)	169.0

Symmetry transformations used to generate equivalent atoms:
#1 -x+1,-y+2,-z+1 #2 -x,-y+2,-z+1 #3 -x+1,-y+2,-z+2

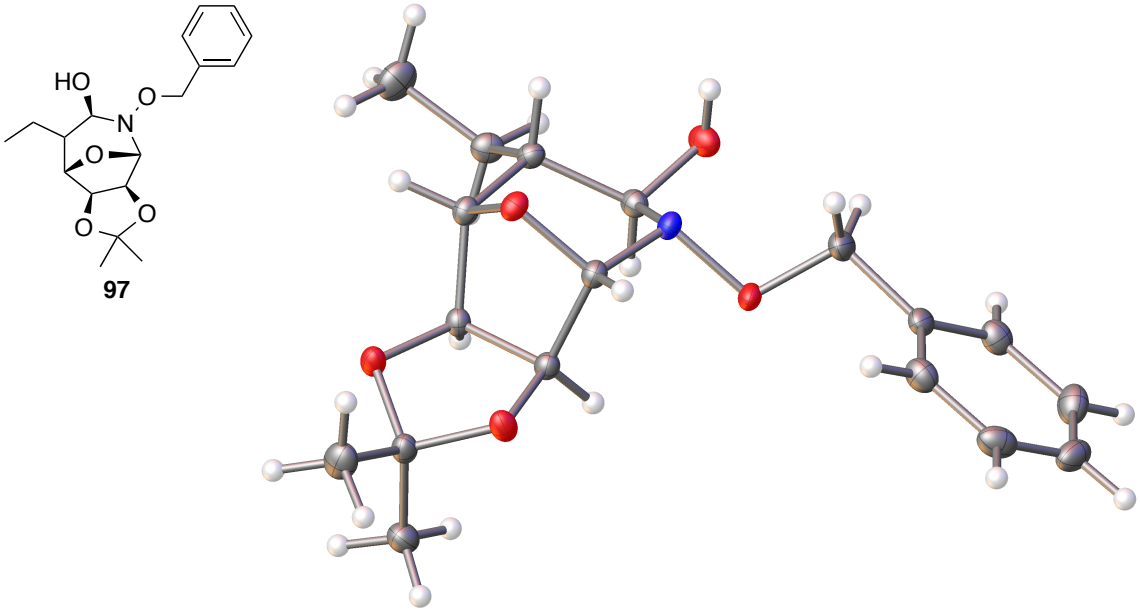

Figure A.3.3 Thermal ellipsoid plot of **97** at 50% probability. Hydrogen atoms are represented as spheres of arbitrary radius. Grey = carbon, red = oxygen, blue = nitrogen.

Table A.3.9. Crystal data and structure refinement for **97**.

Identification code	kb003	
Empirical formula	$C_{36}H_{50}N_2O_{10}$	
Formula weight	670.78	
Temperature	293(2) K	
Wavelength	0.71073 Å	
Crystal system	Triclinic	
Space group	P-1	
Unit cell dimensions	*a* = 10.5811(3) Å	α = 95.6920(10)°.
	b = 10.6861(4) Å	β = 103.3680(10)°.
	c = 17.8639(6) Å	γ = 115.7510(10)°.
Volume	1723.45(10) $Å^3$	
Z	2	
Density (calculated)	1.293 Mg/m^3	
Absorption coefficient	0.094 mm^{-1}	
F(000)	720	
Crystal size	0.26 x 0.16 x 0.10 mm^3	
Theta range for data collection	2.17 to 29.13°.	
Index ranges	-14<=h<=14, -14<=k<=14, -24<=l<=24	
Reflections collected	39853	
Independent reflections	9290 [R(int) = 0.0347]	
Completeness to theta = 29.13°	99.9 %	
Absorption correction	SADABS	
Max. and min. transmission	0.9905 and 0.9764	
Refinement method	Full-matrix least-squares on F^2	
Data / restraints / parameters	9290 / 0 / 439	
Goodness-of-fit on F^2	1.016	
Final R indices [I>2sigma(I)]	R1 = 0.0411, wR2 = 0.1019	
R indices (all data)	R1 = 0.0594, wR2 = 0.1128	
Largest diff. peak and hole	0.369 and -0.225 $e.Å^{-3}$	

Table A.3.10. Bond lengths [Å] and angles [°] for **97**.

O(1)-C(9)	1.4225(13)	C(16)-C(17)	1.3824(19)
O(1)-C(3)	1.4562(13)	C(16)-H(16A)	0.9300
N(1)-O(5)	1.4511(12)	C(17)-C(18)	1.3949(17)
N(1)-C(9)	1.4697(14)	C(17)-H(17A)	0.9300
N(1)-C(1)	1.4717(14)	C(18)-H(18A)	0.9300
C(1)-O(4)	1.4092(13)	N(2)-O(10)	1.4512(12)
C(1)-C(2)	1.5367(15)	N(2)-C(27)	1.4702(15)
C(1)-H(1A)	0.9800	N(2)-C(19)	1.4719(15)
O(2)-C(4)	1.4243(13)	O(6)-C(27)	1.4225(13)
O(2)-C(5)	1.4343(13)	O(6)-C(21)	1.4568(13)
C(2)-C(3)	1.5259(15)	O(7)-C(22)	1.4263(13)
C(2)-C(10)	1.5345(15)	O(7)-C(23)	1.4345(13)
C(2)-H(2A)	0.9800	O(8)-C(26)	1.4220(14)
O(3)-C(8)	1.4210(13)	O(8)-C(23)	1.4312(14)
O(3)-C(5)	1.4331(13)	O(9)-C(19)	1.4079(14)
C(3)-C(4)	1.5286(15)	O(9)-H(9B)	0.8200
C(3)-H(3A)	0.9800	O(10)-C(30)	1.4382(14)
O(4)-H(4A)	0.8200	C(19)-C(20)	1.5379(16)
C(4)-C(8)	1.5468(15)	C(19)-H(19A)	0.9800
C(4)-H(4B)	0.9800	C(20)-C(21)	1.5300(16)
O(5)-C(12)	1.4424(14)	C(20)-C(28)	1.5355(15)
C(5)-C(7)	1.5087(16)	C(20)-H(20A)	0.9800
C(5)-C(6)	1.5155(17)	C(21)-C(22)	1.5261(16)
C(6)-H(6A)	0.9600	C(21)-H(21A)	0.9800
C(6)-H(6B)	0.9600	C(22)-C(26)	1.5488(15)
C(6)-H(6C)	0.9600	C(22)-H(22A)	0.9800
C(7)-H(7A)	0.9600	C(23)-C(24)	1.5075(17)
C(7)-H(7B)	0.9600	C(23)-C(25)	1.5123(17)
C(7)-H(7C)	0.9600	C(24)-H(24A)	0.9600
C(8)-C(9)	1.5311(15)	C(24)-H(24B)	0.9600
C(8)-H(8A)	0.9800	C(24)-H(24C)	0.9600
C(9)-H(9A)	0.9800	C(25)-H(25A)	0.9600
C(10)-C(11)	1.5238(17)	C(25)-H(25B)	0.9600
C(10)-H(10A)	0.9700	C(25)-H(25C)	0.9600
C(10)-H(10B)	0.9700	C(26)-C(27)	1.5289(16)
C(11)-H(11A)	0.9600	C(26)-H(26A)	0.9800
C(11)-H(11B)	0.9600	C(27)-H(27A)	0.9800
C(11)-H(11C)	0.9600	C(28)-C(29)	1.5231(17)
C(12)-C(13)	1.5058(16)	C(28)-H(28A)	0.9700
C(12)-H(12A)	0.9700	C(28)-H(28B)	0.9700
C(12)-H(12B)	0.9700	C(29)-H(29A)	0.9600
C(13)-C(14)	1.3896(17)	C(29)-H(29B)	0.9600
C(13)-C(18)	1.3919(17)	C(29)-H(29C)	0.9600
C(14)-C(15)	1.3849(18)	C(30)-C(31)	1.5000(17)
C(14)-H(14A)	0.9300	C(30)-H(30A)	0.9700
C(15)-C(16)	1.383(2)	C(30)-H(30B)	0.9700
C(15)-H(15A)	0.9300	C(31)-C(36)	1.3911(17)

C(31)-C(32)	1.3930(17)	C(5)-C(6)-H(6A)	109.5
C(32)-C(33)	1.3911(18)	C(5)-C(6)-H(6B)	109.5
C(32)-H(32A)	0.9300	H(6A)-C(6)-H(6B)	109.5
C(33)-C(34)	1.387(2)	C(5)-C(6)-H(6C)	109.5
C(33)-H(33A)	0.9300	H(6A)-C(6)-H(6C)	109.5
C(34)-C(35)	1.3836(19)	H(6B)-C(6)-H(6C)	109.5
C(34)-H(34A)	0.9300	C(5)-C(7)-H(7A)	109.5
C(35)-C(36)	1.3835(19)	C(5)-C(7)-H(7B)	109.5
C(35)-H(35A)	0.9300	H(7A)-C(7)-H(7B)	109.5
C(36)-H(36A)	0.9300	C(5)-C(7)-H(7C)	109.5
		H(7A)-C(7)-H(7C)	109.5
C(9)-O(1)-C(3)	103.03(8)	H(7B)-C(7)-H(7C)	109.5
O(5)-N(1)-C(9)	105.04(8)	O(3)-C(8)-C(9)	109.70(9)
O(5)-N(1)-C(1)	107.90(8)	O(3)-C(8)-C(4)	104.85(8)
C(9)-N(1)-C(1)	113.58(9)	C(9)-C(8)-C(4)	102.99(9)
O(4)-C(1)-N(1)	108.62(9)	O(3)-C(8)-H(8A)	112.9
O(4)-C(1)-C(2)	111.66(9)	C(9)-C(8)-H(8A)	112.9
N(1)-C(1)-C(2)	110.27(9)	C(4)-C(8)-H(8A)	112.9
O(4)-C(1)-H(1A)	108.7	O(1)-C(9)-N(1)	106.93(8)
N(1)-C(1)-H(1A)	108.7	O(1)-C(9)-C(8)	104.25(9)
C(2)-C(1)-H(1A)	108.7	N(1)-C(9)-C(8)	114.18(9)
C(4)-O(2)-C(5)	107.23(8)	O(1)-C(9)-H(9A)	110.4
C(3)-C(2)-C(10)	114.44(9)	N(1)-C(9)-H(9A)	110.4
C(3)-C(2)-C(1)	109.82(9)	C(8)-C(9)-H(9A)	110.4
C(10)-C(2)-C(1)	110.28(9)	C(11)-C(10)-C(2)	113.77(10)
C(3)-C(2)-H(2A)	107.3	C(11)-C(10)-H(10A)	108.8
C(10)-C(2)-H(2A)	107.3	C(2)-C(10)-H(10A)	108.8
C(1)-C(2)-H(2A)	107.3	C(11)-C(10)-H(10B)	108.8
C(8)-O(3)-C(5)	107.17(8)	C(2)-C(10)-H(10B)	108.8
O(1)-C(3)-C(2)	107.57(9)	H(10A)-C(10)-H(10B)	107.7
O(1)-C(3)-C(4)	102.96(8)	C(10)-C(11)-H(11A)	109.5
C(2)-C(3)-C(4)	113.98(9)	C(10)-C(11)-H(11B)	109.5
O(1)-C(3)-H(3A)	110.7	H(11A)-C(11)-H(11B)	109.5
C(2)-C(3)-H(3A)	110.7	C(10)-C(11)-H(11C)	109.5
C(4)-C(3)-H(3A)	110.7	H(11A)-C(11)-H(11C)	109.5
C(1)-O(4)-H(4A)	109.5	H(11B)-C(11)-H(11C)	109.5
O(2)-C(4)-C(3)	109.79(9)	O(5)-C(12)-C(13)	108.56(9)
O(2)-C(4)-C(8)	104.26(8)	O(5)-C(12)-H(12A)	110.0
C(3)-C(4)-C(8)	103.72(9)	C(13)-C(12)-H(12A)	110.0
O(2)-C(4)-H(4B)	112.8	O(5)-C(12)-H(12B)	110.0
C(3)-C(4)-H(4B)	112.8	C(13)-C(12)-H(12B)	110.0
C(8)-C(4)-H(4B)	112.8	H(12A)-C(12)-H(12B)	108.4
C(12)-O(5)-N(1)	108.25(8)	C(14)-C(13)-C(18)	119.08(11)
O(3)-C(5)-O(2)	104.16(8)	C(14)-C(13)-C(12)	120.41(11)
O(3)-C(5)-C(7)	108.08(9)	C(18)-C(13)-C(12)	120.47(11)
O(2)-C(5)-C(7)	108.84(9)	C(15)-C(14)-C(13)	120.67(12)
O(3)-C(5)-C(6)	111.18(9)	C(15)-C(14)-H(14A)	119.7
O(2)-C(5)-C(6)	110.45(9)	C(13)-C(14)-H(14A)	119.7
C(7)-C(5)-C(6)	113.66(10)	C(16)-C(15)-C(14)	119.99(12)

C(16)-C(15)-H(15A)	120.0	C(23)-C(24)-H(24A)	109.5
C(14)-C(15)-H(15A)	120.0	C(23)-C(24)-H(24B)	109.5
C(17)-C(16)-C(15)	120.09(12)	H(24A)-C(24)-H(24B)	109.5
C(17)-C(16)-H(16A)	120.0	C(23)-C(24)-H(24C)	109.5
C(15)-C(16)-H(16A)	120.0	H(24A)-C(24)-H(24C)	109.5
C(16)-C(17)-C(18)	119.98(12)	H(24B)-C(24)-H(24C)	109.5
C(16)-C(17)-H(17A)	120.0	C(23)-C(25)-H(25A)	109.5
C(18)-C(17)-H(17A)	120.0	C(23)-C(25)-H(25B)	109.5
C(13)-C(18)-C(17)	120.16(11)	H(25A)-C(25)-H(25B)	109.5
C(13)-C(18)-H(18A)	119.9	C(23)-C(25)-H(25C)	109.5
C(17)-C(18)-H(18A)	119.9	H(25A)-C(25)-H(25C)	109.5
O(10)-N(2)-C(27)	106.07(8)	H(25B)-C(25)-H(25C)	109.5
O(10)-N(2)-C(19)	105.46(8)	O(8)-C(26)-C(27)	109.63(9)
C(27)-N(2)-C(19)	113.46(9)	O(8)-C(26)-C(22)	104.63(9)
C(27)-O(6)-C(21)	102.76(8)	C(27)-C(26)-C(22)	103.09(9)
C(22)-O(7)-C(23)	106.91(8)	O(8)-C(26)-H(26A)	112.9
C(26)-O(8)-C(23)	107.08(8)	C(27)-C(26)-H(26A)	112.9
C(19)-O(9)-H(9B)	109.5	C(22)-C(26)-H(26A)	112.9
C(30)-O(10)-N(2)	108.79(8)	O(6)-C(27)-N(2)	106.69(9)
O(9)-C(19)-N(2)	108.85(9)	O(6)-C(27)-C(26)	104.57(9)
O(9)-C(19)-C(20)	112.29(9)	N(2)-C(27)-C(26)	114.55(9)
N(2)-C(19)-C(20)	110.61(9)	O(6)-C(27)-H(27A)	110.3
O(9)-C(19)-H(19A)	108.3	N(2)-C(27)-H(27A)	110.3
N(2)-C(19)-H(19A)	108.3	C(26)-C(27)-H(27A)	110.3
C(20)-C(19)-H(19A)	108.3	C(29)-C(28)-C(20)	113.51(10)
C(21)-C(20)-C(28)	114.25(10)	C(29)-C(28)-H(28A)	108.9
C(21)-C(20)-C(19)	109.96(9)	C(20)-C(28)-H(28A)	108.9
C(28)-C(20)-C(19)	109.74(9)	C(29)-C(28)-H(28B)	108.9
C(21)-C(20)-H(20A)	107.5	C(20)-C(28)-H(28B)	108.9
C(28)-C(20)-H(20A)	107.5	H(28A)-C(28)-H(28B)	107.7
C(19)-C(20)-H(20A)	107.5	C(28)-C(29)-H(29A)	109.5
O(6)-C(21)-C(22)	103.34(8)	C(28)-C(29)-H(29B)	109.5
O(6)-C(21)-C(20)	107.46(9)	H(29A)-C(29)-H(29B)	109.5
C(22)-C(21)-C(20)	114.11(9)	C(28)-C(29)-H(29C)	109.5
O(6)-C(21)-H(21A)	110.6	H(29A)-C(29)-H(29C)	109.5
C(22)-C(21)-H(21A)	110.6	H(29B)-C(29)-H(29C)	109.5
C(20)-C(21)-H(21A)	110.6	O(10)-C(30)-C(31)	107.28(10)
O(7)-C(22)-C(21)	110.21(9)	O(10)-C(30)-H(30A)	110.3
O(7)-C(22)-C(26)	104.19(9)	C(31)-C(30)-H(30A)	110.3
C(21)-C(22)-C(26)	103.42(9)	O(10)-C(30)-H(30B)	110.3
O(7)-C(22)-H(22A)	112.8	C(31)-C(30)-H(30B)	110.3
C(21)-C(22)-H(22A)	112.8	H(30A)-C(30)-H(30B)	108.5
C(26)-C(22)-H(22A)	112.8	C(36)-C(31)-C(32)	119.09(11)
O(8)-C(23)-O(7)	103.96(9)	C(36)-C(31)-C(30)	119.42(11)
O(8)-C(23)-C(24)	108.42(10)	C(32)-C(31)-C(30)	121.49(12)
O(7)-C(23)-C(24)	109.11(10)	C(33)-C(32)-C(31)	120.13(12)
O(8)-C(23)-C(25)	111.04(10)	C(33)-C(32)-H(32A)	119.9
O(7)-C(23)-C(25)	110.83(10)	C(31)-C(32)-H(32A)	119.9
C(24)-C(23)-C(25)	113.06(11)	C(34)-C(33)-C(32)	120.16(12)

C(34)-C(33)-H(33A)	119.9	C(34)-C(35)-H(35A)	119.9
C(32)-C(33)-H(33A)	119.9	C(36)-C(35)-H(35A)	119.9
C(35)-C(34)-C(33)	119.81(12)	C(35)-C(36)-C(31)	120.67(11)
C(35)-C(34)-H(34A)	120.1	C(35)-C(36)-H(36A)	119.7
C(33)-C(34)-H(34A)	120.1	C(31)-C(36)-H(36A)	119.7
C(34)-C(35)-C(36)	120.12(13)		

Table A.3.11. Torsion angles [°] for **97**.

O(5)-N(1)-C(1)-O(4)	-74.95(10)	O(3)-C(8)-C(9)-O(1)	-83.65(10)
C(9)-N(1)-C(1)-O(4)	169.04(9)	C(4)-C(8)-C(9)-O(1)	27.57(10)
O(5)-N(1)-C(1)-C(2)	162.39(8)	O(3)-C(8)-C(9)-N(1)	160.03(8)
C(9)-N(1)-C(1)-C(2)	46.38(12)	C(4)-C(8)-C(9)-N(1)	-88.75(10)
O(4)-C(1)-C(2)-C(3)	-164.66(9)	C(3)-C(2)-C(10)-C(11)	69.06(13)
N(1)-C(1)-C(2)-C(3)	-43.81(12)	C(1)-C(2)-C(10)-C(11)	-166.54(10)
O(4)-C(1)-C(2)-C(10)	68.32(12)	N(1)-O(5)-C(12)-C(13)	164.91(9)
N(1)-C(1)-C(2)-C(10)	-170.82(9)	O(5)-C(12)-C(13)-C(14)	-72.42(14)
C(9)-O(1)-C(3)-C(2)	-74.00(10)	O(5)-C(12)-C(13)-C(18)	109.57(12)
C(9)-O(1)-C(3)-C(4)	46.69(10)	C(18)-C(13)-C(14)-C(15)	1.12(18)
C(10)-C(2)-C(3)-O(1)	-176.58(9)	C(12)-C(13)-C(14)-C(15)	-176.92(11)
C(1)-C(2)-C(3)-O(1)	58.78(11)	C(13)-C(14)-C(15)-C(16)	0.35(19)
C(10)-C(2)-C(3)-C(4)	69.94(12)	C(14)-C(15)-C(16)-C(17)	-1.6(2)
C(1)-C(2)-C(3)-C(4)	-54.70(12)	C(15)-C(16)-C(17)-C(18)	1.4(2)
C(5)-O(2)-C(4)-C(3)	-132.01(9)	C(14)-C(13)-C(18)-C(17)	-1.35(18)
C(5)-O(2)-C(4)-C(8)	-21.43(11)	C(12)-C(13)-C(18)-C(17)	176.68(11)
O(1)-C(3)-C(4)-O(2)	83.06(10)	C(16)-C(17)-C(18)-C(13)	0.12(19)
C(2)-C(3)-C(4)-O(2)	-160.75(9)	C(27)-N(2)-O(10)-C(30)	116.48(10)
O(1)-C(3)-C(4)-C(8)	-27.88(10)	C(19)-N(2)-O(10)-C(30)	-122.90(10)
C(2)-C(3)-C(4)-C(8)	88.31(10)	O(10)-N(2)-C(19)-O(9)	74.81(10)
C(9)-N(1)-O(5)-C(12)	-132.25(9)	C(27)-N(2)-C(19)-O(9)	-169.53(9)
C(1)-N(1)-O(5)-C(12)	106.28(10)	O(10)-N(2)-C(19)-C(20)	-161.38(9)
C(8)-O(3)-C(5)-O(2)	-34.14(11)	C(27)-N(2)-C(19)-C(20)	-45.71(12)
C(8)-O(3)-C(5)-C(7)	-149.79(9)	O(9)-C(19)-C(20)-C(21)	164.51(9)
C(8)-O(3)-C(5)-C(6)	84.82(11)	N(2)-C(19)-C(20)-C(21)	42.70(12)
C(4)-O(2)-C(5)-O(3)	34.57(11)	O(9)-C(19)-C(20)-C(28)	-69.00(12)
C(4)-O(2)-C(5)-C(7)	149.68(10)	N(2)-C(19)-C(20)-C(28)	169.18(9)
C(4)-O(2)-C(5)-C(6)	-84.89(11)	C(27)-O(6)-C(21)-C(22)	-46.67(10)
C(5)-O(3)-C(8)-C(9)	130.55(9)	C(27)-O(6)-C(21)-C(20)	74.31(10)
C(5)-O(3)-C(8)-C(4)	20.56(11)	C(28)-C(20)-C(21)-O(6)	178.08(9)
O(2)-C(4)-C(8)-O(3)	0.53(11)	C(19)-C(20)-C(21)-O(6)	-58.02(11)
C(3)-C(4)-C(8)-O(3)	115.47(9)	C(28)-C(20)-C(21)-C(22)	-67.99(12)
O(2)-C(4)-C(8)-C(9)	-114.24(9)	C(19)-C(20)-C(21)-C(22)	55.91(12)
C(3)-C(4)-C(8)-C(9)	0.70(11)	C(23)-O(7)-C(22)-C(21)	132.61(9)
C(3)-O(1)-C(9)-N(1)	74.64(10)	C(23)-O(7)-C(22)-C(26)	22.23(11)
C(3)-O(1)-C(9)-C(8)	-46.64(10)	O(6)-C(21)-C(22)-O(7)	-82.56(10)
O(5)-N(1)-C(9)-O(1)	179.31(8)	C(20)-C(21)-C(22)-O(7)	161.09(9)
C(1)-N(1)-C(9)-O(1)	-63.01(11)	O(6)-C(21)-C(22)-C(26)	28.32(10)
O(5)-N(1)-C(9)-C(8)	-65.94(11)	C(20)-C(21)-C(22)-C(26)	-88.03(11)
C(1)-N(1)-C(9)-C(8)	51.75(12)	C(26)-O(8)-C(23)-O(7)	35.34(11)

C(26)-O(8)-C(23)-C(24)	151.34(10)
C(26)-O(8)-C(23)-C(25)	-83.89(11)
C(22)-O(7)-C(23)-O(8)	-35.79(11)
C(22)-O(7)-C(23)-C(24)	-151.30(10)
C(22)-O(7)-C(23)-C(25)	83.58(11)
C(23)-O(8)-C(26)-C(27)	-131.16(9)
C(23)-O(8)-C(26)-C(22)	-21.18(11)
O(7)-C(22)-C(26)-O(8)	-0.68(11)
C(21)-C(22)-C(26)-O(8)	-115.94(9)
O(7)-C(22)-C(26)-C(27)	113.98(9)
C(21)-C(22)-C(26)-C(27)	-1.28(11)
C(21)-O(6)-C(27)-N(2)	-75.62(10)
C(21)-O(6)-C(27)-C(26)	46.12(10)
O(10)-N(2)-C(27)-O(6)	178.63(8)
C(19)-N(2)-C(27)-O(6)	63.33(11)
O(10)-N(2)-C(27)-C(26)	63.44(11)
C(19)-N(2)-C(27)-C(26)	-51.86(12)
O(8)-C(26)-C(27)-O(6)	83.98(10)
C(22)-C(26)-C(27)-O(6)	-27.01(11)
O(8)-C(26)-C(27)-N(2)	-159.60(9)
C(22)-C(26)-C(27)-N(2)	89.41(10)
C(21)-C(20)-C(28)-C(29)	-62.96(14)
C(19)-C(20)-C(28)-C(29)	173.02(10)
N(2)-O(10)-C(30)-C(31)	162.52(10)
O(10)-C(30)-C(31)-C(36)	-76.15(14)
O(10)-C(30)-C(31)-C(32)	103.07(13)
C(36)-C(31)-C(32)-C(33)	-0.51(18)
C(30)-C(31)-C(32)-C(33)	-179.74(11)
C(31)-C(32)-C(33)-C(34)	0.97(19)
C(32)-C(33)-C(34)-C(35)	-0.3(2)
C(33)-C(34)-C(35)-C(36)	-0.8(2)
C(34)-C(35)-C(36)-C(31)	1.26(19)
C(32)-C(31)-C(36)-C(35)	-0.60(18)
C(30)-C(31)-C(36)-C(35)	178.64(11)

Symmetry transformations used to generate equivalent atoms:
#1 -x+1,-y+1,-z #2 -x+1,-y+1,-z+1

Table A.3.12. Hydrogen bonds for **97** [Å and °].

D-H...A	d(D-H)	d(H...A)	d(D...A)	<(DHA)
O(4)-H(4A)...O(1)#1	0.82	2.16	2.9708(12)	172.1
O(9)-H(9B)...O(6)#2	0.82	2.16	2.9815(12)	179.6

Symmetry transformations used to generate equivalent atoms:
#1 -x+1,-y+1,-z #2 -x+1,-y+1,-z+1

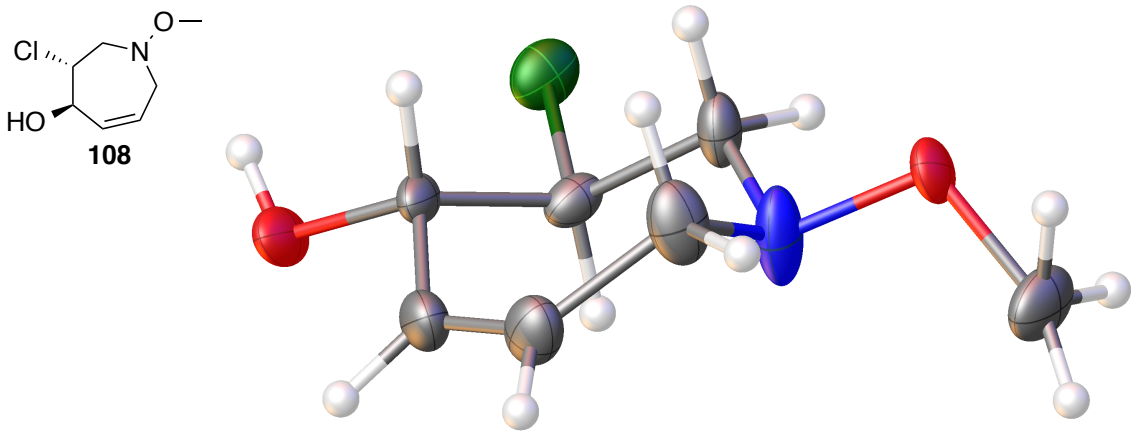

Figure A.3.4. Thermal ellipsoid plot of azepine **108** at 50% probability. Hydrogen atoms are represented as spheres of arbitrary radius. Gray = carbon, red = oxygen, blue = nitrogen, green = chlorine.

Table A.3.13. Crystal data and structure refinement for **108**.

CCDC no.	1028235	
Identification code	klb008_0m	
Empirical formula	C7 H7 Cl N O2	
Formula weight	172.59	
Temperature	100.15 K	
Wavelength	0.71073 Å	
Crystal system	Monoclinic	
Space group	*C*2/c	
Unit cell dimensions	a = 24.849(3) Å	α = 90°.
	b = 4.7231(5) Å	β = 103.467(2)°.
	c = 14.8643(17) Å	γ = 90°.
Volume	1696.6(3) $Å^3$	
Z	8	
Density (calculated)	1.351 Mg/m^3	
Absorption coefficient	0.400 mm^{-1}	
F(000)	712	
Crystal size	0.159 x 0.063 x 0.057 mm^3	
Theta range for data collection	1.685 to 26.426°.	
Index ranges	-30<=h<=30, -5<=k<=5, -18<=l<=18	
Reflections collected	12847	
Independent reflections	1736 [R(int) = 0.0616]	
Completeness to theta = 25.242°	100.0 %	
Absorption correction	Semi-empirical from equivalents	
Max. and min. transmission	0.7454 and 0.6525	
Refinement method	Full-matrix least-squares on F^2	
Data / restraints / parameters	1736 / 6 / 106	
Goodness-of-fit on F^2	1.000	
Final R indices [I>2sigma(I)]	R1 = 0.0562, wR2 = 0.1727	
R indices (all data)	R1 = 0.0797, wR2 = 0.1969	
Extinction coefficient	n/a	
Largest diff. peak and hole	0.894 and -0.478 $e.Å^{-3}$	

Table A.3.14. Bond lengths [Å] and angles [°] for **108**.

C(1)-C(2)	1.522(4)
C(1)-N(1)	1.471(4)
C(2)-C(3)	1.523(4)
C(2)-Cl(1)	1.812(3)
C(3)-C(4)	1.505(5)
C(3)-O(1)	1.423(3)
C(4)-C(5)	1.315(5)
C(5)-C(6)	1.498(5)
C(6)-N(1)	1.484(5)
C(7)-O(2)	1.426(4)
C(7)-O(2A)	1.598(13)
N(1)-O(2)	1.423(4)
N(1)-O(2A)	0.964(12)
N(1)-C(1)-C(2)	112.3(3)
C(1)-C(2)-Cl(1)	105.1(2)
C(3)-C(2)-C(1)	114.8(3)
C(3)-C(2)-Cl(1)	108.4(2)
C(4)-C(3)-C(2)	111.1(2)
O(1)-C(3)-C(2)	112.5(3)
O(1)-C(3)-C(4)	106.4(2)
C(5)-C(4)-C(3)	126.6(3)
C(4)-C(5)-C(6)	125.1(3)
N(1)-C(6)-C(5)	109.8(3)
C(1)-N(1)-C(6)	111.4(3)
O(2)-N(1)-C(1)	104.2(3)
O(2)-N(1)-C(6)	106.6(3)
O(2A)-N(1)-C(1)	130.0(8)
O(2A)-N(1)-C(6)	117.8(8)
C(7)-O(2)-N(1)	107.1(3)
N(1)-O(2A)-C(7)	125.0(11)

Table A.3.15. Torsion angles [°] for **108**.

C(1)-C(2)-C(3)-C(4)	-71.9(3)
C(1)-C(2)-C(3)-O(1)	169.0(3)
C(1)-N(1)-O(2)-C(7)	-136.7(3)
C(1)-N(1)-O(2A)-C(7)	101.7(11)
C(2)-C(1)-N(1)-C(6)	-78.1(4)
C(2)-C(1)-N(1)-O(2)	167.3(3)
C(2)-C(1)-N(1)-O(2A)	90.8(10)
C(2)-C(3)-C(4)-C(5)	56.7(4)
C(3)-C(4)-C(5)-C(6)	-2.2(6)
C(4)-C(5)-C(6)-N(1)	-59.3(5)
C(5)-C(6)-N(1)-C(1)	83.6(4)
C(5)-C(6)-N(1)-O(2)	-163.4(3)
C(5)-C(6)-N(1)-O(2A)	-86.8(9)
C(6)-N(1)-O(2)-C(7)	105.5(3)
C(6)-N(1)-O(2A)-C(7)	-89.9(11)
N(1)-C(1)-C(2)-C(3)	72.1(4)
N(1)-C(1)-C(2)-Cl(1)	-169.0(2)
O(1)-C(3)-C(4)-C(5)	179.4(3)
O(2)-C(7)-O(2A)-N(1)	-10.4(9)
O(2)-N(1)-O(2A)-C(7)	9.2(8)
O(2A)-C(7)-O(2)-N(1)	6.0(5)
O(2A)-N(1)-O(2)-C(7)	-8.8(8)
Cl(1)-C(2)-C(3)-C(4)	171.0(2)
Cl(1)-C(2)-C(3)-O(1)	51.9(3)

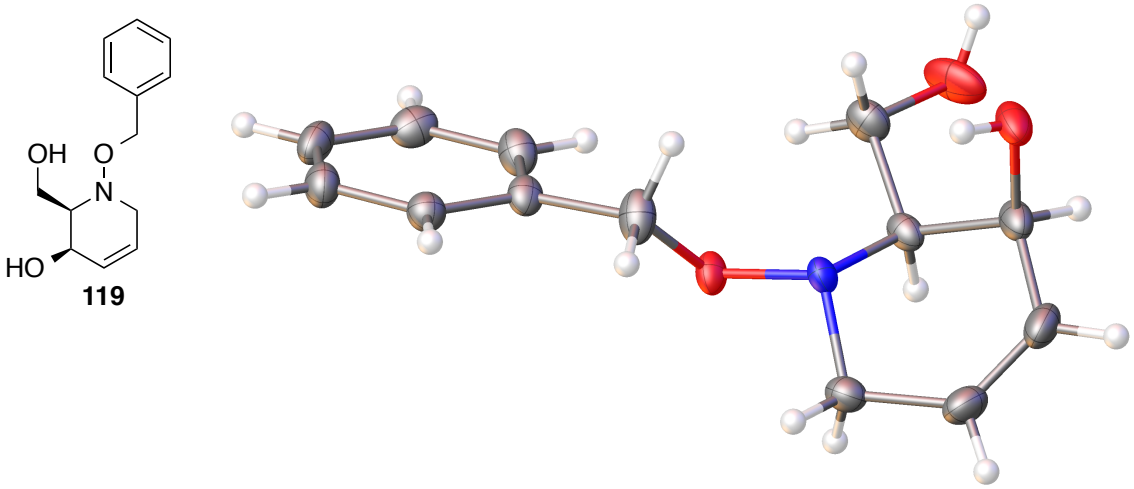

Figure A.3.5. Thermal ellipsoid plot of tetrahydropyridine **119** at 50% probability. Hydrogen atoms are represented as spheres of arbitrary radius. Gray = carbon, red = oxygen, blue = nitrogen.

Table A.3.16. Crystal data and structure refinement for **119**.

CCDC no.	1028236	
Identification code	klb009_0m	
Empirical formula	C26 H34 N2 O6	
Formula weight	470.55	
Temperature	99.65 K	
Wavelength	0.71073 Å	
Crystal system	Triclinic	
Space group	*P*-1	
Unit cell dimensions	*a* = 9.9549(4) Å	α = 106.4607(7)°.
	b = 11.3328(5) Å	β = 101.6175(7)°.
	c = 11.8818(5) Å	γ = 100.1738(7)°.
Volume	1219.60(9) $Å^3$	
Z	2	
Density (calculated)	1.281 Mg/m^3	
Absorption coefficient	0.091 mm^{-1}	
F(000)	504	
Crystal size	0.161 x 0.126 x 0.072 mm^3	
Theta range for data collection	1.854 to 26.413°.	
Index ranges	-12<=h<=12, -14<=k<=14, -14<=l<=14	
Reflections collected	23662	
Independent reflections	5015 [R(int) = 0.0515]	
Completeness to theta = 25.242°	100.0 %	
Absorption correction	Semi-empirical from equivalents	
Max. and min. transmission	0.7454 and 0.7196	
Refinement method	Full-matrix least-squares on F^2	
Data / restraints / parameters	5015 / 0 / 317	
Goodness-of-fit on F^2	1.000	
Final R indices [I>2sigma(I)]	R1 = 0.0367, wR2 = 0.0677	
R indices (all data)	R1 = 0.0618, wR2 = 0.0727	
Extinction coefficient	n/a	
Largest diff. peak and hole	0.209 and -0.188 $e.Å^{-3}$	

Table A.3.17. Bond lengths [Å] and angles [°] for **119**.

C(14)-C(15)	1.4928(18)	O(4)-C(17)-C(18)	112.60(10)
C(14)-N(2)	1.4654(16)	C(19)-C(18)-C(17)	112.10(10)
C(15)-C(16)	1.3203(18)	N(2)-C(18)-C(17)	107.16(10)
C(16)-C(17)	1.4974(17)	N(2)-C(18)-C(19)	111.69(10)
C(17)-C(18)	1.5323(17)	O(5)-C(19)-C(18)	107.66(10)
C(17)-O(4)	1.4369(15)	O(6)-C(20)-C(21)	106.61(10)
C(18)-C(19)	1.5120(17)	C(22)-C(21)-C(20)	120.88(13)
C(18)-N(2)	1.4757(15)	C(26)-C(21)-C(20)	120.31(12)
C(19)-O(5)	1.4286(14)	C(26)-C(21)-C(22)	118.80(13)
C(20)-C(21)	1.4999(17)	C(23)-C(22)-C(21)	120.32(14)
C(20)-O(6)	1.4366(14)	C(24)-C(23)-C(22)	120.30(14)
C(21)-C(22)	1.3855(18)	C(23)-C(24)-C(25)	119.86(14)
C(21)-C(26)	1.3837(18)	C(24)-C(25)-C(26)	119.89(14)
C(22)-C(23)	1.3860(19)	C(21)-C(26)-C(25)	120.82(14)
C(23)-C(24)	1.374(2)	C(14)-N(2)-C(18)	109.55(10)
C(24)-C(25)	1.379(2)	O(6)-N(2)-C(14)	103.67(9)
C(25)-C(26)	1.3821(18)	O(6)-N(2)-C(18)	106.96(9)
N(2)-O(6)	1.4588(12)	C(20)-O(6)-N(2)	107.97(8)
C(1)-C(2)	1.4917(19)	N(1)-C(1)-C(2)	109.19(11)
C(1)-N(1)	1.4653(16)	C(3)-C(2)-C(1)	122.54(14)
C(2)-C(3)	1.3216(19)	C(2)-C(3)-C(4)	122.00(13)
C(3)-C(4)	1.4948(19)	C(3)-C(4)-C(5)	111.16(11)
C(4)-C(5)	1.5294(18)	O(1)-C(4)-C(3)	110.80(11)
C(4)-O(1)	1.4366(15)	O(1)-C(4)-C(5)	111.44(11)
C(5)-C(6)	1.5135(18)	C(6)-C(5)-C(4)	112.03(11)
C(5)-N(1)	1.4702(15)	N(1)-C(5)-C(4)	105.42(10)
C(6)-O(2)	1.4267(15)	N(1)-C(5)-C(6)	111.74(10)
C(7)-C(8)	1.5016(18)	O(2)-C(6)-C(5)	108.65(11)
C(7)-O(3)	1.4305(15)	O(3)-C(7)-C(8)	109.43(10)
C(8)-C(9)	1.3918(18)	C(9)-C(8)-C(7)	121.74(12)
C(8)-C(13)	1.3875(17)	C(13)-C(8)-C(7)	119.48(12)
C(9)-C(10)	1.3824(18)	C(13)-C(8)-C(9)	118.64(12)
C(10)-C(11)	1.3852(18)	C(10)-C(9)-C(8)	120.81(12)
C(11)-C(12)	1.3807(19)	C(9)-C(10)-C(11)	119.99(13)
C(12)-C(13)	1.3851(18)	C(12)-C(11)-C(10)	119.67(13)
N(1)-O(3)	1.4535(13)	C(11)-C(12)-C(13)	120.28(13)
		C(12)-C(13)-C(8)	120.60(13)
N(2)-C(14)-C(15)	110.45(11)	C(1)-N(1)-C(5)	110.04(10)
C(16)-C(15)-C(14)	122.24(13)	O(3)-N(1)-C(1)	106.10(9)
C(15)-C(16)-C(17)	122.23(12)	O(3)-N(1)-C(5)	108.29(9)
C(16)-C(17)-C(18)	111.51(11)	C(7)-O(3)-N(1)	106.43(9)
O(4)-C(17)-C(16)	110.43(10)		

Table A.3.18. Torsion angles [°] for **119**.

C(14)-C(15)-C(16)-C(17)	1.9(2)	C(15)-C(16)-C(17)-C(18)	12.64(18)
C(14)-N(2)-O(6)-C(20)	-120.51(10)	C(15)-C(16)-C(17)-O(4)	-113.35(14)
C(15)-C(14)-N(2)-C(18)	-54.91(13)	C(16)-C(17)-C(18)-C(19)	-169.57(10)
C(15)-C(14)-N(2)-O(6)	-168.80(10)	C(16)-C(17)-C(18)-N(2)	-46.69(14)

C(17)-C(18)-C(19)-O(5)	-62.84(13)
C(17)-C(18)-N(2)-C(14)	69.77(12)
C(17)-C(18)-N(2)-O(6)	-178.49(9)
C(18)-N(2)-O(6)-C(20)	123.76(10)
C(19)-C(18)-N(2)-C(14)	-167.10(10)
C(19)-C(18)-N(2)-O(6)	-55.36(12)
C(20)-C(21)-C(22)-C(23)	-177.60(12)
C(20)-C(21)-C(26)-C(25)	177.77(12)
C(21)-C(20)-O(6)-N(2)	174.53(9)
C(21)-C(22)-C(23)-C(24)	-0.3(2)
C(22)-C(21)-C(26)-C(25)	-0.69(19)
C(22)-C(23)-C(24)-C(25)	-0.5(2)
C(23)-C(24)-C(25)-C(26)	0.7(2)
C(24)-C(25)-C(26)-C(21)	-0.1(2)
C(26)-C(21)-C(22)-C(23)	0.86(19)
N(2)-C(14)-C(15)-C(16)	18.79(18)
N(2)-C(18)-C(19)-O(5)	176.88(10)
O(4)-C(17)-C(18)-C(19)	-44.78(14)
O(4)-C(17)-C(18)-N(2)	78.09(13)
O(6)-C(20)-C(21)-C(22)	91.95(14)
O(6)-C(20)-C(21)-C(26)	-86.48(14)
C(1)-C(2)-C(3)-C(4)	-1.7(2)
C(1)-N(1)-O(3)-C(7)	112.31(11)
C(2)-C(1)-N(1)-C(5)	55.71(14)
C(2)-C(1)-N(1)-O(3)	172.64(10)
C(2)-C(3)-C(4)-C(5)	-14.86(19)
C(2)-C(3)-C(4)-O(1)	109.64(15)
C(3)-C(4)-C(5)-C(6)	171.02(11)
C(3)-C(4)-C(5)-N(1)	49.28(14)
C(4)-C(5)-C(6)-O(2)	58.70(14)
C(4)-C(5)-N(1)-C(1)	-72.46(12)
C(4)-C(5)-N(1)-O(3)	171.98(9)
C(5)-N(1)-O(3)-C(7)	-129.59(11)
C(6)-C(5)-N(1)-C(1)	165.61(11)
C(6)-C(5)-N(1)-O(3)	50.05(13)
C(7)-C(8)-C(9)-C(10)	-175.87(13)
C(7)-C(8)-C(13)-C(12)	175.27(13)
C(8)-C(7)-O(3)-N(1)	171.39(10)
C(8)-C(9)-C(10)-C(11)	0.6(2)
C(9)-C(8)-C(13)-C(12)	-0.5(2)
C(9)-C(10)-C(11)-C(12)	-0.3(2)
C(10)-C(11)-C(12)-C(13)	-0.4(2)
C(11)-C(12)-C(13)-C(8)	0.8(2)
C(13)-C(8)-C(9)-C(10)	-0.2(2)
N(1)-C(1)-C(2)-C(3)	-17.85(19)
N(1)-C(5)-C(6)-O(2)	176.75(10)
O(1)-C(4)-C(5)-C(6)	46.89(15)
O(1)-C(4)-C(5)-N(1)	-74.86(13)
O(3)-C(7)-C(8)-C(9)	-45.44(18)
O(3)-C(7)-C(8)-C(13)	138.89(12)

Table A.3.19. Hydrogen bonds for **119** [Å and °].

D-H...A	d(D-H)	d(H...A)	d(D...A)	<(DHA)
O(1)-H(1)...O(5)#1	0.84	1.97	2.7226(13)	148.4
O(2)-H(2A)...O(1)#2	0.84	1.87	2.6837(13)	164.4
O(4)-H(4)...O(2)#3	0.837(16)	1.950(16)	2.7199(14)	152.4(15)
O(5)-H(5)...O(4)#4	0.832(16)	1.896(17)	2.7070(14)	164.5(17)

Symmetry transformations used to generate equivalent atoms:
#1 -x,-y+1,-z+1 #2 -x+1,-y+1,-z+2 #3 -x+1,-y+1,-z+1
#4 -x,-y+1,-z

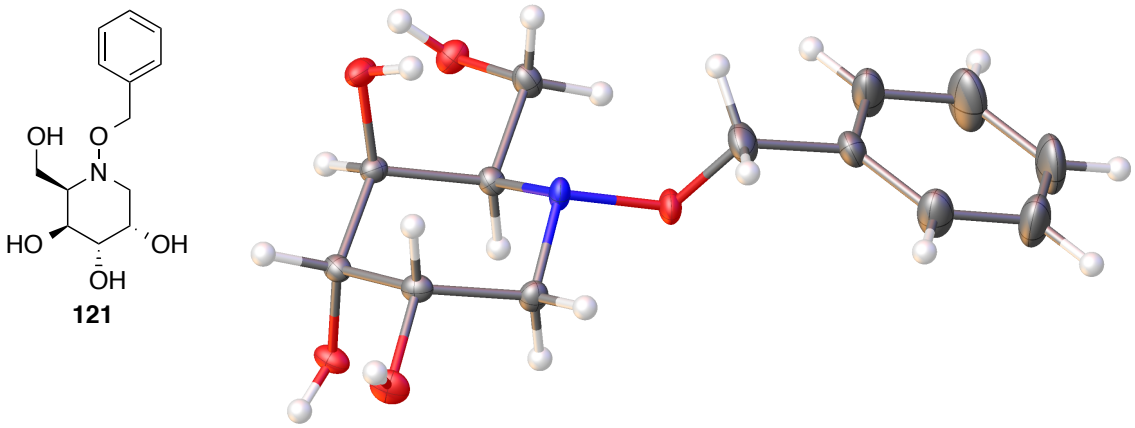

Figure A.3.6. Thermal ellipsoid plot of polyhydroxylated piperidine **121**. Hydrogen atoms are represented as spheres of arbitrary radius. Gray = carbon, red = oxygen, blue = nitrogen.

Table A.3.20. Crystal data and structure refinement for **121**.

CCDC no.	1028237	
Identification code	klb010_0m	
Empirical formula	C26 H38 N2 O10	
Formula weight	538.58	
Temperature	99.65 K	
Wavelength	0.71073 Å	
Crystal system	Triclinic	
Space group	*P*-1	
Unit cell dimensions	a = 5.3906(3) Å	α = 112.4571(11)°.
	b = 15.9299(9) Å	β = 97.7331(11)°.
	c = 17.3564(10) Å	γ = 99.3952(11)°.
Volume	1326.85(13) $Å^3$	
Z	2	
Density (calculated)	1.348 Mg/m^3	
Absorption coefficient	0.104 mm^{-1}	
F(000)	576	
Crystal size	0.401 x 0.191 x 0.176 mm^3	
Theta range for data collection	1.300 to 30.593°.	
Index ranges	-7<=h<=7, -22<=k<=22, -24<=l<=24	
Reflections collected	33786	
Independent reflections	8134 [R(int) = 0.0579]	
Completeness to theta = 25.242°	100.0 %	
Absorption correction	Semi-empirical from equivalents	
Max. and min. transmission	0.7461 and 0.6922	
Refinement method	Full-matrix least-squares on F^2	
Data / restraints / parameters	8134 / 0 / 376	
Goodness-of-fit on F^2	1.000	
Final R indices [I>2sigma(I)]	R1 = 0.0467, wR2 = 0.1191	
R indices (all data)	R1 = 0.0775, wR2 = 0.1352	
Extinction coefficient	n/a	
Largest diff. peak and hole	0.406 and -0.296 $e.Å^{-3}$	

Table A.3.21. Bond lengths [Å] and angles [°] for **121**.

C(1)-C(2)	1.5303(18)	C(3)-C(2)-C(1)	110.44(10)
C(1)-N(1)	1.4736(17)	O(1)-C(2)-C(1)	109.92(10)
C(2)-C(3)	1.5126(18)	O(1)-C(2)-C(3)	108.33(10)
C(2)-O(1)	1.4354(15)	C(2)-C(3)-C(4)	108.38(10)
C(3)-C(4)	1.5209(18)	O(2)-C(3)-C(2)	110.20(11)
C(3)-O(2)	1.4243(15)	O(2)-C(3)-C(4)	108.74(10)
C(4)-C(5)	1.5323(18)	C(3)-C(4)-C(5)	111.04(11)
C(4)-O(3)	1.4182(15)	O(3)-C(4)-C(3)	106.47(10)
C(5)-C(6)	1.5310(18)	O(3)-C(4)-C(5)	111.66(11)
C(5)-N(1)	1.4813(16)	C(6)-C(5)-C(4)	111.36(11)
C(6)-O(4)	1.4253(16)	N(1)-C(5)-C(4)	108.96(10)
C(7)-C(8)	1.526(3)	N(1)-C(5)-C(6)	111.05(10)
C(7)-C(8A)	1.489(3)	O(4)-C(6)-C(5)	109.98(10)
C(7)-O(5)	1.4350(16)	O(5)-C(7)-C(8)	102.87(17)
C(8)-C(9)	1.3900	O(5)-C(7)-C(8A)	109.19(17)
C(8)-C(13)	1.3900	C(9)-C(8)-C(7)	120.0(3)
C(9)-C(10)	1.3900	C(9)-C(8)-C(13)	120.0
C(10)-C(11)	1.3900	C(13)-C(8)-C(7)	120.0(3)
C(11)-C(12)	1.3900	C(10)-C(9)-C(8)	120.0
C(12)-C(13)	1.3900	C(9)-C(10)-C(11)	120.0
C(8A)-C(13A)	1.3900	C(12)-C(11)-C(10)	120.0
C(8A)-C(9A)	1.3900	C(11)-C(12)-C(13)	120.0
C(13A)-C(12A)	1.3900	C(12)-C(13)-C(8)	120.0
C(12A)-C(11A)	1.3900	C(13A)-C(8A)-C(7)	120.5(3)
C(11A)-C(10A)	1.3900	C(13A)-C(8A)-C(9A)	120.0
C(10A)-C(9A)	1.3900	C(9A)-C(8A)-C(7)	119.2(3)
N(1)-O(5)	1.4575(13)	C(8A)-C(13A)-C(12A)	120.0
C(14)-C(15)	1.5243(18)	C(13A)-C(12A)-C(11A)	120.0
C(14)-N(2)	1.4716(17)	C(12A)-C(11A)-C(10A)	120.0
C(15)-C(16)	1.5200(18)	C(9A)-C(10A)-C(11A)	120.0
C(15)-O(6)	1.4251(15)	C(10A)-C(9A)-C(8A)	120.0
C(16)-C(17)	1.5251(18)	C(1)-N(1)-C(5)	109.79(10)
C(16)-O(7)	1.4257(16)	O(5)-N(1)-C(1)	104.45(9)
C(17)-C(18)	1.5293(18)	O(5)-N(1)-C(5)	104.98(9)
C(17)-O(8)	1.4270(16)	C(7)-O(5)-N(1)	109.50(9)
C(18)-C(19)	1.5335(18)	N(2)-C(14)-C(15)	108.50(11)
C(18)-N(2)	1.4695(16)	C(14)-C(15)-C(16)	110.63(10)
C(19)-O(9)	1.4297(16)	O(6)-C(15)-C(14)	109.53(11)
C(20)-C(21)	1.5095(17)	O(6)-C(15)-C(16)	110.03(11)
C(20)-O(10)	1.4324(18)	C(15)-C(16)-C(17)	109.70(11)
C(21)-C(22)	1.3900	O(7)-C(16)-C(15)	111.63(11)
C(21)-C(26)	1.3900	O(7)-C(16)-C(17)	107.61(10)
C(22)-C(23)	1.3900	C(16)-C(17)-C(18)	111.82(11)
C(23)-C(24)	1.3900	O(8)-C(17)-C(16)	110.06(10)
C(24)-C(25)	1.3900	O(8)-C(17)-C(18)	110.80(11)
C(25)-C(26)	1.3900	C(17)-C(18)-C(19)	111.04(11)
N(2)-O(10)	1.4540(14)	N(2)-C(18)-C(17)	106.73(10)
		N(2)-C(18)-C(19)	110.37(11)
N(1)-C(1)-C(2)	108.76(10)	O(9)-C(19)-C(18)	111.51(11)

O(10)-C(20)-C(21)	105.62(12)	C(25)-C(26)-C(21)	120.0
C(22)-C(21)-C(20)	119.39(9)	C(18)-N(2)-C(14)	110.65(10)
C(22)-C(21)-C(26)	120.0	O(10)-N(2)-C(14)	106.01(10)
C(26)-C(21)-C(20)	120.59(9)	O(10)-N(2)-C(18)	104.87(9)
C(21)-C(22)-C(23)	120.0	C(20)-O(10)-N(2)	109.12(10)
C(24)-C(23)-C(22)	120.0		
C(25)-C(24)-C(23)	120.0		
C(26)-C(25)-C(24)	120.0		

Table A.3.22. Torsion angles [°] for **121**.

C(1)-C(2)-C(3)-C(4)	57.08(13)	O(1)-C(2)-C(3)-C(4)	177.51(9)
C(1)-C(2)-C(3)-O(2)	-61.80(13)	O(1)-C(2)-C(3)-O(2)	58.64(13)
C(1)-N(1)-O(5)-C(7)	121.05(11)	O(2)-C(3)-C(4)-C(5)	63.69(13)
C(2)-C(1)-N(1)-C(5)	63.20(12)	O(2)-C(3)-C(4)-O(3)	-174.56(10)
C(2)-C(1)-N(1)-O(5)	175.31(9)	O(3)-C(4)-C(5)-C(6)	62.85(13)
C(2)-C(3)-C(4)-C(5)	-56.11(13)	O(3)-C(4)-C(5)-N(1)	-59.97(13)
C(2)-C(3)-C(4)-O(3)	65.64(13)	O(5)-C(7)-C(8)-C(9)	-103.4(3)
C(3)-C(4)-C(5)-C(6)	-178.48(10)	O(5)-C(7)-C(8)-C(13)	77.2(3)
C(3)-C(4)-C(5)-N(1)	58.70(13)	O(5)-C(7)-C(8A)-C(13A)	99.8(3)
C(4)-C(5)-C(6)-O(4)	60.08(13)	O(5)-C(7)-C(8A)-C(9A)	-73.8(3)
C(4)-C(5)-N(1)-C(1)	-61.96(13)	C(14)-C(15)-C(16)-C(17)	-52.96(14)
C(4)-C(5)-N(1)-O(5)	-173.72(9)	C(14)-C(15)-C(16)-O(7)	66.23(13)
C(5)-N(1)-O(5)-C(7)	-123.43(11)	C(14)-N(2)-O(10)-C(20)	-105.72(12)
C(6)-C(5)-N(1)-C(1)	175.04(10)	C(15)-C(14)-N(2)-C(18)	-65.77(13)
C(6)-C(5)-N(1)-O(5)	63.27(12)	C(15)-C(14)-N(2)-O(10)	-178.93(10)
C(7)-C(8)-C(9)-C(10)	-179.4(3)	C(15)-C(16)-C(17)-C(18)	54.02(14)
C(7)-C(8)-C(13)-C(12)	179.4(3)	C(15)-C(16)-C(17)-O(8)	-69.58(13)
C(7)-C(8A)-C(13A)-C(12A)	-173.6(3)	C(16)-C(17)-C(18)-C(19)	-179.34(10)
C(7)-C(8A)-C(9A)-C(10A)	173.7(3)	C(16)-C(17)-C(18)-N(2)	-59.00(13)
C(8)-C(7)-C(8A)-C(13A)	106(2)	C(17)-C(18)-C(19)-O(9)	-52.84(15)
C(8)-C(7)-C(8A)-C(9A)	-68(2)	C(17)-C(18)-N(2)-C(14)	65.06(13)
C(8)-C(7)-O(5)-N(1)	172.28(17)	C(17)-C(18)-N(2)-O(10)	178.94(10)
C(8)-C(9)-C(10)-C(11)	0.0	C(18)-N(2)-O(10)-C(20)	137.16(12)
C(9)-C(8)-C(13)-C(12)	0.0	C(19)-C(18)-N(2)-C(14)	-174.18(11)
C(9)-C(10)-C(11)-C(12)	0.0	C(19)-C(18)-N(2)-O(10)	-60.29(13)
C(10)-C(11)-C(12)-C(13)	0.0	C(20)-C(21)-C(22)-C(23)	-178.32(12)
C(11)-C(12)-C(13)-C(8)	0.0	C(20)-C(21)-C(26)-C(25)	178.30(12)
C(13)-C(8)-C(9)-C(10)	0.0	C(21)-C(20)-O(10)-N(2)	-172.96(10)
C(8A)-C(7)-C(8)-C(9)	83(2)	C(21)-C(22)-C(23)-C(24)	0.0
C(8A)-C(7)-C(8)-C(13)	-97(2)	C(22)-C(21)-C(26)-C(25)	0.0
C(8A)-C(7)-O(5)-N(1)	172.99(17)	C(22)-C(23)-C(24)-C(25)	0.0
C(8A)-C(13A)-C(12A)-C(11A)	0.0	C(23)-C(24)-C(25)-C(26)	0.0
C(13A)-C(8A)-C(9A)-C(10A)	0.0	C(24)-C(25)-C(26)-C(21)	0.0
C(13A)-C(12A)-C(11A)-C(10A)	0.0	C(26)-C(21)-C(22)-C(23)	0.0
C(12A)-C(11A)-C(10A)-C(9A)	0.0	N(2)-C(14)-C(15)-C(16)	58.47(14)
C(11A)-C(10A)-C(9A)-C(8A)	0.0	N(2)-C(14)-C(15)-O(6)	179.93(10)
C(9A)-C(8A)-C(13A)-C(12A)	0.0	N(2)-C(18)-C(19)-O(9)	-171.00(11)
N(1)-C(1)-C(2)-C(3)	-61.18(13)	O(6)-C(15)-C(16)-C(17)	-174.12(10)
N(1)-C(1)-C(2)-O(1)	179.34(9)	O(6)-C(15)-C(16)-O(7)	-54.93(13)
N(1)-C(5)-C(6)-O(4)	-178.31(10)	O(7)-C(16)-C(17)-C(18)	-67.61(13)

O(7)-C(16)-C(17)-O(8)	168.80(10)
O(8)-C(17)-C(18)-C(19)	-56.16(14)
O(8)-C(17)-C(18)-N(2)	64.18(13)
O(10)-C(20)-C(21)-C(22)	72.71(14)
O(10)-C(20)-C(21)-C(26)	-105.59(12)

Table A.3.23. Hydrogen bonds for **121** [Å and °].

D-H...A	d(D-H)	d(H...A)	d(D...A)	<(DHA)
O(2)-H(2A)...O(8)#1	0.84	1.83	2.6499(13)	163.8
O(3)-H(3A)...O(4)#2	0.84	1.87	2.7132(13)	176.5
O(6)-H(6)...O(7)#3	0.84	2.06	2.8814(13)	165.8
O(7)-H(7)...O(1)	0.84	1.94	2.7666(13)	170.2
O(8)-H(8)...O(9)#3	0.84	2.01	2.7652(14)	148.7
O(9)-H(9B)...O(1)#1	0.84	2.12	2.9047(14)	154.4
O(4)-H(4A)...N(1)#4	0.82(2)	2.16(2)	2.9729(14)	171.5(19)

Symmetry transformations used to generate equivalent atoms:
#1 -x,-y+1,-z #2 -x,-y+2,-z+1 #3 x+1,y,z
#4 x-1,y,z